Distribution Independent Data-Driven Design and Analysis of Optimal Fault Detection Systems

Von der Fakultät für Ingenieurwissenschaften,
Abteilung Elektrotechnik und Informationstechnik
der Universität Duisburg-Essen

zur Erlangung des akademischen Grades

Doktor der Ingenieurwissenschaften

genehmigte Dissertation

von

Ting Xue
aus
Shaanxi, V.R. China

1. Gutachter: Prof. Dr.-Ing Steven X. Ding
2. Gutachter: Prof. Dr. Hao Ye
Tag der mündlichen Prüfung: 28.10.2020

DOI: 10.17185/duepublico/73290
URN: urn:nbn:de:hbz:464-20201112-085044-4

Acknowledgements

Upon the completion of this work and my Ph.D. study in the Institute for Automatic Control and Complex Systems (AKS) at the University of Duisburg-Essen, I would like to express the most sincere gratitude to my respectable mentor, Prof. Dr.-Ing. Steven X. Ding, for his valuable guidance to my Ph.D. study and scientific research work over the past four years. I am appreciated greatly for his continuous support, encouragement, insightful discussions, and constructive suggestions to my research work all the time. Without his precious supervision, it would be impossible for me to finish the work at this level. I would also like to thank Prof. Dr. Hao Ye for his interest in my work and being my reviewer.

My heartfelt thanks must go to Prof. Maiying Zhong for her valuable support, guidance, and discussions on this work. I am grateful for her consistent patience and cooperation in my research work. Besides, I would like to thank Dr. Linlin Li, Dr. Lijia Luo, Dr. Xin Peng, and Dr. Changsheng Hua for their constructive comments, valuable suggestions, and discussions on the topics related to this work.

Many thanks also go to my nice AKS colleagues, Christopher Reimann, Yuhong Na, Micha Obergfell, Frederik Hesselmann, Tianyu Liu, Caroline Charlotte Zhu, Deyu Zhang, Jiarui Zhang, Yannian Liu, Tieqiang Wang, Hogir Rafiq, and Darshan Gandhi, for their kind support and help to me during my study in AKS. Particularly, I am grateful for the valuable support of Micha Obergfell, Frederik Hesselmann, and Caroline Charlotte Zhu to this work. My sincere appreciation also goes to the former colleagues, Prof. Baozhu Du, Prof. Qing Gao, Dr. Dong Zhao, Dr. Lu Qian, Dr. Yunsong Xu, Dr. Huayun Han, Dr. Hongtian Chen, Dr. Fangzhou Fu, Han Yu, and Dr. Yang Song. They have given me great help both in research and life. I would also like to thank Dr.-Ing Birgit Köppen-Seliger and Dr.-Ing Chris Louen, who have offered me much help and suggestions to my research and the students supervision. I would also like to thank Mrs. Sabine Bay, Mr. Klaus Göbel, and Mr. Ulrich Janzen for all their valuable help during my study in AKS. I will treasure the precious time spend with them in AKS.

At last, I am deeply indebted to my parents, my sisters, and my brother for their unconditional love, complete support, understanding, and encouragement for all of my decisions in these years.

Duisburg, in August 2020 Ting Xue

Contents

List of Figures

List of Tables

List of Notations

Abbreviations

Abbreviation	Expansion
CVaR	conditional value-at-risk
DIO	distribution independent optimization
DRO	distributionally robust optimization
DCC	distributionally robust chance constraint
DJCC	distributionally robust joint chance constraint
FAR	false alarm rate
FD	fault detection
FDR	fault detection rate
FP	fractional programming
GMM	Gaussian mixture model
KDE	kernel density estimation
LCF	left coprime factorization
LTI	linear time-invariant
MDR	missed detection rate
PDF	probability density function
PI	proportional-integral
RO	robust optimization
SDP	semidefinite programming
SKR	stable kernel representation
SP	semidefinite programming
SVD	singular value decomposition
WC-CVaR	worst-case conditional value-at-risk

Mathematical notations

Notation	Description
$\forall$	for all
$\exists$	exists
$\in$	belong to
$\bigcup$	union
$\Longrightarrow$	imply
$\Longleftrightarrow$	equivalent to
$\|\| \cdot \|\|$	Euclidean norm of a vector
$\|\| \cdot \|\|_2$	$\mathcal{L}_2$ norm of a signal
$\|\| \cdot \|\|_F$	Frobenius norm of a matrix
$\Pr\{\cdot\}$	the probability of $\{\cdot\}$
$\mathrm{Tr}\{\cdot\}$	the trace of $\{\cdot\}$
$\mathrm{rank}\{\cdot\}$	the rank of $\{\cdot\}$
$\lambda_{max}\{\cdot\}$	maximal generalized eigenvalue of $\{\cdot\}$
$\max\{\cdot\}$	maximum of $\{\cdot\}$
$\min\{\cdot\}$	minimum of $\{\cdot\}$
$\mathcal{RH}_\infty$	the set of all stable transfer matrices
$\mathbb{R}^n$	space of n-dimensional vectors
$\mathbb{R}^{n\times m}$	space of n by m matrices
$\mathbb{S}_+^n$	set of positive semidefinite symmetrical matrices in $\mathbb{R}^{n\times n}$
$\mathbb{P}_\xi$	probability distribution for ξ.
$\mathbb{E}[\cdot]$	expectation of $[\cdot]$.
$\mathbb{E}_{\mathbb{P}_\xi}[\cdot]$	expectation of $[\cdot]$ with respect to $\mathbb{P}_\xi$.
$\mathbb{V}[\cdot]$	covariance of $[\cdot]$.
a^+	$\max\{a, 0\}$ for $a \in \mathbb{R}$.
$\hat{\mathbf{x}}$	estimate of the state vector $\mathbf{x}$
$\mathbf{x}$	a vector
$\mathbf{X}$	a matrix
$\mathbf{X}^T$	transport of $\mathbf{X}$
$\mathbf{X}^{-1}$	inverse of $\mathbf{X}$

1 Introduction

1.1 Background and motivations

Modern industrial systems are increasingly automated and highly integrated with the rapid development of computer science, mechanical engineering, electronics and information techniques. This, undoubtedly, gives rise to the increases in scale and complexity of such systems due to the embedded large amounts of components and the interactions of them. Consequently, issues of safety and reliability are significantly important for advanced engineering systems corrupted with disturbances and faults or failures. Especially for the safety-critical plants, e.g., nuclear reactors, aircraft, high-speed trains and chemical processes, etc., a fault or a failure might cause serious casualties, environmental pollution and heavy economic loss, etc. Therefore, it is of practical significance to monitor anomalies in systems so as to take appropriate reactions timely, thus preventing secondary damages and catastrophic consequences as well as enabling a better maintenance schedule.

In response to the ever-growing demands for high levels of safety and reliability of modern industrial processes, great interest has been stimulated in the study on fault detection (FD) and fault diagnosis both in the research and application communities, see, e.g., [56, 2, 12, 22, 84, 20, 43]. Terminologically, a fault is considered as an unexpected change of system behavior hampering nominal operation and eventually delivering unacceptable performance deterioration of the system, which is generally caused by the malfunction of actuators, sensors or process components. FD is the simplest but essential task of fault diagnosis and further fault-tolerant control that aims to detect the occurrence of faults in the functional units of processes [12, 22]. Besides, practical engineering processes are inevitably corrupted with environmental disturbances, which constitute the main sources of false and missed detection of faults. Driven by these observations, study on FD subject to disturbances is practically meaningful and remains an active research topic worth investigated thoroughly.

1.1.1 Fault detection for dynamic processes

Over the past few decades, a rich body of achievements on FD have been reported, including the hardware redundancy based technique and the analytical redundancy based

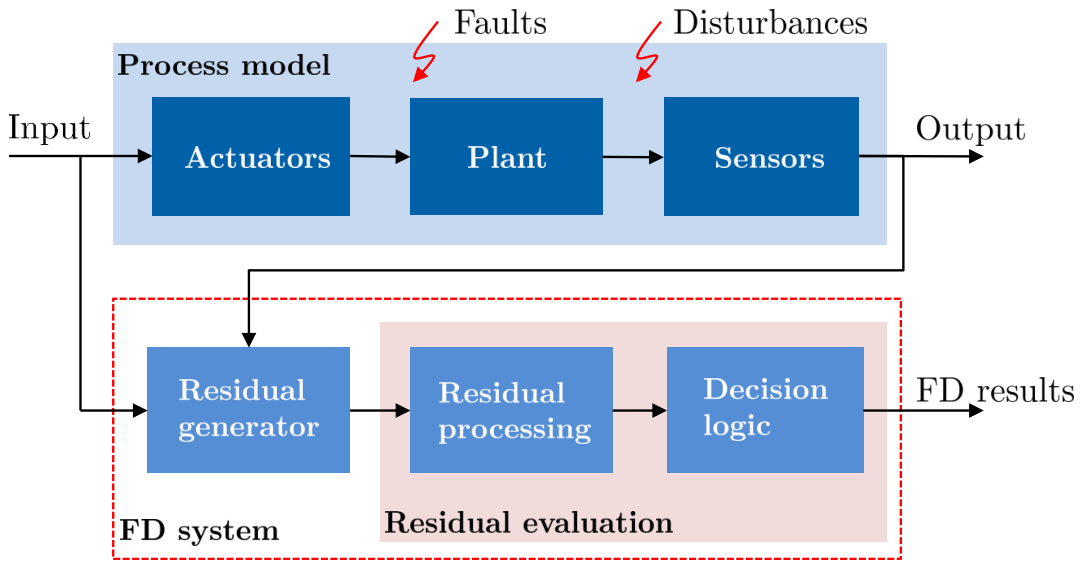

Figure 1.1: Schematic diagram of model-based FD systems.

technique [22, 12]. In hardware redundancy based FD, a redundant process is constructed using identical hardware components. By comparing the outputs of process components and the redundant ones, a fault can then be detected for real-time monitoring. Compelling advantages of this technique lie in the high reliability and the direct achievability of fault isolation [22], while the expensive costs of redundant hardware hinder its applications in practice. To alleviate this drawback, analytical redundancy based FD has obtained ongoing attention, which, as per the adoption of an analytical system model, can be roughly categorized into the model-based schemes and the data-driven methods.

In the framework of model-based FD, a so-called residual signal is generated to capture the difference between the measured system output and the model-based estimate. Then a residual evaluation function and an appropriate threshold are determined in the residual processing unit, in terms of which a decision logic is carried out to detect the occurrence of a fault, as shown in Fig. 1.1. Noteworthy merit of model-based FD lies in its capability of dealing with process dynamics. Plenty of mature results in control engineering community thus provide powerful tools for the investigation of this technique. According to the way of residual generation, existing model-based FD achievements fall into three classes, i.e., the observer-based methods [28, 87, 55], the parity space-based schemes [5, 88] and the parameter estimation approaches [86, 50]. Remarkably, the achievability of successful FD highly relies on a well-established analytical model of the supervised process. In practical applications, unfortunately, establishing an elaborate system model is becoming time- and efforts-consuming with the continuously rising scales and complexity of modern engineering

processes.

With the advent of data and information explosion age, the hinder of dispensing with analytical process model has led to a new surge of research attention on data-driven FD very recently, thanks to its capability of extracting process operating information completely from process input and output (I/O) data [84, 20, 40, 83]. Roughly speaking, data-driven FD approaches are typically classified into the multivariate analysis (MVA) methods, e.g., principal component analysis [75, 72] and independent component analysis [47, 92, 6, 8], the statistical learning schemes [26, 51, 4], e.g., neural network [7], Fisher discriminate analysis [27], K-nearest neighbor [59] and decision tree [64], etc., and the subspace technique aided approaches [48, 57, 21]. Among the involved results, MVA and statistical learning schemes generally work well in the FD for static processes. In contrast, the methodology of subspace technique aided FD outperforms the others for its efficiency in coping with the process dynamics [21]. The core idea behind it is to construct a residual generator directly using process I/O data without identifying sophisticated system models.

In the research line of subspace technique aided data-driven FD, residual evaluation has only been sporadically studied so far, despite its key role in safeguarding satisfactory FD performance. From the viewpoint of modeling, disturbances in the monitored system are generally concerned to be stochastic process and measurement noises. This, on the one hand, is reasonable in practical applications and, on the other hand, require for system identification purpose [40]. On account of this, the well studied statistical hypothesis test methods are apt to be applied for residual evaluation under the assumption of knowing exact probability distribution for noises. In this fashion, the residual evaluation function is set as a test statistic of residual and a threshold is then determined towards expected FD performance criteria, e.g., missed detection rate (MDR), false alarm rate (FAR) and fault detection rate (FDR) [24, 20, 52].

It is worth emphasizing that conventional statistical hypothesis test methods commonly work well with perfect distribution knowledge of noises, which, however, is inaccessible in practical applications. To mitigate this drawback, increasing attention has been paid to estimating the distributional information of residual from historical data by using the techniques such as kernel density estimation (KDE), histogram and Gaussian mixture model (GMM) [85, 73, 38], so that the statistical hypothesis test methods can be applied for residual evaluation, see, for instance, [31, 34]. Despite the reported successes, achieving a perfect estimation of probability distribution using process I/O data remains a time- and efforts-consuming task concerning the requirement for sufficiently large sample sets under all possible operating scenarios of the monitored process. Besides, derivations of the empirical estimate of probability distribution from the real one are generally inevitable due to the limited number of samples. This would give rise to unreliable FD results

when an over-optimistic threshold is set under certain distribution estimate. In other words, the predefined FD performance under true probability distributions might fail to be satisfied. For these concerns, issues of data-driven FD in dynamic processes suffering from distributional ambiguity of noises and faults remain to be addressed properly towards satisfactory FD performance.

1.1.2 Stochastic optimization

In terms of handling optimization problems dispensing with exact distribution knowledge of random variables, a surge of interest in the stochastic optimization has emerged in recent years, e.g., [58, 3, 29], and increasing applications have been exhibited in various fields, e.g., decision-making [69, 93, 82], robust control [71, 25, 76], dimension reduction [74], classification [54, 53] and fault diagnosis [45, 89, 90], etc. In line of this research, distributionally robust optimization (DRO) is one of the most popular topics. Rather than making specific distribution assumptions on random variables, a so-called ambiguity set is constituted to characterize a family of probability distributions sharing common properties, e.g., the moments, the probability density function (PDF) and the support or the combination of them [25]. The involved chance constraints over random variables are then posted as distributionally robust chance constraints (DCCs). To this extent, the derived solution to the targeting optimization problem is thus feasible to all probability distributions belonging to the predefined ambiguity set [19, 29]. That means the optimization problem with DCCs is a worst-case formulation regarding the distribution uncertainties.

From the perspective of ambiguity set modeling, the knowledge of mean and covariance matrix (sometimes in combination with the support information) are mostly used [29]. One natural merit of the mean-covariance based ambiguity set lies in the easy accessibility of the mean and covariance matrix with high probability from historical data. Meanwhile, at the level of algorithm, the mean and covariance matrix related DCCs can usually be converted into deterministic conditions, which greatly simplifies the targeting optimization objectives for the design and analysis purposes. Especially, thanks to the arising efforts in the connections of DCCs and conditional Value-at-Risk (CVaR) as well as the worst-case CVaR (WC-CVaR) in risk theory, the mean-covariance involved DRO problems have been eventually reformulated as deterministic robust optimization (RO) problems and effectively addressed by means of the techniques of semidefinite programming (SDP) or stochastic programming (SP), see, e.g., [30, 94, 3, 39].

In data-driven framework, the true mean and covariance matrix of a random variable are usually inaccessible and the empirical values of them are instead estimated based on process data. Even though the empirical estimates are close to the true ones with high

probability when the size of the sample set is sufficiently large, the estimation uncertainties are theoretically inevitable due to the finite number of samples. Particularly, in our context of FD, the samples in faulty cases are commonly scarce. Besides, the perturbation of the operating point or the change of distribution profiles of random variables may occur during process operation. For these concerns, investigation of the robustness of DRO under moments uncertainties is practically meaningful but theoretically challenging [19].

1.2 Objective of the work

Motivated by the above observations, this thesis is devoted to the design and analysis of data-driven FD systems for stochastic dynamic processes subject to distributional ambiguity of noises and faults. More specifically, the main objectives of this thesis are stated as follows:

- Propose a performance-oriented configuration of FD systems. On this basis, address data-driven design issues of optimal FD systems for stochastic linear discrete-time processes such that the residual generator, residual evaluator and FD performance criteria can be synthesized in an integrated manner.
- Formulate design issues of data-driven FD systems as tractable distribution independent optimization (DIO) problems based on the mean-covariance based ambiguity sets without posing specific distribution assumptions on noises and faults.
- Develop algorithms to solve the formulated DIO problems. Analytical solutions of the targeting problems and the existence conditions are exploited.
- Investigate the robustness of the developed FD systems over the moments uncertainties caused by the estimation errors due to the limited number of historical process I/O samples. Analyze the confidence levels of the achieved FD performance criteria in the probabilistic context quantitatively.

1.3 Outline of the thesis

This thesis consists of eight chapters, which are structured in Fig. 1.2. The major objectives and contributions of each chapter are briefly summarized as follows.

Chapter 1: Introduction

In this chapter, the background, motivations, objectives and the organization of this work are presented.

Chapter 2: Preliminaries of data-driven FD for dynamic processes

In this chapter, preliminaries of data-driven FD for dynamic processes are demonstrated. Basic concepts in the FD field and the schematic structure of subspace technique aided FD system are first overviewed. Then several algorithms for the data-driven construction of a residual generator are recalled, followed by a brief review of residual evaluation schemes. Finally, a short introduction of stochastic optimization is given accompanied with the modeling of ambiguity set.

Chapter 3: A DIO approach to the design of FD systems

This chapter focuses on developing a DIO approach to address design issues of data-driven FD systems. By constructing a parity relation based residual generator using process I/O data, the mean-covariance based ambiguity sets are introduced to characterize the distribution knowledge of residuals in fault-free and faulty cases, respectively. In the context of minimizing the MDR for a prescribed FAR, the design of FD systems is then formulated as a vector-valued DIO problem in terms of the means and covariance matrices, providing an integrated design of the residual generator, the residual evaluation function, and the threshold. An iterative parametric algorithm is applied to solve the targeting DIO problem and the worst-case FAR and MDR criteria are analyzed quantitatively.

Chapter 4: An improved DIO method for FD and analytical algorithms

This chapter demonstrates an improved DIO approach to the data-driven design of FD systems towards minimizing the MDR for a given FAR. Along the research line of Chapter 3, the design of FD systems is formulated as a stochastic optimization problem with DCCs with respect to the mean-covariance based ambiguity sets. Moreover, it is proven rigorously that the targeting FD issue can be addressed by solving a generalized eigenvalue-eigenvector problem and an analytical solution is thus achieved by means of singular value decomposition (SVD). Tight upper bounds of FAR and MDR are derived without distribution assumption. The existence condition of the optimal solution is also studied.

Chapter 5: Matrix-valued DIO approaches to FD systems design

This chapter presents matrix-valued solutions to the DIO approach aided design of data-driven FD systems. By introducing a parameter matrix to the parity relation based residual generator, three kinds of configurations of FD systems are proposed in the context of minimizing the MDR for a prescribed FAR under consideration of available moments information of faults, namely the multicvector-valued design method, WC-CVaR aided design method and the optimal matrix-valued design scheme. Furthermore, matrix-valued solutions to the DIO method aided FD without fault information are discussed.

Chapter 6: Performance analysis of FD systems under moments uncertainties

In this chapter, performance analysis of the data-driven FD systems developed in Chapters 3–5 is performed under consideration of the estimation uncertainties in means and covariance matrices of residuals in fault-free and faulty cases. To this end, the mean-covariance based ambiguity sets with norm-bounded and box-type uncertainties are first modeled. On this basis, the robustness of the FD systems against the moments uncertainties is investigated and the worst-case FAR and MDR are suggested quantitatively. By establishing analytical relationships between the sample numbers and the moments uncertainties, confidence levels of the achieved FAR and MDR criteria are further studied in the probabilistic context.

Chapter 7: Benchmark study and real-time implementation

In this chapter, applications of the proposed design and analysis approaches in Chapters 3–6 are illustrated on a laboratory setup of three-tank system. The effectiveness of the developed vector-valued and matrix-valued DIO methods have been verified through simulation and experimental results. The robustness of the FD systems over moments uncertainties is also demonstrated.

Chapter 8: Conclusions and future work

This chapter concludes the thesis and discusses the future scopes.

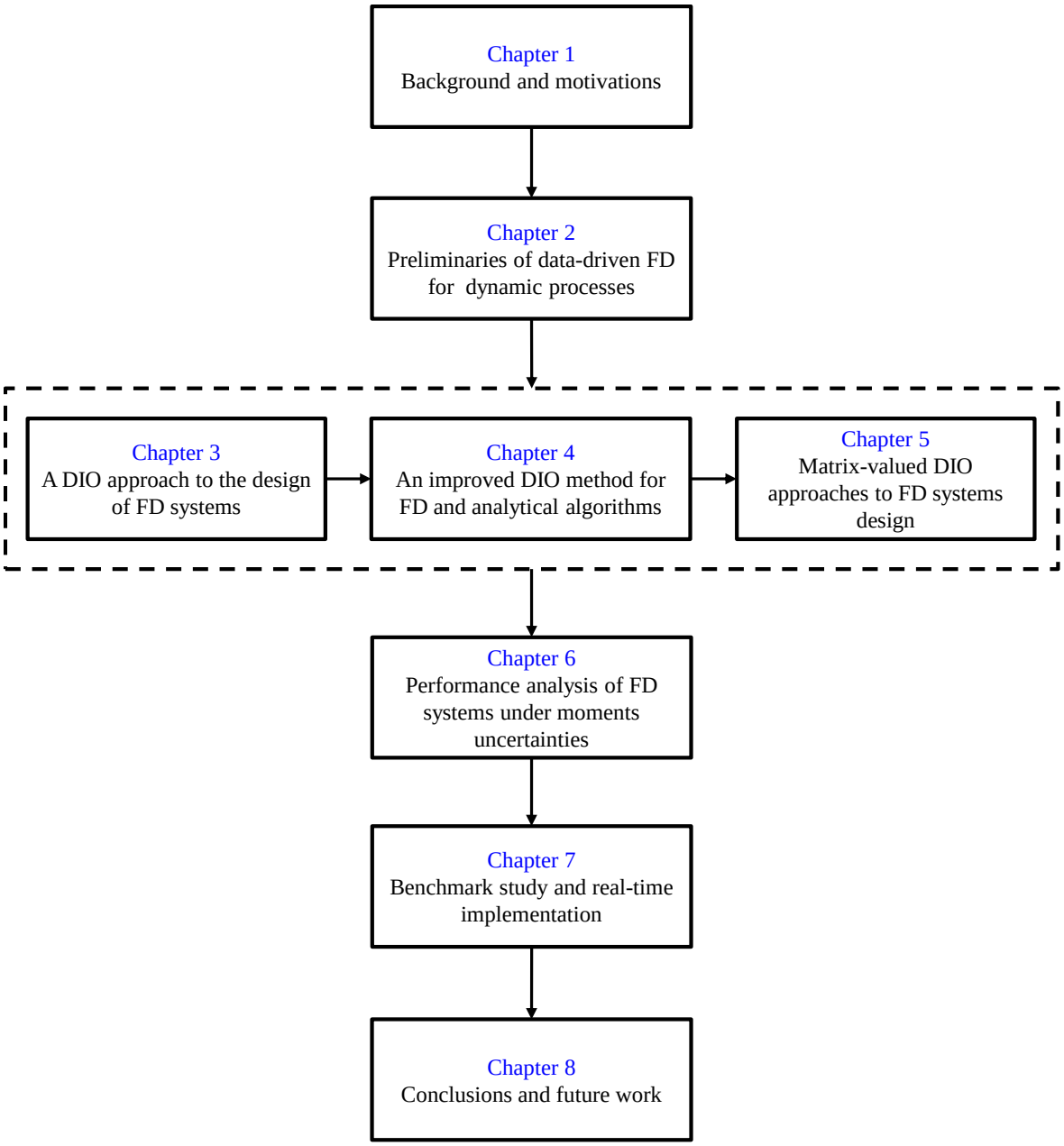

Figure 1.2: Organization of the chapters

2 Preliminaries of data-driven FD for dynamic processes

In this chapter, preliminaries of data-driven FD for stochastic linear dynamic processes and stochastic optimization are reviewed. Firstly, mathematical descriptions of stochastic linear dynamic processes are given. Then basic knowledge of subspace technique aided data-driven FD is presented, which, to be more specific, includes the residual generation and residual evaluation. Moreover, the basis of stochastic optimization and ambiguity set modeling are introduced, followed by a brief summary and notes.

2.1 Mathematical description of linear dynamic processes

2.1.1 Modeling of linear dynamic processes

We start with considering a linear discrete time-invariant system in nominal operation modeled by

$$\begin{cases} \mathbf{x}(k+1) = \mathbf{A}\mathbf{x}(k) + \mathbf{B}\mathbf{u}(k),\ \mathbf{x}_0 = \mathbf{x}(0) \\ \mathbf{y}(k) = \mathbf{C}\mathbf{x}(k) + \mathbf{D}\mathbf{u}(k) \end{cases} \tag{2.1}$$

where $\mathbf{x} \in \mathbb{R}^n$, $\mathbf{u} \in \mathbb{R}^l$, $\mathbf{y} \in \mathbb{R}^m$ are the state, input and output vectors, respectively, $\mathbf{x}_0$ is the initial state of the system, $\mathbf{A}$, $\mathbf{B}$, $\mathbf{C}$, $\mathbf{D}$ are real constant system matrices with appropriate dimensions. The dynamics of the state-space model (2.1) can also be described as follows

$$\mathbf{y}(z) = \mathbf{G}_{yu}(z)\mathbf{u}(z) \tag{2.2}$$

where $\mathbf{G}_{yu}(z) = \mathbf{C}(z\mathbf{I}-\mathbf{A})^{-1}\mathbf{B}+\mathbf{D}$ is the transfer function matrix from input to output and can be abbreviated to $\mathbf{G}_{yu}(z) = (\mathbf{A}, \mathbf{B}, \mathbf{C}, \mathbf{D})$. Since there are infinite state-space representations of the monitored process, it is assumed throughout this thesis that $(\mathbf{A}, \mathbf{B}, \mathbf{C}, \mathbf{D})$ is a minimal realization of $\mathbf{G}_{yu}(z)$, i.e., $(\mathbf{A}, \mathbf{B})$ is controllable and $(\mathbf{A}, \mathbf{C})$ is observable.

Concerning the system (2.1) corrupted with noises and faults, a stochastic linear discrete-time process is modeled as follows

$$\begin{cases} \mathbf{x}(k+1) = \mathbf{A}\mathbf{x}(k) + \mathbf{B}\mathbf{u}(k) + \mathbf{B}_f\mathbf{f}(k) + \boldsymbol{\omega}(k),\ \mathbf{x}_0 = \mathbf{x}(0) \\ \mathbf{y}(k) = \mathbf{C}\mathbf{x}(k) + \mathbf{D}\mathbf{u}(k) + \mathbf{D}_f\mathbf{f}(k) + \boldsymbol{\upsilon}(k) \end{cases} \tag{2.3}$$

where $\mathbf{f} \in \mathbb{R}^p$, $\boldsymbol{\omega} \in \mathbb{R}^n$, $\boldsymbol{\upsilon} \in \mathbb{R}^m$ are the fault, process and measurement noise vectors, respectively, $\mathbf{B}_f$, $\mathbf{D}_f$ are time-invariant matrices that indicate the influence of fault to the system dynamics. Noise signals $\boldsymbol{\omega}(k)$, $\boldsymbol{\upsilon}(k)$ are assumed to be white random sequences statistically independent of $\mathbf{x}_0$, $\mathbf{u}(k)$ and $\mathbf{f}(k)$.

Without loss of generality, the faults in system (2.3) are considered to be additive faults, which occur without changing the system stability. From the viewpoint of modeling, additive faults are broadly categorized into the following three classes, i.e.,

- Actuator faults $\mathbf{f}_A$: these faults would cause changes in the actuator response to the input commend $\mathbf{u}(k)$. The system (2.3) with actuator fault is then modeled by setting $\mathbf{B}_f = \mathbf{B}$, $\mathbf{D}_f = \mathbf{D}$.
- Sensor faults $\mathbf{f}_S$: these faults would directly influence the process measurement $\mathbf{y}(k)$. The system (2.3) with sensor faults is modeled by setting $\mathbf{B}_f = \mathbf{0}$, $\mathbf{D}_f = \mathbf{I}$.
- Process faults $\mathbf{f}_P$: the malfunctions in process are termed processes faults. With the use of $\mathbf{D}_\mathrm{p}$ to determine the location and type of $\mathbf{f}_P$, the system (2.3) with process faults is obtained with $\mathbf{B}_f = \mathbf{B}_\mathrm{p}$, $\mathbf{D}_f = \mathbf{D}_\mathrm{p}$.

Let $\mathbf{f} = \begin{bmatrix}\mathbf{f}_A^T & \mathbf{f}_S^T & \mathbf{f}_P^T\end{bmatrix}^T$, $\mathbf{B}_f = [\mathbf{B} \quad \mathbf{0} \quad \mathbf{B}_\mathrm{p}]$, $\mathbf{D}_f = [\mathbf{D} \quad \mathbf{I} \quad \mathbf{D}_\mathrm{p}]$. The dynamics of a system with actuator faults, sensor faults and process faults can be intuitively described by (2.3).

2.1.2 Coprime factorization technique

Coprime factorization technique is used to factorize a transfer matrix into two stable and coprime transfer matrices, which provides another alternative description of system dynamics. Below we first present the definition of left coprime factorization (LCF).

Definition 2.1. *(Left coprime factorization (LCF) [22]) A factorization* $\mathbf{G}(z) = \hat{\mathbf{M}}^{-1}(z)\hat{\mathbf{N}}(z)$ *is said to be an LCF of* $\mathbf{G}(z)$ *if (i)* $\hat{\mathbf{N}}(z) \in \mathcal{RH}_\infty$ *and* $\hat{\mathbf{M}}(z) \in \mathcal{RH}_\infty$ *and (ii) there exist* $\hat{\mathbf{Y}}(z) \in \mathcal{RH}_\infty$ *and* $\hat{\mathbf{X}}(z) \in \mathcal{RH}_\infty$ *such that*

$$\hat{\mathbf{N}}(z)\hat{\mathbf{X}}(z) + \hat{\mathbf{M}}(z)\hat{\mathbf{Y}}(z) = \mathbf{I}. \tag{2.4}$$

Followed by Definition 2.1, a state-space computation algorithm of an LCF is presented in the following lemma.

Lemma 2.1. *[22] Suppose* $\mathbf{G}$ *is a proper real-rational transfer matrix with a state space realization* $(\mathbf{A}, \mathbf{B}, \mathbf{C}, \mathbf{D})$*, and it is stabilizable and detectable. Let* $\mathbf{L}$ *be so that* $\mathbf{A} - \mathbf{LC}$ *is Schur matrix (i.e., its eigenvalues are inside the unit circle on the complex plane). Define*

$$\hat{\mathbf{M}}(z) = (\mathbf{A} - \mathbf{LC},\ -\mathbf{L},\ \mathbf{C}, \mathbf{I}),\ \hat{\mathbf{N}}(z) = (\mathbf{A} - \mathbf{LC},\ \mathbf{B} - \mathbf{LD},\ \mathbf{C}, \mathbf{D}). \tag{2.5}$$

Then $\mathbf{G}(z) = \hat{\mathbf{M}}^{-1}(z)\hat{\mathbf{N}}(z)$ *is the LCF of* $\mathbf{G}(z)$*. Moreover, the so-called Bezout identity (2.4) holds with*

$$\hat{\mathbf{X}}(z) = (\mathbf{A}+\mathbf{BF},\, \mathbf{L},\, \mathbf{C}+\mathbf{DF}, \mathbf{I})\,,\ \hat{\mathbf{Y}}(z) = (\mathbf{A}+\mathbf{BF},\, -\mathbf{L},\, \mathbf{F}, \mathbf{0})$$

and $\mathbf{A}+\mathbf{BF}$ *being a Schur matrix.*

Under assumption of the system (2.1) being controllable and observable, according to Lemma 2.1, an LCF of transform matrix $\mathbf{G}_{yu}(z)$ is obtained as

$$\mathbf{G}_{yu}(z) = \hat{\mathbf{M}}^{-1}(z)\hat{\mathbf{N}}(z) \tag{2.6}$$

with $\hat{\mathbf{M}}(z)$, $\hat{\mathbf{N}}(z)$ given in (2.5). Alternatively, the system (2.1) can be represented in the following form

$$\forall \mathbf{u}(z),\ \begin{bmatrix} -\hat{\mathbf{N}}(z) & \hat{\mathbf{M}}(z) \end{bmatrix} \begin{bmatrix} \mathbf{u}(z) \\ \mathbf{y}(z) \end{bmatrix} = 0. \tag{2.7}$$

Equation (2.7) is known as a kernel representation of the system (2.1). More generally, the stable kernel representation (SKR) is defined as follows.

Definition 2.2. *(Stable kernel representation (SKR) [23]) Given system (2.1), a stable linear system* $\mathcal{K}$ *driven by* $\mathbf{u}(z)$, $\mathbf{y}(z)$ *and satisfying*

$$\forall \mathbf{u}(z),\ \mathcal{K} \begin{bmatrix} \mathbf{u}(z) \\ \mathbf{y}(z) \end{bmatrix} = 0 \tag{2.8}$$

is called SKR of (2.1).

It is evident that $\mathcal{K} = \begin{bmatrix} -\hat{\mathbf{N}}(z) & \hat{\mathbf{M}}(z) \end{bmatrix}$ is an SKR of the system (2.1). One point worth emphasizing is that the SKR of the concerned system is not unique by noting the nonunique realization of an LCF. More details about the relationship between different realizations of LCF can be referred to [22, 91].

2.2 Residual generation techniques

In the framework of analytical redundancy based FD, an FD system consists of two parts termed the residual generation and residual evaluation, as sketched in Fig. 1.1 in Chapter 1. In this part, the subspace technique aided data-driven constructions of a residual generator are first reviewed.

Roughly speaking, a residual generator is constructed to check the consistency of the real monitored system and the redundant process driven by the same input [12]. In general, the estimate of system output is created using the process model and the difference of it

from the real measured output is adopted as a residual signal. Under ideal conditions, the residual should be zero in fault-free case and nonzero with the presence of faults. Denote by $\mathbf{r}(k)$ the residual signal, given system (2.1), $\mathbf{r}(k)$ should satisfy [22]

i) in fault-free case,

$$\forall \mathbf{u}(k),\, \mathbf{x}_0,\, \lim_{k\to\infty} \mathbf{r}(k) = \mathbf{0}, \tag{2.9}$$

ii) when some possible faults present,

$$\mathbf{r}(k) \neq \mathbf{0}. \tag{2.10}$$

Concerning these characteristics, an SKR is actually a parametrized realization of residual generator for the system (2.1), that is

$$\mathbf{r}(z) = \begin{bmatrix} -\hat{\mathbf{M}}(z) & \hat{\mathbf{N}}(z) \end{bmatrix} \begin{bmatrix} \mathbf{u}(z) \\ \mathbf{y}(z) \end{bmatrix}. \tag{2.11}$$

Correspondingly, an observer-based online realization of (2.11) is constructed as follows

$$\begin{cases} \hat{\mathbf{x}}(k+1) = \mathbf{A}\hat{\mathbf{x}}(k) + \mathbf{B}\mathbf{u}(k) + \mathbf{L}(\mathbf{y}(k) - \hat{\mathbf{y}}(k)) \\ \hat{\mathbf{y}}(k) = \mathbf{C}\hat{\mathbf{x}}(k) + \mathbf{D}\mathbf{u}(k) \\ \mathbf{r}(k) = \mathbf{y}(k) - \hat{\mathbf{y}}(k) \end{cases} \tag{2.12}$$

where $\hat{\mathbf{x}} \in \mathbb{R}^n$, $\hat{\mathbf{y}} \in \mathbb{R}^m$ are the estimates of $\mathbf{x}$, $\mathbf{y}$, respectively, $\mathbf{L}$ is the observer gain matrix stabilizing $(\mathbf{A} - \mathbf{LC})$. It is noteworthy that (2.12) is also known as a fault detection filter in the model-based FD concept.

Together with Definition 2.2 and the residual generator (2.11), the following theorem is achieved intuitively.

Theorem 2.1. *[23] Given process model (2.3), a linear discrete time-invariant dynamic system is a residual generator if and only if it is an SKR of (2.1).*

2.2.1 I/O data models

To achieve a data-driven implementation of the residual generator (2.11), establishing the so-called I/O data model to link the analytical model with process I/O data is necessary. In what follows, three kinds of I/O data models are first introduced to this end, based on which the subspace technique aided algorithms for residual generation are studied.

For ease of presentation, the following notations are introduced. For a vector $\boldsymbol{\xi} \in \mathbb{R}^{k_\xi}$ and integer $s > 0$, let

$$\boldsymbol{\xi}_s(k) = \begin{bmatrix} \boldsymbol{\xi}(k-s) \\ \boldsymbol{\xi}(k-s+1) \\ \vdots \\ \boldsymbol{\xi}(k) \end{bmatrix} \in \mathbb{R}^{(s+1)k_\xi}, \ \boldsymbol{\Xi}_k = \begin{bmatrix} \boldsymbol{\xi}(k) & \boldsymbol{\xi}(k+1) & \cdots & \boldsymbol{\xi}(k+N-1) \end{bmatrix} \in \mathbb{R}^{Nk_\xi}$$

$$\boldsymbol{\Xi}_{k,s} = \begin{bmatrix} \boldsymbol{\xi}_s(k) & \boldsymbol{\xi}_s(k+1) & \cdots & \boldsymbol{\xi}_s(k+N-1) \end{bmatrix} = \begin{bmatrix} \boldsymbol{\Xi}_{k-s} \\ \boldsymbol{\Xi}_{k-s+1} \\ \vdots \\ \boldsymbol{\Xi}_k \end{bmatrix} \in \mathbb{R}^{(s+1)k_\xi \times N} \tag{2.13}$$

where $\boldsymbol{\xi}$ can be $\mathbf{x}$, $\mathbf{u}$, $\mathbf{y}$, $\mathbf{f}$, $\boldsymbol{\omega}$, $\boldsymbol{\upsilon}$ with k_ξ being n, l, m, p correspondingly. Corresponding to state-space representation (2.3), the following parity relation based process model can be established

$$\mathbf{y}_s(k) = \boldsymbol{\Gamma}_s \mathbf{x}(k-s) + \mathbf{H}_{u,s}\mathbf{u}_s(k) + \mathbf{H}_{f,s}\mathbf{f}_s(k) + \mathbf{H}_{\omega,s}\boldsymbol{\omega}_s(k) + \boldsymbol{\upsilon}_s(k) \tag{2.14}$$

where $s \geq n$ and

$$\boldsymbol{\Gamma}_s = \begin{bmatrix} \mathbf{C} \\ \mathbf{CA} \\ \vdots \\ \mathbf{CA}^s \end{bmatrix}, \quad \mathbf{H}_{u,s} = \begin{bmatrix} \mathbf{D} & 0 & \cdots & 0 \\ \mathbf{CB} & \mathbf{D} & \cdots & 0 \\ \vdots & \ddots & \ddots & \vdots \\ \mathbf{CA}^{s-1}\mathbf{B} & \cdots & \mathbf{CB} & \mathbf{D} \end{bmatrix} \tag{2.15}$$

$\mathbf{H}_{\omega,s}$ and $\mathbf{H}_{f,s}$ are obtained by replacing $(\mathbf{B}, \mathbf{D})$ in $\mathbf{H}_{us}$ with $(\mathbf{I}, \mathbf{0})$ and $(\mathbf{B}_f, \mathbf{D}_f)$, respectively. On this basis, an I/O data model of system (2.3) for fault-free case (i.e., $\mathbf{f}(k) = 0$), is given by

$$\mathbf{Y}_{k,s}(k) = \boldsymbol{\Gamma}_s \mathbf{X}_{k-s} + \mathbf{H}_{u,s}\mathbf{U}_{k,s}(k) + \mathbf{H}_{\omega,s}\boldsymbol{\Omega}_{k,s}(k) + \boldsymbol{\Upsilon}_{k,s}(k) \tag{2.16}$$

where $\mathbf{X}_{k-s}$ has the same structure of $\boldsymbol{\Xi}_k$ with respect to replacing $\boldsymbol{\xi}$ with $\mathbf{x}$, $\mathbf{Y}_{k,s}$, $\mathbf{U}_{k,s}$, $\boldsymbol{\Omega}_{k,s}$, $\boldsymbol{\Upsilon}_{k,s}$ are in form of $\boldsymbol{\Xi}_{k,s}$ by replacing $\boldsymbol{\xi}$ with $\mathbf{y}$, $\mathbf{u}$, $\boldsymbol{\omega}$, $\boldsymbol{\upsilon}$, respectively. The item $\mathbf{H}_{\omega,s}\boldsymbol{\Omega}_{k,s}(k) + \boldsymbol{\Upsilon}_{k,s}(k)$ represents the influence of noises to the process output.

By introducing a so-called innovation sequence denoted by $\mathbf{e}(k) = \mathbf{y}(k) - \hat{\mathbf{y}}(k)$, it is derived from (2.12) that

$$\begin{cases} \hat{\mathbf{x}}(k+1) = \mathbf{A}\hat{\mathbf{x}}(k) + \mathbf{B}\mathbf{u}(k) + \mathbf{L}\mathbf{e}(k) = \mathbf{A}_L\hat{\mathbf{x}}(k) + \mathbf{B}_L\mathbf{u}(k) + \mathbf{L}\mathbf{y}(k) \\ \mathbf{y}(k) = \mathbf{C}\hat{\mathbf{x}}(k) + \mathbf{D}\mathbf{u}(k) + \mathbf{e}(k) \end{cases} \tag{2.17}$$

where $\mathbf{A}_L = \mathbf{A} - \mathbf{LC}$, $\mathbf{B}_L = \mathbf{B} - \mathbf{LD}$. Alternative I/O data models of system (2.3) for fault-free case can then be obtained as follows

$$\mathbf{Y}_{k,s} = \mathbf{\Gamma}_s \hat{\mathbf{X}}_{k-s} + \mathbf{H}_{u,s}\mathbf{U}_{k,s} + \mathbf{H}_{e,s}\mathbf{E}_{k,s} \tag{2.18}$$

$$\left(\mathbf{I} - \mathbf{H}^L_{y,s}\right)\mathbf{Y}_{k,s} = \mathbf{\Gamma}^L_s \hat{\mathbf{X}}_{k-s} + \mathbf{H}^L_{u,s}\mathbf{U}_{k,s} + \mathbf{E}_{k,s} \tag{2.19}$$

where $\mathbf{E}_{k,s}$ are given in form of (2.13) with $\boldsymbol{\xi}$ replaced by $\mathbf{e}$ and

$$\mathbf{H}_{e,s} = \begin{bmatrix} \mathbf{I} & \mathbf{0} & \cdots & \mathbf{0} \\ \mathbf{CL} & \mathbf{I} & \cdots & \mathbf{0} \\ \vdots & \ddots & \ddots & \vdots \\ \mathbf{CA}^{s-1}\mathbf{L} & \cdots & \mathbf{CL} & \mathbf{I} \end{bmatrix}, \quad \mathbf{\Gamma}^L_s = \begin{bmatrix} \mathbf{C} \\ \mathbf{CA}_L \\ \vdots \\ \mathbf{CA}^s_L \end{bmatrix}$$

$$\mathbf{H}^L_{y,s} = \begin{bmatrix} \mathbf{0} & \mathbf{0} & \cdots & \mathbf{0} \\ \mathbf{CL} & \mathbf{0} & \cdots & \mathbf{0} \\ \vdots & \ddots & \ddots & \vdots \\ \mathbf{CA}^{s-1}_L\mathbf{L} & \cdots & \mathbf{CL} & \mathbf{0} \end{bmatrix}, \quad \mathbf{H}^L_{u,s} = \begin{bmatrix} \mathbf{D} & \mathbf{0} & \cdots & \mathbf{0} \\ \mathbf{CB}_L & \mathbf{D} & \cdots & \mathbf{0} \\ \vdots & \ddots & \ddots & \vdots \\ \mathbf{CA}^{s-1}_L\mathbf{B}_L & \cdots & \mathbf{CB}_L & \mathbf{D} \end{bmatrix}$$

with $\mathbf{H}^L_{y,s} \in \mathbb{R}^{(s+1)m\times(s+1)m}$ and $\mathbf{H}_{e,s} \in \mathbb{R}^{(s+1)m\times(s+1)m}$.

2.2.2 Subspace technique aided residual generation

Based on Definition 2.2 and the parity relation based process model (2.14), we recall the following data-driven realization of SKR.

Definition 2.3. *(Data-driven realization of SKR [23]) Given system (2.1), matrix $\boldsymbol{\mathcal{K}}_{d,s}$ is called a data-driven realization of the SKR, if for some positive integer s, it holds*

$$\forall \mathbf{u}_s(k),\, \mathbf{x}_0,\quad \boldsymbol{\mathcal{K}}_{d,s}\begin{bmatrix} \mathbf{u}_s(k) \\ \mathbf{y}_s(k) \end{bmatrix} = 0. \tag{2.20}$$

On this basis, a data-driven realization of residual generator (2.11) is obtained as follows

$$\mathbf{r}(k) = \boldsymbol{\mathcal{K}}_{d,s}\begin{bmatrix} \mathbf{u}_s(k) \\ \mathbf{y}_s(k) \end{bmatrix}. \tag{2.21}$$

Notably, the key point of constructing residual generator (2.21) lies in the identification of $\boldsymbol{\mathcal{K}}_{d,s}$. Keeping this in mind, corresponding to the I/O data models (2.18), (2.19) and (2.16), below we successively show three subspace technique aided residual generation schemes by using process I/O data.

- **Scheme I**

  It follows from (2.17) that

$$\hat{\mathbf{x}}(k) = \mathbf{A}_L^{\rho}\hat{\mathbf{x}}(k-\rho) + \sum_{i=1}^{\rho} \mathbf{A}_L^{i-1} \begin{bmatrix} \mathbf{B}_L & \mathbf{L} \end{bmatrix} \begin{bmatrix} \mathbf{u}_s(k) \\ \mathbf{y}_s(k) \end{bmatrix}. \tag{2.22}$$

  Note that $\mathbf{A}_L^{\rho} \approx 0$ holds for a large integer $\rho > 0$, it immediately follows

$$\hat{\mathbf{x}}(k) \approx \sum_{i=1}^{\rho} \mathbf{A}_L^{i-1} \begin{bmatrix} \mathbf{B}_L & \mathbf{L} \end{bmatrix} \begin{bmatrix} \mathbf{u}_s(k) \\ \mathbf{y}_s(k) \end{bmatrix}. \tag{2.23}$$

  By constructing the following data stacks

$$\mathbf{Z}_{k-\rho,\rho-1} = \begin{bmatrix} \mathbf{Y}_{k-\rho,\rho-1} \\ \mathbf{U}_{k-\rho,\rho-1} \end{bmatrix}$$

  the I/O data model (2.18) can then be re-written as

$$\mathbf{Y}_{k,s} \approx \mathbf{\Pi}_{s,\rho-1}\mathbf{Z}_{k-\rho,\rho-1} + \mathbf{H}_{u,s}\mathbf{U}_{k,s} + \mathbf{H}_{e,s}\mathbf{E}_{k,s} \tag{2.24}$$

  where $\mathbf{\Pi}_{s,\rho-1} = [\mathbf{\Pi}_{s,\rho-1,u} \quad \mathbf{\Pi}_{s,\rho-1,y}]$ with

$$\mathbf{\Pi}_{s,\rho-1,u} = \mathbf{\Gamma}_s \begin{bmatrix} \mathbf{A}_L^{\rho-1}\mathbf{B}_L & \cdots & \mathbf{B}_L \end{bmatrix}, \ \mathbf{\Pi}_{s,\rho-1,y} = \mathbf{\Gamma}_s \begin{bmatrix} \mathbf{A}_L^{\rho-1}\mathbf{L} & \cdots & \mathbf{L} \end{bmatrix}.$$

  Once the matrix $\mathbf{\Pi}_{s,\rho-1}$, $\mathbf{H}_{u,s}$ are identified using process I/O data, according to Definition 2.3, a residual generator can then be constructed online by

$$\mathbf{r}(k+\rho) = \mathbf{y}_s(k+\rho) - \mathbf{\Pi}_{s,\rho-1}\mathbf{z}_{\rho-1}(k) - \mathbf{H}_{u,s}\mathbf{u}_s(k+\rho). \tag{2.25}$$

  The algorithm is summarized in Algorithm 2.2.1.

- **Scheme II**

  Given I/O data model (2.19) and $\rho > 0$ such that (2.23) holds, we have

$$\mathbf{Y}_{k,s} = \mathbf{\Pi}_{s,\rho-1}^{L}\mathbf{Z}_{k-\rho,\rho-1} + \mathbf{H}_{u,s}^{L}\mathbf{U}_{k,s} + \mathbf{H}_{y,s}^{L}\mathbf{Y}_{k,s} + \mathbf{E}_{k,s} \tag{2.27}$$

Algorithm 2.2.1 Construction of residual generator (2.25)

1: Collect process I/O data in fault-free case and construct $\mathbf{Z}_{k-\rho,\rho-1}$, $\mathbf{U}_{k,s}$, $\mathbf{Y}_{k,s}$.

2: Identify the matrices $\mathbf{\Pi}_{s,\rho-1}$, $\mathbf{H}_{u,s}$ by solving the following least square problem (with QR-decomposition technique as presented in Algorithm 9.3 in [20])

$$\min_{\mathbf{\Pi}_{s,\rho-1},\mathbf{H}_{u,s}} \|\mathbf{Y}_{k,s} - \mathbf{\Pi}_{s,\rho-1}\mathbf{Z}_{k-\rho,\rho-1} - \mathbf{H}_{u,s}\mathbf{U}_{k,s}\|_F. \tag{2.26}$$

3: Compute the residual sequence online with (2.25).

where $\mathbf{\Pi}_{s,\rho-1}^L = \begin{bmatrix}\mathbf{\Pi}_{s,\rho-1,u}^L & \mathbf{\Pi}_{s,\rho-1,y}^L\end{bmatrix}$ with

$$\mathbf{\Pi}_{s,\rho-1,u}^L = \mathbf{\Gamma}_s^L \begin{bmatrix}\mathbf{A}_L^{\rho-1}\mathbf{B}_L & \cdots & \mathbf{B}_L\end{bmatrix}, \ \mathbf{\Pi}_{s,\rho-1,y} = \mathbf{\Gamma}_s^L \begin{bmatrix}\mathbf{A}_L^{\rho-1}\mathbf{L} & \cdots & \mathbf{L}\end{bmatrix}.$$

The following approximation of (2.27) is then obtained for a sufficient large ρ

$$\mathbf{Y}_k \approx \sum_{i=1}^{\rho+s} \mathbf{C}\mathbf{A}_L^{i-1} \begin{bmatrix}\mathbf{B}_L & \mathbf{L}\end{bmatrix} \begin{bmatrix}\mathbf{U}_{k-i} \\ \mathbf{Y}_{k-i}\end{bmatrix} + \mathbf{D}\mathbf{U}_k + \mathbf{E}_k = \mathbf{\Theta} \begin{bmatrix}\mathbf{Z}_{k-s-1,s+\rho-1} \\ \mathbf{U}_k\end{bmatrix}$$

with $\mathbf{\Theta} = \begin{bmatrix}\mathbf{C}\mathbf{A}_L^{s+\rho-1}\mathbf{B} & \cdots & \mathbf{C}\mathbf{B}, \ \mathbf{C}\mathbf{A}_L^{s+\rho-1}\mathbf{L} & \cdots & \mathbf{C}\mathbf{L}, \ \mathbf{D}\end{bmatrix}$.

By identifying $\mathbf{\Theta}$ using process I/O data and constructing the matrices $\mathbf{\Pi}_{s,\rho-1}^L$, $\mathbf{H}_{u,s}^L$ and $\mathbf{H}_{y,s}^L$ based on it, the residual generator is then given in the following form

$$\mathbf{r}(k+\rho) = \left(\mathbf{I} - \mathbf{H}_{y,s}^L\right)\mathbf{y}_s(k+\rho) - \mathbf{\Pi}_{s,\rho-1}^L \mathbf{z}_{\rho-1}(k) - \mathbf{H}_{u,s}^L \mathbf{u}_s(k+\rho). \tag{2.28}$$

The algorithm is summarized in Algorithm 2.2.2.

- **Scheme III**

  Consider the fault-free case with $\mathbf{f}(k) = 0$ and rewrite the model (2.14) as follows

$$\begin{bmatrix}\mathbf{y}_s(k) \\ \mathbf{u}_s(k)\end{bmatrix} = \begin{bmatrix}\mathbf{\Gamma}_s & \mathbf{H}_{u,s} \\ 0 & \mathbf{I}\end{bmatrix} \begin{bmatrix}\mathbf{x}(k-s) \\ \mathbf{u}_s(k)\end{bmatrix} + \begin{bmatrix}\mathbf{H}_{\omega,s}\boldsymbol{\omega}_s(k) + \boldsymbol{\upsilon}_s(k) \\ 0\end{bmatrix}. \tag{2.30}$$

  Denote by $\mathbf{\Gamma}_s^\perp \in \mathbb{R}^{((s+1)m-n)\times(s+1)m}$ the null space of $\mathbf{\Gamma}_s$, i.e., $\mathbf{\Gamma}_s^\perp\mathbf{\Gamma}_s = 0$. Let

$$\mathbf{\Psi}_s = \begin{bmatrix}\mathbf{\Gamma}_s & \mathbf{H}_{u,s} \\ 0 & \mathbf{I}\end{bmatrix}, \ \mathbf{\Psi}_s^\perp = \begin{bmatrix}\mathbf{\Gamma}_s^\perp & -\mathbf{\Gamma}_s^\perp\mathbf{H}_{u,s}\end{bmatrix} \in \mathbb{R}^{((s+1)m-n)\times(s+1)(l+m)}.$$

  It is evident that $\mathbf{\Psi}_s^\perp\mathbf{\Psi}_s = 0$. Recalling Definition 2.3, matrix $\mathbf{\Psi}_s^\perp$ is actually a data-driven realization of SKR of the system (2.1) and can thus be identified for residual generation purpose. To this end, it yields from (2.16) that

$$\begin{bmatrix}\mathbf{Y}_{k,s} \\ \mathbf{U}_{k,s}\end{bmatrix} = \mathbf{\Psi}_s \begin{bmatrix}\mathbf{X}_{k-s} \\ \mathbf{U}_{k,s}\end{bmatrix} + \begin{bmatrix}\mathbf{H}_{\omega,s}\mathbf{\Omega}_{k,s} + \mathbf{\Upsilon}_{k,s} \\ 0\end{bmatrix}. \tag{2.31}$$

Algorithm 2.2.2 Construction of residual generator (2.28)

1: Collect process I/O data in fault-free case and form $\mathbf{Z}_{k-\rho,\rho-1}$, $\mathbf{U}_{k,s}$, $\mathbf{Y}_{k,s}$.

2: Solve the following least square estimation problem with QR-decomposition technique

$$\min_{\mathbf{\Theta}} \left\| \mathbf{Y}_k - \mathbf{\Theta} \begin{bmatrix}\mathbf{Z}_{k-s-1,s+\rho-1} \\ \mathbf{U}_k\end{bmatrix} \right\|_F \tag{2.29}$$

3: Identify the matrices $\mathbf{\Pi}_{s,\rho-1}^L$, $\mathbf{H}_{u,s}^L$ and $\mathbf{H}_{y,s}^L$ from $\mathbf{\Theta}$.

4: Compute the residual sequence online with (2.28).

Denote by $\mathbf{Z}_p = \mathbf{Z}_{k-s-1,s}$, $\mathbf{Z}_f = \mathbf{Z}_{k,s}$. For a large integer $s >> n$, it holds

$$\begin{aligned}\frac{1}{N}\mathbf{Z}_f\mathbf{Z}_p^T &= \mathbf{\Psi}_s\left(\frac{1}{N}\begin{bmatrix}\mathbf{X}_{k-s}\\ \mathbf{U}_{k,s}\end{bmatrix}\mathbf{Z}_p^T + \frac{1}{N}\begin{bmatrix}\mathbf{H}_{\omega,s}\mathbf{\Omega}_{k,s}+\mathbf{\Upsilon}_{k,s}\\ 0\end{bmatrix}\mathbf{Z}_p^T\right)\\ &\approx \mathbf{\Psi}_s\left(\frac{1}{N}\begin{bmatrix}\mathbf{X}_{k-s}\\ \mathbf{U}_{k,s}\end{bmatrix}\mathbf{Z}_p^T\right).\end{aligned}$$

Under assumption of

$$rank\left(\frac{1}{N}\begin{bmatrix}\mathbf{X}_{k-s}\\ \mathbf{U}_{k,s}\end{bmatrix}Z_p^T\right) = n + l(s+1) \tag{2.32}$$

the matrix $\mathbf{\Psi}_s^\perp$ then exists guaranteeing $\mathbf{\Psi}_s^\perp\left(\frac{1}{N}\mathbf{Z}_f\mathbf{Z}_p^T\right) = 0$. Do an SVD on $\frac{1}{N}\mathbf{Z}_f\mathbf{Z}_p^T$

$$\frac{1}{N}\mathbf{Z}_f\mathbf{Z}_p^T = [\mathbf{U}_1 \quad \mathbf{U}_2]\begin{bmatrix}\mathbf{\Lambda}_1 & 0\\ 0 & \mathbf{\Lambda}_2(\approx 0)\end{bmatrix}\begin{bmatrix}\mathbf{V}_1^T\\ \mathbf{V}_2^T\end{bmatrix}.$$

We then have

$$\mathbf{\Psi}_s^\perp = \mathbf{U}_2^T. \tag{2.33}$$

It is remarkable that the condition (2.32) is usually ensured when the system is excited sufficiently. This has been well studied in literature [40]. In what follows, we assume by default that (2.32) holds true except where otherwise stated.

Let $\mathbf{\Psi}_s^\perp = \begin{bmatrix}\mathbf{\Psi}_{y,s}^\perp & -\mathbf{\Psi}_{u,s}^\perp\end{bmatrix}$ with $\mathbf{\Psi}_{y,s}^\perp \in \mathbb{R}^{((s+1)m-n)\times(s+1)m}$. It then holds [21]

$$\mathbf{\Psi}_{y,s}^\perp\mathbf{\Gamma}_s = 0, \quad \mathbf{\Psi}_{u,s}^\perp = \mathbf{\Gamma}_s^\perp\mathbf{H}_{u,s} = \mathbf{\Psi}_{y,s}^\perp\mathbf{H}_{u,s} \tag{2.34}$$

where $\mathbf{\Psi}_{y,s}^\perp = \mathbf{\Gamma}_s^\perp$ is the so-called parity space. The following parity relation based residual generator is thus constructed

$$\mathbf{r}(k) = \mathbf{\Psi}_s^\perp\begin{bmatrix}\mathbf{y}_s(k)\\ \mathbf{u}_s(k)\end{bmatrix} = \mathbf{\Psi}_{y,s}^\perp\mathbf{y}_s(k) - \mathbf{\Psi}_{u,s}^\perp\mathbf{u}_s(k). \tag{2.35}$$

Together with (2.14), the dynamics of residual generator (2.35) is governed by

$$\mathbf{r}(k) = \mathbf{\Psi}_{y,s}^\perp\left(\mathbf{H}_{f,s}\mathbf{f}_s(k) + \mathbf{H}_{\omega,s}\boldsymbol{\omega}_s(k) + \boldsymbol{\upsilon}_s(k)\right). \tag{2.36}$$

We summary the construction of residual generator (2.35) in Algorithm 2.2.3.

As a short summary, in the Schemes I and II, the residual generators (2.25) and (2.28) are depending on the process input. In contrast, the residual generator (2.35) obtained with

Algorithm 2.2.3 Construction of residual generator (2.35)

1: Collect process I/O data in fault-free case and form $\mathbf{Z}_p$, $\mathbf{Z}_f$.
2: Do an SVD on $\frac{1}{N}\mathbf{Z}_f\mathbf{Z}_p$ and then compute $\mathbf{\Psi}_s^\perp$ with (2.33). Form matrices $\mathbf{\Psi}_{y,s}^\perp$, $\mathbf{\Psi}_{u,s}^\perp$.
3: Compute the residual signal online with (2.35).

Scheme III is decoupled of the system input in an ideal situation. Meanwhile, the online realization of (2.35) requires lower computational load in contrast with (2.25) and (2.28). In the subsequent study, Scheme III will be applied for residual generation except where otherwise stated.

From the viewpoint of online realization, the residual generator (2.35) is computationally cumbersome due to the data stacking operations and the delivered residual vector might contain redundant information and thus less robust against noises. Remembering the observer-based implementation of SKR, a fault detection filter-like configuration of (2.35) is demonstrated in the following lemma, a detailed declaration of which is referred to [23].

Lemma 2.2. *[23] Given system (2.30) and $\mathbf{\Psi}_s^\perp$ in (2.33), denote by $\boldsymbol{\psi}_s^\perp = [\boldsymbol{\psi}_{s,y}^\perp \quad -\boldsymbol{\psi}_{s,u}^\perp] \in \mathbb{R}^{(s+1)m}$ a row vector of $\mathbf{\Psi}_s^\perp$ satisfying $\boldsymbol{\psi}_{s,y}^\perp \mathbf{\Gamma}_s = 0$. An observer-based realization of residual generator (2.35) for given $\boldsymbol{\psi}_s^\perp$ can be*

$$\begin{cases} \mathbf{x}_o(k+1) = \mathbf{A}_o\mathbf{x}_o(k) + \mathbf{B}_o\mathbf{u}(k) + \mathbf{L}_o\mathbf{y}(k) \\ \mathrm{r}(k) = \mathbf{g}_o\mathbf{y}(k) - \mathbf{c}_o\mathbf{x}_o(k) - \mathbf{d}_o\mathbf{u}(k) \end{cases} \tag{2.37}$$

where $\mathbf{x}_o \in \mathbb{R}^{k_{o,x}}$, $\mathrm{r} \in \mathbb{R}$, $\mathbf{c}_o = [0 \quad \cdots \quad 0 \quad 1]$, $\mathbf{g}_o = \boldsymbol{\psi}_{s,y,s}^\perp$, $\mathbf{d}_o = \boldsymbol{\psi}_{s,u,s}^\perp$ and

$$\mathbf{A}_o = \begin{bmatrix} 0 & 0 & \cdots & 0 \\ 1 & 0 & \cdots & 0 \\ \vdots & \ddots & \ddots & \vdots \\ 0 & \cdots & 1 & 0 \end{bmatrix} \in \mathbb{R}^{s\times s},\ \mathbf{L}_o = -\begin{bmatrix} \boldsymbol{\psi}_{s,y,1}^\perp \\ \boldsymbol{\psi}_{s,y,2}^\perp \\ \vdots \\ \boldsymbol{\psi}_{s,y,s}^\perp \end{bmatrix},\ \mathbf{B}_o = \begin{bmatrix} \boldsymbol{\psi}_{s,u,1}^\perp \\ \boldsymbol{\psi}_{s,u,2}^\perp \\ \vdots \\ \boldsymbol{\psi}_{s,u,s}^\perp \end{bmatrix}$$

with $\boldsymbol{\psi}_{s,y,i}^\perp$ being the $(m(i-1)+1 : im)$ columns of $\boldsymbol{\psi}_{s,y}^\perp$ and $\boldsymbol{\psi}_{s,u,i}^\perp$ the $(l(i-1)+1 : il)$ columns of $\boldsymbol{\psi}_{s,u}^\perp$ with $i = 1, 2, \ldots, s$, respectively.

Remark 2.1. *Note that the residual generated in (2.37) is a scalar signal whilst a residual vector is usually required to achieve reliable FD results. Towards an m-dimensional residual generator, one simple way is to construct m observer-based residual generators in form of (2.37) and then form a residual vector directly, i.e.,*

$$\begin{cases} \mathbf{x}_{o,i}(k+1) = \mathbf{A}_{o,i}\mathbf{x}_{o,i}(k) + \mathbf{B}_{o,i}\mathbf{u}(k) + \mathbf{L}_{o,i}\mathbf{y}_i(k) \\ r_i(k) = g_{o,i}y_i(k) - \mathbf{c}_{o,i}\mathbf{x}_{o,i}(k) - \mathbf{d}_{o,i}\mathbf{u}(k),\ i = 1, 2, \ldots, m \\ \mathbf{r}(k) = [r_1(k) \ \ r_2(k) \ \ \cdots \ \ r_m(k)]^T \in \mathbb{R}^m \end{cases} \tag{2.38}$$

where $\mathbf{x}_{o,i} \in \mathbb{R}^{k_{o,x}}$ *and* $r_i \in \mathbb{R}$ *denote the state and residual of the i-th observer excited by the i-th output* y_i *and process input* $\mathbf{u}$*, respectively, matrices* $\mathbf{A}_{o,i}$*,* $\mathbf{B}_{o,i}$*,* $\mathbf{L}_{o,i}$*,* $g_{o,i}$*,* $\mathbf{c}_{o,i}$*,* $\mathbf{d}_{o,i}$ *are correspondingly in form of* $\mathbf{A}_o$*,* $\mathbf{B}_o$*,* $\mathbf{L}_o$*,* g_o*,* $\mathbf{c}_o$*,* $\mathbf{d}_o$ *as given in Lemma 2.2 with* $\mathbf{y}$ *substituted by* y_i*. Other algorithms for the construction of an m-dimensional residual generator is referred to [23].*

2.3 Residual evaluation schemes

Followed by residual generation, another essential part of an FD system is residual evaluation, which involves the determination of residual evaluation function $J(\mathbf{r})$, threshold J_{th} and decision logic. Roughly speaking, there are two residual evaluation strategies for FD purpose, namely the norm-based methods and the statistical hypothesis test schemes.

2.3.1 Norm-based methods

The norm-based residual evaluation strategy is usually adopted for FD concerning the disturbances being norm-bounded. Typically, the L_2-norm and L_∞-norm of residual signal are the two most popular choices for residual evaluation function. In the fashion of L_2-norm, the residual evaluation function and threshold are determined as

$$J_2(\mathbf{r}) = \|\mathbf{r}(k)\|_2 = \sqrt{\mathbf{r}^T(k)\mathbf{r}(k)}, \quad J_{2,th} = \sup_{\mathbf{f}=0} J_2(\mathbf{r}). \tag{2.39}$$

The occurrence of a fault can then be detected by using the following decision logic

$$\begin{cases} J_2(\mathbf{r}) \leq J_{2,\text{th}}, & \Rightarrow \text{no fault alarm} \\ J_2(\mathbf{r}) > J_{2,\text{th}}, & \Rightarrow \text{ fault alarm.} \end{cases} \tag{2.40}$$

Similarly, the L_∞-norm based residual evaluation function and threshold are set as

$$J_\infty(\mathbf{r}) = \|\mathbf{r}(k)\|_\infty = \sup_k \sqrt{\mathbf{r}^T(k)\mathbf{r}(k)}, \quad J_{\infty,th} = \sup_{\mathbf{f}=0} J_\infty(\mathbf{r}). \tag{2.41}$$

The following decision logic is thus used for FD

$$\begin{cases} J_\infty(\mathbf{r}) \leq J_{\infty,th}, & \Rightarrow \text{no fault alarm} \\ J_\infty(\mathbf{r}) > J_{\infty,th}, & \Rightarrow \text{ fault alarm.} \end{cases} \tag{2.42}$$

2.3.2 Statistical hypothesis test methods

Statistical hypothesis test methods are commonly used to deal with residual evaluation issues subject to stochastic noises. In this research line, the residual evaluation function is

generally set as a test statistic of residual sequence and a threshold is then determined towards acceptable FD performance in terms of FAR, FDR and MDR, etc.

It is worth mentioning that the likelihood ratio test scheme is one of the most powerful hypothesis test technique according to the Neyman–Pearson lemma [62]. In the framework of likelihood ratio test, a likelihood function of residual is defined, i.e., $\hbar(\mathbf{r}|\boldsymbol{\theta})$ with $\boldsymbol{\theta}$ being a parameter carrying fault information. Denote by $\boldsymbol{\theta} = \boldsymbol{\theta}_0$ in fault-free case and $\boldsymbol{\theta} = \boldsymbol{\theta}_f$ in faulty case. The residual evaluation function $J(\mathbf{r})$ can then be defined as

$$J(\mathbf{r}) = \frac{\hbar(\mathbf{r}|\boldsymbol{\theta}_0)}{\hbar(\mathbf{r}|\boldsymbol{\theta}_f)} \tag{2.43}$$

which is a so-called likelihood ratio function. By introducing a null hypothesis $\mathcal{H}_0$ and an alternative hypothesis $\mathcal{H}_1$ as follows

$$\mathcal{H}_0 : \boldsymbol{\theta} = \boldsymbol{\theta}_0, \quad \mathcal{H}_1 : \boldsymbol{\theta} = \boldsymbol{\theta}_f \tag{2.44}$$

a threshold J_{th} is then determined with respect to the following decision logic

$$\begin{cases} J(\mathbf{r}) \leq J_{th}, & \Rightarrow \text{no fault alarm} \\ J(\mathbf{r}) > J_{th}, & \Rightarrow \text{fault alarm} \end{cases} \tag{2.45}$$

such that

$$\Pr\{J(\mathbf{r}) > J_{th}|\mathcal{H}_0\} = \alpha \tag{2.46}$$

where α is an acceptable significance level of the probability rejecting $\mathcal{H}_0$ in favor of $\mathcal{H}_1$. In FD fashion, α is termed as the FAR.

Under assumption of known probability distribution for noises, the PDF of residual is usually chosen as the likelihood function $\hbar(\mathbf{r}|\boldsymbol{\theta})$. Especially when the noises are considered to be Gaussian distributed, the residual evaluation function in (2.43) is actually a T^2 test statistic of residual that relies merely on the mean and covariance matrix of residual vector. These results have been illustrated broadly in plenty of achievements, see, e.g., [12, 22, 23]. Nevertheless, in practical applications the requirement for exact probability distributions for noises and faults is difficulty to be fulfilled.

2.3.3 Performance assessment

In terms of assessing the performance of FD systems regarding residual evaluation function $J(\mathbf{r})$, threshold J_{th} and decision logic (2.45), the definitions of FAR, FDR and MDR in the probabilistic context are first introduce as follows [22].

Definition 2.4. *(False alarm rate (FAR)) The conditional probability*

$$P_{FAR} := \Pr\{J(\mathbf{r}) > J_{th} | \mathbf{f} = 0\} \tag{2.47}$$

is called the FAR.

Definition 2.5. *(Missed detection rate (MDR)) The conditional probability*

$$P_{MDR} := \Pr\{J(\mathbf{r}) \leq J_{th} | \mathbf{f} \neq 0\} \tag{2.48}$$

is called the MDR.

Definition 2.6. *(Fault detection rate (FDR)) The conditional probability*

$$P_{FDR} := \Pr\{J(\mathbf{r}) > J_{th} | \mathbf{f} \neq 0\} \tag{2.49}$$

is called the FDR.

It is obvious that $P_{FDR} = 1 - P_{MDR}$. In the framework of statistical hypothesis test based residual evaluation, when the probability distributions for noises and faults are known, the threshold can be determined towards minimizing the MDR (or maximizing the FDR) for a given acceptable FAR or minimizing the FAR for a prescribed MDR (or FDR). In the application of norm-based residual evaluation, zero FAR is achieved by using (2.39) or (2.41) while the MDR might be very poor because of the impossibility of decreasing the FAR and MDR simultaneously only by adjusting the threshold.

As stated before, the assumption of knowing exact probability distributions for noises and faults made in the statistical hypothesis test based residual evaluation is often, unfortunately, unrealistic in practical applications. And the mainstream of mitigating this deficiency that estimating the distributional information from historical data might cause unreliable FD results due to the estimation errors caused by the finite number of samples. Very recently, stochastic optimization technique has attracted increasing attention towards addressing design issues under distributional ambiguity, which provides a good jumping-off point for newer approaches to performance-oriented optimal FD without precise probability distributions for noises and faults.

2.4 Basics of stochastic optimization

In this part, basic knowledge of stochastic optimization is presented serving as the preliminary of subsequent study on the design and analysis of optimal FD systems for stochastic dynamic processes.

2.4.1 Distributionally robust chance constraints

The concept of chance constraint was proposed in 1958 by Charnes and Cooper [11] and great efforts have been made on this topic since then, see e.g., [60, 65, 82, 93]. In the paradigm of chance constraint, a deterministic constraint regarding a random variable is supposed to be satisfied with a certain probability. That is, given a random variable $\boldsymbol{\xi} \in \mathbb{R}^n$ following probability distribution $\mathbb{P}_\xi$ and decision vector $\mathbf{w} \in \mathbb{R}^n$ such that a constraint $L(\boldsymbol{\xi}, \mathbf{w}) \geq 0$ holds with

$$\Pr\{L(\boldsymbol{\xi}, \mathbf{w}) \geq 0\} \leq \alpha \tag{2.50}$$

where $\alpha \in (0, 1)$. Obviously, the condition (2.46) posed guaranteeing FAR performance is actually a chance constraint. Note that the condition (2.50) is formulated conceptually but restricted in practical applications due to the inaccessible exact knowledge of $\mathbb{P}_\xi$.

As a natural extension of (2.50), the so-called distributionally robust chance constraint (DCC) has been proposed to immunize the exact distribution requirement in chance constraints. In DCC framework, $\mathbb{P}_\xi$ is assumed to be within the ambiguity set $\mathcal{P}$ that shares common distributional properties and the constraint (2.50) then holds over $\mathcal{P}$, i.e.,

$$\sup_{\mathbb{P}_\xi \in \mathcal{P}} \Pr\{L(\boldsymbol{\xi}, \mathbf{w}) \geq 0\} \leq \alpha. \tag{2.51}$$

It is clear that DCC (2.51) gives the worst-case measure of condition (2.50) with respect to characterizing the distributional uncertainty with ambiguity set $\mathcal{P}$. In other words, (2.51) is robust against the distributional uncertainty in $\mathbb{P}_\xi$.

More generally, concerning multiple constraints $L_i(\boldsymbol{\xi}, \mathbf{w}) \geq 0$, $i = 1, 2, \ldots, m$ over $(\boldsymbol{\xi}, \mathbf{w})$, the following formulation termed distributionally robust joint chance constraints (DJCCs) is introduced

$$\sup_{\mathbb{P}_\xi \in \mathcal{P}} \Pr\{L_i(\boldsymbol{\xi}, \mathbf{w}) \geq 0,\ i = 1, 2, \ldots, m\} \leq \alpha \tag{2.52}$$

which reduces to a DCC (2.51) when $m = 1$.

2.4.2 Worst-case conditional Value-at-Risk

CVaR is arguably one of the most popular coherent risk measures of uncertainties that are broadly utilized in economics [15, 78, 94]. The definition of CVaR is given below.

Definition 2.7. *(Conditional Value-at-Risk(CVaR) [93]) Given a loss function $L(\boldsymbol{\xi}) : \mathbb{R}^n \to \mathbb{R}$ over random variable $\boldsymbol{\xi} \in \mathbb{R}^n$ obeying probability distribution $\mathbb{P}_\xi$, and a tolerance $\rho \in (0, 1)$, the CVaR at level ρ with respect to $\mathbb{P}_\xi$ is defined as*

$$\mathbb{P}_\xi - \mathrm{CVaR}_\rho\left(L(\boldsymbol{\xi})\right) = \inf_{\eta \in \mathbb{R}} \left\{ \eta + \frac{1}{\rho} \mathbb{E}_{\mathbb{P}_\xi}\left[(L(\boldsymbol{\xi}) - \eta)^+\right] \right\}. \tag{2.53}$$

It is notable that CVaR essentially evaluates the conditional expectation of loss above the $(1-\rho)$-quantile of the loss distribution [93]. When the infimum is attended in (2.53), we have $\mathbb{P}_\xi - \mathrm{CVaR}_\rho(L(\boldsymbol{\xi}) = \Pr\{L(\boldsymbol{\xi}) \leq \eta\} \geq 1-\rho$. Thanks to the properties of monotone, homogeneous and convex of CVaR with respect to $L(\boldsymbol{\xi})$, it is usually applied to approximate the chance constraint (2.50). Unfortunately, the application of CVaR constraints still requires the precise knowledge of $\mathbb{P}_\xi$, which is difficult to access in practice.

To alleviate the CVaR in (2.53) against the distributional ambiguity, similar to (2.51), we introduce the so-called WC-CVaR with respect to the ambiguity set $\mathcal{P}$ taking the following form

$$\sup_{\mathbb{P}_\xi \in \mathcal{P}} \mathbb{P}_\xi - \mathrm{CVaR}_\rho\left(L(\boldsymbol{\xi})\right) \leq 0. \tag{2.54}$$

Note that, for any loss function $L(\boldsymbol{\xi})$, it holds

$$\Pr\left\{L(\boldsymbol{\xi}) \leq \mathbb{P}_\xi - \mathrm{CVaR}_\rho\left(L(\boldsymbol{\xi})\right)\right\} \geq 1-\rho. \tag{2.55}$$

We thus always have

$$\sup_{\mathbb{P}_\xi \in \mathcal{P}} \mathbb{P}_\xi - \mathrm{CVaR}_\rho\left(L(\boldsymbol{\xi})\right) \leq 0 \Rightarrow \sup_{\mathbb{P}_\xi \in \mathcal{P}} \Pr\left(L(\boldsymbol{\xi}) \geq 0\right) \leq \rho. \tag{2.56}$$

In this regard, the WC-CVaR condition (2.54) provides a conservative approximation for the DCC in form of (2.51). Because of the convexity of WC-CVaR, tractability of WC-CVaR conditions has been extensively studied by means of SDP and SP, see, e.g., [76, 82, 93]. The connection between the WC-CVaR conditions and DCCs is the key ingredient of this thesis, we defer to the formalities in Chapters 4–6.

2.4.3 Distributionally robust optimization

DRO is an important topic in stochastic optimization that optimizes the targeting objective in worst-case setting over an ambiguity set constituted in terms of partial distributional information [17, 70]. To be more specific, consider a standard DRO problem in the following form

$$\mathcal{Z}_{DRO}(\boldsymbol{\xi}, \mathbf{w}) = \min_{\mathbf{w} \in \mathcal{W}} \sup_{\mathbb{P}_\xi \in \mathcal{P}} \mathbb{E}_{\mathbb{P}_\xi}\left[h(\mathbf{w}, \boldsymbol{\xi})\right] \tag{2.57}$$

where $\mathbf{w}$ is a decision variable belonging to a given set $\mathcal{W}$ in space $\mathbb{R}^n$, $h(\mathbf{w}, \boldsymbol{\xi})$ represents the objective function. It is seen that, the optimal decision variable $\mathbf{w}$ obtained by solving (2.57) would minimize the supremum expectation of objective function $h(\mathbf{w}, \boldsymbol{\xi})$ for a family of probability distributions $\mathbb{P}_\xi \in \mathcal{P}$.

It is worth mentioning that DRO can be regarded as an extension of SP and RO defined in the deterministic optimization context [17]. When the ambiguity set $\mathcal{P}$ is specified for a

certain distribution $\mathbb{P}_\xi$, i.e., $\mathcal{P} = \{\mathbb{P}_\xi\}$, the DRO problem (2.57) would degenerate into an SP problem in the following form

$$\mathcal{Z}_{SP}(\boldsymbol{\xi}, \mathbf{w}) = \min_{\mathbf{w}\in\mathcal{W}} \mathbb{E}_{\mathbb{P}_\xi}\left[h(\mathbf{w}, \boldsymbol{\xi})\right]. \tag{2.58}$$

When the ambiguity set $\mathcal{P}$ is modeled only with the support of random variable $\boldsymbol{\xi}$, i.e., $\mathcal{P} = \{\mathbb{P}_\xi \in \mathbb{R}^n | \Pr\{\boldsymbol{\xi} \in \boldsymbol{\mathcal{U}}\} = 1\}$, the problem (2.57) is reduced to a RO problem as follows

$$\mathcal{Z}_{RO}(\boldsymbol{\xi}, \mathbf{w}) = \min_{\mathbf{w}\in\mathcal{W}} \sup_{\boldsymbol{\xi}\in\boldsymbol{\mathcal{U}}} h(\mathbf{w}, \boldsymbol{\xi}). \tag{2.59}$$

In comparison with SP, DRO can efficiently cope with the uncertainties in probability distributions with the introduction of ambiguity set, instead of presumption on the distribution of random variables as made in SP. Moreover, by modeling the ambiguity set in combination with partial distribution knowledge except for support, DRO can deliver a less conservative result in contrast with RO.

2.4.4 Ambiguity set modeling

Considering the interplay between objective function and DCCs in stochastic optimization, the modeling of ambiguity set is significant towards a tractable DRO problem. Generally speaking, an ambiguity set should be constructed according to the following principles [36]:

- containing the true probability distribution of random variables at least with high confidence levels if not possible,
- facilitating the computational handling such that a tractable reformulation of targeting DRO problem can be obtained and
- being as small as possible with the first condition satisfied to relieve the conservatism of the optimal solution.

With these in mind, various ambiguity set models have been studied, see, e.g., [14, 16, 17, 79], that can be roughly divided into the following categories according to the type of the information they used.

1) *Moments.* The second-order moments information, i.e., the mean and covariance matrix, are mostly used in ambiguity set. Mathematically, given $\boldsymbol{\xi} \in \mathbb{R}^n$ obeying probability distribution $\mathbb{P}_\xi$ with mean $\bar{\boldsymbol{\xi}}$ and covariance matrix $\boldsymbol{\Sigma}$, a mean-covariance based ambiguity set is defined as follows

$$\mathcal{P} = \left\{ \mathbb{P}_\xi \in \mathcal{L} \,\middle|\, \mathbb{E}[\boldsymbol{\xi}] = \bar{\boldsymbol{\xi}},\ \mathbb{V}[\boldsymbol{\xi}] = \boldsymbol{\Sigma} \in \mathbb{S}_+^n \right\} \tag{2.60}$$

where $\mathcal{L}$ is the set of all valid probability distributions in space $\mathbb{R}^n$. Consider $\bar{\boldsymbol{\xi}}$, $\boldsymbol{\Sigma}$ vary in the confidence regions being polytopes, the nested moment ambiguity sets have been studied in [36].

2) *Empirical PDF.* The availability of empirical distribution knowledge from historical data prompts us to constitute the ambiguity set with empirical PDF. In this fashion, the estimation errors are generally modeled by the limited statistical distances, e.g., ϕ-divergence, Kullback–Leibler (KL) divergence [49] and Wasserstein metric [13, 14, 39, 80], etc. As an example, when the statistical distance is defined with KL-divergence, an ambiguity set can be defined as

$$\mathcal{P} = \left\{ \mathbb{P}_\xi \in \mathcal{L} \,\middle|\, D_{KL}\left(p||\hat{p}\right) \leq \delta, p = \frac{d\mathbb{P}_\xi}{d\boldsymbol{\xi}} \right\} \tag{2.61}$$

where p and $\hat{p}$ are the true PDF of $\boldsymbol{\xi}$ and its empirical estimate, respectively, δ is given representing the tolerance upper bound of the distance between p and $\hat{p}$ and $D_{KL}\left(p||\hat{p}\right) = \int p(\boldsymbol{\xi}) \ln\left(\frac{p(\boldsymbol{\xi})}{\hat{p}(\boldsymbol{\xi})}\right) d\boldsymbol{\xi}$ is the KL-divergence of p and $\hat{p}$. When one order Wasserstein metric [16] is used as distance measure of two PDFs, the following ambiguity set is constituted

$$\mathcal{P} = \left\{ \mathbb{P}_\xi \in \mathcal{L} \,\middle|\, D_{\mathrm{w}}(\mathbb{P}_\xi, \hat{\mathbb{P}}_\xi) \leq \delta \right\} \tag{2.62}$$

where $\hat{\mathbb{P}}_\xi$ is the empirical estimate of $\mathbb{P}_\xi$, the Wasserstein metric

$$D_{\mathrm{w}}(\mathbb{P}_\xi, \hat{\mathbb{P}}_\xi) = \sup_{g \in \mathcal{G}} \left\{ \int_{\mathcal{D}} g(\boldsymbol{\xi}) \mathbb{P}_\xi(d\boldsymbol{\xi}) - \int_{\mathcal{D}} g(\boldsymbol{\xi}) \hat{\mathbb{P}}_\xi(d\boldsymbol{\xi}) \right\}$$

measures the distance between $\mathbb{P}_\xi$ and $\hat{\mathbb{P}}_\xi$ with $\mathcal{G}$ being the space of Lipschitz continuous functions satisfying $|g(\boldsymbol{\xi}_1) - g(\boldsymbol{\xi}_2)| \leq \mu(\boldsymbol{\xi}_1, \boldsymbol{\xi}_2)$, $\forall \boldsymbol{\xi}_1, \boldsymbol{\xi}_2 \in \mathcal{D}$, $\mu(\boldsymbol{\xi}_1, \boldsymbol{\xi}_2)$ is the metric between $\boldsymbol{\xi}_1$ and $\boldsymbol{\xi}_2$. In practice, these ambiguity sets are usually approximated with the scenario-wised formulation in data-driven framework [39, 80].

3) *Structural information.* The information referring to symmetry, unimodality, α-unimodality and independence, etc., are generally enrolled into an ambiguity set to capture the structural information of the marginal distribution of random variables [36]. This is commonly neglected in moments based ambiguity sets. As an example, a median-absolute deviation ambiguity set is presented as follows

$$\mathcal{P} = \left\{ \mathbb{P}_\xi \in \mathcal{L} \,\middle|\, \begin{array}{l} \mathbb{P}_\xi \text{ is symmetric with center } \mathbf{m} \\ \mathbb{E}_{\mathbb{P}_\xi}[|\boldsymbol{\xi} - \mathbf{m}|] \leq \mathbf{d} \end{array} \right\} \tag{2.63}$$

where $\mathbf{d}$ is the bound of median absolute deviation.

Remembering the rules of ambiguity set modeling, the mean-covariance based ambiguity sets (in some situations in combination with the structural information) are mostly utilized. The merits are mainly in twofold. Firstly, the empirical mean and covariance matrix can usually be estimated with high probability from data when the number of samples is large enough. Simultaneously, the computational load is much less expensive in comparison with the cost of estimating the empirical knowledge of PDF. Secondly, the tractability of DCCs and WC-CVaR conditions with respect to (2.60) has been widely studied in a rich body of literature, in most of which the underlying DCCs are addressed in a deterministic manner, see, e.g., [19, 42, 53, 81]. To that extent, the involved handling is, indeed, distribution independent, which facilitates the subsequent design and analysis.

2.5 Summary and notes

This chapter has reviewed the preliminaries of data-driven FD for stochastic linear dynamic processes and basic knowledge of stochastic optimization. Firstly, mathematical descriptions of stochastic linear dynamic systems have been presented. By recalling the definitions of coprime factorization and SKR, three subspace technique aided schemes have been given for the data-driven construction of a residual generator. Then the norm-based and statistical hypothesis test based residual evaluation strategies were introduced for residual evaluation purpose. Finally, basic concepts of stochastic optimization have been demonstrated, which serves an essential part of subsequent synthesis and analysis of optimal FD systems in data-driven framework, as will be investigated in Chapters 3–6.

3 A DIO approach to the design of FD systems

As demonstrated in Chapter 2, a data-driven dynamic FD system typically consists of the residual generation and residual evaluation units with a decision-maker embedded and these parts are generally designed separately. So far, a great number of literature on residual generation have been reported and few efforts have been made on the issues of residual evaluation despite its essential role in safeguarding satisfactory FD performance. Conventionally, the statistical hypothesis test methods are prone to be used for residual evaluation under assumption of knowing exact probability distribution for stochastic noises. In practical applications, this presumption is notoriously unrealistic. Hence, research on the data-driven FD for stochastic dynamic processes subject to distributional ambiguity remains an open topic.

Inspired by the merits of the DRO technique in dealing with the distribution ambiguity as introduced in Chapter 2, this chapter confines to a DIO approach to data-driven FD, allowing a performance-oriented integrated design of the residual generator, the residual evaluation function and the threshold. With the introduction of mean-covariance based ambiguity sets, the design of FD systems is formulated as a stochastic optimization problem with DCCs in the context of minimizing the MDR for a prescribed FAR. Without posing specific distribution assumptions on noises and faults, a DIO description of the targeting problem is achieved in terms of the means and covariance matrices of residuals in fault-free and faulty cases. An iterative parametric algorithm is then developed to solve the DIO problem. Furthermore, the worst-case FAR and MDR are exploited and a geometric interpretation is given to gain a deeper insight into the DIO solution.

3.1 Preliminaries and problem formulation

3.1.1 Configuration of data-driven dynamic FD systems

Consider a stochastic linear discrete-time system modeled by

$$\begin{cases} \mathbf{x}(k+1) = \mathbf{A}\mathbf{x}(k) + \mathbf{B}\mathbf{u}(k) + \mathbf{B}_f\mathbf{f}(k) + \boldsymbol{\omega}(k) \\ \mathbf{y}(k) = \mathbf{C}\mathbf{x}(k) + \mathbf{D}\mathbf{u}(k) + \mathbf{D}_f\mathbf{f}(k) + \boldsymbol{\upsilon}(k) \end{cases} \tag{3.1}$$

where $\mathbf{x} \in \mathbb{R}^n$, $\mathbf{u} \in \mathbb{R}^l$, $\mathbf{y} \in \mathbb{R}^m$, $\mathbf{f} \in \mathbb{R}^p$, $\boldsymbol{\omega} \in \mathbb{R}^n$, $\boldsymbol{\upsilon} \in \mathbb{R}^m$ are the state, input, output, fault, process and measurement noise vectors, respectively, $\mathbf{A}$, $\mathbf{B}$, $\mathbf{C}$, $\mathbf{D}$, $\mathbf{B}_f$, $\mathbf{D}_f$ are unknown

time-invariant system matrices with appropriate dimensions. It is assumed that the fault $\mathbf{f}(k)$ is a random vector with nonzero mean and the noises $\boldsymbol{\omega}(k)$, $\boldsymbol{\upsilon}(k)$ are zero-mean white sequences statistically independent of $\mathbf{u}(k)$, $\mathbf{x}(0)$ and $\mathbf{f}(k)$.

Given state-space description (3.1), an I/O data model, i.e., (2.14) with $s \geq n$, is obtained as follows

$$\begin{bmatrix} \mathbf{y}_s(k) \\ \mathbf{u}_s(k) \end{bmatrix} = \boldsymbol{\Psi}_s \begin{bmatrix} \mathbf{x}(k-s) \\ \mathbf{u}_s(k) \end{bmatrix} + \begin{bmatrix} \mathbf{H}_{f,s}\mathbf{f}_s(k) + \mathbf{H}_{\omega,s}\boldsymbol{\omega}_s(k) + \boldsymbol{\upsilon}_s(k) \\ 0 \end{bmatrix}. \tag{3.2}$$

Recall $\boldsymbol{\Psi}_s^{\perp} = \begin{bmatrix} \boldsymbol{\Psi}_{y,s}^{\perp} & -\boldsymbol{\Psi}_{u,s}^{\perp} \end{bmatrix} \in \mathbb{R}^{\gamma \times (s+1)(l+m)}$ satisfying $\boldsymbol{\Psi}_s^{\perp}\boldsymbol{\Psi}_s = 0$ with $\boldsymbol{\Psi}_{y,s}^{\perp} \in \mathbb{R}^{\gamma \times (s+1)m}$ and $\gamma = (s+1)m - n$. Let $\boldsymbol{\varphi}_s(k) = \mathbf{H}_{\omega,s}\boldsymbol{\omega}_s(k) + \boldsymbol{\upsilon}_s(k)$. A subspace technique aided residual generator is then constructed as follows

$$\mathbf{z}(k) = \boldsymbol{\Psi}_s^{\perp} \begin{bmatrix} \mathbf{y}_s(k) \\ \mathbf{u}_s(k) \end{bmatrix} \tag{3.3}$$

$$= \boldsymbol{\Psi}_{y,s}^{\perp} \left(\mathbf{H}_{f,s}\mathbf{f}_s(k) + \boldsymbol{\varphi}_s(k) \right) \tag{3.4}$$

$$r(k) = \mathbf{w}^T \mathbf{z}(k) \tag{3.5}$$

where $r \in \mathbb{R}$ is the residual signal, $\mathbf{w} \in \mathbb{R}^{\gamma}$ is a nonzero parameter vector in the parity space spanned by $\boldsymbol{\Psi}_{y,s}^{\perp}$. The dynamics of residual generator is governed by (3.4), and (3.3) is suggested for online realization. As demonstrated in Section 2.2.2, the matrices $\boldsymbol{\Psi}_s^{\perp}$ and $\boldsymbol{\Psi}_{y,s}^{\perp}$ can be identified with Algorithm 2.2.3 by using process I/O data.

Followed by residual generation, the residual evaluation function $J(r)$ and a threshold J_{th} should be determined appropriately such that the occurrence of a fault can be detected by using the following decision logic

$$\begin{cases} J(r) \leq J_{th}, & \Rightarrow \text{no fault alarm} \\ J(r) > J_{th}, & \Rightarrow \text{fault alarm.} \end{cases} \tag{3.6}$$

The configuration diagram of data-driven FD systems is demonstrated in Fig. 3.1.

Recalling the definitions of FAR and MDR in Section 2.3.3, we then formulate the design of FD system regarding $\mathbf{w}$, $J(r)$ and J_{th} in the context of minimizing the MDR for a given acceptable FAR as following SP problem

$$\min_{\mathbf{w} \neq 0,\, J(r),\, J_{th}} \quad \beta \tag{3.7}$$

$$\text{s.t.} \quad \begin{cases} \Pr\{J(r) > J_{th} | \mathbf{f} = 0\} \leq \alpha_0 \\ \Pr\{J(r) \leq J_{th} | \mathbf{f} \neq 0\} \leq \beta \end{cases} \tag{3.8}$$

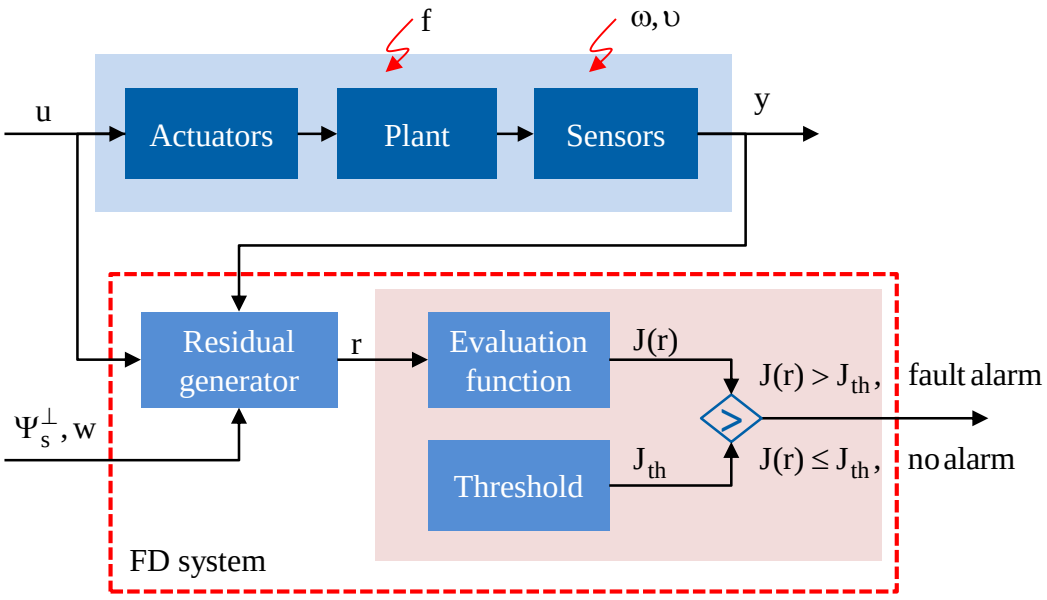

Figure 3.1: Schematic diagram of data-driven FD systems.

where $\alpha_0 \in (0,1)$ is a given upper bound of FAR, $\beta \in (0,1)$ is the upper bound of MDR, respectively. It is remarkable that the chance constraints in (3.8) restrict the FAR and MDR being not larger than α_0 and β, respectively.

In case of knowing exact probability distribution of noises, statistical hypothesis test methods presented in Section 2.3.2 are usually applied for residual evaluation by setting the residual evaluation function $J(r)$ as a test statistic of residual r and then determining the threshold J_{th} with FAR not larger than α_0. According to Neyman–Pearson lemma, a minimal MDR can be delivered in this context [23]. Thus, when the distributional profile of noises is known exactly, the FD problem (3.7)–(3.8) can be directly solved with statistical hypothesis test methods. In engineering applications, precise distribution knowledge of noises and faults is often, unfortunately, inaccessible and the statistical hypothesis test based threshold setting is sensitive to the distribution drifts of noises, which may result in poor FAR and MDR for online FD.

3.1.2 Problem formulation

To address FD system design issues under mild conditions, we can reasonably assume that the true probability distribution of $\mathbf{z}(k)$, i.e., $\mathbb{P}_z$, belongs to a predefined ambiguity set both in fault-free and faulty cases. That is, given distribution ambiguity sets $\mathcal{P}_0$ for

fault-free scenario and $\mathcal{P}_f$ for the faulty scenario, it holds

$$\begin{cases} \mathbb{P}_z \in \mathcal{P}_0, & \text{for} \quad \mathbf{f} = 0 \\ \mathbb{P}_z \in \mathcal{P}_f, & \text{for} \quad \mathbf{f} \neq 0. \end{cases} \tag{3.9}$$

Regarding ambiguity sets $\mathcal{P}_0$ and $\mathcal{P}_f$, the following distributionally robust FD problem is formulated towards minimizing the MDR for a given acceptable FAR, i.e.,

$$\min_{\mathbf{w}\neq 0,\, J(r),\, J_{th}} \quad \beta \tag{3.10}$$

$$\text{s.t.} \quad \begin{cases} \sup\limits_{\mathbb{P}_z \in \mathcal{P}_0} \Pr\{J(r) > J_{th}\} \leq \alpha_0 \\ \sup\limits_{\mathbb{P}_z \in \mathcal{P}_f} \Pr\{J(r) \leq J_{th}\} \leq \beta \end{cases} \tag{3.11}$$

which is an SP problem with DCCs. Without precise knowledge or specific assumption on the distributions for noises and faults, the first DCC in (3.11) guarantees the FAR not larger than α_0 over $\mathcal{P}_0$ and the second DCC suggests the MDR not larger than β over $\mathcal{P}_f$.

Without loss of generality, we define the residual evaluation function and threshold as

$$J(r) = |r(k)|, \; J_{th} = b \tag{3.12}$$

where $b > 0$. By substituting (3.5) into (3.12), the problem (3.10)–(3.11) is further re-written as follows

$$\min_{\mathbf{w}\neq 0,\, b>0} \quad \beta \tag{3.13}$$

$$\text{s.t.} \quad \begin{cases} \sup\limits_{\mathbb{P}_z \in \mathcal{P}_0} \Pr\left\{|\mathbf{w}^T\mathbf{z}| > b\right\} \leq \alpha_0 \\ \sup\limits_{\mathbb{P}_z \in \mathcal{P}_f} \Pr\left\{|\mathbf{w}^T\mathbf{z}| \leq b\right\} \leq \beta. \end{cases} \tag{3.14}$$

It is remarkable that the design of FD systems for stochastic dynamic process (3.1) has been formulated as the problem (3.13)–(3.14). The advantages of this formulation in contrast with the problem (3.7)–(3.8) are in the following aspects.

- It provides a performance-oriented integrated design of FD systems by incorporating the criteria of FAR and MDR with the residual generator, residual evaluation function and threshold setting.
- The demand for exact distribution knowledge of noises and faults, as required in statistical hypothesis test methods, is alleviated by introducing the ambiguity sets $\mathcal{P}_0$ and $\mathcal{P}_f$ to specify families of distributions of $\mathbf{z}(k)$ in fault-free and faulty cases, respectively.

- In this sense, the upper bounds of FAR and MDR derived by solving (3.13)–(3.14) are achievable under any probability distributions for noises $\boldsymbol{\omega}(k)$, $\boldsymbol{\upsilon}(k)$ and fault $\mathbf{f}(k)$ supporting $\mathbb{P}_z \in \mathcal{P}_0$ in fault-free case and $\mathbb{P}_z \in \mathcal{P}_f$ in faulty case. It implies the robustness of the solution to (3.13)–(3.14) against the distributional ambiguity.

Hence, the problems to be addressed in this chapter are formulated as follows:

- With respect to appropriately modeled ambiguity sets $\mathcal{P}_0$, $\mathcal{P}_f$, solve the problem (3.13)–(3.14) for parameter vector $\mathbf{w}$ and threshold b without posing distribution assumptions on noises and faults and

- Develop a data-driven realization of the designed FD system including offline design and online implementation.

3.2 Distribution independent optimal FD

In this section, a DIO scheme is proposed to address the FD problem (3.13)–(3.14) without presumption on the distributions for noises and faults. To this end, the mean-covariance based ambiguity sets are first established, based on which a distribution independent description of the FD problem (3.13)–(3.14) is formulated in the probabilistic context. Then an iterative parametric algorithm is developed, followed by a data-driven implementation of the FD system.

3.2.1 Mean-covariance based ambiguity sets

Note that the core of addressing the problem (3.13)–(3.14) lies in handling the DCCs (3.14), which highly relies on the models of ambiguity sets $\mathcal{P}_0$ and $\mathcal{P}_f$.

As introduced in Section 2.4.4, various forms of ambiguity set are available, among which the mean-covariance based model is mostly used in engineering applications for the common availability of second-order moments information using historical data and its computational tractability under certain conditions [36, 79, 93]. For these merits, in what follows we model the ambiguity sets $\mathcal{P}_0$ and $\mathcal{P}_f$ in terms of the mean and covariance matrix of $\mathbf{z}(k)$. Denote by

$$\begin{aligned}\mathbf{z}_0(k) &= \mathbf{z}(k)|_{\mathbf{f}(k)=0}, \quad \bar{\mathbf{z}}_0 = \mathbb{E}[\mathbf{z}_0], \quad \boldsymbol{\Sigma}_{z_0} = \mathbb{V}[\mathbf{z}_0]\\ \mathbf{z}_f(k) &= \mathbf{z}(k)|_{\mathbf{f}(k)\neq 0}, \quad \bar{\mathbf{z}}_f = \mathbb{E}[\mathbf{z}_f], \quad \boldsymbol{\Sigma}_{z_f} = \mathbb{V}[\mathbf{z}_f].\end{aligned}$$

Let $\bar{\boldsymbol{\omega}}_s = \mathbb{E}[\boldsymbol{\omega}_s]$, $\bar{\boldsymbol{\upsilon}}_s = \mathbb{E}[\boldsymbol{\upsilon}_s]$, $\boldsymbol{\Sigma}_\omega = \mathbb{V}[\boldsymbol{\omega}_s]$, $\boldsymbol{\Sigma}_\upsilon = \mathbb{V}[\boldsymbol{\upsilon}_s]$, $\bar{\mathbf{f}}_s = \mathbb{E}[\mathbf{f}_s] \neq 0$, $\boldsymbol{\Sigma}_f = \mathbb{V}[\mathbf{f}_s]$. It is

derived from (3.4) that

$$\bar{\mathbf{z}}_0 = \boldsymbol{\Psi}_{y,s}^{\perp}\bar{\boldsymbol{\varphi}}_s,\ \boldsymbol{\Sigma}_{z_0} = \boldsymbol{\Psi}_{y,s}^{\perp}\boldsymbol{\Sigma}_{\varphi}(\boldsymbol{\Psi}_{y,s}^{\perp})^T \tag{3.15}$$

$$\bar{\mathbf{z}}_f = \bar{\mathbf{z}}_0 + \bar{\mathbf{H}}_{f,s}\bar{\mathbf{f}}_s,\ \boldsymbol{\Sigma}_{z_f} = \boldsymbol{\Sigma}_{z_0} + \bar{\mathbf{H}}_{f,s}\boldsymbol{\Sigma}_f\bar{\mathbf{H}}_{f,s}^T \tag{3.16}$$

where $\bar{\boldsymbol{\varphi}}_s = \mathbf{H}_{\omega,s}\bar{\boldsymbol{\omega}}_s + \bar{\boldsymbol{\upsilon}}_s$, $\boldsymbol{\Sigma}_{\varphi} = \mathbb{V}[\boldsymbol{\varphi}_s] = \mathbf{H}_{\omega,s}\boldsymbol{\Sigma}_{\omega}\mathbf{H}_{\omega,s}^T + \boldsymbol{\Sigma}_{\upsilon}$, $\bar{\mathbf{H}}_{f,s} = \boldsymbol{\Psi}_{y,s}^{\perp}\mathbf{H}_{f,s}$. We then construct the ambiguity set $\mathcal{P}_0$ as follows

$$\mathcal{P}_0 = \left\{ \mathbb{P}_z \in \mathcal{L} \,\middle|\, \mathbb{E}[\mathbf{z}] = \bar{\mathbf{z}}_0,\ \ \mathbb{V}[\mathbf{z}] = \boldsymbol{\Sigma}_{z_0} \in \mathbb{S}_+^{\gamma} \right\} \tag{3.17}$$

where $\mathcal{L}$ is the set of all valid probability distributions in space $\mathbb{R}^{\gamma}$. Similarly, the ambiguity set $\mathcal{P}_f$ is modeled as

$$\mathcal{P}_f = \left\{ \mathbb{P}_z \in \mathcal{L} \,\middle|\, \mathbb{E}[\mathbf{z}] = \bar{\mathbf{z}}_f,\ \ \mathbb{V}[\mathbf{z}] = \boldsymbol{\Sigma}_{z_f} \in \mathbb{S}_+^{\gamma} \right\}. \tag{3.18}$$

Remark 3.1. *In general, real values of $\bar{\mathbf{z}}_0$, $\boldsymbol{\Sigma}_{z_0}$, $\bar{\mathbf{z}}_f$, $\boldsymbol{\Sigma}_{z_f}$ are unavailable in practical applications and their empirical estimates are usually obtained using process I/O data. When the sample number is sufficiently large, the empirical estimates are considered to be close to the true values with high probability and thus temporarily assumed to be known exactly. The estimation error involved issues will be discussed in Chapter 6.*

3.2.2 Problem reformulation

Since the residual evaluation function $J(r)$ in (3.12) is a two-sided test statistic of residual and the condition $|\mathbf{w}^T\mathbf{z}| > b$ is nonconvex, it is difficult to deal with the DCCs (3.14) directly. One alternative solution is to reformulate the problem (3.13)–(3.14) in terms of two one-sided test statistics of residual. It yields from (3.4) and (3.12) that

$$J(r) = |\mathbf{w}^T\mathbf{z}(k)| = \begin{cases} \mathbf{w}^T\mathbf{z}(k), & \text{for} \quad \mathbf{w}^T\mathbf{z}(k) > 0 \\ -\mathbf{w}^T\mathbf{z}(k), & \text{for} \quad \mathbf{w}^T\mathbf{z}(k) \le 0. \end{cases} \tag{3.19}$$

According to Bonferroni's inequality, we have, for the first DCC in (3.14), it holds

$$\begin{aligned} \sup_{\mathbb{P}_z\in\mathcal{P}_0} \Pr\left\{|\mathbf{w}^T\mathbf{z}| > b\right\} &= \sup_{\mathbb{P}_z\in\mathcal{P}_0} \Pr\left\{\mathbf{w}^T\mathbf{z} > b \ \text{ or } \ -\mathbf{w}^T\mathbf{z} > b\right\} \\ &\le \sup_{\mathbb{P}_z\in\mathcal{P}_0} \Pr\left\{\mathbf{w}^T\mathbf{z} > b | \mathbf{w}^T\mathbf{z} > 0\right\} + \sup_{\mathbb{P}_z\in\mathcal{P}_0} \Pr\left\{-\mathbf{w}^T\mathbf{z} > b | \mathbf{w}^T\mathbf{z} \le 0\right\} \\ &\le \alpha_0 \end{aligned}$$

if the following inequalities hold true

$$\sup_{\mathbb{P}_z\in\mathcal{P}_0} \Pr\left\{\mathbf{w}^T\mathbf{z} > b | \mathbf{w}^T\mathbf{z} > 0\right\} \le \frac{\alpha_0}{2},\ \ \sup_{\mathbb{P}_z\in\mathcal{P}_0} \Pr\left\{-\mathbf{w}^T\mathbf{z} > b | \mathbf{w}^T\mathbf{z} \le 0\right\} \le \frac{\alpha_0}{2}.$$

In this context, the FD problem (3.13)–(3.14) can be addressed by solving the following two optimization problems, wherein one-sided evaluation functions are adopted.

1) When $\mathbf{w}^T\mathbf{z}(k) > 0$, i.e., $J(r) = \mathbf{w}^T\mathbf{z}(k)$. Regarding decision logic (3.6), a one-sided FD problem is constructed as

$$\min_{\mathbf{w}\neq 0,\, b>0} \quad \beta \tag{3.20}$$

$$\text{s.t.} \quad \begin{cases} \sup\limits_{\mathbb{P}_z\in\mathcal{P}_0} \Pr\left\{\mathbf{w}^T\mathbf{z}(k) > b\right\} \leq \frac{\alpha_0}{2} \\ \sup\limits_{\mathbb{P}_z\in\mathcal{P}_f} \Pr\left\{\mathbf{w}^T\mathbf{z}(k) \leq b\right\} \leq \beta. \end{cases} \tag{3.21}$$

2) When $\mathbf{w}^T\mathbf{z}(k) < 0$, i.e., $J(r) = -\mathbf{w}^T\mathbf{z}(k)$. Regarding decision logic (3.6), a one-sided FD problem is constructed as

$$\min_{\mathbf{w}\neq 0,\, b>0} \quad \beta \tag{3.22}$$

$$\text{s.t.} \quad \begin{cases} \sup\limits_{\mathbb{P}_z\in\mathcal{P}_0} \Pr\left\{-\mathbf{w}^T\mathbf{z}(k) > b\right\} \leq \frac{\alpha_0}{2} \\ \sup\limits_{\mathbb{P}_z\in\mathcal{P}_f} \Pr\left\{-\mathbf{w}^T\mathbf{z}(k) \leq b\right\} \leq \beta. \end{cases} \tag{3.23}$$

It is obvious that the optimal solution to FD problem (3.20)–(3.21) solves the problem (3.22)–(3.23) by substituting the parameter vector $\mathbf{w}$ with $-\mathbf{w}$. Besides, by solving (3.20)–(3.21) for $\mathbf{w}$, b, β, the FAR of the FD system can be ensured not larger than α_0 and MDR not greater than β with respect to using (3.12) for residual evaluation. Thus, below we will focus on solving the FD problem (3.20)–(3.21), the core of which lies in the handling of DCCs (3.21) in a deterministic manner.

3.2.3 Distribution independent FD

In order to deal with the DCCs in (3.21) in the probabilistic context, the following theorem is first referred.

Theorem 3.1. *[53] Given a random vector $\boldsymbol{\xi} \in \mathbb{R}^n$ with mean $\bar{\boldsymbol{\xi}}$ and covariance matrix $\boldsymbol{\Sigma} \in \mathbb{S}_+^\gamma$, i.e., $\boldsymbol{\xi} \sim (\bar{\boldsymbol{\xi}}, \boldsymbol{\Sigma})$, for a convex set S, it holds*

$$\sup_{\boldsymbol{\xi}\sim(\bar{\boldsymbol{\xi}},\boldsymbol{\Sigma})} \Pr\{\boldsymbol{\xi} \in S\} = \frac{1}{1+d^2}$$

with $d^2 = \inf\limits_{\boldsymbol{\xi}\in S} (\boldsymbol{\xi} - \bar{\boldsymbol{\xi}})^T \boldsymbol{\Sigma}^{-1} (\boldsymbol{\xi} - \bar{\boldsymbol{\xi}})$.

Based on Theorem 3.1, the following lemma for our study can be achieved.

Lemma 3.1. *[53] Given a random vector* $\boldsymbol{\xi} \in \mathbb{R}^n$ *with* $\boldsymbol{\xi} \sim (\bar{\boldsymbol{\xi}}, \boldsymbol{\Sigma})$, $\mathbf{w} \neq 0$ *and* b, *such that* $\mathbf{w}^T\bar{\boldsymbol{\xi}} \leq b$ *and* $\rho \in [0, 1)$, *the condition*

$$\inf_{\boldsymbol{\xi}\sim(\bar{\boldsymbol{\xi}},\boldsymbol{\Sigma})} \Pr\{\mathbf{w}^T\boldsymbol{\xi} \leq b\} \geq 1 - \rho$$

holds if and only if

$$b - \mathbf{w}^T\bar{\boldsymbol{\xi}} \geq \kappa(\rho)\sqrt{\mathbf{w}^T\boldsymbol{\Sigma}\mathbf{w}}$$

with $\kappa(\rho) = \sqrt{\frac{1-\rho}{\rho}}$, *when* $\mathbf{w}^T\bar{\boldsymbol{\xi}} > b$, $\inf_{\boldsymbol{\xi}\sim(\bar{\boldsymbol{\xi}},\boldsymbol{\Sigma})} \Pr\{\mathbf{w}^T\boldsymbol{\xi} \leq b\} = 0$.

Note that Lemma 3.1 provides a deterministic formulation of a DCC in terms of mean and covariance matrix. On this basis, given ambiguity set $\mathcal{P}_0$ in (3.17), it holds for the first DCC in (3.21) with $\mathbf{w}^T\bar{\mathbf{z}}_0 < b$ that

$$\begin{aligned} \sup_{\mathbb{P}_z\in\mathcal{P}_0} \Pr\left\{\mathbf{w}^T\mathbf{z}(k) > b\right\} \leq \frac{\alpha_0}{2} \quad &\Leftrightarrow \quad \inf_{\mathbb{P}_z\in\mathcal{P}_0} \Pr\left\{\mathbf{w}^T\mathbf{z}(k) \leq b\right\} \geq 1 - \frac{\alpha_0}{2} \\ &\Leftrightarrow \quad b - \mathbf{w}^T\bar{\mathbf{z}}_0 \geq \bar{\kappa}(\alpha_0)\sqrt{\mathbf{w}^T\boldsymbol{\Sigma}_{z_0}\mathbf{w}} \end{aligned} \tag{3.24}$$

where $\bar{\kappa}(\alpha_0) = \kappa(\frac{\alpha_0}{2}) = \sqrt{\frac{2-\alpha_0}{\alpha_0}}$. Similarly, given $\mathcal{P}_f$ in (3.18), the second DCC in (3.21) with $\mathbf{w}^T\bar{\mathbf{z}}_f > b$ is reformulated as follows

$$\begin{aligned} \sup_{\mathbb{P}_z\in\mathcal{P}_f} \Pr\left\{\mathbf{w}^T\mathbf{z}(k) \leq b\right\} \leq \beta \quad &\Leftrightarrow \quad \inf_{\mathbb{P}_z\in\mathcal{P}_f} \Pr\left\{\mathbf{w}^T\mathbf{z}(k) > b\right\} \geq 1 - \beta \\ &\Leftrightarrow \quad \inf_{\mathbb{P}_z\in\mathcal{P}_f} \Pr\left\{-\mathbf{w}^T\mathbf{z}(k) < -b\right\} \geq 1 - \beta \\ &\Leftrightarrow \quad -b + \mathbf{w}^T\bar{\mathbf{z}}_f \geq \kappa(\beta)\sqrt{\mathbf{w}^T\boldsymbol{\Sigma}_{z_f}\mathbf{w}} \end{aligned} \tag{3.25}$$

where $\kappa(\beta) = \sqrt{\frac{1-\beta}{\beta}}$. In the cases of $\mathbf{w}$ designed such that $\mathbf{w}^T\bar{\mathbf{z}}_0 \geq b$ and $\mathbf{w}^T\bar{\mathbf{z}}_f \leq b$, it is obvious that the MDR and FAR would be one, which is meaningless for our FD purpose and thus are discarded. Together with (3.24) and (3.25), the FD problem (3.20)–(3.21) is equally re-written as the following distribution independent form

$$\max_{\mathbf{w}\neq 0,\, b>0} \quad \beta \tag{3.26}$$

$$\text{s.t.} \quad \begin{cases} b - \mathbf{w}^T\bar{\mathbf{z}}_0 \geq \bar{\kappa}(\alpha_0)\sqrt{\mathbf{w}^T\boldsymbol{\Sigma}_{z_0}\mathbf{w}} \\ -b + \mathbf{w}^T\bar{\mathbf{z}}_f \geq \kappa(\beta)\sqrt{\mathbf{w}^T\boldsymbol{\Sigma}_{z_f}\mathbf{w}}. \end{cases} \tag{3.27}$$

This formulation is a second-order cone programming (SOCP) problem that is obviously independent of the probability distributions of noises and faults. In the next subsection, the optimal solution of the FD problem (3.26)–(3.27) is studied.

3.2.4 Optimal solution and algorithms

It is derived from (3.27) that

$$\bar{\kappa}(\alpha_0)\sqrt{\mathbf{w}^T\mathbf{\Sigma}_{z_0}\mathbf{w}} - \mathbf{w}_1^T\bar{\mathbf{z}}_0 \leq b \leq \mathbf{w}^T\bar{\mathbf{z}}_f - \kappa(\beta)\sqrt{\mathbf{w}^T\mathbf{\Sigma}_{z_f}\mathbf{w}}. \tag{3.28}$$

It follows

$$\kappa(\beta)\sqrt{\mathbf{w}^T\mathbf{\Sigma}_{z_f}\mathbf{w}} + \bar{\kappa}(\alpha_0)\sqrt{\mathbf{w}^T\mathbf{\Sigma}_{z_0}\mathbf{w}} \leq \mathbf{w}^T(\bar{\mathbf{z}}_f - \bar{\mathbf{z}}_0). \tag{3.29}$$

Note that the value of $\|\mathbf{w}\|$ would not influence the optimal solution of β regarding (3.29). We can without loss of generality set

$$\mathbf{w}^T(\bar{\mathbf{z}}_f - \bar{\mathbf{z}}_0) = 1 \tag{3.30}$$

and then

$$\kappa(\beta)\sqrt{\mathbf{w}^T\mathbf{\Sigma}_{z_f}\mathbf{w}} + \bar{\kappa}(\alpha_0)\sqrt{\mathbf{w}^T\mathbf{\Sigma}_{z_0}\mathbf{w}} \leq 1 \tag{3.31}$$

holds, which delivers

$$\kappa(\beta) \leq \frac{1 - \bar{\kappa}(\alpha_0)\sqrt{\mathbf{w}^T\mathbf{\Sigma}_{z_0}\mathbf{w}}}{\sqrt{\mathbf{w}^T\mathbf{\Sigma}_{z_f}\mathbf{w}}}. \tag{3.32}$$

Since β has the opposite monotonicity with $\kappa(\beta)$, we then have

$$\min_{\mathbf{w}\neq 0} \ \beta \ \Leftrightarrow \ \max_{\mathbf{w}\neq 0} \ \kappa(\beta) \ \Leftrightarrow \ \max_{\mathbf{w}\neq 0} \ \frac{1 - \bar{\kappa}(\alpha_0)\sqrt{\mathbf{w}^T\mathbf{\Sigma}_{z_0}\mathbf{w}}}{\sqrt{\mathbf{w}^T\mathbf{\Sigma}_{z_f}\mathbf{w}}}. \tag{3.33}$$

Together with (3.30) and (3.33), we can rewrite the problem (3.26)–(3.27) as follows

$$\max_{\mathbf{w}} \ \frac{1 - \bar{\kappa}(\alpha_0)\sqrt{\mathbf{w}^T\mathbf{\Sigma}_{z_0}\mathbf{w}}}{\sqrt{\mathbf{w}^T\mathbf{\Sigma}_{z_f}\mathbf{w}}} \quad \text{s.t.} \quad \mathbf{w}^T(\bar{\mathbf{z}}_f - \bar{\mathbf{z}}_0) = 1 \tag{3.34}$$

which is a fractional programming (FP) problem according to [68]. After solving the problem (3.34) for an optimal $\mathbf{w}$, the equalities in (3.28) hold at this optimum. And then we have

$$\kappa(\beta) = \frac{1 - \bar{\kappa}(\alpha_0)\sqrt{\mathbf{w}^T\mathbf{\Sigma}_{z_0}\mathbf{w}}}{\sqrt{\mathbf{w}^T\mathbf{\Sigma}_{z_f}\mathbf{w}}} \tag{3.35}$$

$$\beta = \frac{1}{1 + \kappa^2(\beta)} \tag{3.36}$$

$$\begin{aligned} b &= \bar{\kappa}(\alpha_0)\sqrt{\mathbf{w}^T\mathbf{\Sigma}_{z_f}\mathbf{w}} - \mathbf{w}^T\bar{\mathbf{z}}_0 \\ &= \mathbf{w}^T\bar{\mathbf{z}}_f - \kappa(\beta)\sqrt{\mathbf{w}^T\mathbf{\Sigma}_{z_f}\mathbf{w}}. \end{aligned} \tag{3.37}$$

Therefore, the key point of solving the problem (3.26)–(3.27) lies in solving the FP problem (3.34). Up to now, various parametric algorithms and software have been

developed to deal with this kind of FP problems, e.g., the iterative least square [53] and quadratic search methods [42]. Here an iterative least square scheme is applied to this end. Let

$$\ell(\mathbf{w}) = 1 - \bar{\kappa}(\alpha_0)\sqrt{\mathbf{w}^T\boldsymbol{\Sigma}_{z_0}\mathbf{w}}, \quad g(\mathbf{w}) = \sqrt{\mathbf{w}^T\boldsymbol{\Sigma}_{z_f}\mathbf{w}}. \tag{3.38}$$

The problem (3.34) is re-written as follows

$$\max_{\mathbf{w}} \ \frac{\ell(\mathbf{w})}{g(\mathbf{w})} \quad \text{s.t.} \quad \mathbf{w}^T(\bar{\mathbf{z}}_f - \bar{\mathbf{z}}_0) = 1. \tag{3.39}$$

By introducing a parameter $\lambda \geq 0$, the problem (3.39) can then be addressed by iteratively solving the following SOCP problem for a fixed λ

$$\max_{\mathbf{w}} \ \ell(\mathbf{w}) - \lambda g(\mathbf{w}) \quad \text{s.t.} \quad \mathbf{w}^T(\bar{\mathbf{z}}_f - \bar{\mathbf{z}}_0) = 1. \tag{3.40}$$

With respect to updating λ with

$$\lambda = \frac{\ell(\mathbf{w}_*)}{g(\mathbf{w}_*)}, \ \mathbf{w}_* = \arg\max_{\mathbf{w}} \ \ell(\mathbf{w}) - \lambda g(\mathbf{w}) \tag{3.41}$$

an optimal $\mathbf{w}$ to (3.34) is then achieved until a predefined criterion is achieved.

Regarding solving the SOCP problem (3.40), denote by $\mathbf{F} \in \mathbb{R}^{\gamma\times(\gamma-1)}$ an orthogonal matrix whose columns span the subspace orthogonal to $\bar{\mathbf{z}}_f - \bar{\mathbf{z}}_0$, $\mathbf{q} \in \mathbb{R}^{\gamma-1}$. Let

$$\mathbf{w} = \bar{\mathbf{w}}_0 + \mathbf{F}\mathbf{q}, \ \bar{\mathbf{w}}_0 = \frac{\bar{\mathbf{z}}_f - \bar{\mathbf{z}}_0}{\|\bar{\mathbf{z}}_f - \bar{\mathbf{z}}_0\|_2^2}. \tag{3.42}$$

The condition $\mathbf{w}^T(\bar{\mathbf{z}}_f - \bar{\mathbf{z}}_0) = 1$ holds obviously. Then the problem (3.40) is re-written as an unconstrained SOCP problem in the following form

$$\max_{\mathbf{q}} \ \left\{1 - \bar{\kappa}^2(\alpha_0)\left\|\boldsymbol{\Sigma}_{z_0}^{1/2}(\bar{\mathbf{w}}_0 + \mathbf{F}\mathbf{q})\right\|_2^2 - \lambda^2\left\|\boldsymbol{\Sigma}_{z_f}^{1/2}(\bar{\mathbf{w}}_0 + \mathbf{F}\mathbf{q})\right\|_2^2\right\}$$

which equals to

$$\min_{\mathbf{q}} \ \left\{\bar{\kappa}^2(\alpha_0)\left\|\boldsymbol{\Sigma}_{z_0}^{1/2}(\bar{\mathbf{w}}_0 + \mathbf{F}\mathbf{q})\right\|_2^2 + \lambda^2\left\|\boldsymbol{\Sigma}_{z_f}^{1/2}(\bar{\mathbf{w}}_0 + \mathbf{F}\mathbf{q})\right\|_2^2\right\}. \tag{3.43}$$

To handle the problem (3.43), the following lemma is recalled.

Lemma 3.2. *[37] For any vectors* $\mathbf{a}$, $\mathbf{c}$ *and any matrix* $\mathbf{M}$ *and for all* $\epsilon > 0$, *we have*

$$(\mathbf{a}+\mathbf{c})^T\mathbf{M}(\mathbf{a}+\mathbf{c}) \leq \left(1 + \frac{1}{\epsilon}\right)\mathbf{a}^T\mathbf{M}\mathbf{a} + (1+\epsilon)\mathbf{c}^T\mathbf{M}\mathbf{c}.$$

A proposition of Lemma 3.2 can then be obtained as follows.

Algorithm 3.2.4 Iterative least square method for solving (3.40)

1: Given $\lambda > 0$, sufficient small $\epsilon > 0$, $\tau_0 > 0$, $\Delta > 0$, compute $\bar{\mathbf{w}}_0$, $\mathbf{F}$. Let

$$\mathbf{G} = \lambda^2 \mathbf{F}^T \Sigma_{z_0} \mathbf{F}, \quad \mathbf{H} = \bar{\kappa}^2(\alpha_0) \mathbf{F}^T \Sigma_{z_f} \mathbf{F}$$
$$\mathbf{g} = \lambda^2 \mathbf{F}^T \Sigma_{z_0} \bar{\mathbf{w}}_0, \quad \mathbf{h} = \bar{\kappa}^2(\alpha_0) \mathbf{F}^T \Sigma_{z_f} \bar{\mathbf{w}}_0.$$

2: Initialize $\xi_1 = 1$, $\zeta_1 = 1$, $\delta_1 = 1$, $i = 1$.

3: Do the following computation until $|\delta_{i+1} - \delta_i| \leq \epsilon$, i.e.,

$$\mathbf{K} = \tfrac{1}{\zeta_i}\mathbf{G} + \tfrac{1}{\xi_i}\mathbf{H} + \Delta \mathbf{I}, \quad \mathbf{Q} = -\left(\tfrac{1}{\zeta_i}\mathbf{g} + \tfrac{1}{\xi_i}\mathbf{h}\right), \quad \mathbf{q}_i = \mathbf{K}^{-1}\mathbf{Q}$$
$$\mathbf{w}^i = \bar{\mathbf{w}}_0 + \mathbf{F}\mathbf{q}_i, \quad \zeta_{i+1} = \sqrt{\lambda (\mathbf{w}^i)^T \Sigma_{z_0} \mathbf{w}^i}, \quad \xi_{i+1} = \sqrt{\bar{\kappa}(\alpha_0) (\mathbf{w}^i)^T \Sigma_{z_f} \mathbf{w}^i}$$
$$\delta_{i+1} = \tfrac{\zeta_{i+1} + \xi_{i+1}}{2}, \quad i \leftarrow i + 1.$$

4: Assign $\mathbf{w}_* = \mathbf{w}^{i-1}$.

Proposition 3.1. *For any vector* $\mathbf{a}$*, matrix* $\mathbf{M}$ *and* $\epsilon > 0$*, it holds*

$$\mathbf{a}^* = \arg\min_{\mathbf{a}} \ \mathbf{a}^T \mathbf{M} \mathbf{a} = \arg \inf_{\mathbf{a}, \epsilon > 0} \left(\epsilon + \frac{1}{\epsilon}\right) \mathbf{a}^T \mathbf{M} \mathbf{a}.$$

Based on Lemma 3.2 and Proposition 3.1, we introduce parameters $\eta > 0,\ \mu > 0$ and rewrite the problem (3.43) as follows

$$\inf_{\mathbf{q},\, \eta>0,\, \mu>0} \left\{ \eta + \frac{\bar{\kappa}^2(\alpha_0)}{\eta} \left\| \mathbf{\Sigma}_{z_0}^{1/2} (\bar{\mathbf{w}}_0 + \mathbf{F}\mathbf{q}) \right\|_2^2 + \mu + \frac{\lambda^2}{\mu} \left\| \mathbf{\Sigma}_{z_f}^{1/2} (\bar{\mathbf{w}}_0 + \mathbf{F}\mathbf{q}) \right\|_2^2 \right\} \tag{3.44}$$

which can be solved with an iterative least square algorithm, as presented in **Algorithm** 3.2.4, in which the iteration is stopped when the error between two steps is smaller than a predefined sufficient small tolerance.

By solving the optimal $\mathbf{w}$ with Algorithm 3.2.4, the optimal solutions of $\beta,\ b$ are further achieved with (3.36) and (3.37), respectively. As a summary, the algorithm for solving the FD problem (3.26)–(3.27) is given in **Algorithm** 3.2.5.

As mentioned before, the optimal solutions of $\mathbf{w}$, b, β obtained by solving the problem (3.26)–(3.27) also address the problem (3.22)–(3.23) by replacing $\mathbf{w}$ with $-\mathbf{w}$. Since the DCCs (3.14) hold if the DCCs (3.21) and (3.23) hold, the solutions $\mathbf{w}$, b, β to (3.26)–(3.27) thus solve the original FD problem (3.13)–(3.14). We thus give the following theorem.

Theorem 3.2. *The optimal solution to the DIO problem (3.26)–(3.27) is given in (3.35)–(3.37), which solve the FD problem (3.13)–(3.14).*

Algorithm 3.2.5 Optimal solution to the DIO problem (3.26)–(3.27)

1: Given a small $\tau_1 > 0$, set $j = 1$, $\lambda = \lambda_1$.

2: Solve the problem (3.40) with Algorithm 3.2.4 for $\mathbf{w}_*$, Let $\mathbf{w}^j = \mathbf{w}_*$.

3: Repeat the following process until $\lambda_j > \lambda_{j+1}$ and $\lambda_j > \lambda_{j-1}$ hold simultaneously

$$\lambda_{j+1} = \frac{1 - \bar{\kappa}(\alpha_0)\sqrt{(\mathbf{w}^j)^T \mathbf{\Sigma}_{z_0} \mathbf{w}^j}}{\sqrt{(\mathbf{w}^j)^T \mathbf{\Sigma}_{z_f} \mathbf{w}^j}}, \; j \leftarrow j + 1.$$

4: Let $\mathbf{w} = \mathbf{w}^j$, $\kappa(\beta) = \lambda_j$. Compute β, b by (3.36) and (3.37), respectively.

5: Return $\mathbf{w}$, β, b.

3.2.5 Data-driven implementation

The above presented solution to the FD problem (3.13)–(3.14) provides an integrated design of FD systems regarding residual generator, residual evaluation function, threshold, FDR and MDR criteria without distribution assumptions on noises and faults. In this part, a data-driven implementation of the designed FD system is presented, which includes the offline design and online FD, as show in Fig. 3.2.

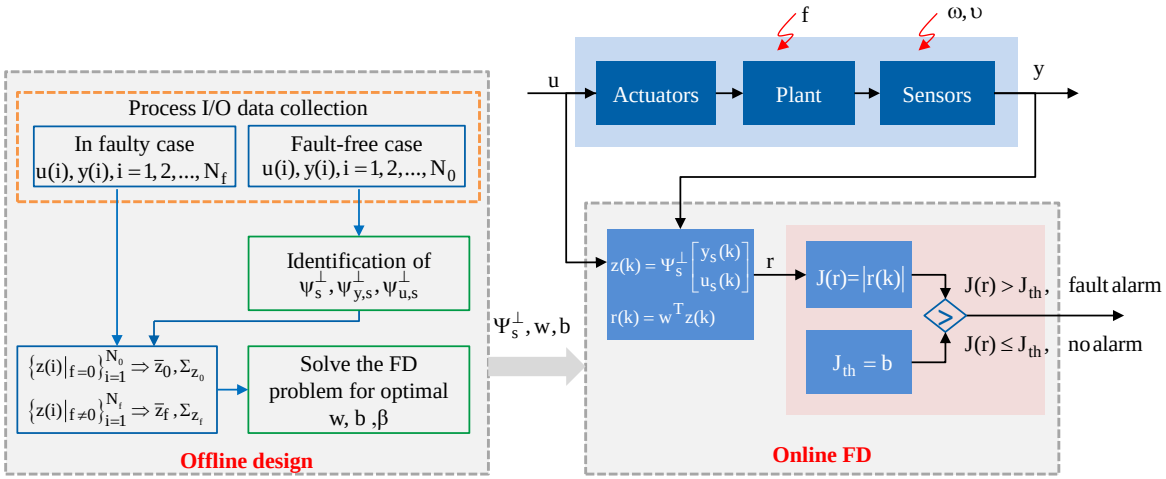

Figure 3.2: DIO method aided data-driven configuration of FD systems

In the stage of offline design, the matrix $\mathbf{\Psi}_s^\perp$ is identified using process I/O data with Algorithm 2.2.3. The sample sets $\{\mathbf{z}_0(i)\}_{i=1}^{N_0}$ in fault-free case and $\{\mathbf{z}_f(i)\}_{i=1}^{N_f}$ in the concerned faulty case are then constructed using (3.3), where N_0, N_f are given large enough sample numbers. The means $\bar{\mathbf{z}}_0$, $\bar{\mathbf{z}}_f$ and covariance matrices $\mathbf{\Sigma}_{z_0}$, $\mathbf{\Sigma}_{z_f}$ are thus

Algorithm 3.2.6 Data-driven implementation of DIO method aided FD systems

Offline design

1: Collect process I/O data in fault-free and the concerned faulty cases.
2: Identify $\mathbf{\Psi}_s^\perp$ with Algorithm 2.2.3 by using process I/O data in fault-free case.
3: Construct sample sets $\{\mathbf{z}_0(i)\}_{i=1}^{N_0}$ and $\{\mathbf{z}_f(i)\}_{i=1}^{N_f}$. Compute the empirical means $\bar{\mathbf{z}}_0$, $\bar{\mathbf{z}}_f$ and covariance matrices $\mathbf{\Sigma}_{z_0}$, $\mathbf{\Sigma}_{z_f}$.
4: Given $\alpha_0 \in (0,1)$, solve the FD problem (3.20)–(3.21) with Algorithm 3.2.5 for optimal $\mathbf{w}$, b, β. Compute $\boldsymbol{\vartheta}$, J_{th} with (3.47).

Online FD

1: Compute residual $r(k)$ and $J(r)$ with (3.48) and (3.12) at time step k, respectively.
2: Perform (3.6) to detect the occurrence of a fault.

estimated by

$$\bar{\mathbf{z}}_0 = \frac{1}{N_0}\sum_{i=1}^{N_0}\mathbf{z}_0(i),\ \mathbf{\Sigma}_{z_0} = \frac{1}{N_0}\sum_{i=1}^{N_0}(\mathbf{z}_0(i)-\bar{\mathbf{z}}_0)(\mathbf{z}_0(i)-\bar{\mathbf{z}}_0)^T \tag{3.45}$$

$$\bar{\mathbf{z}}_f = \frac{1}{N_f}\sum_{i=1}^{N_f}\mathbf{z}_f(i),\ \mathbf{\Sigma}_{z_f} = \frac{1}{N_f}\sum_{i=1}^{N_f}(\mathbf{z}_f(i)-\bar{\mathbf{z}}_f)(\mathbf{z}_f(i)-\bar{\mathbf{z}}_f)^T. \tag{3.46}$$

Given an appropriate $\alpha_0 \in (0,1)$, Algorithm 3.2.5 is then applied to solve the FD problem (3.26)–(3.27) for $\mathbf{w}$, b, β. Let

$$\boldsymbol{\vartheta} = \mathbf{w}^T\mathbf{\Psi}_s^\perp,\quad J_{th} = b. \tag{3.47}$$

In the stage of online FD, a residual signal at time step k is generated with

$$r(k) = \boldsymbol{\vartheta}\begin{bmatrix}\mathbf{y}_s(k)\\ \mathbf{u}_s(k)\end{bmatrix}. \tag{3.48}$$

By computing the residual evaluation function $J(r)$ and threshold with (3.12), the occurrence of a fault is then detected by performing the decision logic (3.6). The algorithm is summarized in **Algorithm** 3.2.6. As discussed in Section 3.2.2, the FAR of the designed FD system is ensured not greater than α_0 and the MDR not larger than β with respect to $\mathbb{P}_z \in \mathcal{P}_0$ in fault-free case and $\mathbb{P}_z \in \mathcal{P}_f$ in faulty case.

3.3 Discussion

In the above study, the design of FD systems regarding a two-sided residual evaluation function is formulated as the problem (3.13)–(3.14), which is further re-written as two one-sided DIO problems in form of (3.26)–(3.27) and then solved with an iterative parametric

algorithm. To gain a deeper insight, in this section we give two additional remarks about the worst-case FAR and MDR and a geometric interpretation of the optimal solution.

3.3.1 Worst-case FAR and MDR

In Section 3.2.2, we have represented the DCCs (3.14) with DCCs (3.21) and (3.23) as sufficient conditions by using Bonferroni's inequality. To explain this point better, we introduce the following theorems as side results of Theorem 3.1.

Theorem 3.3. *Given* $\boldsymbol{\xi} \in \mathbb{R}^n$ *with* $\boldsymbol{\xi} \sim (\bar{\boldsymbol{\xi}}, \boldsymbol{\Sigma})$, $\mathbf{w} \neq 0$ *and* $b > 0$ *such that* $|\mathbf{w}^T\bar{\boldsymbol{\xi}}| \leq b$, $\rho \in (0,1)$, *if*

$$b - |\mathbf{w}^T\bar{\boldsymbol{\xi}}| \geq \bar{\kappa}(\rho)\sqrt{\mathbf{w}^T\boldsymbol{\Sigma}\mathbf{w}} \tag{3.49}$$

holds with $\bar{\kappa}(\rho) = \sqrt{\frac{2-\rho}{\rho}}$, *then the condition*

$$\sup_{\boldsymbol{\xi}\sim(\bar{\boldsymbol{\xi}},\boldsymbol{\Sigma})} \Pr\left\{\left|\mathbf{w}^T\boldsymbol{\xi}\right| > b\right\} \leq \rho \tag{3.50}$$

holds true, when $|\mathbf{w}^T\bar{\boldsymbol{\xi}}| > b$, $\sup_{\boldsymbol{\xi}\sim(\bar{\boldsymbol{\xi}},\boldsymbol{\Sigma})} \Pr\left\{\left|\mathbf{w}^T\boldsymbol{\xi}\right| > b\right\} = 1$.

Proof. See the Appendix A.1. □

Theorem 3.4. *Given* $\boldsymbol{\xi} \in \mathbb{R}^n$ *with* $\boldsymbol{\xi} \sim (\bar{\boldsymbol{\xi}}, \boldsymbol{\Sigma})$, $\mathbf{w} \neq 0$ *and* $b > 0$ *such that* $|\mathbf{w}^T(\bar{\boldsymbol{\xi}})| \geq b$, $\rho \in (0,1)$, *the condition*

$$-b + |\mathbf{w}^T\bar{\boldsymbol{\xi}}| \geq \kappa(\rho)\sqrt{\mathbf{w}^T\boldsymbol{\Sigma}\mathbf{w}} \tag{3.51}$$

holds with $\kappa(\rho) = \sqrt{\frac{1-\rho}{\rho}}$ *if and only if*

$$\sup_{\xi\sim(\bar{\boldsymbol{\xi}},\boldsymbol{\Sigma})} \Pr\left\{\left|\mathbf{w}^T\boldsymbol{\xi}\right| \leq b\right\} \leq \rho \tag{3.52}$$

holds true, when $|\mathbf{w}^T\bar{\boldsymbol{\xi}}| < b$, $\sup_{\boldsymbol{\xi}\sim(\bar{\boldsymbol{\xi}},\boldsymbol{\Sigma})} \Pr\left\{\left|\mathbf{w}^T\boldsymbol{\xi}\right| \leq b\right\} = 1$.

Proof. See the Appendix A.2. □

Based on Theorems 3.3 and 3.4, the FD problem (3.20)–(3.21) can be substituted by

$$\min_{\mathbf{w}\neq 0,\, b>0} \quad \beta \tag{3.53}$$

$$\text{s.t.} \quad \begin{cases} b - |\mathbf{w}^T\bar{\mathbf{z}}_0| \geq \bar{\kappa}(\alpha_0)\sqrt{\mathbf{w}^T\boldsymbol{\Sigma}_{z_0}\mathbf{w}} \\ -b + |\mathbf{w}^T\bar{\mathbf{z}}_f| \geq \kappa(\beta)\sqrt{\mathbf{w}^T\boldsymbol{\Sigma}_{z_f}\mathbf{w}}. \end{cases} \tag{3.54}$$

By eliminating b from (3.54) and further re-written the problem (3.53)–(3.54) as follows

$$\max_{\mathbf{w}} \ \frac{1 - \bar{\kappa}(\alpha_0)\sqrt{\mathbf{w}^T\boldsymbol{\Sigma}_{z_0}\mathbf{w}}}{\sqrt{\mathbf{w}^T\boldsymbol{\Sigma}_{z_f}\mathbf{w}}} \quad \text{s.t.} \quad |\mathbf{w}^T\bar{\mathbf{z}}_f| - |\mathbf{w}^T\bar{\mathbf{z}}_0| = 1 \tag{3.55}$$

which is obviously identical with the FD problem (3.34) with $|\mathbf{w}^T\bar{\mathbf{z}}_f| - |\mathbf{w}^T\bar{\mathbf{z}}_0| > 0$. Algorithm 3.2.5 can then be used intuitively to solve (3.55). It is remarkable that $|\mathbf{w}^T\bar{\mathbf{z}}_f| - |\mathbf{w}^T\bar{\mathbf{z}}_0| > 0$ surely holds under assumption of $\bar{\mathbf{z}}_0 = 0$ and this assumption is without loss of generality since data can always be pre-processed so to comply with this assumption. When $\bar{\mathbf{z}}_0 \neq 0$ for the nonzero mean noises, the primary residual signal $\mathbf{z}(k)$ can be redefined as $\widetilde{\mathbf{z}}(k) = \mathbf{\Psi}_s^{\perp}\begin{bmatrix}\mathbf{y}_s(k)\\ \mathbf{u}_s(k)\end{bmatrix} - \bar{\mathbf{z}}_0$ such that $\mathbb{E}[\widetilde{\mathbf{z}}] = 0$ holds in fault-free case.

In summary, we solve the one-sided FD problem (3.20)–(3.21) for the optimal solutions of $\mathbf{w}$, b, β, as given in (3.35)–(3.37), respectively. Then, with respect to using the two-sided test statistic (3.12) and decision logic (3.6) for residual evaluation, the FAR and MDR of the FD system can be achieved satisfying

$$P_{FAR} \leq \alpha_0,\ P_{MDR} \leq \beta$$

for noises and faults supporting $\mathbb{P}_z \in \mathcal{P}_0$ in fault-free case and $\mathbb{P}_z \in \mathcal{P}_f$ in faulty case.

Remark 3.2. *It is worth emphasizing that the proposed DIO approach to FD with respect to solving (3.13)–(3.14) provides quantitative upper bounds of FAR and MDR in the probabilistic context, without special distribution assumptions on noises and faults. In case that the probability distributions for noises and faults are known in specific forms, the well-established (generalized) likelihood ratio method is apt to be applied to solve the problem (3.10)–(3.11), which will achieve a tighter upper bound of MDR for an identical FAR due to the additional distributional information except for mean and covariance matrix.*

3.3.2 Geometric interpretation

In the fashion of statistical learning, FD issue can be regarded as a binary classification problem, i.e., the fault-free class and the faulty class. The FD problem (3.13)–(3.14) is formulated aiming to find a hyperplane such that these two classes can be separated with minimum missed classification probabilities, i.e., the FAR and MDR. In this context, a geometric interpretation of the achieved solution is given below.

Since the solution to FD problem (3.13)–(3.14) is achieved by addressing (3.34), we start with using Lagrangian multiplier method to cope with (3.34). By introducing parameter vectors $\boldsymbol{\varsigma}$, $\boldsymbol{\zeta}$, a Lagrangian function corresponding to (3.34) is constructed as follows [41]

$$\mathcal{L}(\mathbf{w}, \lambda_1, \lambda_2, \boldsymbol{\varsigma}, \boldsymbol{\zeta}) = \min_{\mathbf{w},\lambda_1} \max_{\lambda_2,\boldsymbol{\varsigma},\boldsymbol{\zeta}} \bar{\kappa}(\alpha_0)\mathbf{w}^T\mathbf{\Sigma}_{z_0}^{\frac{1}{2}}\boldsymbol{\varsigma} + \lambda_1\mathbf{w}^T\mathbf{\Sigma}_{z_f}^{\frac{1}{2}}\boldsymbol{\varsigma} + \lambda_2(1 - \mathbf{w}^T(\bar{\mathbf{z}}_f - \bar{\mathbf{z}}_0)) \quad (3.56)$$

with $\|\boldsymbol{\varsigma}\|_2 \leq 1$, $\|\boldsymbol{\zeta}\|_2 \leq 1$. Given $\lambda_2\bar{\mathbf{z}}_f - \lambda_1\mathbf{\Sigma}_{z_f}^{\frac{1}{2}}\boldsymbol{\zeta} = \lambda_2\bar{\mathbf{z}}_0 + \bar{\kappa}(\alpha_0)\mathbf{\Sigma}_{z_0}^{\frac{1}{2}}\boldsymbol{\varsigma}$, i.e., $\bar{\mathbf{z}}_f - \lambda_1\mathbf{\Sigma}_{z_f}^{\frac{1}{2}}\boldsymbol{\zeta} =$

$\bar{\mathbf{z}}_0 + \bar{\kappa}(\alpha_0)\boldsymbol{\Sigma}_{z_0}^{\frac{1}{2}}\boldsymbol{\varsigma}$ with $\|\boldsymbol{\varsigma}\|_2 \leq \frac{1}{\lambda_2}, \|\boldsymbol{\zeta}\|_2 \leq \frac{1}{\lambda_2}$, the problem (3.56) is re-written as

$$\begin{aligned}\mathcal{L}(\mathbf{w}, \lambda_1, \lambda_2, \boldsymbol{\varsigma}, \boldsymbol{\zeta}) &= \max_{\|\boldsymbol{\varsigma}\|_2 \leq 1, \|\boldsymbol{\zeta}\|_2 \leq 1, \lambda_1} \lambda_2 : \lambda_2 \bar{\mathbf{z}}_f - \lambda_1 \boldsymbol{\Sigma}_{z_f}^{\frac{1}{2}} \boldsymbol{\zeta} = \lambda_2 \bar{\mathbf{z}}_0 + \bar{\kappa}(\alpha_0)\boldsymbol{\Sigma}_{z_0}^{\frac{1}{2}}\boldsymbol{\varsigma} \\ &= \min_{\|\boldsymbol{\varsigma}\|_2 \leq \frac{1}{\lambda_2}, \|\boldsymbol{\zeta}\|_2 \leq \frac{1}{\lambda_2}, \lambda_1} \frac{1}{\lambda_2} : \bar{\mathbf{z}}_f - \lambda_1 \boldsymbol{\Sigma}_{z_f}^{\frac{1}{2}} \boldsymbol{\zeta} = \bar{\mathbf{z}}_0 + \bar{\kappa}(\alpha_0)\boldsymbol{\Sigma}_{z_0}^{\frac{1}{2}}\boldsymbol{\varsigma}. \quad (3.57)\end{aligned}$$

At the optimum, it holds

$$\lambda_2 = \lambda_1 \left\| \boldsymbol{\Sigma}_{z_f}^{\frac{1}{2}} \mathbf{w} \right\|_2 + \bar{\kappa}(\alpha_0) \left\| \boldsymbol{\Sigma}_{z_0}^{\frac{1}{2}} \mathbf{w} \right\|_2 = 1, \ \lambda_1 = \kappa(\beta). \quad (3.58)$$

The formulation (3.57) admits a Mahalanobis distance based geometric interpretation of (3.58). Consider two ellipsoids centered with mean and shaped obeying covariance matrix in the following form

$$\mathcal{E}_0 = \left\{ \mathbf{z}_0 := \bar{\mathbf{z}}_0 + \bar{\kappa}(\alpha_0)\boldsymbol{\Sigma}_{z_0}^{\frac{1}{2}}\boldsymbol{\varsigma}, \ \ \|\boldsymbol{\varsigma}\|_2 \leq 1 \right\}, \ \mathcal{E}_f = \left\{ \mathbf{z}_f := \bar{\mathbf{z}}_f + \kappa(\beta)\boldsymbol{\Sigma}_{z_f}^{\frac{1}{2}}\boldsymbol{\zeta}, \ \ \|\boldsymbol{\zeta}\|_2 \leq 1 \right\}$$

which specify two groups of instances whose Mahalanobis distance to the center satisfies

$$\mathcal{M}_0 = \left\| \boldsymbol{\Sigma}_{z_0}^{-\frac{1}{2}} (\mathbf{z}_0 - \bar{\mathbf{z}}_0) \right\|_2 \leq \bar{\kappa}(\alpha_0), \ \mathcal{M}_f = \left\| \boldsymbol{\Sigma}_{z_f}^{-\frac{1}{2}} (\mathbf{z}_f - \bar{\mathbf{z}}_f) \right\|_2 \leq \kappa(\beta).$$

The optimal solution (3.58) is then interpreted as that a $\mathbf{w}$ is fund achieving the ellipsoids $\mathcal{E}_0$, $\mathcal{E}_f$ being tangentially intersected, such that a minimum MDR $\beta = \frac{1}{1+\kappa^2(\beta)}$ is achieved for a given FAR not larger than $\alpha_0 = \frac{2}{1+\bar{\kappa}^2(\alpha_0)}$ with Mahalanobis distances $\mathcal{M}_0 \leq \bar{\kappa}(\alpha_0)$ and $\mathcal{M}_f \leq \kappa(\beta)$.

3.4 Summary and notes

In this chapter, a DIO scheme has been presented to address design issues of data-driven FD systems subject to distributional ambiguity of noises and faults. Rather than posing specific distribution assumptions on noises and faults as made in conventional hypothesis test methods, ambiguity sets have been introduced to characterize families of probability distributions with common mean and covariance matrix both for fault-free and faulty cases. On this basis, the FD systems design has been formulated as an SP problem with DCCs in the context of minimizing the MDR for a prescribed FAR. A distribution independent solution to the targeting problem has been developed, which provides an integrated synthesis of the residual generator, residual evaluation function and threshold. Moreover, a data-driven implementation of the designed FD system has been given. To a better understanding, the worst-case FAR and MDR and a geometric interpretation of the solution have been discussed.

4 An improved DIO method for FD and analytical algorithms

A DIO approach has been demonstrated in Chapter 3 towards an integrated design of FD systems, achieving a minimum MDR for a given acceptable FAR without precise distribution knowledge of noises and faults. The basic idea behind this approach is to formulate the FAR and MDR involved DCCs as distribution independent conditions and then solve the DIO problem with iterative parametric algorithms. In the offline design procedure, the DCCs with residual evaluation function being two-sided test statistic of residual are decomposed into two conditions with one-sided test statistics and the FAR criterion is then derived using Bonferroni's inequality. It is worth mentioning that this handling would result in a conservative upper bound of FAR. On the other hand, despite various iterative parametric algorithms for solving DIO problems, the computational cost is generally expensive for the cases involving high dimensional process variables and a closed-form solution is rarely available [41]. Searching for an analytical solution to the DIO method aided FD is thus of practical importance but theoretically challenging.

Motivated by these concerns, this chapter confines to an improved DIO approach to the design of data-driven FD systems, providing tighter upper bounds of FAR and MDR without precise distribution knowledge of noises and faults. On the basis of a data-driven construction of a parity relation based residual generator, a two-sided test statistic of residual is applied as residual evaluation function, and then the design of FD systems is formulated as an SP problem with DCCs towards minimizing the MDR for a prescribed FAR. It is rigorously proven that the targeting problem can be addressed by solving a generalized eigenvalue-eigenvector problem. An analytical solution is thus obtained by means of an SVD. The existence condition of the optimal solution is also studied analytically. At the end of this chapter, a short discussion is given concerning two special cases of FD missing fault information and deterministic fault detection.

4.1 Problem formulation

For the purpose of FD in stochastic linear discrete-time systems of form (3.1), we recall the residual generator (3.3)–(3.5) to generate the residual signal using process I/O data. Considering the situation of unknown exact distributions for noises and faults, we refer

to the mean-covariance based ambiguity sets $\mathcal{P}_0$ in (3.17) and $\mathcal{P}_f$ in (3.18) to specify groups of probability distributions of $\mathbf{z}(k)$ in fault-free and faulty cases, respectively. In this context, given known means $\bar{\mathbf{z}}_0$, $\bar{\mathbf{z}}_f$ and covariance matrices $\mathbf{\Sigma}_{z_0}$, $\mathbf{\Sigma}_{z_f}$, the residual evaluation function $J(r)$ and threshold J_{th} are without loss of generality defined as follows

$$J(r) = (r(k) - \bar{r}_0)^2, \ J_{th} = 1 \tag{4.1}$$

where $\bar{r}_0 = \mathbf{w}^T \bar{\mathbf{z}}_0$. The following decision logic is then used to for online FD

$$\begin{cases} J(r) \leq J_{th} & \Rightarrow \quad \text{no fault alarm} \\ J(r) > J_{th} & \Rightarrow \quad \text{fault alarm.} \end{cases} \tag{4.2}$$

The design of FD systems thus lies in the design of parameter vector $\mathbf{w}$.

Towards minimizing the MDR for a given FAR, we substitute (3.5) into (4.1) and formulate the design of FD system regarding parameter vector $\mathbf{w}$ as an SP problem with DCCs in the following form

$$\min_{\mathbf{w} \neq 0} \ \beta \tag{4.3}$$

$$\text{s.t.} \quad \begin{cases} \sup\limits_{\mathbb{P}_z \in \mathcal{P}_0} \Pr\left\{(\mathbf{w}^T(\mathbf{z} - \bar{\mathbf{z}}_0))^2 > 1\right\} \leq \alpha_0 \\ \sup\limits_{\mathbb{P}_z \in \mathcal{P}_f} \Pr\left\{(\mathbf{w}^T(\mathbf{z} - \bar{\mathbf{z}}_0))^2 \leq 1\right\} \leq \beta \end{cases} \tag{4.4}$$

where $\alpha_0 \in (0, 1)$ is a given upper bound of FAR and $\beta \in (0, 1)$ the upper bound of MDR.

Due to the DCCs (4.4), it remains a challenging task to find the optimal solution to the FD problem (4.3)–(4.4) in an analytical manner. To deal with this issue, the main objectives of this chapter are as follows:

- Study the deterministic formulations of the DCCs (4.4) in the probabilistic context such that the tighter upper bounds of FAR and MDR can be achieved and
- Develop an analytical solution to the FD problem (4.3)–(4.4) without specific distribution assumptions on noises and faults.

4.2 An improved DIO approach to FD

In this part, an improved DIO approach is demonstrated for the design of FD systems by solving the problem (4.3)–(4.4). To this end, distribution independent representations of the DCCs in (4.4) are first studied.

4.2.1 Deterministic description of DCCs

As demonstrated in Chapter 3, the first DCC in (4.4) can be handled by decomposing the two-sided residual evaluation function into two one-sided test statistics of residual due to its nonconvexity, then the FAR criterion is obtained using Bonferroni's inequality. Unfortunately, this approximation will lead to a quite conservative FAR. To alleviate this deficiency, below an equivalent deterministic formulation of the first DCC in (4.4) is investigated according to the connections between DCCs and WC-CVaR constraints [66].

Recall the definition of CVaR given in 2.7. The following theorems are referred at first.

Theorem 4.1. *[93] Let $L(\boldsymbol{\xi}) : \mathbb{R}^n \to \mathbb{R}$ be a continuous loss function that is either concave or quadratic in $\boldsymbol{\xi}$ (possibly nonconcave). Then the following equivalence holds*

$$\mathcal{Z}(\rho, L(\boldsymbol{\xi})) = \sup_{\mathbb{P}_\xi \in \mathcal{P}} \mathbb{P}_\xi - \mathrm{CVaR}_\rho\left(L(\boldsymbol{\xi})\right) \leq 0 \quad \Leftrightarrow \quad \inf_{\mathbb{P}_\xi \in \mathcal{P}} \Pr\left(L(\boldsymbol{\xi}) \leq 0\right) \geq 1 - \rho$$

where $\mathcal{P}$ is a mean-covariance based ambiguity set of $\mathbb{P}_\xi$, $\mathcal{Z}(\rho, L(\boldsymbol{\xi}))$ is a WC-CVaR *condition.*

Theorem 4.2. *[76] Given $\boldsymbol{\xi} \in \mathbb{R}^n$ following probability distribution $\mathbb{P}_\xi$ with $\mathbb{E}[\boldsymbol{\xi}] = \bar{\boldsymbol{\xi}}$ and $\mathbb{V}[\boldsymbol{\xi}] = \boldsymbol{\Sigma}$, let the second-order moment matrix be*

$$\mathbf{M}_\xi = \begin{bmatrix} \boldsymbol{\Sigma} + \bar{\boldsymbol{\xi}}\bar{\boldsymbol{\xi}}^T & \bar{\boldsymbol{\xi}} \\ \bar{\boldsymbol{\xi}}^T & 1 \end{bmatrix}. \tag{4.5}$$

Define an ambiguity set

$$\mathcal{P} = \left\{ \mathbb{P}_\xi \,\middle|\, \int \begin{bmatrix} \boldsymbol{\xi}^T & 1 \end{bmatrix}^T \cdot \begin{bmatrix} \boldsymbol{\xi}^T & 1 \end{bmatrix} d\mathbb{P}_\xi = \mathbf{M}_\xi \right\}$$

and a loss function $L(\boldsymbol{\xi}) = \boldsymbol{\xi}^T\mathbf{E}\boldsymbol{\xi} + 2\mathbf{e}_1^T\boldsymbol{\xi} + \mathrm{e}_0$ with $\mathbf{E} \in \mathbb{S}_+^n$, $\mathbf{e}_1 \in \mathbb{R}^n$, $\mathrm{e}_0 \in \mathbb{R}$. Then the WC-CVaR *is equivalent to the following tractable SDP*

$$\begin{aligned} \sup_{\mathbb{P}_\xi \in \mathcal{P}} \mathbb{P} - \mathrm{CVaR}_\rho\left(L(\boldsymbol{\xi})\right) \quad = \quad & \inf_{\eta, \mathbf{K}} \ \eta + \frac{1}{\rho}\,\mathrm{Tr}\left(\mathbf{M}_\xi \mathbf{K}\right) \\ & \text{s.t.} \quad \mathbf{K} \in \mathbb{S}_+^{n+1},\ \eta \in \mathbb{R},\ \mathbf{K} - \begin{bmatrix} \mathbf{E} & \mathbf{e}_1 \\ \mathbf{e}_1^T & \mathrm{e}_0 - \eta \end{bmatrix} \succeq 0. \end{aligned}$$

Theorem 4.3. *[76] Using the notations in Theorem 4.2, given $\bar{\boldsymbol{\xi}} = 0$, $\boldsymbol{\Sigma} \in \mathbb{S}_+^n$ and loss function $L(\boldsymbol{\xi}) = \boldsymbol{\xi}^T\mathbf{E}\boldsymbol{\xi} + \mathrm{e}_0$, then*

$$\sup_{\mathbb{P}_\xi \in \mathcal{P}} \mathbb{P} - \mathrm{CVaR}_\rho\left(L(\boldsymbol{\xi})\right) \quad = \quad \mathrm{e}_0 + \frac{1}{\rho}\,\mathrm{Tr}\left(\boldsymbol{\Sigma}\mathbf{E}\right).$$

Based on Theorems 4.2 and 4.3, the following theorem can be achieved.

Theorem 4.4. *Given $\boldsymbol{\xi} \in \mathbb{R}^n$ obeying probability distribution $\mathbb{P}_\xi$ with $\mathbb{E}[\boldsymbol{\xi}] = \bar{\boldsymbol{\xi}}$, $\mathbb{V}[\boldsymbol{\xi}] = \boldsymbol{\Sigma} \in \mathbb{S}_+^n$, define a mean-covariance based ambiguity set $\mathcal{P}$. For $\alpha \in (0, 1)$, the condition*

$$\sup_{\mathbb{P}_\xi \in \mathcal{P}} \Pr\left\{(\mathbf{w}^T(\boldsymbol{\xi} - \bar{\boldsymbol{\xi}}))^2 > 1\right\} \leq \alpha \tag{4.6}$$

holds if and only if

$$\nu(\alpha)\sqrt{\mathbf{w}^T\boldsymbol{\Sigma}\mathbf{w}} \leq 1 \tag{4.7}$$

with $\nu(\alpha) = \sqrt{1/\alpha}$.

Proof. Denote by $\boldsymbol{\zeta} = \boldsymbol{\xi} - \bar{\boldsymbol{\xi}}$ obeying distribution $\mathbb{P}_\zeta$ with $\mathbb{E}[\boldsymbol{\zeta}] = 0$, $\mathbb{V}[\boldsymbol{\zeta}] = \mathbb{V}[\boldsymbol{\xi}] = \boldsymbol{\Sigma} \in \mathbb{S}_+^n$. Define an ambiguity set $\mathcal{P} = \{\mathbb{P}_\zeta \in \mathcal{L} \,|\mathbb{E}[\boldsymbol{\zeta}] = 0,\ \mathbb{V}[\boldsymbol{\zeta}] = \boldsymbol{\Sigma}\}$ and a function of $\boldsymbol{\zeta}$ by

$$\mathcal{F}(\boldsymbol{\zeta}) = \boldsymbol{\zeta}^T\mathbf{Q}\boldsymbol{\zeta} - 1,\ \mathbf{Q} = \mathbf{w}\mathbf{w}^T. \tag{4.8}$$

According to Theorem 4.1, the following expression regarding the condition (4.6) holds

$$\begin{aligned} \sup_{\mathbb{P}_\xi \in \mathcal{P}} \Pr\left\{(\ \mathbf{w}^T(\boldsymbol{\xi} - \bar{\boldsymbol{\xi}}))^2 > 1\right\} \leq \alpha \quad &\Leftrightarrow \quad \sup_{\mathbb{P}_\zeta \in \mathcal{P}} \Pr\left\{\mathcal{F}(\boldsymbol{\zeta}) > 0\right\} \leq \alpha \\ &\Leftrightarrow \quad \inf_{\mathbb{P}_\zeta \in \mathcal{P}} \Pr\left\{\mathcal{F}(\boldsymbol{\zeta}) \leq 0\right\} \geq 1 - \alpha. \end{aligned} \tag{4.9}$$

Note that $\mathcal{F}(\boldsymbol{\zeta})$ is a quadratic function over $\boldsymbol{\zeta}$. It is known from Theorem 4.2 that (4.9) holds if and only if

$$\sup_{\mathbb{P}_\zeta \in \mathcal{P}} \mathbb{P} - \mathrm{CVaR}_\alpha\left(\mathcal{F}\left(\boldsymbol{\zeta}\right)\right) \leq 0 \tag{4.10}$$

Referring to Theorem 4.3, we have (4.10) equals to

$$-1 + \frac{1}{\alpha}\mathrm{Tr}\left(\boldsymbol{\Sigma}\mathbf{Q}\right) \leq 0. \tag{4.11}$$

Together with (4.8)–(4.10) and (4.11), the condition (4.6) then holds if and only if

$$\frac{1}{\alpha}\left(\mathbf{w}^T\boldsymbol{\Sigma}\mathbf{w}\right) \leq 1$$

which clearly delivers (4.7). The proof is completed. □

According to Theorem 4.4, the first DCC in (4.4) is equally described as the following distribution independent form

$$\nu(\alpha_0)\sqrt{\mathbf{w}^T\boldsymbol{\Sigma}_{z_0}\mathbf{w}} \leq 1 \tag{4.12}$$

where $\nu(\alpha_0) = \sqrt{1/\alpha_0}$. In order to deal with the second DCC in (4.4) in deterministic manner, we further propose the following theorem.

Theorem 4.5. *Using the notations in Theorem 4.4, let* $\kappa(\alpha) = \sqrt{(1-\alpha)/\alpha}$. *Given a constant vector* $\mathbf{g} \in \mathbb{R}^n$ *with* $|\mathbf{w}^T(\bar{\boldsymbol{\xi}} - \mathbf{g})| \geq 1$, *the condition*

$$\sup_{\mathbb{P}_\xi \in \mathcal{P}} \Pr\left\{(\mathbf{w}^T(\boldsymbol{\xi} - \mathbf{g}))^2 \leq 1\right\} \leq \alpha \tag{4.13}$$

holds if and only if

$$\sqrt{\mathbf{w}^T(\bar{\boldsymbol{\xi}} - \mathbf{g})(\bar{\boldsymbol{\xi}} - \mathbf{g})^T\mathbf{w}} - 1 \geq \kappa(\alpha)\sqrt{\mathbf{w}^T\boldsymbol{\Sigma}\mathbf{w}}. \tag{4.14}$$

When $|\mathbf{w}^T(\bar{\boldsymbol{\xi}} - \mathbf{g})| < 1$, *it holds* $\sup_{\mathbb{P}_\xi \in \mathcal{P}} \Pr\left\{(\mathbf{w}^T(\boldsymbol{\xi} - \mathbf{g}))^2 \leq 1\right\} = 1$.

Proof. Let $\boldsymbol{\varsigma} = \boldsymbol{\xi} - \mathbf{g}$, $\mathcal{D} = \left\{\mathbb{P}_\varsigma \in \mathcal{L} \,\middle|\, \mathbb{E}[\boldsymbol{\varsigma}] = \bar{\boldsymbol{\xi}} - \mathbf{g} = \bar{\boldsymbol{\varsigma}},\ \mathbb{V}[\boldsymbol{\varsigma}] = \boldsymbol{\Sigma} \in \mathbb{S}_+^n\right\}$. It is noted from Theorem 3.4 that, for $|\mathbf{w}^T\bar{\boldsymbol{\varsigma}}| \leq 1$, it holds

$$\begin{aligned} \text{Eq. (4.13)} \ &\Leftrightarrow \ \sup_{\mathbb{P}_\varsigma \in \mathcal{D}} \Pr\left\{(\ \mathbf{w}^T\boldsymbol{\varsigma})^2 \leq 1\right\} \leq \alpha \Leftrightarrow \sup_{\mathbb{P}_\varsigma \in \mathcal{D}} \Pr\left\{|\mathbf{w}^T\boldsymbol{\varsigma}| \leq 1\right\} \leq \alpha \\ &\Leftrightarrow \ \sqrt{\mathbf{w}^T\bar{\boldsymbol{\varsigma}}\bar{\boldsymbol{\varsigma}}^T\mathbf{w}} - 1 \geq \kappa(\alpha)\sqrt{\mathbf{w}^T\boldsymbol{\Sigma}\mathbf{w}}. \end{aligned} \tag{4.15}$$

The substitution of $\bar{\boldsymbol{\varsigma}} = \bar{\boldsymbol{\xi}} - \mathbf{g}$ to (4.15) delivers (4.14). When $|\mathbf{w}^T\bar{\boldsymbol{\varsigma}}| > 1$, we have $\sup_{\mathbb{P}_\varsigma \in \mathcal{D}} \Pr\left\{(\mathbf{w}^T\boldsymbol{\varsigma})^2 \leq 1\right\} = \sup_{\mathbb{P}_\varsigma \in \mathcal{D}} \Pr\left\{|\mathbf{w}^T\boldsymbol{\varsigma}| \leq 1\right\} = 1$. The proof is completed. □

Let $\kappa(\beta) = \sqrt{(1-\beta)/\beta}$, $\tilde{\mathbf{z}}_f = \bar{\mathbf{z}}_f - \bar{\mathbf{z}}_0$. Based on Theorem 4.5, the second DCC in (4.4) is then equally substituted by the following deterministic constraint

$$\sqrt{\mathbf{w}^T\tilde{\mathbf{z}}_f\tilde{\mathbf{z}}_f^T\mathbf{w}} - \kappa(\beta)\sqrt{\mathbf{w}^T\boldsymbol{\Sigma}_{z_f}\mathbf{w}} \geq 1. \tag{4.16}$$

Combining with (4.12) and (4.16), the FD problem (4.6)–(4.7) is thus equally reformulated as the following distribution independent form

$$\min_{\mathbf{w} \neq 0} \quad \beta \tag{4.17}$$

$$\text{s.t.} \quad \begin{cases} \nu(\alpha_0)\sqrt{\mathbf{w}^T\boldsymbol{\Sigma}_{z_0}\mathbf{w}} \leq 1 \\ \sqrt{\mathbf{w}^T\tilde{\mathbf{z}}_f\tilde{\mathbf{z}}_f^T\mathbf{w}} - \kappa(\beta)\sqrt{\mathbf{w}^T\boldsymbol{\Sigma}_{z_f}\mathbf{w}} \geq 1. \end{cases} \tag{4.18}$$

Now the remaining task is to solve the DIO problem (4.17)–(4.18). Though various parametric algorithms, e.g., the iterative least square [53] and the quadratic interpolation schemes [41], can be applied to this end, achieving an analytical solution to this problem remains difficult and a rigorous analysis of the FD results is then intractable. In the upcoming subsection we propose an SVD-based algorithm to address the FD problem (4.17)–(4.18) analytically.

4.2.2 Analytical optimal solution

It follows from (4.18) that

$$\nu(\alpha_0)\sqrt{\mathbf{w}^T\mathbf{\Sigma}_{z_0}\mathbf{w}} \leq 1 \leq \sqrt{\mathbf{w}^T\tilde{\mathbf{z}}_f\tilde{\mathbf{z}}_f^T\mathbf{w}} - \kappa(\beta)\sqrt{\mathbf{w}^T\mathbf{\Sigma}_{z_f}\mathbf{w}}. \tag{4.19}$$

Let

$$\mathcal{C}(\mathbf{w}) = \frac{\sqrt{\mathbf{w}^T\tilde{\mathbf{z}}_f\tilde{\mathbf{z}}_f^T\mathbf{w}} - \nu(\alpha_0)\sqrt{\mathbf{w}^T\mathbf{\Sigma}_{z_0}\mathbf{w}}}{\sqrt{\mathbf{w}^T\mathbf{\Sigma}_{z_f}\mathbf{w}}}. \tag{4.20}$$

We then have

$$0 < \kappa(\beta) \leq \mathcal{C}(\mathbf{w}). \tag{4.21}$$

Since $\kappa(\beta)$ has the opposite monotonicity with β, the objective of minimizing β in (4.17) can be achieved by maximizing $\kappa(\beta)$. Simultaneously, it obviously holds at the maximum of $\kappa(\beta)$ that

$$\kappa(\beta) = \mathcal{C}(\mathbf{w}),\ \nu(\alpha_0)\sqrt{\mathbf{w}^T\mathbf{\Sigma}_{z_0}\mathbf{w}} = 1. \tag{4.22}$$

Because if $\mathbf{w}$ delivers $\nu(\alpha_0)\sqrt{\mathbf{w}^T\mathbf{\Sigma}_{z_0}\mathbf{w}} < 1$, we can always find another $\mathbf{w}$ achieving a larger $\kappa(\beta)$. In this regard, the problem (4.17)–(4.18) can be solved by addressing

$$\max_{\mathbf{w}\neq 0}\ \mathcal{C}(\mathbf{w}) \tag{4.23}$$

$$\text{s.t.}\quad \nu(\alpha_0)\sqrt{\mathbf{w}^T\mathbf{\Sigma}_{z_0}\mathbf{w}} = 1,\ \mathcal{C}(\mathbf{w}) > 0. \tag{4.24}$$

Note that the constraint $\nu(\alpha_0)\sqrt{\mathbf{w}^T\mathbf{\Sigma}_{z_0}\mathbf{w}} = 1$ in (4.24) can always be satisfied by multiplying a constant to the optimal solution of $\mathbf{w}$ to the following problem

$$\max_{\mathbf{w}\neq 0}\ \mathcal{C}(\mathbf{w}) \quad \text{s.t.} \quad \mathcal{C}(\mathbf{w}) > 0. \tag{4.25}$$

We thus temporally omit the first constraint in (4.24) and focus on solving the problem (4.25). The following theorem is proposed to this aim.

Theorem 4.6. *The solution to the problem (4.25) can be achieved by solving the following generalized eigenvalue-eigenvector problem*

$$\max_{\mathbf{w}\neq 0}\ \frac{\mathbf{w}^T\tilde{\mathbf{\Sigma}}\mathbf{w}}{\mathbf{w}^T\mathbf{\Sigma}_{z_f}\mathbf{w}} \tag{4.26}$$

where $\tilde{\mathbf{\Sigma}} = \tilde{\mathbf{z}}_f\tilde{\mathbf{z}}_f^T - \nu^2(\alpha_0)\mathbf{\Sigma}_{z_0}$. *Do an SVD on* $\mathbf{\Sigma}_{z_f}^{\frac{1}{2}}$, *i.e.,* $\mathbf{\Sigma}_{z_f}^{\frac{1}{2}} = \mathbf{U}\begin{bmatrix}\mathbf{S} & 0\end{bmatrix}\mathbf{V}^T$, $\mathbf{U}\mathbf{U}^T = \mathbf{I}$, $\mathbf{V}\mathbf{V}^T = \mathbf{I}$. *The optimal solution of* $\mathbf{w}$ *to (4.26) is obtained as*

$$\mathbf{w} = \mathbf{U}\mathbf{S}^{-1}\mathbf{v} \tag{4.27}$$

where $\mathbf{v}$ *solves*

$$\mathbf{v}^T(\lambda_m\mathbf{I} - \mathbf{S}^{-1}\mathbf{U}^T\tilde{\mathbf{\Sigma}}\mathbf{U}\mathbf{S}^{-1})\mathbf{v} = 0,\ \mathbf{v}^T\mathbf{v} = 1 \tag{4.28}$$

with $\lambda_m > 0$ *being the maximum eigenvalue of matrix* $\mathbf{S}^{-1}\mathbf{U}^T\tilde{\mathbf{\Sigma}}\mathbf{U}\mathbf{S}^{-1}$.

Proof. For $\mathbf{w} \neq 0$, $\tilde{\mathbf{z}}_f \neq 0$, let $t(\mathbf{w}) = \frac{\sqrt{\mathbf{w}^T\tilde{\mathbf{z}}_f\tilde{\mathbf{z}}_f^T\mathbf{w}}}{\sqrt{\mathbf{w}^T\boldsymbol{\Sigma}_{z_f}\mathbf{w}}}$, $h(\mathbf{w}) = \frac{\nu(\alpha_0)\sqrt{\mathbf{w}^T\boldsymbol{\Sigma}_{z_0}\mathbf{w}}}{\sqrt{\mathbf{w}^T\boldsymbol{\Sigma}_{z_f}\mathbf{w}}}$ with $t(\mathbf{w}) > h(\mathbf{w}) > 0$ and

$$\mathcal{C}(\mathbf{w}) = t(\mathbf{w}) - h(\mathbf{w}),\ \mathcal{H}(\mathbf{w}) = t^2(\mathbf{w}) - h^2(\mathbf{w}).$$

Since $t(\mathbf{w})$ and $h(\mathbf{w})$ are scalars, there without loss of generality exists $\mu(\mathbf{w}) \in (0,1)$ such that $h(\mathbf{w}) = \mu(\mathbf{w})t(\mathbf{w})$. Then, we have $\mathcal{C}(\mathbf{w}) = (1-\mu(\mathbf{w}))t(\mathbf{w})$ and

$$\mathcal{H}(\mathbf{w}) = (1-\mu^2(\mathbf{w}))t^2(\mathbf{w}) = \frac{(1+\mu(\mathbf{w}))\mathcal{C}^2(\mathbf{w})}{1-\mu(\mathbf{w})}.$$

Because of $\mathcal{C}(\mathbf{w}) > 0$, it is easy to verify that

$$\frac{\partial\mathcal{H}(\mathbf{w})}{\partial\mathcal{C}(\mathbf{w})} = 2\mathcal{C}(\mathbf{w})\frac{1+\mu(\mathbf{w})}{1-\mu(\mathbf{w})} > 0$$

which means $\mathcal{H}(\mathbf{w})$ has the same monotonicity with $\mathcal{C}(\mathbf{w})$ over $\mathbf{w}$. Then it follows

$$\mathbf{w} = \arg\max_{\mathbf{w}\neq 0}\ \mathcal{C}(\mathbf{w}) = \arg\max_{\mathbf{w}\neq 0}\ \mathcal{H}(\mathbf{w}).$$

Submitting $t(\mathbf{w})$, $h(\mathbf{w})$ into $\mathcal{H}(\mathbf{w})$, the solution of (4.25) is then obtained by solving (4.26). Note that (4.26) is a generalized eigenvalue-eigenvector problem and thus is solved by (4.27) by means of an SVD with $\lambda_m = \max_{\mathbf{w}\neq 0}\frac{\mathbf{w}^T\tilde{\boldsymbol{\Sigma}}\mathbf{w}}{\mathbf{w}^T\boldsymbol{\Sigma}_{z_f}\mathbf{w}} > 0$. The proof is completed. □

Now we consider the constraint $\nu(\alpha_0)\sqrt{\mathbf{w}^T\boldsymbol{\Sigma}_{z_0}\mathbf{w}} = 1$ in (4.24). As mentioned before, we can obviously determine the optimal $\mathbf{w}$ by dividing $\mathbf{w}$ in (4.27) with a constant such that this equality holds without changing the maximum of $\mathcal{C}(\mathbf{w})$. The following theorem is thus achieved.

Theorem 4.7. *The optimal solution to the problem (4.17)–(4.18) can be obtained by solving (4.26) such that* $\nu(\alpha_0)\sqrt{\mathbf{w}^T\boldsymbol{\Sigma}_{z_0}\mathbf{w}} = 1$. *At the optimum, it holds* $\kappa(\beta) = \mathcal{C}(\mathbf{w})$.

Denote by $\mathbf{w}_*$ the optimal solution of $\mathbf{w}$ to the problem (4.17)–(4.18). According to Theorems 4.6 and 4.7, we have

$$\mathbf{w}_* = \frac{\mathbf{w}}{\nu(\alpha_0)\sqrt{\mathbf{w}^T\boldsymbol{\Sigma}_{z_0}\mathbf{w}}} \tag{4.29}$$

with $\mathbf{w}$ being given in (4.27) and

$$\kappa(\beta) = \mathcal{C}(\mathbf{w}_*) = \frac{\sqrt{\mathbf{w}_*^T\tilde{\mathbf{z}}_f\tilde{\mathbf{z}}_f^T\mathbf{w}_*} - 1}{\sqrt{\mathbf{w}_*^T\Sigma_{z_f}\mathbf{w}_*}},\ \beta = \frac{1}{1+\kappa^2(\beta)}. \tag{4.30}$$

So far, analytical solutions of $\mathbf{w}$, β to the FD problem (4.17)–(4.18) are achieved by means of SVD technique. The algorithm is summarized in Algorithm 4.2.7. From the

Algorithm 4.2.7 Analytical solution to the FD problem (4.17)–(4.18)

1: Given an appropriate $\alpha_0 \in (0,1)$, $\bar{\mathbf{z}}_0 \neq \bar{\mathbf{z}}_f$, $\mathbf{\Sigma}_{z_0}$, $\mathbf{\Sigma}_{z_f} \in \mathbb{S}_+^\gamma$, do an SVD on $\mathbf{\Sigma}_{z_f}^{\frac{1}{2}}$ and compute $\mathbf{w}$ with (4.27) by solving (4.28) for $\mathbf{v}$.
2: Compute $\mathbf{w}_*$ and β with (4.29) and (4.30), respectively.

viewpoint of computation, it is worth mentioning that the key of the proposed analytical algorithm lies in solving the generalized eigenvalue-eigenvector problem (4.26), which can be addressed efficiently by means of the well-developed SVD techniques [18], the worst-case computational complexity is $O(\gamma^3)$. Nowadays, various iterative numerical algorithms have been proposed to solve generalized eigenvalue-eigenvector problems, which involve comparable lower computational cost than $O(\gamma^3)$, especially for high dimensional random variables, see, for instance, [32, 33, 67]. In comparison, the existing parametric algorithms, e.g., the iterative least-square method presented in [53], would involve the worst-case computational complexity not smaller than $O(\gamma^3)$, meanwhile, an analytical solution is unavailable for further FD performance analysis.

Remark 4.1. *As illustrated in Section 3.2.3, the parameter vector* $\mathbf{w}$ *to the problem (3.13)–(3.14) is obtained by solving the FD problem (3.20)–(3.21) and then the FAR criterion is obtained according to Bonferroni inequality. In other words, constraints (3.21) hold as sufficient conditions of (3.14). While as proven before, (4.18) provide sufficient and necessary conditions to DCCs (4.4). Comparing (3.27) and (4.18), we can see that they are in the same form with* $\bar{\kappa}(\alpha_0)$ *in place of* $\nu(\alpha_0)$ *for* $\bar{\mathbf{z}}_0 = 0$ *and* $b = 1$*. Because* $\bar{\kappa}(\alpha_{0,1}) = \nu(\alpha_{0,2})$ *with* $\alpha_{0,1}, \alpha_{0,2} \in (0,1)$ *leads to* $\alpha_{0,2} < \alpha_{0,1}$*, we can then conclude that, for an identical upper bound of MDR, i.e.,* β*, a smaller upper bound of FAR can be achieved by using the improved DIO method.*

Remark 4.2. *Algorithm 4.2.7 can be directly applied to solve the distribution independent FD problems (3.24)–(3.25) and (3.26)–(3.27). In this manner, not only a closed-form solution can be delivered but also a comparable lower computational load in contrast with Algorithm 3.2.5.*

4.2.3 Existence condition of the optimal solution

It is observed from Theorem 4.6 that there naturally exists a lower bound of α_0 to guarantee the existence of $\mathbf{w}$, such that $\lambda_m > 0$ holds to ensure $\kappa(\beta) > 0$. Since $\kappa(\beta)$ decreases monotonically with the increase of β and the decrease of α_0, we study the existence condition of the optimal solution to problem (4.17)–(4.18) by setting $\beta = 1$. In this context, $\kappa(\beta) = 0$ holds. Denote by α_0^l the lower bound of α_0. Let $\nu(\alpha_0^l) = \sqrt{1/\alpha_0^l}$. It

yields from (4.19) that

$$\nu^2(\alpha_0^l) := \max_{\mathbf{w}\neq 0} \frac{\mathbf{w}^T\tilde{\mathbf{z}}_f\tilde{\mathbf{z}}_f^T\mathbf{w}}{\mathbf{w}^T\boldsymbol{\Sigma}_{z_0}\mathbf{w}} \tag{4.31}$$

which is a generalized eigenvalue-eigenvector problem. Do an SVD on $\boldsymbol{\Sigma}_{z_0}^{\frac{1}{2}}$, i.e., $\boldsymbol{\Sigma}_{z_0}^{\frac{1}{2}} = \bar{\mathbf{U}}\begin{bmatrix}\bar{\mathbf{S}} & 0\end{bmatrix}\bar{\mathbf{V}}^T$, $\bar{\mathbf{U}}\bar{\mathbf{U}}^T = \mathbf{I}$, $\bar{\mathbf{V}}\bar{\mathbf{V}}^T = \mathbf{I}$. The optimal solution of $\mathbf{w}$ to (4.31) is achieved as

$$\mathbf{w} = \bar{\mathbf{U}}\bar{\mathbf{S}}^{-1}\bar{\mathbf{v}} \tag{4.32}$$

with $\bar{\mathbf{v}}$ solving the following equations

$$\bar{\mathbf{v}}^T(\bar{\lambda}_m\mathbf{I} - \bar{\mathbf{S}}^{-1}\bar{\mathbf{U}}^T\tilde{\mathbf{z}}_f\tilde{\mathbf{z}}_f^T\bar{\mathbf{U}}\bar{\mathbf{S}}^{-1})\bar{\mathbf{v}} = 0,\ \bar{\mathbf{v}}^T\bar{\mathbf{v}} = 1 \tag{4.33}$$

where $\bar{\lambda}_m = \lambda_{max}\left\{\bar{\mathbf{S}}^{-1}\bar{\mathbf{U}}^T\tilde{\mathbf{z}}_f\tilde{\mathbf{z}}_f^T\bar{\mathbf{U}}\bar{\mathbf{S}}^{-1}\right\}$. Due to $\bar{\mathbf{S}}^{-1}\bar{\mathbf{U}}^T\tilde{\mathbf{z}}_f\tilde{\mathbf{z}}_f^T\bar{\mathbf{U}}\bar{\mathbf{S}}^{-1}$ is a rank-one matrix, it then holds

$$\bar{\lambda}_m = \tilde{\mathbf{z}}_f^T\boldsymbol{\Sigma}_{z_0}^{-1}\tilde{\mathbf{z}}_f. \tag{4.34}$$

We intuitively have $\nu^2(\alpha_0^l) = \bar{\lambda}_m = \tilde{\mathbf{z}}_f^T\boldsymbol{\Sigma}_{z_0}^{-1}\tilde{\mathbf{z}}_f$ and then

$$\alpha_0^l = \frac{1}{\tilde{\mathbf{z}}_f^T\boldsymbol{\Sigma}_{z_0}^{-1}\tilde{\mathbf{z}}_f}. \tag{4.35}$$

Moreover, note that $\alpha_0^l \in (0,\ 1)$, it should hold $\tilde{\mathbf{z}}_f^T\boldsymbol{\Sigma}_{z_0}^{-1}\tilde{\mathbf{z}}_f > 1$. Recalling the dynamics of residual generator in (3.4), we have $\tilde{\mathbf{z}}_f = \bar{\mathbf{z}}_f - \bar{\mathbf{z}}_0 = \bar{\mathbf{H}}_{f,s}\bar{\mathbf{f}}_s$ and then

$$\tilde{\mathbf{z}}_f^T\boldsymbol{\Sigma}_{z_0}^{-1}\tilde{\mathbf{z}}_f = \left\|\boldsymbol{\Sigma}_{z_0}^{-\frac{1}{2}}\bar{\mathbf{H}}_{f,s}\bar{\mathbf{f}}_s\right\|_2^2 > 1 \tag{4.36}$$

should hold. It implies that the magnitude of $\bar{\mathbf{f}}_s$ should satisfy (4.36) such that an MDR smaller than one can be ensured for a given appropriate $\alpha_0 \in \left(\alpha_0^l,\ 1\right)$. The following theorem is thus achieved.

Theorem 4.8. *Given $\bar{\mathbf{z}}_0,\ \bar{\mathbf{z}}_f \in \mathbb{R}^\gamma$, $\boldsymbol{\Sigma}_{z_0},\ \boldsymbol{\Sigma}_{z_f} \in \mathbb{S}_+^\gamma$, if (4.36) holds true, an optimal solution of (4.17)–(4.18) exists on condition that $\alpha_0 \in \left(\alpha_0^l,\ 1\right)$ with α_0^l given in (4.35).*

It is noted from (4.35) that α_0^l gets smaller with the increase of the magnitude of $\bar{\mathbf{f}}$ for a given s and

$$\left\|\boldsymbol{\Sigma}_{z_0}^{-\frac{1}{2}}\bar{\mathbf{H}}_{f,s}\bar{\mathbf{f}}_s\right\|_2 \leq \left\|\boldsymbol{\Sigma}_{z_0}^{-\frac{1}{2}}\bar{\mathbf{H}}_{f,s}\right\|_\infty \left\|\bar{\mathbf{f}}_s\right\|_2 = \sigma_1\left\|\bar{\mathbf{f}}_s\right\|_2 \tag{4.37}$$

with σ_1 being the maximum singular value of matrix $\boldsymbol{\Sigma}_{z_0}^{-\frac{1}{2}}\bar{\mathbf{H}}_{f,s}$. Then, if

$$\left\|\bar{\mathbf{f}}_s\right\|_2 \leq \sigma_1^{-1} \tag{4.38}$$

the fault with magnitude not larger than σ_1^{-1} cannot be detected. The following theorem is thus derived providing a necessary condition of the worst-case fault detectability.

Theorem 4.9. *Given $\bar{\mathbf{z}}_0 \in \mathbb{R}^\gamma$, $\boldsymbol{\Sigma}_{z_0} \in \mathbb{S}_+^\gamma$, if a fault $\mathbf{f}(k)$ with $\mathbb{E}[\mathbf{f}] = \bar{\mathbf{f}}$ leading to (4.38), the worst-case FAR would be one.*

Algorithm 4.2.8 Data-driven realization of FD systems using improved DIO method

Offline design

1: Collect process I/O data in fault-free and concerned faulty cases. Identify the matrix $\mathbf{\Psi}_s^{\perp}$ using Algorithm 2.2.3.
2: Generate residual samples with (3.3) using process I/O data in fault-free and faulty cases. Then compute $\bar{\mathbf{z}}_0$, $\bar{\mathbf{z}}_f$, $\mathbf{\Sigma}_{z_0}$, $\mathbf{\Sigma}_{z_f}$ with (3.45).
3: Compute α_0^l using (4.35) and set $\alpha_0 \in (\alpha_0^l, 1)$.
4: Solve $\mathbf{w}_*$, β using Algorithm 4.2.7 and then compute $\boldsymbol{\vartheta}$, $\bar{r}_0$ with (4.39).

Online FD

1: Compute residual $r(k)$ and $J(r)$ with (4.40) at time step k.
2: Perform (4.2) to detect the occurrence of a fault.

4.2.4 Data-driven implementation

A data-driven realization of the above designed FD system is described in Algorithm 4.2.8. In the offline design stage, the residual generator (3.3) is first constructed by identifying the matrix $\mathbf{\Psi}_s^{\perp}$ using process I/O data. Then the empirical means $\bar{\mathbf{z}}_0$, $\bar{\mathbf{z}}_f$ and covariance matrices $\mathbf{\Sigma}_{z_0}$, $\mathbf{\Sigma}_{z_f}$ are computed with (3.45)–(3.46). Before solving the FD problem (4.3)–(4.4), an appropriate $\alpha_0 \in (\alpha_0^l, 1)$ should be set for the considered fault so as to ensure the existence of the optimal solution. By using Algorithm 4.2.7, the optimal parameter vector $\mathbf{w}_*$ is then obtained. Let

$$\boldsymbol{\vartheta} = \mathbf{w}_*^T \mathbf{\Psi}_s^{\perp}, \quad \bar{r}_0 = \mathbf{w}_*^T \bar{\mathbf{z}}_0. \tag{4.39}$$

For online FD purpose, compute the residual sequence and residual evaluation function in time step k by

$$r(k) = \boldsymbol{\vartheta} \begin{bmatrix} \mathbf{y}_s(k) \\ \mathbf{u}_s(k) \end{bmatrix}, \quad J(r) = (r(k) - \bar{r}_0)^2. \tag{4.40}$$

Then the occurrence of a fault can be detected by using the decision logic (4.2) with $J_{th} = 1$. The FAR and MDR are ensured not larger than α_0 and β, respectively.

4.3 Special cases discussion

In this part, we discuss the analytical solutions of the distribution independent FD problem (4.17)–(4.18) in two special scenarios, i.e., missing fault formation and the fault being deterministic signal. Some interesting results are presented below.

4.3.1 FD missing fault information

In some engineering applications, prior knowledge of faults and even historical process I/O samples in faulty case is unavailable, which result in inaccessible mean and covariance matrix of residual in faulty case and then infeasible solution of the proposed DIO method. In this situation, we propose to formulate the design of FD system regarding $\mathbf{w}$, residual evaluation function and threshold given in (4.1) as follows

$$\max_{\mathbf{w}\neq 0} \quad \left\|\mathbf{w}^T\bar{\mathbf{H}}_{f,s}\right\|_2^2 \quad \text{s.t.} \quad \sup_{\mathbb{P}_z\in\mathcal{P}_0} \Pr\left\{(\mathbf{w}^T(\mathbf{z}-\bar{\mathbf{z}}_0))^2>1\right\}\leq\alpha_0. \tag{4.41}$$

In this formulation, the DCC ensures FAR no larger than a given $\alpha_0\in(0,1)$, the objective, i.e., $\max_{\mathbf{w}\neq 0}\left\|\mathbf{w}^T\bar{\mathbf{H}}_{f,s}\right\|_2^2$, is posed aiming to minimize the MDR. Since for fixed threshold $J_{th}=1$, maximizing $\left\|\mathbf{w}^T\bar{\mathbf{H}}_{f,s}\right\|_2^2$ means minimizing the probability of $(\mathbf{w}^T(\mathbf{z}_f-\bar{\mathbf{z}}_0))^2=\left\|\mathbf{w}^T\bar{\mathbf{H}}_{f,s}\mathbf{f}_s\right\|_2^2\leq\left\|\mathbf{w}^T\bar{\mathbf{H}}_{f,s}\right\|_2^2\|\mathbf{f}_s\|_2^2\leq 1$ for unknown fault modes, i.e., minimizing the MDR.

According to Theorem 4.4, the problem (4.41) can be reformulated as follows

$$\max_{\mathbf{w}\neq 0} \quad \left\|\mathbf{w}^T\bar{\mathbf{H}}_{f,s}\right\|_2^2 \quad \text{s.t.} \quad \nu(\alpha_0)\sqrt{\mathbf{w}^T\boldsymbol{\Sigma}_{z_0}\mathbf{w}}\leq 1 \tag{4.42}$$

which follows

$$\max_{\mathbf{w}\neq 0} \quad \left\|\mathbf{w}^T\bar{\mathbf{H}}_{f,s}\right\|_2^2 \quad \text{s.t.} \quad \mathbf{w}^T\boldsymbol{\Sigma}_{z_0}\mathbf{w}\leq\alpha_0. \tag{4.43}$$

By introducing a Lagrangian function $L(\mathbf{w},\lambda)=-\left\|\mathbf{w}^T\bar{\mathbf{H}}_{f,s}\right\|_2^2+\lambda\left(\mathbf{w}^T\boldsymbol{\Sigma}_{z_0}\mathbf{w}-\alpha_0\right)$ with $\lambda\geq 0$, it holds at the optimum that

$$\frac{\partial L(\mathbf{w},\lambda)}{\partial\mathbf{w}}=0,\ \frac{\partial L(\mathbf{w},\lambda)}{\partial\lambda}=0 \ \Rightarrow\ \bar{\mathbf{H}}_{f,s}\bar{\mathbf{H}}_{f,s}^T\mathbf{w}=\lambda\boldsymbol{\Sigma}_{z_0}\mathbf{w},\ \mathbf{w}^T\boldsymbol{\Sigma}_{z_0}\mathbf{w}=\alpha_0. \tag{4.44}$$

Do an SVD on $\boldsymbol{\Sigma}_{z_0}^{\frac{1}{2}}$, the optimal solution of (4.43) is then obtained as

$$\mathbf{w}=\sqrt{\alpha_0}\bar{\mathbf{U}}\bar{\mathbf{S}}^{-1}\bar{\mathbf{v}} \tag{4.45}$$

with $\bar{\mathbf{v}}$ solving the equations (4.33). Then it obviously holds for $\bar{\lambda}_m$ given in (4.34) that

$$\max_{\mathbf{w}\neq 0}\left\|\mathbf{w}^T\bar{\mathbf{H}}_{f,s}\right\|_2^2=\alpha_0\bar{\lambda}_m.$$

Note that a fault can be detected on condition that $\alpha_0\bar{\lambda}_m>1$, i.e., $\sqrt{\bar{\lambda}_m}>\nu(\alpha_0)$. From the viewpoint of geometric, the residual evaluation function given in (4.1) is actually a Mahalanobis distance of $\mathbf{z}$ from the mean vector $\bar{\mathbf{z}}_0$, i.e., $(\mathbf{w}^T(\mathbf{z}-\bar{\mathbf{z}}_0))^2=\alpha_0\left\|\bar{\mathbf{v}}^T\bar{\mathbf{S}}^{-1}\bar{\mathbf{U}}^T(\mathbf{z}-\bar{\mathbf{z}}_0)\right\|_2^2$. In this context, given the FAR not greater than α_0, it is easy to understand that, a fault is expected to be detected when the Mahalanobis distance of $\mathbf{z}$ from $\bar{\mathbf{z}}_0$ in the direction of $\tilde{\mathbf{v}}$ is larger than $\nu(\alpha_0)$.

4.3.2 Deterministic fault detection

Consider the situation that the concerned fault is deterministic, i.e., $\mathbb{V}[\mathbf{f}] = 0$, then $\mathbf{\Sigma}_{z_0} = \mathbf{\Sigma}_{z_f}$. With respect to the FD problem (4.3)–(4.4), a distribution independent form of it can then be described by (4.17)–(4.18) with $\mathbf{\Sigma}_{z_f} = \mathbf{\Sigma}_{z_0}$, i.e.,

$$\min_{\mathbf{w}\neq 0} \quad \beta \tag{4.46}$$

$$\text{s.t.} \quad \begin{cases} \nu(\alpha_0)\sqrt{\mathbf{w}^T\mathbf{\Sigma}_{z_0}\mathbf{w}} \leq 1 \\ \sqrt{\mathbf{w}^T\tilde{\mathbf{z}}_f\tilde{\mathbf{z}}_f^T\mathbf{w}} - \kappa(\beta)\sqrt{\mathbf{w}^T\mathbf{\Sigma}_{z_0}\mathbf{w}} \geq 1. \end{cases} \tag{4.47}$$

which, according to the results in Section 4.2.2, can be solved by addressing

$$\max_{\mathbf{w}\neq 0} \quad \frac{\mathbf{w}^T\tilde{\mathbf{z}}_f\tilde{\mathbf{z}}_f^T\mathbf{w}}{\mathbf{w}^T\mathbf{\Sigma}_{z_0}\mathbf{w}} \quad \text{s.t.} \quad \nu(\alpha_0)\sqrt{\mathbf{w}^T\mathbf{\Sigma}_{z_0}\mathbf{w}} = 1. \tag{4.48}$$

To this end, we first solve the unconstrained problem $\max_{\mathbf{w}\neq 0} \frac{\mathbf{w}^T\tilde{\mathbf{z}}_f\tilde{\mathbf{z}}_f^T\mathbf{w}}{\mathbf{w}^T\mathbf{\Sigma}_{z_0}\mathbf{w}}$ for $\mathbf{w}$ by means of SVD, the solution is given in (4.32). Then the optimal solution $\mathbf{w}_*$ to (4.46)–(4.47) can be obtained by dividing a constant to $\mathbf{w}$ in (4.32) such that $\nu(\alpha_0)\sqrt{\mathbf{w}_*^T\mathbf{\Sigma}_{z_0}\mathbf{w}_*} = 1$ holds. At the optimum, we have

$$\mathbf{w}_* = \frac{\mathbf{w}}{\nu(\alpha_0)\sqrt{\mathbf{w}^T\mathbf{\Sigma}_{z_0}\mathbf{w}}}, \ \kappa(\beta) = \sqrt{\bar{\lambda}_m} - \nu(\alpha_0), \ \beta = \frac{1}{1+\kappa^2(\beta)} \tag{4.49}$$

with $\mathbf{w}$ and $\bar{\lambda}_m$ being given in (4.32) and (4.34), respectively. To ensure $\kappa(\beta) > 0$, the prescribed FAR should be given such that $\alpha_0 \in (\alpha_0^l, 1)$, as summarized in Theorem 4.8.

On the other hand, given acceptable FAR and MDR, we can derive a sufficient condition of the existence of the optimal solution to the problem (4.47)–(4.46) with respect to the magnitude of fault. It yields from the DCCs (4.47) that

$$\mathbf{w}^T\left(\tilde{\mathbf{z}}_f\tilde{\mathbf{z}}_f^T - (\kappa(\beta)+\nu(\alpha_0))^2\mathbf{\Sigma}_{z_0}\right)\mathbf{w} \geq 0.$$

Therefore, a nonzero $\mathbf{w}$ exists on condition that

$$\left\|\mathbf{\Sigma}_{z_0}^{-\frac{1}{2}}\tilde{\mathbf{z}}_f\right\|_2 = \left\|\mathbf{\Sigma}_{z_0}^{-\frac{1}{2}}\bar{\mathbf{H}}_{f,s}\bar{\mathbf{f}}_s\right\|_2 \geq \kappa(\beta) + \nu(\alpha_0). \tag{4.50}$$

It implies that, a deterministic fault $\mathbf{f}$ can be detected with FAR and MDR not larger than α_0 and β, respectively, on condition that (4.50) holds.

Hence, when no fault information is available, another alternative solution is to set a so-called reference constant fault vector with $\bar{\mathbf{f}} = \mathbf{f}_{ref} \neq 0$, $\mathbb{V}[\mathbf{f}] = 0$ and then solve the FD problem (4.46)–(4.47) for an optimal $\mathbf{w}_*$. In this context, any fault with the magnitude of mean larger than $\mathbf{f}_{ref}$ can be detected with probability not smaller than $1-\beta$ for given FAR no larger than α_0. Besides, the value of $\mathbf{f}_{ref}$ for expected α_0, β can be determined according to (4.50).

4.4 Summary and notes

In this chapter, an improved DIO approach has been developed for the design of data-driven FD systems achieving a minimum MDR for a given FAR. By constructing the residual generator using process I/O data, the FD issue subject to distributional ambiguity has been formulated as an SP problem with DCCs. Then an equivalent DIO representation of the targeting FD problem has been derived. It has been further proven that the formulated DIO problem can be addressed by solving a generalized eigenvalue-eigenvector problem. An analytical solution has thus been achieved by means of an SVD. Moreover, the existence condition of the optimal solution has been studied. In comparison with the DIO method in Chapter 3, a tighter upper bound of MDR for an identical FAR can be achieved with a lower computational cost. In the end, alternative solutions to the improved DIO approach aided FD in the situations of inaccessible fault information and deterministic faults have been discussed.

5 Matrix-valued DIO approaches to FD systems design

In Chapters 3 and 4, vector-valued DIO approaches have been studied to cope with data-driven FD issues for stochastic dynamic processes, in which the fault is considered to be in a certain mode with features of mean and covariance matrix of residual. Despite the achieved results, the following concerns arising from the perspective of practical application are worth mentioning.

- The introduced parameter vector is designed such that the residual signal is mostly sensitive to the concerned fault mode. In practice, however, the underlying fault in the monitored process is generally unpredictable in advance that a poor MDR might be delivered when a fault occurs deflecting the concerned fault in the offline design stage in type, direction and magnitude, etc.

- In engineering applications, historical process I/O data in some faulty scenarios might be merely accessible, which results in unreliable moments information of residual in faulty cases.

For the first consideration, one natural remedy is to apply a bank of parameter vectors to generate a group of residual generators and each of them is designed to be sensitive to a certain kind of fault pattern, see, e.g., [74, 89]. Nevertheless, this exhaustive strategy might cause a higher FAR on the one hand and, cannot cope well with the faults without reliable moments knowledge on the other hand, as mentioned in the second point.

For the above observations, in this chapter matrix-valued solutions to the DIO scheme aided design of FD systems are developed both for the cases of available and unavailable prior knowledge of faults. With the introduction of a parameter matrix rather than a vector to a data-driven residual generator, the design of FD systems is first formulated as an SP problem with DCCs in the context of minimizing the MDR for a prescribed FAR. Concerning available knowledge of faults in different modes, three configurations of FD systems, named the multivector-valued solution, the WC-CVaR aided solution and the optimal matrix-valued solution, are developed with respect to solving the targeting SP problem by means of SDP. Successively, without fault information, the matrix-valued DIO solutions to the design of FD systems are investigated.

5.1 Problem formulation

On the basis of generating the signal $\mathbf{z}(k) \in \mathbb{R}^{\gamma}$ with (3.3) using process I/O data, we introduce a parameter matrix $\mathbf{W} \in \mathbb{R}^{\gamma \times \eta}$ and construct the residual generator in the following form

$$\mathbf{r}(k) = \mathbf{W}^T \mathbf{z}(k) \tag{5.1}$$

where $\mathbf{r}(k) \in \mathbb{R}^{\eta}$ is the residual vector, $\mathbf{W} \neq 0$. Followed by residual generation, a residual evaluation function $J(\mathbf{r})$ and a threshold J_{th} should be determined such that the occurrence of a fault can be detected by performing

$$\begin{cases} J(\mathbf{r}) > J_{th} & \Rightarrow \text{fault alarm} \\ J(\mathbf{r}) \leq J_{th} & \Rightarrow \text{no alarm.} \end{cases} \tag{5.2}$$

Oriented by the requirement of satisfactory FD performance, we consider to design the matrix $\mathbf{W}$, residual evaluation function $J(\mathbf{r})$ and threshold J_{th} towards minimizing the MDR for a given FAR. Disregarding perfect distributions for noises and faults, we refer to ambiguity sets $\mathcal{P}_0$ in (3.17) and $\mathcal{P}_f$ in (3.18) and formulate the design of FD system as

$$\min_{\mathbf{W} \neq 0,\, J(\mathbf{r}),\, J_{th}} \quad \beta \tag{5.3}$$

$$\text{s.t.} \quad \begin{cases} \sup\limits_{\mathbb{P}_z \in \mathcal{P}_0} \Pr\{J(\mathbf{r}) > J_{th}\} \leq \alpha_0 \\ \sup\limits_{\mathbb{P}_z \in \mathcal{P}_f} \Pr\{J(\mathbf{r}) \leq J_{th}\} \leq \beta \end{cases} \tag{5.4}$$

where $\alpha_0 \in (0, 1)$ is a given upper bound of FAR, $\beta \in (0, 1)$ is the upper bound of MDR. It is remarkable that, when the fault $\mathbf{f}(k)$ is known in prior of certain mode with features of mean and covariance matrix, vector-valued solutions of $\mathbf{W}$ with $\eta = 1$ to the problem (5.3)–(5.4) have been given in Chapters 3 and 4, while a higher MDR might be delivered when a fault occurs in other pattern during online FD. The parameter matrix $\mathbf{W}$ with $\eta > 1$ is adopted for this reason, which allows more freedom of design of FD systems towards a lower MDR.

Hence, the main objectives of this chapter are to address design issues of FD systems with respect to

- solving the FD problem (5.3)–(5.4) with known fault information, the key of which lies in handling the DCCs (5.4) without precise distributional information of noises and faults and
- dealing with the FD problem (5.3)–(5.4) without prior knowledge of fault.

5.2 Multivector-valued design

Despite the unpredictable knowledge of faults in practice, the engineer can usually design FD systems to detect some possible faults in different patterns such that the most of the underlying faults can be detected with high probability. Keeping this in mind, a multivector-valued solution to the FD problem (5.3)–(5.4) is first investigated below.

5.2.1 System configuration

Without loss of generality, we parametrize the fault mode with the features of mean and covariance matrix. Denote by $\mathbf{f}_i(k)$ the fault signal in i-th faulty scenario and

$$\mathbf{z}_{f_i}(k) = \mathbf{z}(k)\,\big|_{\mathbf{f}_i(k)\neq 0}\ ,\ i = 1,\, 2,\, \ldots,\, M$$

where M is the number of the concerned fault patterns. Let $\bar{\mathbf{f}}_{is} = \mathbb{E}[\mathbf{f}_{is}]$, $\mathbf{\Sigma}_{f_{is}} = \mathbb{V}[\mathbf{f}_{is}]$ with $\mathbf{f}_{is}(k) = \mathbf{f}_s(k)|_{\mathbf{f}(k)=\mathbf{f}_i(k)}$. The mean and covariance matrix of $\mathbf{z}_{f_i}(k)$ are obtained as

$$\bar{\mathbf{z}}_{f_i} = \mathbb{E}[\mathbf{z}_{f_i}] = \bar{\mathbf{z}}_0 + \bar{\mathbf{H}}_{f,s}\bar{\mathbf{f}}_{is},\ \mathbf{\Sigma}_{z_{f_i}} = \mathbb{V}[\mathbf{z}_{f_i}] = \mathbf{\Sigma}_{z_0} + \bar{\mathbf{H}}_{f,s}\mathbf{\Sigma}_{f_{is}}\bar{\mathbf{H}}_{f,s}^T.$$

Let P_{f_i} be the probability of the occurrence of i-th fault. It holds

$$\mathrm{P}_{f_i} \in [0,\, 1],\ i = 1,\, 2,\, \ldots,\, M,\ \sum_{i=1}^{M} \mathrm{P}_{f_i} = 1.$$

In case of unavailable prior knowledge of P_{f_i}, we can generally set $\mathrm{P}_{f_i} = \frac{1}{M}$. Given known $\bar{\mathbf{z}}_{f_i}$, $\mathbf{\Sigma}_{z_{f_i}}$, we introduce a family of confidence sets of $\mathbb{P}_z$ for M faulty cases as follows

$$\mathcal{P}_{f_i} = \left\{ \mathbb{P}_z \in \mathcal{L} \,\middle|\, \mathbb{E}[\mathbf{z}] = \bar{\mathbf{z}}_{f_i},\ \ \mathbb{V}[\mathbf{z}] = \mathbf{\Sigma}_{z_{f_i}} \in \mathbb{S}_+^{\gamma} \right\},\ i = 1,\, 2,\, \ldots,\, M \tag{5.5}$$

and redefine the ambiguity set in faulty cases as a set of $\mathcal{P}_{f_i}$, i.e.,

$$\mathcal{P}_f = \bigcup_{i=1}^{M} \mathcal{P}_{f_i},\quad \Pr\{\mathbb{P}_z \in \mathcal{P}_{f_i}\} = \mathrm{P}_{f_i},\ i = 1,\, 2,\, \ldots,\, M. \tag{5.6}$$

On this basis, we rewrite the matrix $\mathbf{W}$ in a column-wised form with $\eta = M$, i.e.,

$$\mathbf{W} = \begin{bmatrix} \mathbf{w}_1 & \mathbf{w}_2 & \cdots & \mathbf{w}_M \end{bmatrix} \in \mathbb{R}^{\gamma\times M} \tag{5.7}$$

where $\mathbf{w}_i \in \mathbb{R}^{\gamma}$ is termed the i-th parameter vector. The residual signal in (5.1) is then obtained as

$$\mathbf{r}(k) = \begin{bmatrix} r_1(k) \\ r_2(k) \\ \vdots \\ r_M(k) \end{bmatrix},\ r_i(k) = \mathbf{w}_i^T\mathbf{z}(k),\ i = 1,\, 2,\, \ldots,\, M. \tag{5.8}$$

In this context, the design of matrix $\mathbf{W}$ is formulated as the design of a bank of parameter vectors $\mathbf{w}_i$, $i = 1, 2, ..., M$. Let

$$\bar{r}_{i,0} = \mathbf{w}_i^T \bar{\mathbf{z}}_0,\ i = 1,\ 2,\ \ldots,\ M. \tag{5.9}$$

Define the residual evaluation functions and thresholds as follows

$$J(r_i) = (r_i(k) - \bar{r}_{i,0})^2,\ J_{th,i} = b_i,\ i = 1,\ 2,\ \ldots,\ M \tag{5.10}$$

where $b_i > 0$. The following decision logic is then used for FD

$$\begin{cases} \exists i, & J(r_i) > J_{th,i} & \Rightarrow & \text{fault alarm} \\ \forall i, & J(r_i) \leq J_{th,i} & \Rightarrow & \text{no alarm.} \end{cases} \tag{5.11}$$

In this formulation, the FD system is actually divided into a bank of subsystems in terms of $\mathbf{w}_i$, b_i, $i = 1,\ 2,\ \ldots\ M$, see the diagram in Fig. 5.1. Analogy to the Definitions 2.47 and 2.48, we define the FAR and MDR with respect to i-th fault mode respectively by

$$P_{FAR_i} = \Pr\{J(r_i) > J_{th,i}\,|\mathbf{f}(k) = 0\} \tag{5.12}$$

$$P_{MDR_i} = \Pr\{J(r_i) \leq J_{th,i}\,|\mathbf{f}_i(k) \neq 0\}. \tag{5.13}$$

By substituting (5.9) into (5.10), the design of $\mathbf{w}_i, , b_i$ for i-th FD subsystem regarding the ambiguity set $\mathcal{P}_{f_i}$ is formulated as follows

$$\min_{\mathbf{w}_i \neq 0,\ b_i > 0} \quad \beta_i \tag{5.14}$$

$$\text{s.t.} \quad \begin{cases} \sup\limits_{\mathbb{P}_z \in \mathcal{P}_0} \Pr\left\{(\mathbf{w}_i^T(\mathbf{z} - \bar{\mathbf{z}}_0))^2 > b_i\right\} \leq \alpha_0 \\ \sup\limits_{\mathbb{P}_z \in \mathcal{P}_{f_i}} \Pr\left\{(\mathbf{w}_i^T(\mathbf{z} - \bar{\mathbf{z}}_0))^2 \leq b_i\right\} \leq \beta_i \end{cases} \tag{5.15}$$

where $\alpha_0 \in (0, 1)$ is the prescribed upper bound of P_{FAR_i}, $\beta_i \in (0, 1)$ is the upper bound of P_{MDR_i}. Clearly, the formulation (5.14)–(5.15) searches for the optimal $\mathbf{w}_i$, b_i towards minimizing the i-th MDR for a given FAR not larger than α_0. In this regard, the original FD problem (5.3)–(5.4) with respect to matrix $\mathbf{W}$ is reformulated as solving a bank of vector-valued problems in form of (5.14)–(5.15) with $i = 1,\ 2,\ \ldots,\ M$ separately.

5.2.2 Optimal solution

Note that the magnitude of $\|\mathbf{w}_i\|_2$, b_i would not influence the optimal solution of problem (5.14)–(5.15). Then, we set $b_i = 1$, $i = 1,\ 2,\ \ldots,\ M$. According to Theorems 4.4 and 4.5,

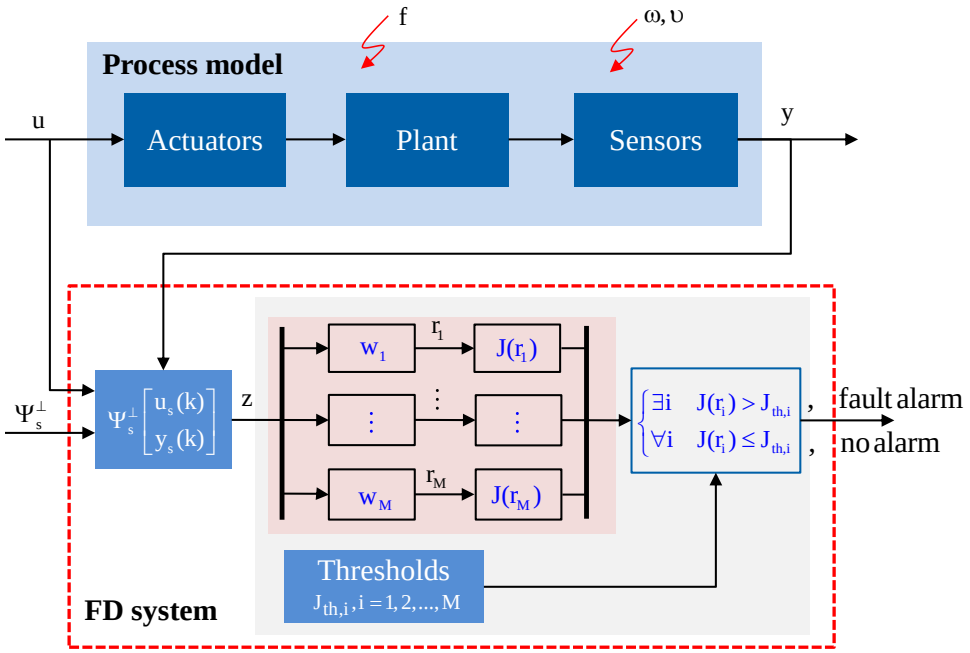

Figure 5.1: Diagram of multivector-valued configuration of FD systems.

the problem (5.14)–(5.15) is equally re-written as the following DIO form

$$\min_{\mathbf{w}_i \neq 0} \quad \beta_i \tag{5.16}$$

$$\text{s.t.} \quad \begin{cases} \nu(\alpha_0)\sqrt{\mathbf{w}_i^T \boldsymbol{\Sigma}_{z_0} \mathbf{w}_i} \leq 1 \\ \sqrt{\mathbf{w}_i^T \tilde{\mathbf{z}}_{f_i} \tilde{\mathbf{z}}_{f_i}^T \mathbf{w}_i} - \kappa(\beta_i)\sqrt{\mathbf{w}^T \boldsymbol{\Sigma}_{z_{f_i}} \mathbf{w}_i} \geq 1. \end{cases} \tag{5.17}$$

where $\nu(\alpha_0) = \sqrt{1/\alpha_0}$, $\kappa(\beta_i) = \sqrt{(1-\beta_i)/\beta_i}$, $\tilde{\mathbf{z}}_{f_i} = \bar{\mathbf{z}}_{f_i} - \bar{\mathbf{z}}_0$.

As presented in Section 4.2.2, an analytical solution to (5.16)–(5.17) can be achieved by means of SVD, as presented in Theorem 4.6. Let $\tilde{\boldsymbol{\Sigma}}_i = \tilde{\mathbf{z}}_{f_i} \tilde{\mathbf{z}}_{f_i}^T - \nu^2(\alpha_0)\boldsymbol{\Sigma}_{z_0}$. Do an SVD on $\boldsymbol{\Sigma}_{z_{f_i}}^{\frac{1}{2}}$, i.e., $\boldsymbol{\Sigma}_{z_{f_i}}^{\frac{1}{2}} = \mathbf{U}_i \left[\mathbf{S}_i \;\; 0\right] \mathbf{V}_i^T$, $\mathbf{U}_i \mathbf{U}_i^T = \mathbf{I}$, $\mathbf{V}_i \mathbf{V}_i^T = \mathbf{I}$. Let

$$\tilde{\mathbf{w}}_i = \mathbf{U}_i \mathbf{S}_i^{-1} \mathbf{v}_i \tag{5.18}$$

with $\mathbf{v}_i$ solving the following equations

$$\mathbf{v}_i^T (\lambda_{m,i} \mathbf{I} - \mathbf{S}_i^{-1} \mathbf{U}_i^T \tilde{\boldsymbol{\Sigma}}_i \mathbf{U}_i \mathbf{S}_i^{-1}) \mathbf{v}_i = 0, \; \mathbf{v}_i^T \mathbf{v}_i = 1 \tag{5.19}$$

where $\lambda_{m,i} = \lambda_{max} \left\{ \mathbf{S}_i^{-1} \mathbf{U}_i^T \tilde{\boldsymbol{\Sigma}}_i \mathbf{U}_i \mathbf{S}_i^{-1} \right\}$. The optimal solutions of $\mathbf{w}_i$, β_i to the problem

(5.16)–(5.17) are then obtained as follows

$$\mathbf{w}_i = \frac{\tilde{\mathbf{w}}_i}{\nu(\alpha_0)\sqrt{\tilde{\mathbf{w}}_i^T \boldsymbol{\Sigma}_{z_0} \tilde{\mathbf{w}}_i}},\ \kappa(\beta_i) = \frac{\sqrt{\mathbf{w}_i^T \tilde{\mathbf{z}}_{f_i} \tilde{\mathbf{z}}_{f_i}^T \mathbf{w}_i} - 1}{\sqrt{\mathbf{w}_i^T \boldsymbol{\Sigma}_{z_{f_i}} \mathbf{w}_i}},\ \beta_i = \frac{1}{1+\kappa^2(\beta_i)}. \tag{5.20}$$

For online realization purpose, the residual vector is generated with (5.8) and then FD is carried out by performing (5.10) and (5.11) with $J_{th,i} = 1$, $i = 1, 2, \ldots, M$. The algorithm for the multivector-valued solution to FD problem (5.3)–(5.4) is summarized in Algorithm 5.2.9.

Remark 5.1. *As mentioned in Section 4.2.3, an appropriate α_0 should be set to guarantee the existence of the optimal solution to the problem (5.16)–(5.17) with $i = 1, 2, \ldots, M$. To this end, denote by $\alpha_{0,i}^l$ the lower bound of α_0 for the i-th faulty case. Recalling (4.35), we then have*

$$\alpha_{0,i}^l = \frac{1}{\tilde{\mathbf{z}}_{f_i}^T \boldsymbol{\Sigma}_{z_0}^{-1} \tilde{\mathbf{z}}_{f_i}}. \tag{5.21}$$

The value of α_0 is thus selected satisfying

$$\alpha_0 \in (\alpha_{0,max}^l, 1),\ \alpha_{0,max}^l = \max_{i=1,2,\ldots,M} \{\alpha_{0,i}^l\}. \tag{5.22}$$

5.2.3 Worst-case FAR and MDR

It is notable that the upper bounds of FAR and MDR for each FD subsystem are tight with respect to the corresponding ambiguity set $\mathcal{P}_{f_i}$, as proven in Chapter 4. Since these subsystems are designed separately, it is necessary to discuss the worst-case FAR and MDR criteria of the FD system regarding $\mathcal{P}_f = \bigcup_{i=1}^{M} \mathcal{P}_{f_i}$.

Algorithm 5.2.9 Multivector-valued configuration of FD systems

Offline design

1: Estimate $\bar{\mathbf{z}}_0, \boldsymbol{\Sigma}_{z_0}, \bar{\mathbf{z}}_{f_i}, \boldsymbol{\Sigma}_{z_{f_i}}, i = 1, 2, ..., M$using process I/O data and compute $\alpha_{0,i}^l$ with (5.21). Set α_0 satisfying (5.22).

2: For $i = 1, 2, \ldots M$, solve (5.19) for $\tilde{\mathbf{w}}_i$ and compute $\mathbf{w}_i$, β_i and $\bar{r}_{i,0}$ with (5.20) and (5.9), respectively.

Online FD

1: Compute $r_i(k)$ and $J(r_i)$ for $i = 1, 2, \ldots M$ with (5.8) and (5.10), respectively.

2: Perform decision logic (5.11) to detect the occurrence of a fault.

According to Definitions 2.47 and 2.48, the FAR and MDR of the multivector-valued FD system can be written as follows

$$P_{FAR} = \Pr\left\{\exists i,\ J(r_i) > J_{th,i} \,|\mathbf{f}(k) = 0\right\} \tag{5.23}$$

$$P_{MDR} = \Pr\left\{\forall i,\ J(r_i) \leq J_{th,i} \,|\mathbf{f}(k) \neq 0\right\}. \tag{5.24}$$

Note from the Bonferroni inequality that

$$\begin{aligned}\sup_{\mathbb{P}_z \in \mathcal{P}_0} \Pr\left\{\exists i, J(r_i) > J_{th,i}\right\} &= \sup_{\mathbb{P}_z \in \mathcal{P}_0} \Pr\left\{\bigcup_{i=1}^{M}\left\{J(r_i) > J_{th,i}\right\}\right\} \\ &\leq \sum_{i=1}^{M} \sup_{\mathbb{P}_z \in \mathcal{P}_0} \Pr\left\{J(r_i) > J_{th,i}\right\} \\ &\leq M\alpha_0. \end{aligned} \tag{5.25}$$

It implies that the worst-case FAR of the FD system is $M\alpha_0$, i.e., $P_{FAR} \leq M\alpha_0$.

For the MDR criterion, we recall the ambiguity set $\mathcal{P}_f$ defined in (5.6) and note that

$$\begin{aligned}\sup_{\mathbb{P}_z \in \mathcal{P}_f} \Pr\left\{\forall i, J(r_i) \leq J_{th,i}\right\} &= 1 - \inf_{\mathbb{P}_z \in \mathcal{P}_f} \Pr\left\{\exists i, J(r_i) > J_{th,i}\right\} \\ &= 1 - \left(1 - \min_{i=1,2,\ldots,M}\left\{\sup_{\mathbb{P}_z \in \mathcal{P}_{f_i}} \Pr\left\{J(r_i) \leq J_{th,i}\right\}\right\}\right) \\ &= \min_{i=1,2,\ldots,M}\{\beta_i\} \end{aligned} \tag{5.26}$$

which shows that the MDR of the FD system is obtained satisfying $P_{MDR} \leq \min_{i=1,2,\ldots,M}\{\beta_i\}$.

From the viewpoint of FD performance evaluation, it should be pointed out that the values $M\alpha_0$ and $\min_{i=1,2,\ldots,M}\{\beta_i\}$ are the worst-case upper bounds of FAR and MDR, respectively, which sometimes are too pessimistic in practical applications. To alleviate this deficiency, the so-called average FAR and MDR criteria are introduced as follows

$$\bar{P}_{FAR} = \frac{1}{M}\sum_{i=1}^{M} P_{FAR_i},\ \bar{P}_{MDR} = \sum_{i=1}^{M} P_{MDR_i}\mathrm{P}_{f_i}. \tag{5.27}$$

In this fashion, the average FAR and MDR of the multivector-valued FD system satisfy

$$\bar{P}_{FAR} \leq \alpha_0,\ \bar{P}_{MDR} \leq \sum_{i=1}^{M} \beta_i \mathrm{P}_{f_i}. \tag{5.28}$$

Together with (5.21) and (5.25), it is remarkable that, the upper bound of P_{FAR_i}, i.e., α_0 in (5.4), should be set satisfying $\alpha_0 \in (\alpha^l_{0,max}, \frac{1}{M}]$ with $\alpha^l_{0,max}$ given in (5.22) because of $P_{FAR} \in [0, 1]$. This fact implies that the upper bound of the feasible interval of α_0 gets

smaller with the increase of the number of fault modes. For this reason, on the one hand, the existence condition of the optimal solution to problem (5.16)–(5.17) might not be ensured when $\exists i,\ \alpha_{0,i}^{l} > \frac{1}{M}$. On the other hand, a much higher MDR would be delivered when a prescribed FAR smaller than $\frac{1}{M}$ is given. For these concerns, the multivector-valued configuration with respect to solving the problem (5.16)–(5.17) is not a good choice to handle design issues of FD systems regarding solving the problem (5.3)–(5.4).

5.3 Worst-case CVaR aided design

To achieve tighter upper bounds of FAR and MDR of the multivector-valued FD system, a WC-CVaR aided solution to (5.3)–(5.4) is proposed in this part.

5.3.1 System configuration

Recalling the column-wised matrix $\mathbf{W}$ in (5.7) and the definitions of P_{FAR_i} in (5.12) and P_{MDR_i} in (5.13), we define the following residual evaluation function and threshold

$$J(\mathbf{r}) = \max_{i=1,\,2,\,\ldots,\,M} J(r_i),\ J_{th} = b \tag{5.29}$$

where $b > 0$, $J(r_i)$ is given in (5.10). In this setting, the FD problem (5.3)–(5.4) with decision logic (5.2) is re-written as follows

$$\min_{\mathbf{w}_i \neq 0,\, i=1,\,2,\,\ldots,\,M,\, b>0} \quad \beta \tag{5.30}$$

$$\text{s.t.} \quad \begin{cases} \sup\limits_{\mathbb{P}_z \in \mathcal{P}_0} \Pr\{J(\mathbf{r}) > b\} \leq \alpha_0 \\ \sup\limits_{\mathbb{P}_z \in \mathcal{P}_f} \Pr\{J(\mathbf{r}) \leq b\} \leq \beta. \end{cases} \tag{5.31}$$

Given $b_i = b$, $i = 1,\,2,\,\ldots,\,M$, it clearly holds

$$\begin{aligned} J(\mathbf{r}) > b \ &\Leftrightarrow \ \max_{i=1,\,2,\,\ldots,\,M} J(r_i) > b \ \Rightarrow \ \exists i,\ J(r_i) > b_i \\ J(\mathbf{r}) \leq b \ &\Leftrightarrow \ \max_{i=1,\,2,\,\ldots,\,M} J(r_i) \leq b \ \Rightarrow \ \forall i,\ J(r_i) \leq b_i \end{aligned}$$

which reveals that the formulation (5.30)–(5.31) allows an integrated design of the parameter vectors $\mathbf{w}_i$, $i = 1,\,2,\,\ldots,\,M$ and the threshold in the context of minimizing the MDR for a prescribed FAR. The diagram of the FD system is sketched in Fig. 5.2.

Note that the key of solving the FD problem (5.30)–(5.31) lies in dealing with the DCCs (5.31), which is notoriously difficult. Thanks to the arising efforts on the study of the connection between DCC and WC-CVaR condition [78, 15, 94, 29, 10], below we endeavor to cope with the DCCs (5.31) with WC-CVaR approximations in the probabilistic context such that the problem (5.30)–(5.31) can be handled with SDP.

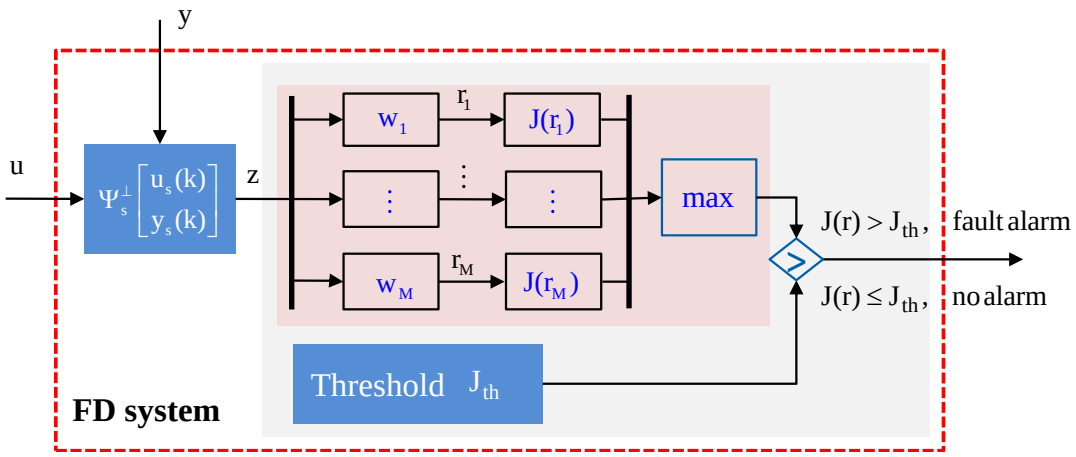

Figure 5.2: Diagram of WC-CVaR aided configuration of FD systems.

5.3.2 Optimal solution

Given $J(r_i)$ in (5.10), we start with introducing the following functions

$$L_i(r_i) = J(r_i) - b,\ i = 1, 2, \ldots, M. \tag{5.32}$$

Let $\tilde{\mathbf{z}} = \mathbf{z} - \bar{\mathbf{z}}_0$, $\mathbf{Q}_i = \mathbf{w}_i\mathbf{w}_i^T$. By substituting (5.10) into (5.32), it follows

$$L_i(r_i) = L_i(\tilde{\mathbf{z}}) = \tilde{\mathbf{z}}^T\mathbf{Q}_i\tilde{\mathbf{z}} - b,\ i = 1, 2, \ldots, M. \tag{5.33}$$

Define a function $L(\tilde{\mathbf{z}})$ over $\tilde{\mathbf{z}}$ in the following form

$$L(\tilde{\mathbf{z}}) = \max_{i=1,2,\ldots,M} L_i(\tilde{\mathbf{z}}). \tag{5.34}$$

For $\mathbf{Q}_i \in \mathbb{S}_+^\gamma$ and the convexity of $L_i(\tilde{\mathbf{z}})$, $i = 1, 2, \ldots, M$, the function $L(\tilde{\mathbf{z}})$ is convex over $\tilde{\mathbf{z}}$. The DCCs in (5.31) therefore satisfy

$$\sup_{\mathbb{P}_z\in\mathcal{P}_0} \Pr\{J(\mathbf{r}) > b\} \le \alpha_0 \quad \Leftrightarrow \quad \inf_{\mathbb{P}_z\in\mathcal{P}_0} \Pr\{L(\tilde{\mathbf{z}}) \le 0\} \ge 1 - \alpha_0 \tag{5.35}$$

$$\sup_{\mathbb{P}_z\in\mathcal{P}_f} \Pr\{J(\mathbf{r}) \le b\} \le \beta \quad \Leftrightarrow \quad \inf_{\mathbb{P}_z\in\mathcal{P}_f} \Pr\{L(\tilde{\mathbf{z}}) \ge 0\} \ge 1 - \beta. \tag{5.36}$$

Towards deterministic representations of DCCs in (5.35)–(5.36), the following theorem according to the results in [93] is first recalled, which suggests a tractable WC-CVaR approximation of a DCC.

Theorem 5.1. *([93] Theorem 3.2) Given $\boldsymbol{\xi} \in \mathbb{R}^n$, strictly positive parameters $\epsilon_i \in \mathcal{A} = \{\epsilon :\ \epsilon > 0\}$ and*

$$L_i(\boldsymbol{\xi}) = \boldsymbol{\xi}^T\mathbf{E}_i\boldsymbol{\xi} + 2\mathbf{e}_i^T\boldsymbol{\xi} + \mathrm{e}_i^0 \tag{5.37}$$

with $\mathbf{E}_i \in \mathbb{S}_+^n$, $\mathrm{e}_i^0 \in \mathbb{R}$, $i = 1, 2, ..., M$, *define a loss function*

$$L^{\epsilon}(\boldsymbol{\xi}) = \max_{i=1,2,...,M} \epsilon_i L_i(\boldsymbol{\xi}). \tag{5.38}$$

For fixed ϵ_i, *it holds*

$$\sup_{\mathbb{P}_\xi \in \mathcal{P}} \mathbb{P} - \mathrm{CVaR}_\rho \left(L^{\epsilon}(\boldsymbol{\xi})\right) \leq 0 \quad \Rightarrow \quad \inf_{\mathbb{P}_\xi \in \mathcal{P}} \Pr\left\{L_i(\boldsymbol{\xi}) \leq 0,\, \forall i = 1, 2, ..., M\right\} \geq 1 - \rho.$$

Note that $\max_{i=1,2,...,M} L_i(\tilde{\mathbf{z}}) \leq 0$ means $L_i(\tilde{\mathbf{z}}) \leq 0$, $\forall i = 1, 2, ..., M$. According to Theorem 5.1, The DCCs in (5.35) can be substituted by

$$\sup_{\mathbb{P}_z \in \mathcal{P}_0} \mathbb{P} - \mathrm{CVaR}_{\alpha_0} \left(L(\tilde{\mathbf{z}})\right) \leq 0. \tag{5.39}$$

Moreover, it has been proven in [76] that a WC-CVaR condition can be described as an SDP, as demonstrated in the following theorem.

Theorem 5.2. *[76] Using the notations in 4.2, given* $\boldsymbol{\xi} \in \mathbb{R}^n$, $\mathbf{M}_\xi$ *in (4.5) and a loss function (5.38) with* $L_i(\boldsymbol{\xi})$ *in (5.37), the* WC-CVaR *is equivalent to a tractable SDP, i.e,*

$$\begin{aligned} \sup_{\mathbb{P}_\xi \in \mathcal{P}} \mathbb{P} - \mathrm{CVaR}_\rho \left(L^{\epsilon}(\boldsymbol{\xi})\right) \quad &= \quad \inf_{\eta, \mathbf{K}} \; \eta + \frac{1}{\rho} \mathrm{Tr}\left(\mathbf{M}_\xi \mathbf{K}\right) \\ s.t. \quad & \mathbf{K} \in \mathbb{S}_+^{n+1},\; \eta \in \mathbb{R} \qquad (5.40) \\ & \mathbf{K} - \begin{bmatrix} \epsilon_i \mathbf{E}_i & \epsilon_i \mathbf{e}_i \\ \epsilon_i \mathbf{e}_i^T & \epsilon_i \mathrm{e}_i^0 - \eta \end{bmatrix} \succeq 0,\; \forall i = 1, 2, \ldots, M. \qquad (5.41) \end{aligned}$$

Theorem 5.2 allows an SDP representation of WC-CVaR condition (5.39) with $\epsilon_i = 1$. Let $\tilde{\mathbf{z}}_0 = \tilde{\mathbf{z}}|_{\mathbf{f}=0}$ and $\boldsymbol{\Omega}_{\tilde{z}_0}$ be the second-order moment matrix of $\tilde{\mathbf{z}}_0$. Due to $\mathbb{E}[\tilde{\mathbf{z}}_0] = 0$, $\mathbb{V}[\tilde{\mathbf{z}}_0] = \boldsymbol{\Sigma}_{z_0}$, we have

$$\boldsymbol{\Omega}_{\tilde{z}_0} = \begin{bmatrix} \boldsymbol{\Sigma}_{z_0} & 0 \\ 0 & 1 \end{bmatrix}. \tag{5.42}$$

The WC-CVaR condition (5.39) thus can be equally re-written as following SDP constraints

$$\begin{cases} \mathbf{K}_0 \in \mathbb{S}_+^{\gamma+1},\; \mathbf{Q}_i \in \mathbb{S}_+^{\gamma},\; \eta \in \mathbb{R},\; b > 0 \\ \eta + \frac{1}{\alpha_0} \mathrm{Tr}\left(\boldsymbol{\Omega}_{\tilde{\mathbf{z}}_0} \mathbf{K}_0\right) \leq 0,\; \mathbf{K}_0 - \begin{bmatrix} \mathbf{Q}_i & 0 \\ 0 & -b - \eta \end{bmatrix} \succeq 0,\; \forall i = 1, 2, \ldots, M. \end{cases} \tag{5.43}$$

Remark 5.2. *It is notable that Theorem 4.2 is the result of Theorem 5.1 with* $M = 1$.

Remark 5.3. *The constraint in (5.43) that equals to (5.39), is a sufficient condition of (5.35). More specifically, for* $\boldsymbol{\epsilon}$ *with entries* $\epsilon_i \in \mathcal{A}$*, given the following sets of* $\mathbf{Q}_i$*,*

$$\begin{aligned}
\mathcal{J}_1(\boldsymbol{\epsilon}) &= \{\mathbf{Q}_i \in \mathbb{S}_+^\gamma \,|\textit{constraints in (5.43)}\} \\
\mathcal{J}_2(\boldsymbol{\epsilon}) &= \left\{ \mathbf{Q}_i \in \mathbb{S}_+^\gamma \,\middle|\, \sup_{\mathbb{P}_z \in \mathcal{P}} \mathbb{P} - \mathrm{CVaR}_{\alpha_0}\left(L(\tilde{\mathbf{z}})\right) \leq 0 \right\} \\
\mathcal{J}_3(\boldsymbol{\epsilon}) &= \left\{ \mathbf{Q}_i \in \mathbb{S}_+^\gamma \,\middle|\, \inf_{\mathbb{P}_z \in \mathcal{P}} \Pr\left\{L_i(\tilde{\mathbf{z}}) \leq 0,\, \forall i = 1, 2, ..., M\right\} \geq 1 - \alpha_0 \right\}
\end{aligned}$$

it then holds $\mathcal{J}_1(\boldsymbol{\epsilon}) = \mathcal{J}_2(\boldsymbol{\epsilon}) \subseteq \mathcal{J}_3(\boldsymbol{\epsilon})$*.*

Next, we devote to dealing with the DCC in (5.36). The following lemma is referred.

Lemma 5.1. *[9] Let* $\mathcal{S} \in \mathbb{R}^n$ *be any Borel measurable set (which is not necessarily convex), and define the worst-case probability* π *as*

$$\pi = \sup_{\mathbb{P}_\xi \in \mathcal{P}} \Pr\left\{\boldsymbol{\xi} \in \mathcal{S}\right\} \tag{5.44}$$

where $\mathcal{P}$ *is the set of* $\mathbb{P}_\xi$ *with mean* $\bar{\boldsymbol{\xi}}$ *and covariance matrix* $\boldsymbol{\Sigma} \in \mathbb{S}_+^n$*. It then holds*

$$\pi = \inf_{\mathbf{K}} \left\{ \mathrm{Tr}(\mathbf{M}_\xi \mathbf{K}) : \mathbf{K} \in \mathbb{S}_+^{n+1},\ \left[\boldsymbol{\xi}^T \ \ 1\right] \mathbf{K} \left[\boldsymbol{\xi}^T \ \ 1\right]^T \geq 1,\ \forall \boldsymbol{\xi} \in \mathcal{S} \right\} \tag{5.45}$$

According to Lemma 5.1, we have the following theorem.

Theorem 5.3. *Using the notations in Theorem 5.1, for fixed* $\epsilon_i \in \mathcal{A}$*, the condition*

$$\sup_{\mathbb{P}_\xi \in \mathcal{P}} \Pr\left\{L^\epsilon(\boldsymbol{\xi}) \leq 0\right\} \leq \rho \tag{5.46}$$

can be substituted by the following SDP

$$\begin{cases} \mathbf{K} \in \mathbb{S}_+^{n+1},\ \tau_i \geq 0 \\ \mathrm{Tr}(\mathbf{M}_\xi \mathbf{K}) \leq \rho,\ \left[\mathbf{K} - \mathrm{diag}(\mathbf{0}, 1)\right] + \sum_{i=1}^{M} \tau_i \begin{bmatrix} \epsilon_i \mathbf{E}_i & \epsilon_i \mathbf{e}_i \\ \epsilon_i \mathbf{e}_i^T & \epsilon_i \mathrm{e}_i^0 \end{bmatrix} \succeq 0. \end{cases} \tag{5.47}$$

Proof. Define a set for random vector $\boldsymbol{\xi}$ by $\mathcal{S} = \{\boldsymbol{\xi} \in \mathbb{R}^n \,|L^\epsilon(\boldsymbol{\xi}) \leq 0\}$. we have

$$\pi = \sup_{\mathbb{P}_\xi \in \mathcal{P}} \Pr\left\{\boldsymbol{\xi} \in \mathcal{S}\right\} = \sup_{\mathbb{P}_\xi \in \mathcal{P}} \Pr\left\{\epsilon_i L_i(\boldsymbol{\xi}) \leq 0,\, \forall i = 1,\, 2,\, \ldots,\, M\right\}.$$

Note that $\forall \boldsymbol{\xi} \in \mathcal{S}$ it holds

$$\epsilon_i L_i(\boldsymbol{\xi}) = \left[\boldsymbol{\xi}^T \ \ 1\right] \begin{bmatrix} \epsilon_i \mathbf{E}_i & \epsilon_i \mathbf{e}_i \\ \epsilon_i \mathbf{e}_i^T & \epsilon_i \mathrm{e}_i^0 \end{bmatrix} \left[\boldsymbol{\xi}^T \ \ 1\right]^T \leq 0,\, \forall i = 1,\, 2,\, \ldots,\, M.$$

Let $\boldsymbol{\varsigma} = \left[\boldsymbol{\xi}^T \;\; 1\right]$. The constraints in π, according to Lemma 5.1, are reformulated as follows

$$\mathbf{K} \in \mathbb{S}_+^{n+1},\, \boldsymbol{\varsigma}\left[\mathbf{K} - \mathrm{diag}(\mathbf{0}, 1)\right]\boldsymbol{\varsigma}^T \geq 0,\;\; \boldsymbol{\varsigma}\begin{bmatrix} \epsilon_i\mathbf{E}_i & \epsilon_i\mathbf{e}_i \\ \epsilon_i\mathbf{e}_i^T & \epsilon_i\mathrm{e}_i^0 \end{bmatrix}\boldsymbol{\varsigma}^T \leq 0, \forall i = 1,\, 2,\, \ldots,\, M$$

for fixed $\epsilon_i \in \mathcal{A}$, which, by using the S-lemma, can be rewritten as

$$\exists \tau_i \geq 0,\; [\mathbf{K} - \mathrm{diag}(\mathbf{0}, 1)] + \sum_{i=1}^{M} \tau_i \begin{bmatrix} \epsilon_i\mathbf{E}_i & \epsilon_i\mathbf{e}_i \\ \epsilon_i\mathbf{e}_i^T & \epsilon_i\mathrm{e}_i^0 \end{bmatrix} \succeq 0.$$

The condition π, therefore, is equally represented by

$$\begin{aligned} \pi \;\; = \;\; & \inf_{\mathbf{K}} \;\; \mathrm{Tr}(\mathbf{M}_\xi \mathbf{K}) \\ & \text{s.t.} \;\; \mathbf{K} \in \mathbb{S}_+^{n+1},\; \tau_i \geq 0,\; [\mathbf{K} - \mathrm{diag}(\mathbf{0}, 1)] + \sum_{i=1}^{M} \tau_i \begin{bmatrix} \epsilon_i\mathbf{E}_i & \epsilon_i\mathbf{e}_i \\ \epsilon_i\mathbf{e}_i^T & \epsilon_i\mathrm{e}_i^0 \end{bmatrix} \succeq 0 \end{aligned}$$

In this context, $\pi \leq \rho$ can be substituted by (5.47). The proof is completed. □

It is remarkable that Theorem 5.3 provides an SDP formulation of a DCC in form of (5.43), in which one ambiguity set with fixed mean and covariance matrix is taken into consideration. In DCC (5.36), a family of ambiguity sets $\mathcal{P}_{f_j} \in \mathcal{P}_f$, $j = 1, 2, ..., M$ are concerned and the results in Theorem 5.3 cannot be applied directly. For this reason, we first consider a single fault mode with respect to ambiguity set $\mathcal{P}_{f_j}$. Let

$$\boldsymbol{\Omega}_{\tilde{z}_j} = \begin{bmatrix} \boldsymbol{\Sigma}_{z_{f_j}} + \bar{\tilde{\mathbf{z}}}_j\bar{\tilde{\mathbf{z}}}_j^T & \bar{\tilde{\mathbf{z}}}_j^T \\ \bar{\tilde{\mathbf{z}}}_j^T & 1 \end{bmatrix},\; \bar{\tilde{\mathbf{z}}}_j = \bar{\mathbf{z}}_{f_j} - \bar{\mathbf{z}}_0 = \bar{\mathbf{H}}_{f,s}\bar{\mathbf{f}}_{js}. \tag{5.48}$$

It yields according to Theorem 5.3 that

$$\begin{aligned} & \sup_{\mathbb{P}_z \in \mathcal{P}_{f_j}} \Pr\left\{L(\tilde{\mathbf{z}}) \leq 0\right\} \leq \beta \\ \Leftrightarrow \;\; & \begin{cases} \mathbf{K}_j \in \mathbb{S}_+^{\gamma+1},\; \tau_{ji} \geq 0,\; i = 1,\, 2,\, \ldots,\, M \\ \mathrm{Tr}(\boldsymbol{\Omega}_{\tilde{z}_j}\mathbf{K}_j) \leq \beta,\; [\mathbf{K}_j - \mathrm{diag}(\mathbf{0}, 1)] + \sum_{i=1}^{M} \tau_{ji} \begin{bmatrix} \mathbf{Q}_i & 0 \\ 0 & -b \end{bmatrix} \succeq 0. \end{cases} \end{aligned} \tag{5.49}$$

Moreover, $\forall \mathcal{P}_{f_j} \in \mathcal{P}_f$, $j = 1, 2, ..., M$, we note that

$$\begin{aligned} \sup_{\mathbb{P}_z \in \mathcal{P}_f} \Pr\left\{L(\tilde{\mathbf{z}}) \leq 0\right\} \leq \beta \;\; & \Leftrightarrow \;\; \max_{\mathcal{P}_{f_j} \in \mathcal{P}_f,\, j=1,2,...,M} \left\{ \sup_{\mathbb{P}_z \in \mathcal{P}_{f_j}} \Pr\left\{L(\tilde{\mathbf{z}}) \leq 0\right\} \right\} \leq \beta \\ & \Leftrightarrow \;\; \sup_{\mathbb{P}_z \in \mathcal{P}_{f_j}} \Pr\left\{L(\tilde{\mathbf{z}}) \leq 0\right\} \leq \beta,\; \forall j = 1, 2, ..., M. \end{aligned}$$

Similar to (5.49), it is intuitive that the DCC in (5.36) can be substituted by

$$\begin{cases} \mathbf{K}_j \in \mathbb{S}_+^{\gamma+1},\ \tau_{ji} \geq 0,\ \mathrm{Tr}(\mathbf{\Omega}_{\tilde{z}_j}\mathbf{K}_j) \leq \beta \\ [\mathbf{K}_j - \mathrm{diag}(\mathbf{0}, 1)] + \sum\limits_{i=1}^{M} \tau_{ji} \begin{bmatrix} \mathbf{Q}_i & 0 \\ 0 & -b \end{bmatrix} \succeq 0,\ \forall i,\ j = 1, 2, ..., M. \end{cases} \tag{5.50}$$

Now the DCCs in (5.35) and (5.36) have been represented by SDP constraints, i.e., (5.38) and (5.50). On this basis, the FD problem (5.30)–(5.31) can be addressed by solving the following SDP problem

$$\min_{\mathbf{K}_0, b, \eta, \mathbf{Q}_i, \mathbf{K}_j, i=1,2,...,M} \quad \beta \tag{5.51}$$

$$\text{s.t.} \begin{cases} \mathbf{K}_0 \in \mathbb{S}_+^{\gamma+1},\ \mathbf{Q}_i \in \mathbb{S}_+^{\gamma},\ \eta \in \mathbb{R},\ b > 0,\ \mathbf{K}_j \in \mathbb{S}_+^{\gamma+1},\ \tau_{ji} \geq 0 \\ \eta + \frac{1}{\alpha_0}\mathrm{Tr}\left(\mathbf{\Omega}_{\tilde{\mathbf{z}}_0}\mathbf{K}_0\right) \leq 0,\ \mathbf{K}_0 - \begin{bmatrix} \mathbf{Q}_i & 0 \\ 0 & -b-\eta \end{bmatrix} \succeq 0 \\ \mathrm{Tr}(\mathbf{\Omega}_{\tilde{z}_j}\mathbf{K}_j) \leq \beta,\ [\mathbf{K}_j - \mathrm{diag}(\mathbf{0}, 1)] + \sum\limits_{i=1}^{M} \tau_{ji} \begin{bmatrix} \mathbf{Q}_i & 0 \\ 0 & -b \end{bmatrix} \succeq 0,\ \forall i, j = 1, 2, ..., M. \end{cases} \tag{5.52}$$

Numerical solution of this problem can be obtained by using the toolboxes such as CVX, OPTI and YALMIP [1], etc.

Because the magnitudes of $\mathbf{Q}_i$, b will not influence the optimal solution of the problem (5.51)–(5.52), we can usually set $b = 1$. By solving this problem for β, $\mathbf{Q}_i$, $i = 1, 2, ..., M$, the residual evaluation function and and threshold in (5.29) can then be applied for online FD by using the decision logic (5.2). In this context, the FAR of the FD system is achieved not larger than α_0 and MDR not greater than β. The design and real-time implementation of WC-CVaR aided FD systems is demonstrated in Algorithm 5.3.10.

Until now, design issues of FD systems in terms of parameter matrix $\mathbf{W}$ are addressed by designing a bank of parameter vectors $\mathbf{w}_i$, $i = 1, 2, ..., M$ in a separated manner, i.e., (5.16)–(5.17), or in an integrated manner, i.e., (5.51)–(5.52).

Remark 5.4. *In comparison with the results obtained in Section 5.2, the formulation (5.51)–(5.52) delivers a much lower bound of MDR for an identical FAR, and vice versa. More specifically, denote by $\mathcal{D}_{\mathrm{se}}$ the set of $\mathbf{W}$ that is constructed by separately solving each entry $\mathbf{w}_i$ satisfying (5.15) and $\mathcal{D}_{\mathrm{wc}}$ the set of $\mathbf{W}$ guaranteeing (5.52), i.e.,*

$$\mathcal{J}_{\mathrm{se}}(\alpha_0) = \left\{\mathbf{W} \in \mathbb{R}^{\gamma \times M} \mid \mathbf{w}_i \ \textit{ satisfying (5.15) with } i = 1, 2, ..., M\right\}$$
$$\mathcal{J}_{\mathrm{wc}}(\alpha_0) = \left\{\mathbf{W} \in \mathbb{R}^{\gamma \times M} \,\middle|\, \mathbf{w}_i\mathbf{w}_i^T = \mathbf{Q}_i,\ i = 1, 2, ..., M,\ \textit{with } \mathbf{Q}_i \textit{ satisfying (5.52)}\right\}$$

Given fixed α_0, it holds $\mathcal{J}_{\mathrm{wc}}(\alpha_0) \subseteq \mathcal{J}_{\mathrm{se}}(\alpha_0)$.

Algorithm 5.3.10 WC-CVaR aided configuration of FD systems

Offline design

1: Estimate $\bar{\mathbf{z}}_0$, $\mathbf{\Sigma}_{z_0}$, $\bar{\mathbf{z}}_{f_i}$, $\mathbf{\Sigma}_{z_{f_i}}$, $i = 1, 2, \ldots, M$ using process I/O data.
2: Solve the SDP problem (5.51)–(5.52) for $\mathbf{Q}_i$, $i = 1, 2, \ldots, M$, β, b.

Online FD

1: At time step k, compute $\mathbf{z}(k)$ with (3.3) using process I/O data.
2: Construct the residual evaluation function $J(\mathbf{r})$ with (5.29) and (5.10).
3: Perform decision logic (5.2) for FD.

Remark 5.5. *It is worth mentioning that the distribution independent conditions (3.27) in Chapter 3 are in essential the closed-forms of SDPs (5.38) and (5.50) as special cases with the quadratic items being zero. A detailed proof is referred to [9].*

5.4 Optimal matrix-valued design

In terms of residual generator (5.1), a 2-norm based residual evaluation function is defined in the following form

$$J(\mathbf{r}) = \|\mathbf{r}(k) - \bar{\mathbf{r}}_0\|_2^2 \tag{5.53}$$

where $\bar{\mathbf{r}}_0 = \mathbf{W}^T\bar{\mathbf{z}}_0$. Remembering $\tilde{\mathbf{z}} = \mathbf{z} - \bar{\mathbf{z}}_0$, it then follows from (5.53) that

$$J(\mathbf{r}) = \left\|\mathbf{W}^T\tilde{\mathbf{z}}(k)\right\|_2^2. \tag{5.54}$$

By without loss of generality setting $J_{th} = 1$ and using the decision logic (5.2), the FD problem (5.3)–(5.4) with respect to $\mathcal{P}_f$ in (5.6) is then reformulated as follows

$$\min_{\mathbf{W}\neq 0} \quad \beta \tag{5.55}$$

$$\text{s.t.} \quad \begin{cases} \sup\limits_{\mathbb{P}_z\in\mathcal{P}_0} \Pr\left\{\left\|\mathbf{W}^T\tilde{\mathbf{z}}\right\|_2^2 > 1\right\} \le \alpha_0 \\ \sup\limits_{\mathbb{P}_z\in\mathcal{P}_f} \Pr\left\{\left\|\mathbf{W}^T\tilde{\mathbf{z}}\right\|_2^2 \le 1\right\} \le \beta \end{cases} \tag{5.56}$$

which provides an integrated design of parameter matrix $\mathbf{W}$, FAR and MDR criteria. The configuration of this optimal matrix-valued FD system is illustrated in Fig. 5.3.

5.4.1 Optimal solution

In order to solve the problem (5.55)–(5.56), a quadratic function of $\tilde{\mathbf{z}}$ is defined as follows

$$L(\tilde{\mathbf{z}}) = \tilde{\mathbf{z}}^T\mathbf{P}\tilde{\mathbf{z}} - 1 \tag{5.57}$$

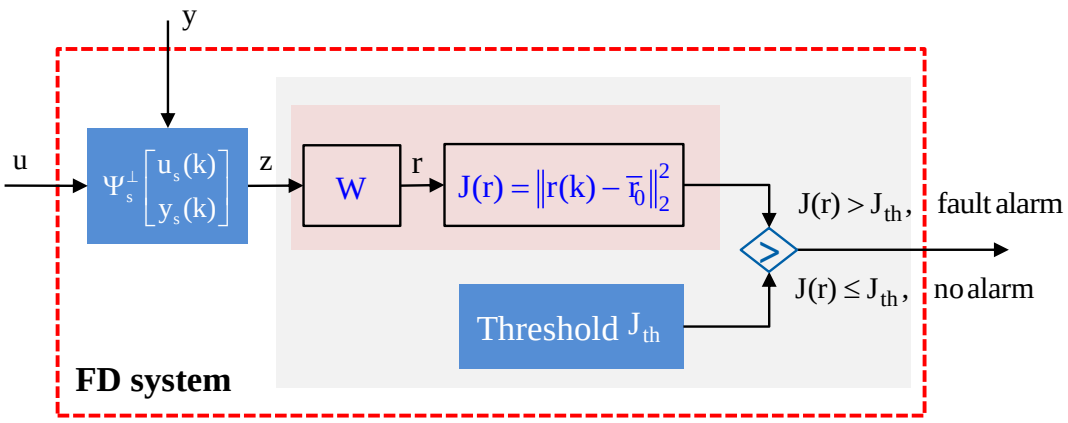

Figure 5.3: Diagram of optimal matrix-valued configuration of FD systems.

where $\mathbf{P} = \mathbf{W}\mathbf{W}^T \in \mathbb{S}_+^\gamma$. Then the first DCC in (5.56) yields

$$\begin{aligned} \sup_{\mathbb{P}_z \in \mathcal{P}_0} \Pr\left\{ \left\| \mathbf{W}^T \tilde{\mathbf{z}} \right\|_2^2 > 1 \right\} &= \sup_{\mathbb{P}_z \in \mathcal{P}_0} \Pr\left\{ L(\tilde{\mathbf{z}}) > 0 \right\} \leq \alpha_0 \\ &\Leftrightarrow \inf_{\mathbb{P}_z \in \mathcal{P}_0} \Pr\left\{ L(\tilde{\mathbf{z}}) \leq 0 \right\} \geq 1 - \alpha_0. \end{aligned} \tag{5.58}$$

Referring to Theorems 4.1 and 4.2, we have

$$\text{Eq. (5.58)} \Leftrightarrow \sup_{\mathbb{P}_z \in \mathcal{P}_0} \mathbb{P}_z\text{–CVaR}_{\alpha_0}(L(\tilde{\mathbf{z}})) = -1 + \frac{1}{\alpha_0} \text{Tr}(\mathbf{\Sigma}_{z_0} \mathbf{P}) \leq 0. \tag{5.59}$$

For the second DCC in (5.56), it follows from Theorem 5.3 that

$$\begin{aligned} \sup_{\mathbb{P}_z \in \mathcal{P}_f} \Pr\left\{ \left\| \mathbf{W}^T \tilde{\mathbf{z}} \right\|_2^2 \leq 1 \right\} &= \max_{j=1,2,\ldots,M} \left\{ \inf_{\mathbf{K}_j, \tau_j} \ \text{Tr}(\mathbf{\Omega}_{\tilde{z}_j} \mathbf{K}_j) \right\} \\ &\text{s.t.} \ \ \mathbf{K}_j \in \mathbb{S}_+^{\gamma+1}, \ \tau_j \geq 0, \ \mathbf{K}_j + \begin{bmatrix} \tau_j \mathbf{P} & 0 \\ 0 & -1 - \tau_j \end{bmatrix} \succeq 0 \end{aligned}$$

where $\mathbf{\Omega}_{\tilde{z}_j}$ is given in (5.48). An SDP representation of the second DCC in (5.56) is then achieved as

$$\mathbf{K}_j \in \mathbb{S}_+^{\gamma+1}, \ \tau_j \geq 0, \ \text{Tr}(\mathbf{\Omega}_{\tilde{z}_j} \mathbf{K}_j) \leq \beta, \ \mathbf{K}_j + \begin{bmatrix} \tau_j \mathbf{P} & 0 \\ 0 & -1 - \tau_j \end{bmatrix} \succeq 0, \ \forall j = 1, 2, \ldots, M. \tag{5.60}$$

Due to (5.59) and (5.60), the FD problem (5.55)–(5.56) is thus re-written as follows

$$\min_{\mathbf{P}, \mathbf{K}_j, \tau_j, j=1,2,\ldots,M} \ \beta \tag{5.61}$$

$$\text{s.t.} \quad \begin{cases} \mathbf{K}_j \in \mathbb{S}_+^{\gamma+1}, \ \mathbf{P} \in \mathbb{S}_+^\gamma, \ \tau_j \geq 0 \\ \text{Tr}(\mathbf{\Sigma}_{z_0} \mathbf{P}) \leq \alpha_0, \ \text{Tr}(\mathbf{\Omega}_{\tilde{\mathbf{z}}_j} \mathbf{K}_j) \leq \beta \\ \mathbf{K}_j + \begin{bmatrix} \tau_j \mathbf{P} & 0 \\ 0 & -1 - \tau_j \end{bmatrix} \succeq 0, \ \forall j = 1, 2, \ldots, M. \end{cases} \tag{5.62}$$

By solving (5.61)–(5.62) for $\mathbf{P}$, β, an optimal solution to $\mathbf{W}$ can be obtained as

$$\mathbf{W} = \mathbf{P}^{\frac{1}{2}}. \tag{5.63}$$

In this regard, the FAR and MDR are achieved not larger than α_0 and β, respectively. The configuration of this optimal matrix-valued FD systems is given in Algorithm 5.4.11.

So far, three DIO configurations of FD systems have been drawn with respect to solving the problem (5.3)–(5.4). For the achieved results, the following two additional remarks are worth mentioning.

- It is observed from (5.10), (5.29) and (5.54) that, the value of residual evaluation functions get larger with the increase of the magnitude of fault $\mathbf{f}_i(k)$, which implies a smaller MDR for a given FAR and fixed threshold. In this sense, the value of $\bar{\mathbf{f}}_{is}$ (or $\bar{\mathbf{z}}_{f_i}$ in ambiguity set $\mathcal{P}_{f_i}$) can be regarded as a reference mean of the i-th fault mode towards FD performance regarding FAR and MDR not poor than α_0 and β, respectively, likewise for the DIO methods in Chapters 3 and 4.

- Since the upper bounds of FAR and MDR are obtained with M groups of the concerned faulty scenarios, i.e., $\mathcal{P}_f = \bigcup_{i=1}^{M} \mathcal{P}_{f_i}$, a fault with probability distribution varying over the set $\mathcal{P}_f$ can then be detected with the above designed FD systems, guaranteeing the MDR not greater than β and FAR not larger than α_0.

For these facts, even though the mean and covariance matrix of residual in each faulty scenario are considered to be constant, the developed FD systems can well handle the faults with time-varying distribution profiles changing in mean and covariance matrix.

On the other hand, in the above discussion the fault mode is characterized by the features of mean and covariance matrix and the information of most of possible fault modes is required towards a lower MDR. As stated before, this kind of exhaustive handling

Algorithm 5.4.11 Optimal matrix-valued configuration of FD systems

Offline design

1: Estimate $\bar{\mathbf{z}}_0$, $\mathbf{\Sigma}_{z_0}$, $\bar{\mathbf{z}}_{f_i}$, $\mathbf{\Sigma}_{z_{f_i}}$, $i = 1, 2, \ldots, M$ using process I/O dtata.
2: Solve the problem (5.61)–(5.62) for $\mathbf{P}$, β and determine $\mathbf{W}$ with (5.63).
3: Compute $\bar{\mathbf{r}}_0 = \mathbf{W}^T \bar{\mathbf{z}}_0$.

Online FD

1: At time step k, generate residual $\mathbf{r}(k)$ with (3.3) and (5.1) and compute residual evaluation function $J(\mathbf{r})$ with (5.53).
2: Perform decision logic (5.2) for FD.

would involve high complexity for implementation in case that the number of fault class and the dimension of residual signal are large. Furthermore, due to the scarcity of data in faulty cases in practical applications, the intrinsic assumption of known mean and covariance matrix of all fault modes is, to some extent, unrealistic. When a fault in new mode occurs, the above developed DIO schemes may lead to a high MDR during online FD. These shortcomings trigger direct matrix-valued solutions to the FD problem (5.3)–(5.4) without knowledge of $\mathcal{P}_f$, as discussed in the forthcoming section.

5.5 Matrix-valued solutions without fault information

Given ambiguity set $\mathcal{P}_0$ in (3.17), residual evaluation function (5.53) and threshold $J_{th} = 1$, we begin with formulating the design of FD systems regarding matrix $\mathbf{W}$ as follows

$$\max_{\mathbf{W}\neq 0} \ \mathrm{Tr}(\bar{\mathbf{H}}_{f,s}^T \mathbf{W}\mathbf{W}^T \bar{\mathbf{H}}_{f,s}) \tag{5.64}$$

$$\text{s.t.} \quad \sup_{\mathbb{P}_z\in\mathcal{P}_0} \Pr\left\{ \left\| \mathbf{W}^T \tilde{\mathbf{z}} \right\|_2^2 > 1 \right\} \leq \alpha_0. \tag{5.65}$$

This formulation is posted towards minimizing the MDR for a given FAR not larger than α_0 despite no fault information is available. More detailedly, the DCC (5.65) clearly restricts the FAR not larger than α_0. With (5.65) ensured, it is observed from (5.54) that the value of $J(\mathbf{r})$ gets larger with the increase of the magnitude of $\mathrm{Tr}(\bar{\mathbf{H}}_{f,s}^T \mathbf{W}\mathbf{W}^T \bar{\mathbf{H}}_{f,s})$ for certain $\mathbf{f}(k)$. In this context, the objective (5.64) delivers a minimum MDR.

Recall the notations $\mathbf{P} = \mathbf{W}\mathbf{W}^T \in \mathbb{S}_+^\gamma$, $L(\tilde{\mathbf{z}}) = \tilde{\mathbf{z}}^T \mathbf{P} \tilde{\mathbf{z}} - 1$. The DCC (5.65), according to Theorem 4.1, is then equally replaced with the following WC-CVaR condition

$$\sup_{\mathbb{P}_z\in\mathcal{P}_0} \mathbb{P} - \mathrm{CVaR}_{\alpha_0}\left(L(\tilde{\mathbf{z}})\right) \leq 0 \tag{5.66}$$

which, due to Theorem 4.3, can be further substituted by the following condition

$$\mathrm{Tr}(\mathbf{\Sigma}_{z_0} \mathbf{P}) \leq \alpha_0. \tag{5.67}$$

The problem (5.64)–(5.65) is thus reformulated as the following SDP problem

$$\max_{\mathbf{P}\neq 0} \ \mathrm{Tr}(\bar{\mathbf{H}}_{f,s}^T \mathbf{P} \bar{\mathbf{H}}_{f,s}) \quad \text{s.t.} \quad \mathbf{P} \in \mathbb{S}_+^\gamma, \ \mathrm{Tr}(\mathbf{\Sigma}_{z_0}\mathbf{P}) \leq \alpha_0. \tag{5.68}$$

Though the simple form of (5.68), an analytical solution is difficult to achieve and the orthogonality of the entries $\mathbf{w}_i$, $i = 1, 2, \ldots, \gamma$ is not specified.

To solve (5.68), let

$$\mathbf{H} = \bar{\mathbf{H}}_{f,s} \bar{\mathbf{H}}_{f,s}^T, \quad \mathbf{W} = \epsilon \tilde{\mathbf{W}} \tag{5.69}$$

with $\epsilon > 0$. By specifying the orthogonality of the column entries of $\mathbf{W}$ with $\tilde{\mathbf{W}}^T\boldsymbol{\Sigma}_{z_0}\tilde{\mathbf{W}} = \mathbf{I}$, the FD problem (5.68) can be re-written as follows

$$\max_{\tilde{\mathbf{W}},\epsilon>0} \quad \mathrm{Tr}(\tilde{\mathbf{W}}^T\mathbf{H}\tilde{\mathbf{W}}) \quad \text{s.t.} \quad \tilde{\mathbf{W}}^T\boldsymbol{\Sigma}_{z_0}\tilde{\mathbf{W}} = \mathbf{I},\ \epsilon^2\gamma \leq \alpha_0. \tag{5.70}$$

Note that $\mathrm{Tr}(\mathbf{W}^T\boldsymbol{\Sigma}_{z_0}\mathbf{W}) = \alpha_0$ holds at the optimum of (5.68). Since if the inequality holds, a larger $\mathrm{Tr}(\bar{\mathbf{H}}_{f,s}^T\mathbf{P}\bar{\mathbf{H}}_{f,s})$ can always be found with respect to $\mathbf{P}$. In this sense, $\epsilon = \sqrt{\frac{\alpha_0}{\gamma}}$ holds in (5.70). And then the solution to (5.70) is obtained by solving the following generatized eigenvalue-eigenvector problem [63]

$$\max_{\tilde{\mathbf{W}},\epsilon>0} \quad \mathrm{Tr}(\tilde{\mathbf{W}}^T\mathbf{H}\tilde{\mathbf{W}}) \quad \text{s.t.} \quad \tilde{\mathbf{W}}^T\boldsymbol{\Sigma}_{z_0}\tilde{\mathbf{W}} = \mathbf{I}. \tag{5.71}$$

Do an SVD on $\boldsymbol{\Sigma}_{z_0}^{\frac{1}{2}}$, i.e., $\boldsymbol{\Sigma}_{z_0}^{\frac{1}{2}} = \bar{\mathbf{U}}[\bar{\mathbf{S}} \quad 0]\tilde{\mathbf{V}}^T$. Let

$$\tilde{\mathbf{w}}_i = \bar{\mathbf{U}}\bar{\mathbf{S}}^{-1}\bar{\mathbf{v}}_i \tag{5.72}$$

with $\bar{\mathbf{v}}_i$ solving the following equations

$$\bar{\mathbf{v}}_i^T(\tilde{\lambda}_{m,i}\mathbf{I} - \bar{\mathbf{S}}^{-1}\bar{\mathbf{U}}^T\mathbf{H}\bar{\mathbf{U}}\bar{\mathbf{S}}^{-1})\bar{\mathbf{v}}_i = 0, \quad \bar{\mathbf{v}}_i^T\bar{\mathbf{v}}_i = 1 \tag{5.73}$$

where $\tilde{\lambda}_{m,i}$ is the i-th largest eigenvalue of $\bar{\mathbf{S}}^{-1}\bar{\mathbf{U}}^T\mathbf{H}\bar{\mathbf{U}}\bar{\mathbf{S}}^{-1}$. Then, the optimal solution of $\tilde{\mathbf{W}} = [\tilde{\mathbf{w}}_1 \quad \tilde{\mathbf{w}}_2 \quad \ldots, \quad \tilde{\mathbf{w}}_\gamma]$ to (5.70) is obtained. Thus, the matrix $\mathbf{W}$ is achieved with

$$\mathbf{W} = \sqrt{\frac{\alpha_0}{\gamma}}\tilde{\mathbf{W}}. \tag{5.74}$$

The orthogonality of the column vectors of $\mathbf{W}$ is surely satisfied. Remembering that a vector-valued solution with $\eta = 1$ has been presented in Section 4.3.1, in this case the optimal solutions to (5.70) and (5.71) are identical. It could be verified that the solution can also be derived using Lagrangian multiplier method.

More generally, we post the constraint $\tilde{\mathbf{W}}^T\tilde{\mathbf{W}} = \mathbf{I}$ to the FD problem (5.68) to specify the orthogonality of the entries of $\mathbf{W}$. The problem (5.68) is then reformulated as follows

$$\max_{\tilde{\mathbf{W}}^T\tilde{\mathbf{W}}=\mathbf{I}} \quad \frac{\mathrm{Tr}(\tilde{\mathbf{W}}^T\mathbf{H}\tilde{\mathbf{W}})}{\mathrm{Tr}(\tilde{\mathbf{W}}^T\boldsymbol{\Sigma}_{z_0}\tilde{\mathbf{W}})}. \tag{5.75}$$

with $\epsilon = \sqrt{\alpha_0/\mathrm{Tr}(\tilde{\mathbf{W}}\boldsymbol{\Sigma}_{z_0}\tilde{\mathbf{W}}^T)}$ guaranteeing $\mathrm{Tr}(\mathbf{W}\boldsymbol{\Sigma}_{z_0}\mathbf{W}^T) = \alpha_0$ at the optimum.

For a global optimal solution to the problem (5.75), various iterative algorithms have been reported, see, e.g., [44, 77, 35]. Here we used the so-called iterative trace ratio (ITR) algorithm presented in [77], as summarized in Algorithm 5.5.12. The convergence of this algorithm and its theoretical background have been studied in [44]. After $\tilde{\mathbf{W}}$ is achieved, the global optimal $\mathbf{W}$ is then obtained as $\mathbf{W} = \epsilon\tilde{\mathbf{W}}$.

Algorithm 5.5.12 Iterative trace ratio method for solving (5.75)

1: Let $\mathbf{\Sigma}_{z_0}^u = \bar{\mathbf{U}}^T \mathbf{\Sigma}_{z_0} \bar{\mathbf{U}}$, $\mathbf{H}^u = \bar{\mathbf{U}}^T \mathbf{H} \bar{\mathbf{U}}$, $\delta > 0$ be a smaller scalar.

2: Initialize $\mathbf{\Phi}^0$ as an arbitrary columnly orthogonal matrix.

3: Perform the following steps until $\|\mathbf{\Phi}^n - \mathbf{\Phi}^{n-1}\|_2 \leq \eta\delta$:

- Compute the trace ratio value θ^n from the projection matrix $\mathbf{\Phi}^{n-1}$, i.e.,

$$\theta^n = \frac{\mathrm{Tr}((\mathbf{\Phi}^{n-1})^T \mathbf{H}^u \mathbf{\Phi}^{n-1})}{\mathrm{Tr}((\mathbf{\Phi}^{n-1})^T \mathbf{\Sigma}_{z_0}^u \mathbf{\Phi}^{n-1})}$$

- Solve the trace difference problem

$$\mathbf{\Phi}^n = \arg \max_{\mathbf{\Phi}^T \mathbf{\Phi} = \mathbf{I}} \mathrm{Tr}(\mathbf{\Phi}^T (\mathbf{H}^u - \theta^n \mathbf{\Sigma}_{z_0}^u) \mathbf{\Phi})$$

  using generalized eigenvalue decomposition, i.e., $\mathbf{\Phi}^n = [\boldsymbol{\phi}_1, \boldsymbol{\phi}_2, \ldots, \boldsymbol{\phi}_\eta]$ with $\boldsymbol{\phi}_i$ solving $(\mathbf{H}^u - \theta^n \mathbf{\Sigma}_{z_0}^u)\boldsymbol{\phi}_i = \tau_i^n \boldsymbol{\phi}_i$, τ_i^n is the i-th largest eigenvalue of $\mathbf{H}^u - \theta^n \mathbf{\Sigma}_{z_0}^u$.

- Set $\mathbf{\Sigma}_{z_0}^\phi = \mathbf{\Phi}^n (\mathbf{\Phi}^n)^T \mathbf{\Sigma}_{z_0}^u \mathbf{\Phi}^n (\mathbf{\Phi}^n)^T$. Do SVD as $\mathbf{\Sigma}_{z_0}^\phi = \mathbf{\Phi}^n \mathbf{\Lambda}^n (\mathbf{\Phi}^n)^T$ for $\mathbf{\Phi}^n$. Set $n + 1 \to n$.

4: Return $\tilde{\mathbf{W}} = \mathbf{\Phi}^n$.

Algorithm 5.5.13 Design and implementation of the FD system without fault information

Offline design

1: Collect process I/O data to identify the matrices $\mathbf{\Psi}_s^\perp$. Construct the residual generator (3.3) and estimate $\bar{\mathbf{z}}_0$ and $\mathbf{\Sigma}_{z_0}$ using process I/O data in fault-free case.

2: Solve the problem (5.75) for $\tilde{\mathbf{W}}$ by using Algorithm 5.5.12 (or solving the SDP problem (5.70), using the solutions (5.74)).

3: Set $\mathbf{W} = \epsilon \tilde{\mathbf{W}}$. Let $\bar{\mathbf{r}}_0 = \mathbf{W}^T \bar{\mathbf{z}}_0$.

Online FD

1: Compute residual sequence $\mathbf{r}(k)$ using (3.3) and (5.1).

2: Compute residual evaluation function $J(\mathbf{r})$ with (5.53).

3: Detect the occurrence of a fault with decision logic (5.2).

Because of the orthogonality of the column vectors of $\mathbf{W}$, $rank(\mathbf{W}) = \gamma$ holds in the solutions (5.74) and (5.75). In this context, the parity space of residual generator specified by $\mathbf{\Psi}_{y,s}^\perp$ has been parameterized by a bank of orthogonal vectors and a fault with appropriate nonzero magnitude can be mostly detected.

For online FD purpose, the residual sequence $\mathbf{r}(k)$ at time step k is first generated using (3.3) and (5.1). Then the residual evaluation is carried out to detect the occurrence of a

fault by performing (5.53) and (5.2). The offline design and real-time realization of the FD system without fault information is given in Algorithm 5.5.13.

Remark 5.6. *It is worth noting that the assumption of known matrix* $\bar{\mathbf{H}}_{f,s}$ *is without loss of generality under consideration of actuator and sensor faults. When actuator faults are concerned, we have* $\mathbf{B}_f = \mathbf{B}$ *and* $\mathbf{D}_f = \mathbf{D}$ *and then* $\bar{\mathbf{H}}_{f,s} = \mathbf{\Psi}_{y,s}^{\perp}\mathbf{H}_{u,s} = \mathbf{\Psi}_{u,s}^{\perp}$ *can be identified using process I/O data. When sensor faults are concerned, it holds* $\mathbf{B}_f = 0$, $\mathbf{D}_f = \mathbf{I}$. *Then the matrix* $\mathbf{H}_{f,s}$ *can be constructed in form of (2.15) and* $\bar{\mathbf{H}}_{f,s}$ *is thus available. When no information of the* $\bar{\mathbf{H}}_{f,s}$ *is available, it is without loss of generality to set* $\bar{\mathbf{H}}_{f,s}\bar{\mathbf{H}}_{f,s}^T = \mathbf{I}$.

5.6 Summary and notes

In this chapter, matrix-valued DIO approaches have been developed for the data-driven design of FD systems. Regarding a family of faults characterized by the features of mean and covariance matrix, a parameter matrix has been introduced to the data-driven construction of residual generator. In the context of minimizing the MDR for a prescribed FAR, the design of FD systems has been formulated as an SP problem with DCCs and three DIO solutions have been proposed, namely the multivector-valued design, the WC-CVaR aided design and the optimal matrix-valued design. Additionally, under consideration of inaccessible fault knowledge, matrix-valued solutions without fault information have also been investigated.

6 Performance analysis of FD systems under moments uncertainties

In Chapters 3–5, design issues of data-driven FD systems have been addressed using DIO approaches, achieving a minimum MDR for a prescribed FAR without specific distribution assumptions on noises and faults. Performance analysis of data-driven FD systems is another important topic that has not gained enough attention yet [24, 46, 52]. As demonstrated before, the mean-covariance based ambiguity sets are introduced to characterize the distribution knowledge of noises and faults so as to obtain DIO formulations of the FD problems. In this context, the first-layer robustness of FD systems against the distributional ambiguity has been well handled, assuming known precise means and covariance matrices. In practice, however, the mean and covariance matrix of residual are estimated from process I/O data and the estimation errors in them are inevitable due primarily to the finite number of samples, especially in faulty scenarios. On account of this, the derived FAR and MDR criteria are undoubtedly credible with the probability smaller than one. These observations stimulate the necessity of performance analysis of distribution independent FD systems against the moments uncertainties in the probabilistic context, which is termed the second-layer robustness study.

This chapter focuses on the performance assessment of FD systems designed using DIO approaches under moments uncertainties. At first, the mean-covariance based ambiguity sets plagued by the norm-bounded and box-type moments uncertainties are established. On this basis, the robustness of FD systems demonstrated in Chapters 3–5 is studied quantitatively. The upper bounds of FAR and MDR in the worst-case setting are derived correspondingly. Moreover, the confidence levels of the derived FAR and MDR criteria are investigated in the probabilistic context by establishing analytical relationships between the sample numbers and the estimation errors.

6.1 Problem formulation

Recall the I/O data model (2.14) as presented in Chapter 2, i.e.,

$$\begin{bmatrix} \mathbf{y}_s(k) \\ \mathbf{u}_s(k) \end{bmatrix} = \boldsymbol{\Psi}_s \begin{bmatrix} \mathbf{x}(k-s) \\ \mathbf{u}_s(k) \end{bmatrix} + \begin{bmatrix} \mathbf{H}_{f,s}\mathbf{f}_s(k) + \mathbf{H}_{\omega,s}\boldsymbol{\omega}_s(k) + \boldsymbol{\upsilon}_s(k) \\ 0 \end{bmatrix}. \tag{6.1}$$

For FD purpose, a data-driven construction of residual generator is given below

$$\mathbf{z}(k) = \mathbf{\Psi}_s^{\perp} \begin{bmatrix} \mathbf{y}_s(k) \\ \mathbf{u}_s(k) \end{bmatrix} \tag{6.2}$$

$$\mathbf{r}(k) = \mathbf{W}^T \mathbf{z}(k) \tag{6.3}$$

where $\mathbf{r}(k) \in \mathbb{R}^{\eta}$, $\mathbf{W} \in \mathbb{R}^{\gamma \times \eta}$, $\eta \geq 1$. When $\eta = 1$, $\mathbf{r}(k)$ and $\mathbf{W}$ reduce to $r(k) \in \mathbb{R}$ and $\mathbf{w} \in \mathbb{R}^{\gamma}$, respectively. By determining the residual evaluation function $J(\mathbf{r})$ and threshold J_{th} appropriately, the occurrence of a fault is then detected by using

$$\begin{cases} J(\mathbf{r}) > J_{th} & \Rightarrow \text{fault alarm} \\ J(\mathbf{r}) \leq J_{th} & \Rightarrow \text{no alarm.} \end{cases} \tag{6.4}$$

As presented previously, $\mathbf{W}$, $J(\mathbf{r})$, J_{th} have been addressed using DIO approaches with respect to the mean-covariance based ambiguity sets $\mathcal{P}_0$ and $\mathcal{P}_f$, wherein the true values of means and covariance matrices, i.e., $\bar{\mathbf{z}}_0$, $\mathbf{\Sigma}_{z_0}$ and $\bar{\mathbf{z}}_f$, $\mathbf{\Sigma}_{z_f}$, are assumed to be known exactly. In practical applications, unfortunately, we can only obtain the empirical estimates of them based on process I/O data. This leads to the uncertainties in $\mathcal{P}_0$, $\mathcal{P}_f$ due to the estimation errors. To be more specific, denote by $\hat{\bar{\mathbf{z}}}_0$, $\hat{\mathbf{\Sigma}}_{z_0}$, $\hat{\bar{\mathbf{z}}}_f$, $\hat{\mathbf{\Sigma}}_{z_f}$ the empirical estimates of $\bar{\mathbf{z}}_0$, $\mathbf{\Sigma}_{z_0}$, $\bar{\mathbf{z}}_f$, $\mathbf{\Sigma}_{z_f}$, respectively. By constructing sample sets $\mathcal{S}_0 = \{\mathbf{z}_0(i)\}_{i=1}^{N_0}$ and $\mathcal{S}_f = \{\mathbf{z}_f(i)\}_{i=1}^{N_f}$ with (6.2) respectively using process I/O data in fault-free and faulty cases, then, over $\mathcal{S}_0$ and $\mathcal{S}_f$, we have

$$\hat{\bar{\mathbf{z}}}_0 = \frac{1}{N_0} \sum_{i=1}^{N_0} \mathbf{z}_0(i), \quad \hat{\mathbf{\Sigma}}_{z_0} = \frac{1}{N_0} \sum_{i=1}^{N_0} (\mathbf{z}_0(i) - \hat{\bar{\mathbf{z}}}_0)(\mathbf{z}_0(i) - \hat{\bar{\mathbf{z}}}_0)^T \tag{6.5}$$

$$\hat{\bar{\mathbf{z}}}_f = \frac{1}{N_f} \sum_{i=1}^{N_f} \mathbf{z}_f(i), \quad \hat{\mathbf{\Sigma}}_{z_f} = \frac{1}{N_f} \sum_{i=1}^{N_f} (\mathbf{z}_f(i) - \hat{\bar{\mathbf{z}}}_f)(z_f(i) - \hat{\bar{\mathbf{z}}}_f)^T. \tag{6.6}$$

Because of the finite sample numbers N_0, N_f, the estimation uncertainties are inevitable and nonnegligible especially for small N_0, N_f. Let $\mathbf{\Delta}_{\bar{z}_0}$, $\mathbf{\Delta}_{\Sigma_{z_0}}$, $\mathbf{\Delta}_{\bar{z}_f}$, $\mathbf{\Delta}_{\Sigma_{z_f}}$ be the uncertainties in means $\bar{\mathbf{z}}_0$, $\bar{\mathbf{z}}_f$ and covariance matrices $\mathbf{\Sigma}_{z_0}$, $\mathbf{\Sigma}_{z_f}$, respectively, and model

$$\bar{\mathbf{z}}_0 = \hat{\bar{\mathbf{z}}}_0 + \mathbf{\Delta}_{\bar{z}_0}, \quad \mathbf{\Sigma}_{z_0} = \hat{\mathbf{\Sigma}}_{z_0} + \mathbf{\Delta}_{\Sigma_{z_0}} \tag{6.7}$$

$$\bar{\mathbf{z}}_f = \hat{\bar{\mathbf{z}}}_f + \mathbf{\Delta}_{\bar{z}_f}, \quad \mathbf{\Sigma}_{z_f} = \hat{\mathbf{\Sigma}}_{z_f} + \mathbf{\Delta}_{\Sigma_{z_f}}. \tag{6.8}$$

Denote by $\mathcal{P}_{0,\Delta_0}$, $\mathcal{P}_{f,\Delta_f}$ the ambiguity sets under moments uncertainties with $\mathbf{\Delta}_0 = \{\mathbf{\Delta}_{\bar{z}_0}, \mathbf{\Delta}_{\Sigma_{z_0}}\}$, $\mathbf{\Delta}_f = \{\mathbf{\Delta}_{\bar{z}_f}, \mathbf{\Delta}_{\Sigma_{z_f}}\}$. Then, with respect to $\mathcal{P}_{0,\Delta_0}$, $\mathcal{P}_{f,\Delta_f}$, the FD problem

towards minimizing the MDR for a given FAR is formulated as follows

$$\min_{\mathbf{W}\neq 0,\, J(\mathbf{r}),\, J_{th}} \quad \beta^{rob} \tag{6.9}$$

$$\text{s.t.} \quad \begin{cases} \sup\limits_{\mathbb{P}_z \in \mathcal{P}_{0,\Delta_0}} \Pr\{J(\mathbf{r}) > J_{th}\} \leq \alpha_0^{rob} \\ \sup\limits_{\mathbb{P}_z \in \mathcal{P}_{f,\Delta_f}} \Pr\{J(\mathbf{r}) \leq J_{th}\} \leq \beta^{rob} \end{cases} \tag{6.10}$$

where $\alpha_0^{rob} \in (0,1)$ is a given upper bound of FAR, $\beta^{rob} \in (0,1)$ the upper bound of MDR under moments uncertainties $\mathbf{\Delta}_0$ and $\mathbf{\Delta}_f$.

Considering $\mathbf{\Delta}_0 \neq 0$, $\mathbf{\Delta}_f \neq 0$ in practical applications, main attention of this chapter is thus focused on the performance evaluation of the distribution independent FD systems demonstrated in Chapters 3–5 under moments uncertainties. The problems are specifically formulated as follows, i.e., given ambiguity sets $\mathcal{P}_{0,\Delta_0}$, $\mathcal{P}_{f,\Delta_f}$,

- solve the problem (6.9)–(6.10) for vector-valued solution $\mathbf{w}$, with residual evaluation function $J(r) = |\ \mathbf{w}^T\mathbf{z}(k)|$ and threshold $J_{th} = b$.
- Solve the problem (6.9)–(6.10) for vector-valued solution $\mathbf{w}$ with residual evaluation function $J(r) = (\ \mathbf{w}^T(\mathbf{z}(k) - \bar{\mathbf{z}}_0))^2$ and threshold $J_{th} = 1$.
- Solve the problem (6.9)–(6.10) for matrix-valued solutions $\mathbf{W}$ with the residual evaluation function $J(\mathbf{r})$ given in forms of (5.10), (5.29) and (5.53) and threshold $J_{th} = 1$, respectively.
- Assess the derived FAR and MDR performance under moments uncertainties in the probabilistic context and exploit the confidence levels of them.

6.2 Ambiguity sets modeling under moments uncertainties

To cope with the formulated problems, we start by modeling the ambiguity sets $\mathcal{P}_{0,\Delta_0}$, $\mathcal{P}_{f,\Delta_f}$ under norm-bounded and box-type moments uncertainties.

6.2.1 Norm-bounded model

Consider the moments uncertainties $\mathbf{\Delta}_{\bar{z}_0}$, $\mathbf{\Delta}_{\bar{z}_f}$, $\mathbf{\Delta}_{\Sigma_{z_0}}$, $\mathbf{\Delta}_{\Sigma_{z_f}}$ being norm-bounded. The ambiguity set $\mathcal{P}_{0,\Delta_0}$ for fault-free case is modeled as follows

$$\mathcal{P}_{0,\Delta_0}(\epsilon_1,\, \epsilon_2) = \left\{ \mathbb{P}_z \in \mathcal{L} \;\middle|\; \begin{array}{l} \mathbf{z} \in \mathcal{M}_0 \\ \mathbb{E}[\mathbf{z}] = \bar{\mathbf{z}}_0,\ \mathbb{V}[\mathbf{z}] = \mathbf{\Sigma}_{z_0} \in \mathbb{S}_+^{\gamma} \\ \left\| \mathbf{\Sigma}_{z_0}^{-\frac{1}{2}} (\bar{\mathbf{z}}_0 - \hat{\bar{\mathbf{z}}}_0) \right\|_2 \leq \epsilon_1 \\ \left\| \mathbf{\Sigma}_{z_0} - \hat{\mathbf{\Sigma}}_{z_0} \right\|_F \leq \epsilon_2 \end{array} \right\} \tag{6.11}$$

where $\mathcal{M}_0$ is the support of $\mathbf{z}_0$, $\mathcal{L}$ is the set of all valid distributions in space $\mathbb{R}^\gamma$, $\epsilon_1,\ \epsilon_2 \geq 0$, $\hat{\bar{\mathbf{z}}}_0$, $\hat{\mathbf{\Sigma}}_{z_0}$ are empirical values of $\bar{\mathbf{z}}_0$, $\mathbf{\Sigma}_{z_0}$, as given in (6.5). Remarkably, the uncertainty in mean is characterized by an ellipsoid of size ϵ_1 centered at $\hat{\bar{\mathbf{z}}}_0$ and, the uncertainty in covariance matrix is specified within a Frobenius-norm ball centered at $\hat{\mathbf{\Sigma}}_{z_0}$ with radius ϵ_2.

Similarly, the ambiguity set $\mathcal{P}_{f,\Delta_f}$ for the faulty case is defined as follows

$$\mathcal{P}_{f,\Delta_f}\left(\epsilon_3,\ \epsilon_4\right) = \left\{ \mathbb{P}_z \in \mathcal{L} \left| \begin{array}{l} \mathbf{z} \in \mathcal{M}_f \\ \mathbb{E}[\mathbf{z}] = \bar{\mathbf{z}}_f,\ \mathbb{V}[\mathbf{z}] = \mathbf{\Sigma}_{z_f} \in \mathbb{S}_+^\gamma \\ \left\| \mathbf{\Sigma}_{z_f}^{-\frac{1}{2}} (\bar{\mathbf{z}}_f - \hat{\bar{\mathbf{z}}}_f) \right\|_2 \leq \epsilon_3 \\ \left\| \mathbf{\Sigma}_{z_f} - \hat{\mathbf{\Sigma}}_{z_f} \right\|_F \leq \epsilon_4 \end{array} \right. \right\} \tag{6.12}$$

where $\mathcal{M}_f$, $\epsilon_3 \geq 0$, $\epsilon_4 \geq 0$ have the same physical meanings with $\mathcal{M}_0$, ϵ_1, ϵ_2 in $\mathcal{P}_{0,\Delta_0}$, respectively. Analogously, the ambiguity sets for the concerned M faulty modes can be established, i.e.,

$$\mathcal{P}_{f_i,\Delta_{f_i}}\left(\epsilon_{3,i},\ \epsilon_{4,i}\right) = \left\{ \mathbb{P}_z \in \mathcal{L} \left| \begin{array}{l} \mathbf{z} \in \mathcal{M}_{f_i} \\ \mathbb{E}[\mathbf{z}] = \bar{\mathbf{z}}_{f_i},\ \mathbb{V}[\mathbf{z}] = \mathbf{\Sigma}_{z_{f_i}} \in \mathbb{S}_+^\gamma \\ \left\| \mathbf{\Sigma}_{z_{f_i}}^{-\frac{1}{2}} (\bar{\mathbf{z}}_{f_i} - \hat{\bar{\mathbf{z}}}_{f_i}) \right\|_2 \leq \epsilon_{3,i} \\ \left\| \mathbf{\Sigma}_{z_{f_i}} - \hat{\mathbf{\Sigma}}_{z_{f_i}} \right\|_F \leq \epsilon_{4,i} \end{array} \right. \right\} \tag{6.13}$$

where $\epsilon_{3,i},\ \epsilon_{4,i} \geq 0,\ \forall,\ i = 1,\ 2,\ ...,\ M$. In this sense, we define $\mathcal{P}_{f,\Delta_f} = \bigcup_{i=1}^{M} \mathcal{P}_{f_i,\Delta_{f_i}}$.

Remark 6.1. *Generally speaking, the uncertainties $\mathbf{\Delta}_{\bar{z}_0}$, $\mathbf{\Delta}_{\bar{z}_f}$, $\mathbf{\Delta}_{\Sigma_{z_0}}$, $\mathbf{\Delta}_{\Sigma_{z_f}}$ are considered to be estimation errors caused by the limited number of samples and the probability distribution being time-invariant, as shown in Fig. 6.1(a). Indeed, the uncertainties caused by the identification errors in $\mathbf{\Psi}_s^\perp$, the perturbations of working point and the drifts of the distribution profile of noises and faults, etc., can also be modeled with $\mathcal{P}_{0,\Delta_0}$ and $\mathcal{P}_{f,\Delta_f}$, as seen in Fig. 6.1(b). In this situation, the $\hat{\bar{\mathbf{z}}}_0$, $\hat{\bar{\mathbf{z}}}_f$, $\hat{\mathbf{\Sigma}}_{z_0}$, $\hat{\mathbf{\Sigma}}_{z_f}$ can be regarded as reference means and covariance matrices.*

6.2.2 Box-type model

By specifying the uncertainties $\mathbf{\Delta}_{\bar{z}_0}$, $\mathbf{\Delta}_{\bar{z}_f}$, $\mathbf{\Delta}_{\Sigma_{z_0}}$, $\mathbf{\Delta}_{\Sigma_{z_f}}$ in box-type, we model the ambiguity set $\mathcal{P}_{0,\Delta_0}$ in the following form

$$\mathcal{P}_{0,\Delta_0}\left(R_0,\ \tau_1,\ \tau_2\right) = \left\{ \mathbb{P}_z \in \mathcal{L} \left| \begin{array}{ll} \mathbb{E}[\mathbf{z}] = \bar{\mathbf{z}}_0,\ \mathbb{V}[\mathbf{z}] = \mathbf{\Sigma}_{z_0} \in \mathbb{S}_+^\gamma & (a) \\ \left(\mathbf{z} - \bar{\mathbf{z}}_0\right)^T \mathbf{\Sigma}_{z_0}^{-1} \left(\mathbf{z} - \bar{\mathbf{z}}_0\right) \leq R_0^2 & (b) \\ (\bar{\mathbf{z}}_0 - \hat{\bar{\mathbf{z}}}_0)^T \mathbf{\Sigma}_{z_0}^{-1} (\bar{\mathbf{z}}_0 - \hat{\bar{\mathbf{z}}}_0) \leq \tau_1 & (c) \\ \mathbf{\Sigma}_{z_0} \preceq \tau_2 \hat{\mathbf{\Sigma}}_{z_0} & (d) \end{array} \right. \right\} \tag{6.14}$$

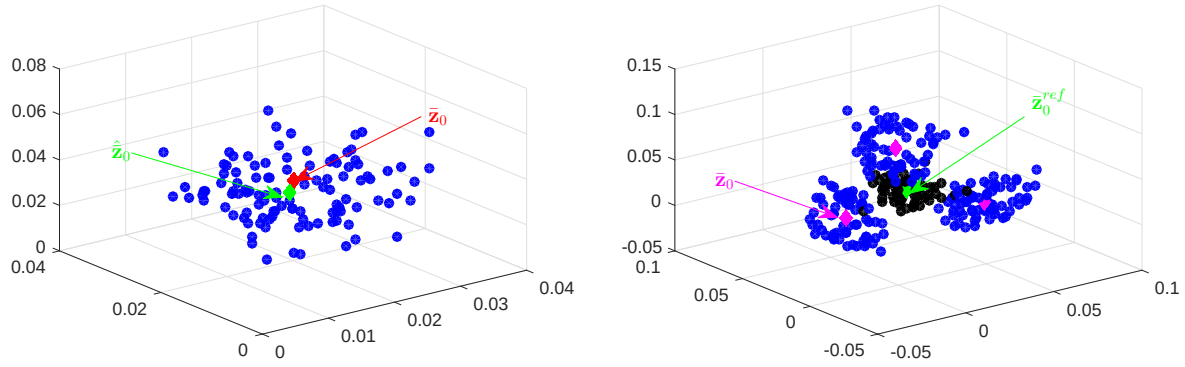

(a) (b)

Figure 6.1: Moments uncertainties: (a) caused by the estimation errors; (b) caused by the modeling uncertainties.

where $R_0 \geq 0$ in (b) determines a ball that contains the entire support of $\mathbf{z}_0$ being with the mean $\bar{\mathbf{z}}_0$ and covariance matrix $\mathbf{\Sigma}_{z_0}$. Conditions (c) and (d) give box-type measures of uncertainties in mean $\bar{\mathbf{z}}_0$ and covariance matrix $\mathbf{\Sigma}_{z_0}$, respectively, with the introduction of parameters $\tau_1 \geq 0$, $\tau_2 \geq 1$.

Similarly, the ambiguity set $\mathcal{P}_{f_i,\Delta_{f_i}}$ for the i-th fault mode is defined as follows

$$\mathcal{P}_{f_i,\Delta_{f_i}}\left(R_{f_i},\, \tau_{3,i},\, \tau_{4,i}\right) = \left\{ \mathbb{P}_z \in \mathcal{L} \;\middle|\; \begin{array}{l} \mathbb{E}[\mathbf{z}] = \bar{\mathbf{z}}_{f_i},\, \mathbb{V}[\mathbf{z}] = \mathbf{\Sigma}_{z_{f_i}} \in \mathbb{S}_+^\gamma \\ \left(\mathbf{z} - \bar{\mathbf{z}}_{f_i}\right)^T \mathbf{\Sigma}_{z_{f_i}}^{-1} \left(\mathbf{z} - \bar{\mathbf{z}}_f\right) \leq R_{f_i}^2 \\ (\bar{\mathbf{z}}_{f_i} - \hat{\bar{\mathbf{z}}}_{f_i})^T \mathbf{\Sigma}_{z_{f_i}}^{-1} (\bar{\mathbf{z}}_{f_i} - \hat{\bar{\mathbf{z}}}_{f_i}) \leq \tau_{3,i} \\ \mathbf{\Sigma}_{z_{f_i}} \preceq \tau_{4,i} \hat{\mathbf{\Sigma}}_{f_i} \end{array} \right\} \tag{6.15}$$

where $R_{f_i} > 0$, $\tau_{3,i} \geq 0$, $\tau_{4,i} \geq 1$, $i = 1, 2, ...M$.

For ease of subsequent discussion, we denote by $\tilde{\mathbf{z}}_{c,0} = \mathbf{z}_0 - \hat{\bar{\mathbf{z}}}_0$, $\tilde{\mathbf{z}}_{c,f_i} = \mathbf{z}_{f_i} - \hat{\bar{\mathbf{z}}}_0$ and

$$\bar{\tilde{\mathbf{z}}}_{c,0} = \bar{\mathbf{z}}_0 - \hat{\bar{\mathbf{z}}}_0,\; \bar{\tilde{\mathbf{z}}}_{c,f_i} = \bar{\mathbf{z}}_{f_i} - \hat{\bar{\mathbf{z}}}_0,\; i = 1, 2, ..., M.$$

The second-order moment matrices of $\tilde{\mathbf{z}}_{c,0}$ and $\tilde{\mathbf{z}}_{c,f_i}$ are given as

$$\mathbf{\Omega}_{\tilde{z}_{c,0}} = \begin{bmatrix} \mathbf{\Sigma}_{z_0} + \bar{\tilde{\mathbf{z}}}_{c,0} \bar{\tilde{\mathbf{z}}}_{c,0}^T & \bar{\tilde{\mathbf{z}}}_{c,0} \\ \bar{\tilde{\mathbf{z}}}_{c,0}^T & 1 \end{bmatrix},\; \mathbf{\Omega}_{\tilde{z}_{c,f_i}} = \begin{bmatrix} \mathbf{\Sigma}_{z_{f_i}} + \bar{\tilde{\mathbf{z}}}_{c,f_i} \bar{\tilde{\mathbf{z}}}_{c,f_i}^T & \bar{\tilde{\mathbf{z}}}_{c,f_i} \\ \bar{\tilde{\mathbf{z}}}_{c,f_i}^T & 1 \end{bmatrix} \tag{6.16}$$

Note from (c) in (6.14) that $\begin{bmatrix} \mathbf{\Sigma}_{z_0} & \bar{\tilde{\mathbf{z}}}_{c,0} \\ \bar{\tilde{\mathbf{z}}}_{c,0}^T & \tau_1 \end{bmatrix} \succeq 0,\;\; \bar{\tilde{\mathbf{z}}}_{c,0} \bar{\tilde{\mathbf{z}}}_{c,0}^T - \tau_1 \mathbf{\Sigma}_{z_0} \preceq 0$. Let

$$\overline{\mathbf{\Omega}}_{\tilde{z}_{c,0}} = \begin{bmatrix} (2+\tau_1)\tau_2 \hat{\mathbf{\Sigma}}_{z_0} & 0 \\ 0 & 1+\tau_1 \end{bmatrix}. \tag{6.17}$$

Then, together with (d), we have

$$\overline{\mathbf{\Omega}}_{\tilde{z}_{c,0}} - \mathbf{\Omega}_{\tilde{z}_{c,0}} = \begin{bmatrix} (2+\tau_1)\tau_2\hat{\mathbf{\Sigma}}_{z_0} - \mathbf{\Sigma}_{z_0} - \bar{\tilde{\mathbf{z}}}_{c,0}\bar{\tilde{\mathbf{z}}}_{c,0}^T & -\bar{\tilde{\mathbf{z}}}_{c,0} \\ -\bar{\tilde{\mathbf{z}}}_{c,0}^T & \tau_1 \end{bmatrix} \succeq 0.$$

This is obtained by noting that $\mathbf{\Pi} = (2+\tau_1)\tau_2\hat{\mathbf{\Sigma}}_{z_0} - \mathbf{\Sigma}_{z_0} - \bar{\tilde{\mathbf{z}}}_{c,0}\bar{\tilde{\mathbf{z}}}_{c,0}^T = 2\tau_2\hat{\mathbf{\Sigma}}_{z_0} - \mathbf{\Sigma}_{z_0} + \tau_1\tau_2\hat{\mathbf{\Sigma}}_{z_0} - \bar{\tilde{\mathbf{z}}}_{c,0}\bar{\tilde{\mathbf{z}}}_{c,0}^T \succeq \mathbf{\Sigma}_{z_0} + \tau_1\mathbf{\Sigma}_{z_0} - \bar{\tilde{\mathbf{z}}}_{c,0}\bar{\tilde{\mathbf{z}}}_{c,0}^T \succeq \mathbf{\Sigma}_{z_0}$ and $\tau_1\mathbf{\Pi} - \bar{\tilde{\mathbf{z}}}_{c,0}\bar{\tilde{\mathbf{z}}}_{c,0}^T \succeq \tau_1\mathbf{\Sigma}_{z_0} - \bar{\tilde{\mathbf{z}}}_{c,0}\bar{\tilde{\mathbf{z}}}_{c,0}^T \succeq 0$. It thus clearly holds, with respect to the ambiguity set (6.14),

$$0 \preceq \mathbf{\Omega}_{\tilde{z}_{c,0}} \preceq \overline{\mathbf{\Omega}}_{\tilde{z}_{c,0}}. \tag{6.18}$$

Analogically, given ambiguity set $\mathcal{P}_{f_i,\Delta_{f_i}}$ in (6.15) we also have

$$0 \preceq \mathbf{\Omega}_{\tilde{z}_{c,f_i}} \preceq \overline{\mathbf{\Omega}}_{\tilde{z}_{c,f_i}} \tag{6.19}$$

for $i = 1, 2, ..., M$ with

$$\overline{\mathbf{\Omega}}_{\tilde{z}_{c,f_i}} = \begin{bmatrix} (2+\tau_{3,i})\tau_{4,i}\hat{\mathbf{\Sigma}}_{z_{f_i}} + (\hat{\bar{\mathbf{z}}}_{f_i} - \hat{\bar{\mathbf{z}}}_0)(\hat{\bar{\mathbf{z}}}_{f_i} - \hat{\bar{\mathbf{z}}}_0)^T & \hat{\bar{\mathbf{z}}}_{f_i} - \hat{\bar{\mathbf{z}}}_0 \\ (\hat{\bar{\mathbf{z}}}_{f_i} - \hat{\bar{\mathbf{z}}}_0)^T & 1+\tau_{3,i} \end{bmatrix}. \tag{6.20}$$

It is remarkable that (6.18) and (6.19) determine box-type uncertainties in the second-order moment matrices $\mathbf{\Omega}_{\tilde{z}_{c,0}}$ and $\mathbf{\Omega}_{\tilde{z}_{c_{f_i}}}$, respectively, in terms of the so-called upper bounds $\overline{\mathbf{\Omega}}_{\tilde{z}_{c,0}}$ and $\overline{\mathbf{\Omega}}_{\tilde{z}_{c_{f_i}}}$ and zero lower bounds.

6.3 Robustness analysis of the FD systems

Regarding the above modeled ambiguity sets, the robustness of the FD systems designed with respect to addressing the problem (6.9)–(6.10) is investigated in this section.

6.3.1 DIO method aided robust FD

Remember that, using the following residual evaluation function and threshold

$$J(r) = |\mathbf{w}^T\mathbf{z}(k)|, \quad J_{th} = b$$

the design of FD systems has been addressed by solving the problem (3.13)–(3.14) with known precise means and covariance matrices of residuals both in fault-free and faulty cases, as demonstrated in Chapter 3. When the uncertainties in means and covariance matrices specified in $\mathcal{P}_{0,\Delta_0}(\epsilon_1, \epsilon_2)$, $\mathcal{P}_{f,\Delta_f}(\epsilon_3, \epsilon_4)$ are concerned, the FD problem (6.9)–(6.10)

is then handled by solving

$$\min_{\mathbf{w}\neq 0,\, b>0} \quad \beta^{rob} \tag{6.21}$$

$$\text{s.t.} \quad \begin{cases} \sup\limits_{\mathbb{P}_z\in\mathcal{P}_{0,\Delta_0}(\epsilon_1,\epsilon_2)} \Pr\left\{\mathbf{w}^T\mathbf{z} > b\right\} \leq \frac{\alpha_0^{rob}}{2} \\ \sup\limits_{\mathbb{P}_z\in\mathcal{P}_{f,\Delta_f}(\epsilon_3,\epsilon_4)} \Pr\left\{\mathbf{w}^T\mathbf{z} \leq b\right\} \leq \beta^{rob}. \end{cases} \tag{6.22}$$

Aiming to cope with this problem, the following lemmas are firstly recalled to handle the DCCs (6.22) in the probabilistic context.

Lemma 6.1. *[53] Given $\epsilon > 0$, $\mathbf{w} \in \mathbb{R}^n$, $\bar{\boldsymbol{\xi}}_0 \in \mathbb{R}^n$ and matrix $\boldsymbol{\Sigma} \in \mathbb{S}_+^n$, the optimal solution of the problem*

$$\mathcal{Q}_1(\bar{\boldsymbol{\xi}}) = \min_{\bar{\boldsymbol{\xi}}} \quad \mathbf{w}^T\bar{\boldsymbol{\xi}} \quad s.t. \quad \left\|\boldsymbol{\Sigma}^{-\frac{1}{2}}(\bar{\boldsymbol{\xi}} - \bar{\boldsymbol{\xi}}_0)\right\|_2 \leq \epsilon$$

is achieved with $\bar{\boldsymbol{\xi}} = \bar{\boldsymbol{\xi}}_0 - \frac{\epsilon\boldsymbol{\Sigma}\mathbf{w}}{\sqrt{\mathbf{w}^T\boldsymbol{\Sigma}\mathbf{w}}}$. At the optimum, it holds $\mathcal{Q}_1(\bar{\boldsymbol{\xi}}) = \mathbf{w}^T\bar{\boldsymbol{\xi}}_0 - \epsilon\sqrt{\mathbf{w}^T\boldsymbol{\Sigma}\mathbf{w}}$.

Lemma 6.2. *[53] Using the notations in Lemma 6.1, the optimal solution of the problem*

$$\mathcal{Q}_2(\boldsymbol{\Sigma}) = \max_{\boldsymbol{\Sigma}} \quad \mathbf{w}^T\boldsymbol{\Sigma}\mathbf{w} \quad s.t. \quad \|\boldsymbol{\Sigma} - \boldsymbol{\Sigma}_0\|_F \leq \epsilon$$

is achieved with $\boldsymbol{\Sigma} = \boldsymbol{\Sigma}_0 + \epsilon\mathbf{I}$. At the optimum, it holds $\mathcal{Q}_2(\boldsymbol{\Sigma}) = \mathbf{w}^T\left(\boldsymbol{\Sigma}_0 + \epsilon\mathbf{I}\right)\mathbf{w}$.

According to Lemmas 6.1 and 6.2, it is obvious that, if

$$b - \mathbf{w}^T\hat{\bar{\mathbf{z}}}_0 \geq \left(\bar{\kappa}(\alpha_0^{rob}) + \epsilon_1\right)\sqrt{\mathbf{w}^T(\hat{\boldsymbol{\Sigma}}_{z_0} + \epsilon_2\mathbf{I})\mathbf{w}} \tag{6.23}$$

holds with $\bar{\kappa}(\alpha_0^{rob}) = \sqrt{(2-\alpha_0^{rob})/\alpha_0^{rob}}$, we then have

$$b - \mathbf{w}^T\bar{\mathbf{z}}_0 \geq \bar{\kappa}(\alpha_0^{rob})\sqrt{\mathbf{w}^T\boldsymbol{\Sigma}_{z_0}\mathbf{w}},\ \forall\,(\bar{\mathbf{z}}_0,\,\boldsymbol{\Sigma}_{z_0}) \in \left\{ (\bar{\mathbf{z}}_0,\,\boldsymbol{\Sigma}_{z_0}) \;\middle|\; \begin{array}{l} \left\|\boldsymbol{\Sigma}_{z_0}^{-\frac{1}{2}}(\bar{\mathbf{z}}_0 - \hat{\bar{\mathbf{z}}}_0)\right\|_2 \leq \epsilon_1 \\ \left\|\boldsymbol{\Sigma}_{z_0} - \hat{\boldsymbol{\Sigma}}_{z_0})\right\|_F \leq \epsilon_2 \end{array} \right\}$$

$$\Leftrightarrow \quad \sup_{\mathbb{P}_z\in\mathcal{P}_{0,\Delta_0}(\epsilon_1,\epsilon_2)} \Pr\left\{\mathbf{w}^T\mathbf{z} > b\right\} \leq \frac{\alpha_0^{rob}}{2}$$

which means the constraint (6.23) holding ensures the first condition in (6.22). Ditto for the faulty case, a deterministic substitution of the second DCC in (6.22) can be obtained, as summarized in the following theorem.

Theorem 6.1. *Given $\mathcal{P}_{0,\Delta_0}(\epsilon_1,\epsilon_2)$ in (6.11) and $\mathcal{P}_{f,\Delta_f}(\epsilon_3,\epsilon_4)$ in (6.12), the first DCC in (6.22) holds if*

$$b - \mathbf{w}^T\hat{\bar{\mathbf{z}}}_0 \geq \left(\bar{\kappa}(\alpha_0^{rob}) + \epsilon_1\right)\sqrt{\mathbf{w}^T(\hat{\boldsymbol{\Sigma}}_{z_0} + \epsilon_2\mathbf{I})\mathbf{w}}. \tag{6.24}$$

Let $\kappa(\beta^{rob}) = \sqrt{(1-\beta^{rob})/\beta^{rob}}$, the second DCC in (6.22) holds if

$$-b + \mathbf{w}^T\hat{\bar{\mathbf{z}}}_f \geq \left(\kappa(\beta^{rob}) + \epsilon_3\right)\sqrt{\mathbf{w}^T(\hat{\boldsymbol{\Sigma}}_{z_f} + \epsilon_4\mathbf{I})\mathbf{w}}. \tag{6.25}$$

According to Theorem 6.1, the problem (6.21)–(6.22) is converted into the following RO problem

$$\min_{\mathbf{w}\neq 0,\, b>0} \quad \beta^{rob} \quad \text{s.t.} \;\; (6.24) \text{ and } (6.25) \tag{6.26}$$

which can be further re-written as follows

$$\min_{\mathbf{w}} \quad \frac{1-\left(\bar{\kappa}(\alpha_0^{rob})+\epsilon_1\right)\sqrt{\mathbf{w}^T(\hat{\mathbf{\Sigma}}_{z_0}+\epsilon_2\mathbf{I})\mathbf{w}}}{\sqrt{\mathbf{w}^T(\hat{\mathbf{\Sigma}}_{z_f}+\epsilon_4\mathbf{I})\mathbf{w}}} \quad \text{s.t.} \quad \mathbf{w}^T(\hat{\bar{\mathbf{z}}}_f-\hat{\bar{\mathbf{z}}}_0)=1. \tag{6.27}$$

It is noteworthy that this problem can be solved with Algorithm 3.2.5. The optimal solutions of $\mathbf{w}$, b, β^{rob} to (6.26) are then obtained as

$$\kappa(\beta^{rob}) = \frac{1-\left(\bar{\kappa}(\alpha_0^{rob})+\epsilon_1\right)\sqrt{\mathbf{w}^T(\hat{\mathbf{\Sigma}}_{z_0}+\epsilon_2\ \mathbf{I})\mathbf{w}}}{\sqrt{\mathbf{w}^T(\hat{\mathbf{\Sigma}}_{z_f}+\epsilon_4\ \mathbf{I})\mathbf{w}}}-\epsilon_3 \tag{6.28}$$

$$\beta^{rob} = \frac{1}{1+\kappa^2(\beta^{rob})} \tag{6.29}$$

$$\begin{aligned} b &= \mathbf{w}^T\hat{\bar{\mathbf{z}}}_0+\left(\bar{\kappa}(\alpha_0^{rob})+\epsilon_1\right)\sqrt{\mathbf{w}^T(\hat{\mathbf{\Sigma}}_{z_0}+\epsilon_2\mathbf{I})\mathbf{w}} \\ &= \mathbf{w}^T\hat{\bar{\mathbf{z}}}_f-(\kappa(\beta^{rob})+\epsilon_3)\sqrt{\mathbf{w}^T(\hat{\mathbf{\Sigma}}_{z_f}+\epsilon_4\ \mathbf{I})\mathbf{w}} \end{aligned} \tag{6.30}$$

In this context, the worst-case FAR and MDR under moments uncertainties are obtained satisfying $P_{FAR}\leq\alpha_0^{rob}$, $P_{MDR}\leq\beta^{rob}$.

To gain a deeper interpretation of the robust optimal solutions (6.28)–(6.30), we make a comparison of them with the ones obtained without moments uncertainties, i.e., (3.35)–(3.37) given in Section 3.3, and have the following observations.

- For an identical upper bound of FAR α_0, it holds

$$\beta^{rob}\geq\beta \tag{6.31}$$

  because $\kappa(\beta^{rob})\leq\kappa(\beta)$ and $\kappa(\beta^{rob})$, $\kappa(\beta)$ have the opposite monotonicity with β^{rob}, β, respectively. It implies, the uncertainties in means and covariance matrices would give rise to the increase of MDR on the one hand and, on the other hand, admits a good robustness against the uncertainties might be caused by the perturbations of operating point, distribution drifts of noises and faults and estimation errors, etc.

- The FD problem (6.27) has the same form of the problem (3.34) with the item $\bar{\kappa}(\alpha_0^{rob})+\epsilon_1$ in place of $\bar{\kappa}(\alpha_0)$. In this context, consider $\bar{\kappa}(\alpha_0^{rob})+\epsilon_1=\bar{\kappa}(\alpha_0)$. Then

$$\alpha_0^{rob}=\frac{2}{1+\left(\bar{\kappa}(\alpha_0)-\epsilon_1\right)^2},\ \alpha_0^{rob}\geq\alpha_0. \tag{6.32}$$

It implies that the worst-case FAR gets larger due to the moments uncertainties. Meanwhile, because of $\bar{\kappa}(\alpha_0^{rob}) > 0$, it should hold $\bar{\kappa}(\alpha_0) > \epsilon_1$, which means $\bar{\kappa}(\alpha_0)$ suggests a tolerance bound of the uncertainties in mean $\mathbf{z}_0$ for given α_0. This point has also been mentioned in [53] from the perspective of classification.

6.3.2 Improved DIO method aided robust FD

In this part, we evaluate the robustness of the improved DIO method aided FD systems in Chapter 4. To this end, consider the following residual evaluation function and threshold

$$J(r) = (\mathbf{w}^T(\mathbf{z}(k) - \hat{\bar{\mathbf{z}}}_0))^2, \ J_{th} = 1. \tag{6.33}$$

The FD problem (6.9)–(6.10) with respect to (6.11) and (6.12) is then re-written as follows

$$\min_{\mathbf{w}\neq 0} \quad \beta^{rob} \tag{6.34}$$

$$\text{s.t.} \quad \begin{cases} \sup\limits_{\mathbb{P}_z \in \mathcal{P}_{0,\Delta_0}(\epsilon_1,\epsilon_2)} \Pr\left\{(\mathbf{w}^T(\mathbf{z} - \hat{\bar{\mathbf{z}}}_0))^2 > 1\right\} \leq \alpha_0^{rob} \\ \sup\limits_{\mathbb{P}_z \in \mathcal{P}_{f,\Delta_f}(\epsilon_3,\epsilon_4)} \Pr\left\{(\mathbf{w}^T(\mathbf{z} - \hat{\bar{\mathbf{z}}}_0))^2 \leq 1\right\} \leq \beta^{rob}. \end{cases} \tag{6.35}$$

To solve this problem, the following lemmas are given as corollaries of Theorem 6.1.

Lemma 6.3. *Given ambiguity set $\mathcal{P}_{0,\Delta_0}(\epsilon_1,\epsilon_2)$ in (6.11), the first DCC in (6.35) holds if*

$$\left(\epsilon_1 + \nu(\alpha_0^{rob})\right)\sqrt{\mathbf{w}^T(\hat{\mathbf{\Sigma}}_{z_0} + \epsilon_2\mathbf{I})\mathbf{w}} \leq 1 \tag{6.36}$$

with $\nu(\alpha_0^{rob}) = \sqrt{1/\alpha_0^{rob}}$.

Proof. Without considering the uncertainties in mean and covariance matrix, it is known form the Theorem 4.4 that the first DCC in (6.35) can be equally converted into

$$1 - \sqrt{\mathbf{w}^T(\bar{\mathbf{z}}_0 - \hat{\bar{\mathbf{z}}}_0)(\bar{\mathbf{z}}_0 - \hat{\bar{\mathbf{z}}}_0)^T\mathbf{w}} \geq \nu(\alpha_0^{rob})\sqrt{\mathbf{w}^T\mathbf{\Sigma}_{z_0}\mathbf{w}} \tag{6.37}$$

It yields $\nu(\alpha_0^{rob})\sqrt{\mathbf{w}^T\mathbf{\Sigma}_{z_0}\mathbf{w}} \leq 1$ on condition that $\bar{\mathbf{z}}_0 = \hat{\bar{\mathbf{z}}}_0$, i.e., $\epsilon_1 = 0$ in $\mathcal{P}_{0,\Delta_0}$. Consider the uncertainty in $\bar{\mathbf{z}}_0$. Note that

$$\left\|\mathbf{w}^T(\bar{\mathbf{z}}_0 - \hat{\bar{\mathbf{z}}}_0)\right\|_2 \leq \left\|\mathbf{w}^T\mathbf{\Sigma}_{z_0}^{\frac{1}{2}}\right\|_2 \left\|\mathbf{\Sigma}_{z_0}^{-\frac{1}{2}}(\bar{\mathbf{z}}_0 - \hat{\bar{\mathbf{z}}}_0)\right\|_2 \leq \epsilon_1 \left\|\mathbf{w}^T\mathbf{\Sigma}_{z_0}^{\frac{1}{2}}\right\|_2. \tag{6.38}$$

Using the result in Lemma 6.2, we have

$$\max_{\left\|\mathbf{\Sigma}_{z_0} - \hat{\mathbf{\Sigma}}_{z_0}\right\|_F \leq \epsilon_2} \mathbf{w}^T\mathbf{\Sigma}_{z_0}\mathbf{w} = \mathbf{w}^T(\hat{\mathbf{\Sigma}}_{z_0} + \epsilon_2\mathbf{I})\mathbf{w}. \tag{6.39}$$

Together with (6.37), (6.38) and (6.39), it is then derived that

$$\begin{aligned}\sqrt{\mathbf{w}^T(\bar{\mathbf{z}}_0-\hat{\bar{\mathbf{z}}}_0)(\bar{\mathbf{z}}_0-\hat{\bar{\mathbf{z}}}_0)^T\ \mathbf{w}}+\nu(\alpha_0^{rob})\sqrt{\mathbf{w}^T\boldsymbol{\Sigma}_{z_0}\mathbf{w}}\ &\le \epsilon_1\left\|\ \mathbf{w}^T\boldsymbol{\Sigma}_{z_0}^{\frac{1}{2}}\right\|_2+\nu(\alpha_0^{rob})\left\|\ \mathbf{w}^T\boldsymbol{\Sigma}_{z_0}^{\frac{1}{2}}\right\|_2\\ &\le \left(\epsilon_1+\nu(\alpha_0^{rob})\right)\sqrt{\mathbf{w}^T(\hat{\boldsymbol{\Sigma}}_{z_0}+\epsilon_2\mathbf{I})\mathbf{w}}.\end{aligned}$$

Hence, if $\left(\epsilon_1+\nu(\alpha_0^{rob})\right)\sqrt{\mathbf{w}^T(\hat{\boldsymbol{\Sigma}}_{z_0}+\epsilon_2\mathbf{I})\mathbf{w}}\le 1$ holds, then (6.37) holds true. The first DCC in (6.35) can thus be substituted by constraint (6.36). The proof is completed. □

Lemma 6.4. *Given ambiguity set $\mathcal{P}_{f,\Delta_f}(\epsilon_3,\,\epsilon_4)$ in (6.12), the second DCC in (6.35) holds if*

$$\sqrt{\mathbf{w}^T(\hat{\bar{\mathbf{z}}}_f-\hat{\bar{\mathbf{z}}}_0)(\hat{\bar{\mathbf{z}}}_f-\hat{\bar{\mathbf{z}}}_0)^T\mathbf{w}}-1\ge\left(\kappa(\beta^{rob})+\epsilon_3\right)\sqrt{\mathbf{w}^T(\hat{\boldsymbol{\Sigma}}_{z_f}+\epsilon_4\mathbf{I})\mathbf{w}}\tag{6.40}$$

holds with $\kappa(\beta^{rob})=\sqrt{(1-\beta^{rob})/\beta^{rob}}$.

Proof. Under no moments uncertainties, it is derived from Theorem 4.5 that the second DCC in (6.35) can be equally converted into

$$\sqrt{\mathbf{w}^T(\bar{\mathbf{z}}_f-\hat{\bar{\mathbf{z}}}_0)(\bar{\mathbf{z}}_f-\hat{\bar{\mathbf{z}}}_0)^T\mathbf{w}}-1\ge\kappa(\beta^{rob})\sqrt{\mathbf{w}^T\boldsymbol{\Sigma}_{z_f}\mathbf{w}}.\tag{6.41}$$

Let $\mathbf{h}=\bar{\mathbf{z}}_f-\hat{\bar{\mathbf{z}}}_0$, $\mathbf{h}_0=\hat{\bar{\mathbf{z}}}_f-\hat{\bar{\mathbf{z}}}_0$. Then $\mathbf{h}-\mathbf{h}_0=\bar{\mathbf{z}}_f-\hat{\bar{\mathbf{z}}}_f$. The uncertainty in $\mathbf{h}$ holds with $\left\|\boldsymbol{\Sigma}_{z_f}^{-\frac{1}{2}}(\mathbf{h}-\mathbf{h}_0)\right\|_2\le\epsilon_3$. Note that

$$\begin{aligned}\min_{\left\|\boldsymbol{\Sigma}_{z_f}^{-\frac{1}{2}}(\bar{\mathbf{z}}_f-\hat{\bar{\mathbf{z}}}_f)\right\|_2\le\epsilon_3}\sqrt{\mathbf{w}^T(\bar{\mathbf{z}}_f-\hat{\bar{\mathbf{z}}}_f)(\bar{\mathbf{z}}_f-\hat{\bar{\mathbf{z}}}_f)^T\mathbf{w}}&=\min_{\left\|\boldsymbol{\Sigma}_{z_f}^{-\frac{1}{2}}(\mathbf{h}-\mathbf{h}_0)\right\|_2\le\epsilon_3}\left\|\mathbf{w}^T\mathbf{h}\right\|_2\\ &=\sqrt{\mathbf{w}^T\mathbf{h}_0\mathbf{h}_0^T\mathbf{w}}-\epsilon_3\sqrt{\mathbf{w}^T\boldsymbol{\Sigma}_{z_f}\mathbf{w}}.\end{aligned}\tag{6.42}$$

The second equality is achieved by using Lagrangian multiplier method. Together with (6.42) and the result in Lemma 6.2, we have, with respect to $\mathcal{P}_{f,\Delta_f}(\epsilon_3,\epsilon_4)$,

$$\begin{aligned}\sqrt{\mathbf{w}^T(\bar{\mathbf{z}}_f-\hat{\bar{\mathbf{z}}}_0)(\bar{\mathbf{z}}_f-\hat{\bar{\mathbf{z}}}_0)^T\mathbf{w}}&\ge\sqrt{\mathbf{w}^T(\hat{\bar{\mathbf{z}}}_f-\hat{\bar{\mathbf{z}}}_0)(\hat{\bar{\mathbf{z}}}_f-\hat{\bar{\mathbf{z}}}_0)^T\mathbf{w}}-\epsilon_3\sqrt{\mathbf{w}^T\boldsymbol{\Sigma}_{z_f}\mathbf{w}}\\ \sqrt{\mathbf{w}^T\boldsymbol{\Sigma}_{z_f}\mathbf{w}}&\le\sqrt{\mathbf{w}^T(\hat{\boldsymbol{\Sigma}}_{z_f}+\epsilon_4\mathbf{I})\mathbf{w}}.\end{aligned}$$

It implies (6.40) holds ensuring (6.41). The second DCC in (6.35) can thus be substituted by (6.40). The proof is completed. □

According to Lemmas 6.3 and 6.4, the FD problem (6.34)–(6.35) is thus solved by addressing

$$\min_{\mathbf{w}\neq 0}\ \beta^{rob}\quad\text{s.t.}\quad\text{(6.36) and (6.40)}.\tag{6.43}$$

Let

$$\mathcal{C}(\mathbf{w}) = \frac{\sqrt{\mathbf{w}^T(\hat{\bar{\mathbf{z}}}_f - \hat{\bar{\mathbf{z}}}_0)(\hat{\bar{\mathbf{z}}}_f - \hat{\bar{\mathbf{z}}}_0)^T\mathbf{w}} - (\epsilon_1 + \nu(\alpha_0^{rob}))\sqrt{\mathbf{w}^T(\hat{\mathbf{\Sigma}}_{z_0} + \epsilon_2\mathbf{I})\mathbf{w}}}{\sqrt{\mathbf{w}^T(\hat{\mathbf{\Sigma}}_{z_f} + \epsilon_4\mathbf{I})\mathbf{w}}}. \tag{6.44}$$

The problem (6.43) is then re-written as follows

$$\max_{\mathbf{w}\neq 0} \ \mathcal{C}(\mathbf{w}) \quad \text{s.t.} \quad (\epsilon_1 + \nu(\alpha_0^{rob}))\sqrt{\mathbf{w}^T(\hat{\mathbf{\Sigma}}_{z_0} + \epsilon_2\mathbf{I})\mathbf{w}} = 1, \ \mathcal{C}(\mathbf{w}) > 0 \tag{6.45}$$

which, according to Theorem 4.6, can be further converted into a generalized eigenvalue-eigenvector problem

$$\max_{\mathbf{w}\neq 0} \ \frac{\mathbf{w}^T\tilde{\mathbf{\Sigma}}_1\mathbf{w}}{\mathbf{w}^T\tilde{\mathbf{\Sigma}}_2\mathbf{w}} \tag{6.46}$$

where $\tilde{\mathbf{\Sigma}}_1 = (\hat{\bar{\mathbf{z}}}_f - \hat{\bar{\mathbf{z}}}_0)(\hat{\bar{\mathbf{z}}}_f - \hat{\bar{\mathbf{z}}}_0)^T - (\epsilon_1 + \nu(\alpha_0^{rob}))^2(\hat{\mathbf{\Sigma}}_{z_0} + \epsilon_2\mathbf{I})$, $\tilde{\mathbf{\Sigma}}_2 = \hat{\mathbf{\Sigma}}_{z_f} + \epsilon_4\mathbf{I}$. And then the SVD technique is applied to solve (6.46) for an optimal $\mathbf{w}$. The optimal solutions to the problem (6.43) are then obtained as

$$\kappa(\beta^{rob}) = \mathcal{C}(\mathbf{w}) - \epsilon_3, \quad \beta^{rob} = \frac{1}{1 + \kappa^2(\beta^{rob})}. \tag{6.47}$$

Similar to the case as discussed in Section 6.3.1, given α_0, β the upper bounds of FAR and MDR achieved by solving the problem (4.17)–(4.18), a larger MDR will be derived due to the uncertainties in means and covariance matrices, i.e., $\beta^{rob} \geq \beta$. Simultaneously, the worst-case FAR is achieved as

$$\alpha_0^{rob} = \frac{1}{(\nu(\alpha_0) - \epsilon_1)^2}, \quad \alpha_0^{rob} \geq \alpha_0. \tag{6.48}$$

It means that the uncertainties in means $\bar{\mathbf{z}}_0$, $\bar{\mathbf{z}}_f$ should be within the ellipsoids of size ϵ_1 and ϵ_3, respectively, such that $\nu(\alpha_0^{rob}) > 0$, $\kappa(\beta^{rob}) > 0$.

Remark 6.2. *Thanks to the discussion in Section 4.2.3, we can directly derive the existence condition of the FD problem (6.43) under moments uncertainties as follows*

$$\alpha_0^{l,rob} = \frac{1}{\bar{\lambda}_m^{rob}} \tag{6.49}$$

where $\bar{\lambda}_m^{rob} = (\hat{\bar{\mathbf{z}}}_f - \hat{\bar{\mathbf{z}}}_0)^T(\hat{\mathbf{\Sigma}}_{z_0} + \epsilon_1\mathbf{I})^{-1}(\hat{\bar{\mathbf{z}}}_f - \hat{\bar{\mathbf{z}}}_0)$. *Hence, the value of* α_0^{rob} *should be set satisfying* $\alpha_0^{rob} \in (\alpha_0^{l,rob}, 1)$ *to guarantee a feasible solution to (6.43).*

6.3.3 Matrix-valued robust FD

With respect to the box-type moments uncertainties, below we focus on the robust versions of matrix-valued FD systems demonstrated in Chapter 5.

Multivector-valued robust FD

Recall the multivector-valued configuration of FD systems with respect to solving a group of problems (5.14)–(5.15) with $i = 1, 2, ..., M$. With $\hat{\bar{\mathbf{z}}}_0$ in place of $\bar{\mathbf{z}}_0$ in (5.9), we define a bank of residual evaluation functions and the threshold as follows

$$J(r_i) = (\mathbf{w}_i^T(\mathbf{z}(k) - \hat{\bar{\mathbf{z}}}_0))^2, \ J_{th} = 1, \ i = 1, 2, ..., M. \tag{6.50}$$

Given ambiguity sets $\mathcal{P}_{0,\Delta_0}(\epsilon_1, \epsilon_2)$ in (6.11) and $\mathcal{P}_{f_i,\Delta_{f_i}}(\epsilon_{3,i}, \epsilon_{4,i})$ in (6.13), a robust multivector-valued solution to the FD problem (6.9)–(6.10) is then achieved by separately solving the following problems

$$\min_{\mathbf{w}_i \neq 0} \ \beta_i^{rob} \tag{6.51}$$

$$\text{s.t.} \quad \begin{cases} \sup\limits_{\mathbb{P}_z \in \mathcal{P}_{0,\Delta_0}(\epsilon_1,\epsilon_2)} \Pr\left\{(\mathbf{w}_i^T(\mathbf{z} - \hat{\bar{\mathbf{z}}}_0))^2 > 1\right\} \leq \alpha_0^{rob} \\ \sup\limits_{\mathbb{P}_z \in \mathcal{P}_{f_i,\Delta_{f_i}}(\epsilon_{3,i},\epsilon_{4,i})} \Pr\left\{(\mathbf{w}_i^T(\mathbf{z} - \hat{\bar{\mathbf{z}}}_0))^2 \leq 1\right\} \leq \beta_i^{rob} \end{cases} \tag{6.52}$$

with $i = 1, 2, \ldots, M$, where $\beta_i^{rob} \in (0, 1)$ represents the upper bound of MDR for the i-th fault mode under moments uncertainties. For the same form of (6.52) with (6.35), a deterministic description of (6.51)–(6.52) is directly obtained as follows

$$\min_{\mathbf{w}_i \neq 0} \ \beta_i^{rob} \tag{6.53}$$

$$\text{s.t.} \quad \begin{cases} \left(\epsilon_1 + \nu(\alpha_0^{rob})\right) \sqrt{\mathbf{w}_i^T(\hat{\mathbf{\Sigma}}_{z_0} + \epsilon_2 \mathbf{I})\mathbf{w}_i} \leq 1 \\ \sqrt{\mathbf{w}^T(\hat{\bar{\mathbf{z}}}_{f_i} - \hat{\bar{\mathbf{z}}}_0)(\hat{\bar{\mathbf{z}}}_{f_i} - \hat{\bar{\mathbf{z}}}_0)^T\mathbf{w}_i} - 1 \geq \left(\kappa(\beta_i^{rob}) + \epsilon_{3,i}\right) \sqrt{\mathbf{w}_i^T(\hat{\mathbf{\Sigma}}_{z_{f_i}} + \epsilon_{4,i}\mathbf{I})\mathbf{w}_i} \end{cases} \tag{6.54}$$

where $\kappa(\beta_i^{rob}) = \sqrt{(1 - \beta_i^{rob})/\beta_i^{rob}}$. By means of Algorithm 4.2.7, the analytical optimal solution of $\mathbf{w}_i$ can then be obtained by means of SVD, and then

$$\kappa(\beta_i^{rob}) = \mathcal{C}(\mathbf{w}_i) - \epsilon_{3,i}, \quad \beta_i^{rob} = \frac{1}{1 + \kappa^2(\beta_i^{rob})} \tag{6.55}$$

where $\mathcal{C}(\mathbf{w}_i)$ is given in (6.44) with $\hat{\bar{\mathbf{z}}}_{f_i}$, $\mathbf{w}_i$, $\epsilon_{4,i}$ in place of $\hat{\bar{\mathbf{z}}}_f$, $\mathbf{w}$, ϵ_4, respectively.

As discussed in Section 5.2.3, the worst-case FAR and MDR with moments uncertainties satisfy

$$P_{FAR} \leq M\alpha_0^{rob}, \ \ P_{MDR} \leq \min_{i=1,2,...,M}\{\beta_i^{rob}\} \tag{6.56}$$

where α_0^{rob} is given in (6.48). It is clear that the uncertainties in means and covariance matrices would cause degradation of FD performance in terms of FAR and MDR, by noting that $\alpha_0^{rob} > \alpha_0$ and $\beta_i^{rob} > \beta_i$ with α_0, β_i derived solving (4.17)–(4.18).

Remark 6.3. *Together with the conclusions in Remarks 5.1 and 6.2, the existence condition of the multivector-valued FD problem under moments uncertainties is*

$$\alpha_0^{rob} \in (\alpha_{0,max}^{l,rob}, 1) \tag{6.57}$$

where $\alpha_{0,max}^{l,rob} = \max\limits_{i=1,2,\ldots,M}\{\alpha_{0,i}^{l,rob}\}$ *with*

$$\alpha_{0,i}^{l,rob} = \frac{1}{\bar{\lambda}_{m,i}^{rob}}, \quad \bar{\lambda}_{m,i}^{rob} = (\hat{\bar{\mathbf{z}}}_{f_i} - \hat{\bar{\mathbf{z}}}_0)^T(\hat{\mathbf{\Sigma}}_{z_0} + \epsilon_1\mathbf{I})^{-1}(\hat{\bar{\mathbf{z}}}_{f_i} - \hat{\bar{\mathbf{z}}}_0). \tag{6.58}$$

WC-CVaR aided robust FD

To study the robustness of the WC-CVaR aided FD with respect to solving the problem (5.3), the following residual evaluation function and threshold are defined

$$J(\mathbf{r}) = \max_{i=1,2,\ldots,M} J(r_i), \ J_{th} = b \tag{6.59}$$

where $J(r_i) = (\mathbf{w}_i^T(\mathbf{z}(k) - \hat{\bar{\mathbf{z}}}_0))^2$. Let $\mathbf{Q}_i = \mathbf{w}_i\mathbf{w}_i^T \in \mathbb{S}_+^\gamma$ and

$$\tilde{\mathbf{z}}_c = \mathbf{z} - \hat{\bar{\mathbf{z}}}_0. \tag{6.60}$$

Define $L_i(\tilde{\mathbf{z}}_c) = J(r_i) - b = \tilde{\mathbf{z}}_c^T\mathbf{Q}_i\tilde{\mathbf{z}}_c - b, \ i = 1, 2, \ldots, M$ and a convex function

$$L(\tilde{\mathbf{z}}_c) = \max_{i=1,2,\ldots,M} L_i(\tilde{\mathbf{z}}_c). \tag{6.61}$$

Regarding the box-type uncertainties specified in (6.14) and (6.15), the FD problem (6.9)–(6.10) with the substitution of (6.59) and (6.61) is re-written as

$$\min_{\mathbf{Q}_i \neq 0,\, i=1,2,\ldots,M,\, b} \quad \beta^{rob} \tag{6.62}$$

$$\text{s.t.} \quad \begin{cases} \sup\limits_{\mathbb{P}_z \in \mathcal{P}_{0,\Delta_0}(R_0,\tau_1,\tau_2)} \Pr\{L(\tilde{\mathbf{z}}_c) > 0\} \leq \alpha_0^{rob} \\ \sup\limits_{\mathbb{P}_z \in \mathcal{P}_{f,\Delta_f}} \Pr\{L(\tilde{\mathbf{z}}_c) \leq 0\} \leq \beta^{rob} \end{cases} \tag{6.63}$$

where $\mathcal{P}_{f,\Delta_f} = \bigcup\limits_{i=1}^{M} \mathcal{P}_{f_i,\Delta_{f_i}}(R_{f_i}, \tau_{3,i}, \tau_{4,i})$. The solution of this problem lies in handling the DCCs (6.63). Due to the moments uncertainties, the extension of the results obtained in Section 5.3.2 is unintuitive. Note that

$$\sup_{\mathbb{P}_z \in \mathcal{P}_{0,\Delta_0}(R_0,\tau_1,\tau_2)} \Pr\{L(\tilde{\mathbf{z}}_c) > 0\} = \sup_{(\bar{\mathbf{z}}_0, \mathbf{\Sigma}_{z_0}) \in \mathcal{U}_0} \sup_{\mathbb{P}_z \in \mathcal{P}_0} \Pr\{L(\tilde{\mathbf{z}}_c) > 0\} \leq \alpha_0^{rob} \tag{6.64}$$

$$\sup_{\mathbb{P}_z \in \mathcal{P}_{f,\Delta_f}} \Pr\{L(\tilde{\mathbf{z}}_c) \leq 0\} = \sup_{(\bar{\mathbf{z}}_{f_i}, \mathbf{\Sigma}_{z_{f_i}}) \in \mathcal{U}_f} \sup_{\mathbb{P}_z \in \mathcal{P}_f} \Pr\{L(\tilde{\mathbf{z}}_c) \leq 0\} \leq \beta^{rob}. \tag{6.65}$$

where $\mathcal{P}_0$, $\mathcal{P}_f$ are given in (3.17) and (5.6), respectively, $\mathcal{U}_0$ is the set of $(\bar{\mathbf{z}}_0, \mathbf{\Sigma}_{z_0})$, i.e.,

$$\mathcal{U}_0 = \left\{ (\bar{\mathbf{z}}_0, \mathbf{\Sigma}_{z_0}) \left| \begin{array}{l} (\bar{\mathbf{z}}_0 - \hat{\bar{\mathbf{z}}}_0)^T \mathbf{\Sigma}_{z_0}^{-1} (\bar{\mathbf{z}}_0 - \hat{\bar{\mathbf{z}}}_0) \leq \tau_1 \\ \mathbf{\Sigma}_{z_0} \preceq \tau_2 \hat{\mathbf{\Sigma}}_0 \end{array} \right. \right\} \tag{6.66}$$

and $\mathcal{U}_f = \bigcup_{i=1}^{M} \mathcal{U}_{f_i}$ with

$$\mathcal{U}_{f_i} = \left\{ (\bar{\mathbf{z}}_{f_i}, \mathbf{\Sigma}_{z_{f_i}}) \left| \begin{array}{l} (\bar{\mathbf{z}}_{f_i} - \hat{\bar{\mathbf{z}}}_{f_i})^T \mathbf{\Sigma}_{z_{f_i}}^{-1} (\bar{\mathbf{z}}_{f_i} - \hat{\bar{\mathbf{z}}}_{f_i}) \leq \tau_{3,i} \\ \mathbf{\Sigma}_{z_{f_i}} \preceq \tau_{4,i} \hat{\mathbf{\Sigma}}_{f_i} \end{array} \right. \right\}. \tag{6.67}$$

On this basis, the inner objectives in (6.64) and (6.65) can be handled with SDPs (5.40) and (5.50), respectively, a detailed proof has been given in Section 5.3.2. Then the equation (6.64) holds on condition that $\mathcal{G}_0 \leq 0$ with

$$\begin{aligned} \mathcal{G}_0 \quad = \quad & \sup_{(\bar{\mathbf{z}}_0, \mathbf{\Sigma}_{z_0}) \in \mathcal{U}_0} \inf_{\eta, \mathbf{K}_0} \eta + \frac{1}{\alpha_0^{rob}} \mathrm{Tr}\left(\mathbf{\Omega}_{z_{c,0}} \mathbf{K}_0\right) \\ \text{s.t.} \quad & \mathbf{K}_0 \in \mathbb{S}_+^{\gamma+1}, \ \eta \in \mathbb{R}, \ \mathbf{K}_0 - \begin{bmatrix} \mathbf{Q}_i & 0 \\ 0 & -b - \eta \end{bmatrix} \succeq 0, \ \forall i = 1, 2, \ldots, M. \end{aligned}$$

Recall the second-order moment matrix of $\tilde{\mathbf{z}}_c$ in fault-free case, i.e., $\mathbf{\Omega}_{\tilde{z}_{c,0}}$ defined in (6.16). Given $(\bar{\mathbf{z}}_0, \mathbf{\Sigma}_{z_0}) \in \mathcal{U}_0$, a box-type confidence region of $\mathbf{\Omega}_{\tilde{z}_{c,0}}$ is given in (6.18), i.e., $0 \preceq \mathbf{\Omega}_{\tilde{z}_{c,0}} \preceq \overline{\mathbf{\Omega}}_{\tilde{z}_{c,0}}$. In this context, the dual formulation of SDP $\mathcal{G}_0$, according to [61], is obtained as follows

$$\begin{aligned} \mathcal{G}_0^d \quad = \quad & \inf_{\eta, \overline{\mathbf{K}}_0, \mathbf{K}_0} \eta + \frac{1}{\alpha_0^{rob}} \mathrm{Tr}\left(\overline{\mathbf{\Omega}}_{\tilde{z}_{c,0}} \overline{\mathbf{K}}_0\right) && (6.68) \\ \text{s.t.} \quad & \overline{\mathbf{K}}_0 - \mathbf{K}_0 \succeq 0, \ \overline{\mathbf{K}}_0 \succeq 0, \ \mathbf{K}_0 \in \mathbb{S}_+^{\gamma+1}, \ \eta \in \mathbb{R} \\ & \mathbf{K}_0 - \begin{bmatrix} \mathbf{Q}_i & 0 \\ 0 & -b - \eta \end{bmatrix} \succeq 0, \ \forall i = 1, 2, \ldots, M. && (6.69) \end{aligned}$$

In this regard, the first DCC in (6.63) is then represented as $\mathcal{G}_0^d \leq 0$.

According to Theorem 5.3, the condition (6.65) is re-written as $\mathcal{G}_f \leq \beta^{rob}$ with

$$\begin{aligned} \mathcal{G}_f \quad = \quad & \sup_{(\bar{\mathbf{z}}_{f_i}, \mathbf{\Sigma}_{z_{f_i}}) \in \mathcal{U}_f} \inf_{\mathbf{K}_{f_j}} \ \mathrm{Tr}(\mathbf{\Omega}_{\tilde{z}_{c,f_j}} \mathbf{K}_{f_j}) \\ \text{s.t.} \quad & \mathbf{K}_{f_j} \in \mathbb{S}_+^{\gamma+1}, \ \tau_{ji} \geq 0 \\ & \left[\mathbf{K}_{f_j} - \mathrm{diag}(\mathbf{0}, 1)\right] + \sum_{i=1}^{M} \tau_{ji} \begin{bmatrix} \mathbf{Q}_i & 0 \\ 0 & -b \end{bmatrix} \succeq 0, \ \forall i, \ j = 1, 2, ..., M \end{aligned}$$

whose dual representation is then achieved as

$$\begin{aligned}\mathcal{G}_f^d \quad = \quad & \inf_{\overline{\mathbf{K}}_{f_j},\mathbf{K}_{f_j}} \ \mathrm{Tr}(\overline{\mathbf{\Omega}}_{\tilde{z}_{c,f_j}}\overline{\mathbf{K}}_{f_j}) && (6.70)\\ \text{s.t.} \quad & \overline{\mathbf{K}}_{f_j}-\mathbf{K}_{f_j}\succeq 0,\ \overline{\mathbf{K}}_{f_j}\succeq 0,\ \mathbf{K}_{f_j}\in\mathbb{S}_+^{\gamma+1},\ \tau_{ji}\geq 0 \\ & \left[\mathbf{K}_{f_j}-\mathrm{diag}(\mathbf{0},1)\right]+\sum_{i=1}^{M}\tau_{ji}\begin{bmatrix}\mathbf{Q}_i & 0\\ 0 & -b\end{bmatrix}\succeq 0,\ \forall i,\ j=1,2,...,M. && (6.71)\end{aligned}$$

Together with (6.68)–(6.69) and (6.70)–(6.71), the FD problem (6.62)–(6.63) can be addressed by solving the following SDP problem

$$\min_{\mathbf{K}_0,\overline{\mathbf{K}}_0,\overline{\mathbf{K}}_{f_j},\mathbf{K}_{f_j},\mathbf{Q}_i,i=1,2,...,M,b,\eta} \quad \beta^{rob} \tag{6.72}$$

$$\text{s.t.} \quad \begin{cases}\overline{\mathbf{K}}_0-\mathbf{K}_0\succeq 0,\ \overline{\mathbf{K}}_0\succeq 0,\ \mathbf{K}_0\in\mathbb{S}_+^{\gamma+1},\ \mathbf{Q}_i\in\mathbb{S}_+^{\gamma},\ \eta\in\mathbb{R},\ b>0\\ \eta+\frac{1}{\alpha_0^{rob}}\mathrm{Tr}\left(\overline{\mathbf{\Omega}}_{\tilde{z}_{c,0}}\overline{\mathbf{K}}_0\right)\leq 0,\ \mathbf{K}_0-\begin{bmatrix}\mathbf{Q}_i & 0\\ 0 & -b-\eta\end{bmatrix}\succeq 0\\ \overline{\mathbf{K}}_{f_j}-\mathbf{K}_{f_j}\succeq 0,\ \overline{\mathbf{K}}_{f_j}\succeq 0,\ \mathbf{K}_{f_j}\in\mathbb{S}_+^{\gamma+1},\ \tau_{ji}\geq 0,\ \mathrm{Tr}(\overline{\mathbf{\Omega}}_{\tilde{z}_{c,f_j}}\overline{\mathbf{K}}_{f_j})\leq\beta^{rob}\\ \left[\mathbf{K}_{f_j}-\mathrm{diag}(\mathbf{0},1)\right]+\sum_{i=1}^{M}\tau_{ji}\begin{bmatrix}\mathbf{Q}_i & 0\\ 0 & -b\end{bmatrix}\succeq 0,\ \forall i,\ j=1,2,...,M.\end{cases} \tag{6.73}$$

We term this formulation as the WC-CVaR aided robust FD problem, the solution of which is not only independent from the distributions for noises and faults but also robust over the uncertainties in means and covariance matrices of residuals both in fault-free and the concerned faulty cases. After obtaining $\mathbf{Q}_i, i=1,2,...,M$, b, online FD is then realized by performing (6.59) and (6.4).

Matrix-valued robust optimal FD

By replacing $\bar{\mathbf{r}}_0$ in (5.54) with $\hat{\bar{\mathbf{r}}}_0=\mathbf{W}^T\hat{\bar{\mathbf{z}}}_0$, we define the residual evaluation function and threshold as follows

$$J(\mathbf{r})=\left\|\mathbf{r}(k)-\hat{\bar{\mathbf{r}}}_0\right\|_2^2,\ J_{th}=1. \tag{6.74}$$

With respect to the ambiguity sets $\mathcal{P}_{0,\Delta_0}(R_0,\tau_1,\tau_2)$ and $\mathcal{P}_{f,\Delta_f}=\bigcup_{i=1}^{M}\mathcal{P}_{f_i,\Delta_{f_i}}(R_{f_i},\tau_{3,i},\tau_{4,i})$, the FD problem (6.9)–(6.10) is re-written as follows

$$\min_{\mathbf{W}\neq 0} \quad \beta^{rob} \tag{6.75}$$

$$\text{s.t.} \quad \begin{cases}\sup\limits_{\mathbb{P}_z\in\mathcal{P}_{0,\Delta_0}(R_0,\tau_1,\tau_2)}\Pr\left\{\left\|\mathbf{W}^T\tilde{\mathbf{z}}_c\right\|_2^2>1\right\}\leq\alpha_0^{rob}\\ \sup\limits_{\mathbb{P}_z\in\mathcal{P}_{f,\Delta_f}}\Pr\left\{\left\|\mathbf{W}^T\tilde{\mathbf{z}}_c\right\|_2^2\leq 1\right\}\leq\beta^{rob}.\end{cases} \tag{6.76}$$

To solve this problem, we consider the following issues

$$\sup_{\mathbb{P}_z\in\mathcal{P}_{0,\Delta_0}(R_0,\tau_1,\tau_2)} \Pr\left\{\left\|\mathbf{W}^T\tilde{\mathbf{z}}_c\right\|_2^2>1\right\} = \sup_{(\bar{\mathbf{z}}_0,\mathbf{\Sigma}_{z_0})\in\mathcal{U}_0}\sup_{\mathbb{P}_z\in\mathcal{P}_0}\Pr\left\{\left\|\mathbf{W}^T\tilde{\mathbf{z}}_c\right\|_2^2>1\right\}\leq\alpha_0^{rob} \quad (6.77)$$

$$\sup_{\mathbb{P}_z\in\mathcal{P}_{f,\Delta_f}} \Pr\left\{\left\|\mathbf{W}^T\tilde{\mathbf{z}}_c\right\|_2^2\leq 1\right\} = \sup_{(\bar{\mathbf{z}}_{f_i},\mathbf{\Sigma}_{z_{f_i}})\in\mathcal{U}_f}\sup_{\mathbb{P}_z\in\mathcal{P}_f}\Pr\left\{\left\|\mathbf{W}^T\tilde{\mathbf{z}}_c\right\|_2^2\leq 1\right\}\leq\beta^{rob}. \quad (6.78)$$

Along the research line of last subsection, conditions (6.77) and (6.78) can be addressed with dual SDPs. Let $\mathbf{P}=\mathbf{W}\mathbf{W}^T$. It is known from Theorems 4.1 that the inner objective of (6.77) can be represented with an SDP, i.e., $\bar{\mathcal{G}}_0\leq 0$ with

$$\begin{aligned}\bar{\mathcal{G}}_0 \quad &= \quad \sup_{(\bar{\mathbf{z}}_0,\mathbf{\Sigma}_{z_0})\in\mathcal{U}_0}\inf_{\eta,\mathbf{K}_0}\eta+\frac{1}{\alpha_0^{rob}}\mathrm{Tr}(\mathbf{\Omega}_{\tilde{z}_{c,0}}\mathbf{K}_0)\\ &\text{s.t.}\quad \mathbf{K}_0\in\mathbb{S}_+^{\gamma+1},\ \eta\in\mathbb{R},\ \ \mathbf{K}_0-\begin{bmatrix}\mathbf{P}&0\\0&-\eta-1\end{bmatrix}\succeq 0\end{aligned}$$

whose dual formulation is given as

$$\begin{aligned}\bar{\mathcal{G}}_0^d \quad &= \quad \inf_{\eta,\overline{\mathbf{K}}_0,\mathbf{K}_0}\eta+\frac{1}{\alpha_0^{rob}}\mathrm{Tr}(\overline{\mathbf{\Omega}}_{\tilde{z}_{c,0}}\overline{\mathbf{K}}_0)\\ &\text{s.t.}\quad \overline{\mathbf{K}}_0-\mathbf{K}_0\succeq 0,\ \overline{\mathbf{K}}_0\succeq 0\\ &\qquad \mathbf{K}_0\in\mathbb{S}_+^{\gamma+1},\ \eta\in\mathbb{R},\ \ \mathbf{K}_0-\begin{bmatrix}\mathbf{P}&0\\0&-\eta-1\end{bmatrix}\succeq 0.\end{aligned}$$

Moreover, it follows from Theorem 5.3 that the condition (6.78) equals to $\bar{\mathcal{G}}_{f_j}\leq\beta^{rob}$, $\forall j=1,2,\ldots,M$ with

$$\begin{aligned}\bar{\mathcal{G}}_{f_j} \quad &= \quad \sup_{(\bar{\mathbf{z}}_{f_i},\mathbf{\Sigma}_{z_{f_i}})\in\mathcal{U}_{f_j}}\inf_{\mathbf{K}_{f_j},\tau_j}\mathrm{Tr}(\mathbf{\Omega}_{\tilde{z}_{c,f_j}}\mathbf{K}_{f_j})\\ &\text{s.t.}\quad \mathbf{K}_{f_j}\in\mathbb{S}_+^{\gamma+1},\ \tau_j\in\mathbb{R},\ \mathbf{K}_{f_j}+\begin{bmatrix}\tau_j\mathbf{P}&0\\0&-1-\tau_j\end{bmatrix}\succeq 0.\end{aligned}$$

Considering the dual form of $\bar{\mathcal{G}}_{f_j}$, i.e.,

$$\begin{aligned}\bar{\mathcal{G}}_{f_j}^d \quad &= \quad \inf_{\overline{\mathbf{K}}_{f_j},\mathbf{K}_{f_j},\tau_j}\mathrm{Tr}(\overline{\mathbf{\Omega}}_{\tilde{z}_{c,f_j}}\overline{\mathbf{K}}_{f_j})\\ &\text{s.t.}\quad \overline{\mathbf{K}}_{f_j}-\mathbf{K}_{f_j}\succeq 0,\ \overline{\mathbf{K}}_{f_j}\succeq 0\\ &\qquad \tau_j\in\mathbb{R},\ \mathbf{K}_{f_j}\in\mathbb{S}_+^{\gamma+1},\ \mathbf{K}_{f_j}+\begin{bmatrix}\tau_j\mathbf{P}&0\\0&-1-\tau_j\end{bmatrix}\succeq 0\end{aligned}$$

the condition (6.77) is then represented with $\max_{i=1,2,\ldots,M}\{\bar{\mathcal{G}}_{f_j}\}\leq\beta^{rob}$, which means $\bar{\mathcal{G}}_{f_j}\leq\beta^{rob}$, $\forall j=1,2,\ldots,M$. The FD problem (6.75)–(6.76) is thus addressed by solving the

following SDP problem

$$\min_{\mathbf{P},\overline{\mathbf{K}}_0,\mathbf{K}_0,\eta,\overline{\mathbf{K}}_{f_j},\mathbf{K}_{f_j},\tau_j,j=1,2,..,M} \quad \beta^{rob} \tag{6.79}$$

$$\text{s.t.} \quad \begin{cases} \overline{\mathbf{K}}_0 - \mathbf{K}_0 \succeq 0,\ \overline{\mathbf{K}}_0 \succeq 0,\ \mathbf{P} \in \mathbb{S}_+^{\gamma},\ \mathbf{K}_0 \in \mathbb{S}_+^{\gamma+1},\ \eta \in \mathbb{R} \\ \eta + \frac{1}{\alpha_0^{rob}} \mathrm{Tr}(\overline{\mathbf{\Omega}}_{\tilde{z}_{c,0}} \overline{\mathbf{K}}_0) \leq 0,\ \mathbf{K}_0 - \begin{bmatrix} \mathbf{P} & 0 \\ 0 & -\eta - 1 \end{bmatrix} \succeq 0 \\ \overline{\mathbf{K}}_{f_j} - \mathbf{K}_{f_j} \succeq 0,\ \overline{\mathbf{K}}_f \succeq 0,\ \mathbf{K}_{f_j} \in \mathbb{S}_+^{\gamma+1},\ \tau_j \in \mathbb{R} \\ \mathrm{Tr}(\overline{\mathbf{\Omega}}_{\tilde{z}_{c,f_j}} \overline{\mathbf{K}}_{f_j}) \leq \beta^{rob},\ \mathbf{K}_{f_j} + \begin{bmatrix} \tau_j \mathbf{P} & 0 \\ 0 & -1 - \tau_j \end{bmatrix} \succeq 0,\ \forall j = 1,\ 2,\ \ldots,\ M. \end{cases} \tag{6.80}$$

As a special case of the matrix-valued optimal solution, the FD issue without fault information has also been studied in Section 5.5, i.e., the FD problem (5.68). With the uncertainties in $\bar{\mathbf{z}}_0$, $\mathbf{\Sigma}_{z_0}$ concerned, the robustness of the solution to (5.68) is briefly studied below.

With respect to the ambiguity set $\mathcal{P}_{0,\Delta_0}(R_0,\ \tau_1,\ \tau_2)$, the FD problem (5.65) subject to moments uncertainties is formulated as follows

$$\max_{\mathbf{W} \neq 0} \quad \mathrm{Tr}(\bar{\mathbf{H}}_{f,s}^T \mathbf{W} \mathbf{W}^T \bar{\mathbf{H}}_{f,s}) \tag{6.81}$$

$$\text{s.t.} \quad \sup_{\mathbb{P}_z \in \mathcal{P}_{0,\Delta_0}(R_0,\tau_1,\tau_2)} \Pr\left\{ \left\| \mathbf{W}^T \tilde{\mathbf{z}}_c \right\|_2^2 > 1 \right\} \leq \alpha_0^{rob}. \tag{6.82}$$

Note that the DCC (6.82) can be re-written as an SDP problem $\bar{\mathcal{G}}_0^d \leq 0$. The problem (6.81)–(6.82) is then solved by addressing

$$\max_{\mathbf{P},\mathbf{K}_0,\overline{\mathbf{K}}_0,\eta} \quad \mathrm{Tr}(\bar{\mathbf{H}}_{f,s}^T \mathbf{P} \bar{\mathbf{H}}_{f,s}) \tag{6.83}$$

$$\text{s.t.} \begin{cases} \overline{\mathbf{K}}_0 - \mathbf{K}_0 \succeq 0,\ \overline{\mathbf{K}}_0 \succeq 0,\ \mathbf{K}_0 \in \mathbb{S}_+^{\gamma+1},\ \mathbf{P} \in \mathbb{S}_+^{\gamma},\ \eta \in \mathbb{R} \\ \eta + \frac{1}{\alpha_0^{rob}} \mathrm{Tr}(\overline{\mathbf{\Omega}}_{\tilde{z}_{c,0}} \overline{\mathbf{K}}_0) \leq 0,\ \mathbf{K}_0 - \begin{bmatrix} \mathbf{P} & 0 \\ 0 & -\eta - 1 \end{bmatrix} \succeq 0. \end{cases} \tag{6.84}$$

Remark 6.4. *In the above discussion, the dual formulation of SDP plays a key role in dealing with the DCCs subject to moments uncertainties. It is remarkable that the strong duality is ensured when the bounds of the involved box-type second-order moment matrices are feasible [61].*

6.4 Probabilistic evaluation

Concerning the moments uncertainties being caused by the estimation errors, the parameters in ambiguity sets $\mathcal{P}_{0,\Delta_0}$, $\mathcal{P}_{f,\Delta_f}$, i.e., ϵ_1, ϵ_2, ϵ_3, ϵ_4, R_0, τ_1, τ_2, R_{f_i}, $\tau_{3,i}$, $\tau_{4,i}$, thus

highly depend upon the sample numbers of process I/O data. In this part, we tackle the determination issue of these parameters, meanwhile, suggest confidence levels of the achieved worst-case FAR and MDR criteria in the probabilistic context.

6.4.1 Parameters determination of ambiguity sets

The following lemma is recalled for the determination of parameters ϵ_1, ϵ_2, ϵ_3, ϵ_4 in ambiguity sets $\mathcal{P}_{0,\Delta_0}(\epsilon_1, \epsilon_2)$ in (6.11) and $\mathcal{P}_{f,\Delta_f}(\epsilon_3, \epsilon_4)$ in (6.12).

Lemma 6.5. *[19] Let $\mathcal{S} = \{\boldsymbol{\xi}(i)\}_{i=1}^{N}$ be a set of N identically independent distributed (i.i.d) samples generated according to the probability distribution of $\boldsymbol{\xi} \in \mathbb{R}^n$. Given $\mathbb{E}[\boldsymbol{\xi}] = \bar{\boldsymbol{\xi}}$, $\mathbb{V}[\boldsymbol{\xi}] = \boldsymbol{\Sigma} \in \mathbb{S}_+^n$, $\|\boldsymbol{\xi}\|_2 \leq R$ and $\delta \in (0,1)$, if $N \geq \left(2 + \sqrt{2\ln(2/\delta)}\right)^2$, then with probability at least $1-\delta$ over the choice of samples, we have*

$$\left\|\boldsymbol{\Sigma}^{-\frac{1}{2}}(\bar{\boldsymbol{\xi}} - \hat{\bar{\boldsymbol{\xi}}})\right\|_2 \leq \mu_1(\delta), \ \left\|\boldsymbol{\Sigma} - \hat{\boldsymbol{\Sigma}}\right\|_F \leq \mu_2(\delta)$$

holds with

$$\mu_1(\delta) = \frac{R}{\sqrt{N}}\left(2 + \sqrt{2\ln(1/\delta)}\right), \ \mu_2(\delta) = \frac{2R^2}{\sqrt{N}}\left(2 + \sqrt{2\ln(2/\delta)}\right) \tag{6.85}$$

where $\hat{\bar{\boldsymbol{\xi}}}$, $\hat{\boldsymbol{\Sigma}}$ are the empirical estimate of $\bar{\boldsymbol{\xi}}$ and $\boldsymbol{\Sigma}$ over $\mathcal{S}$, respectively.

Lemma 6.5 provides analytical relationships between the sample number and the norm bounds of uncertainties in mean and covariance matrix. Given δ_0, $\delta_f \in (0,1)$, i.i.d sample sets $\mathcal{S}_0 = \{\mathbf{z}_0(i)\}_{i=1}^{N_0}$ and $\mathcal{S}_f = \{\mathbf{z}_f(i)\}_{i=1}^{N_f}$ with sample numbers N_0, N_f satisfying

$$N_0 \geq \left(2 + \sqrt{2\ln(2/\delta_0)}\right)^2, \quad N_f \geq \left(2 + \sqrt{2\ln(2/\delta_f)}\right)^2 \tag{6.86}$$

respectively, parameters ϵ_1, ϵ_2, ϵ_3, ϵ_4 are then obtained as

$$\epsilon_1 = \frac{R_0}{\sqrt{N_0}}\left(2 + \sqrt{2\ln(1/\delta_0)}\right), \ \epsilon_2 = \frac{2R_0^2}{\sqrt{N_0}}\left(2 + \sqrt{2\ln(2/\delta_0)}\right) \tag{6.87}$$

$$\epsilon_3 = \frac{R_f}{\sqrt{N_f}}\left(2 + \sqrt{2\ln(1/\delta_f)}\right), \ \epsilon_4 = \frac{2R_f^2}{\sqrt{N_f}}\left(2 + \sqrt{2\ln(2/\delta_f)}\right). \tag{6.88}$$

It clearly holds $\epsilon_1, \epsilon_2 \to 0$ as $N_0 \to \infty$ and $\epsilon_3, \epsilon_4 \to 0$ as $N_f \to \infty$, which implies the empirical estimates of mean and covariance matrix would approach their true values with probability one as sample size goes to infinity.

Regarding the ambiguity sets $\mathcal{P}_{0,\Delta_0}(R_0, \tau_1, \tau_2)$ in (6.14) and $\mathcal{P}_{f_i,\Delta_{f_i}}(R_{f_i}, \tau_{3,i}, \tau_{4,i})$ in (6.15) with box-type moments uncertainties, the following theorem is referred.

Theorem 6.2. *[19] Using the notations in Lemma 6.5, denote by*

$$\hat{R} = \sup_{\boldsymbol{\xi} \in \mathcal{M}_\xi} \left\| \hat{\boldsymbol{\Sigma}}^{-\frac{1}{2}} (\boldsymbol{\xi} - \hat{\bar{\boldsymbol{\xi}}}) \right\|_2 \tag{6.89}$$

with $\mathcal{M}_\xi$ being the known support of $\boldsymbol{\xi}$. For $\delta \in (0,1)$, set $\bar{\delta} = 1 - \sqrt{1-\delta}$, if

$$N > \max\left\{ T_1(\bar{\delta}, \hat{R}), T_2(\bar{\delta}, \hat{R}) \right\} \tag{6.90}$$

holds with $T_1(\bar{\delta}, \hat{R}) = (\hat{R}^2 + 2)^2 T^2(\bar{\delta})$, $T_2(\bar{\delta}, \hat{R}) = (8 + \sqrt{32\ln(4/\bar{\delta})})^2 / (\sqrt{\hat{R} + 4} - \hat{R})^4$, $T(\bar{\delta}) = 2 + \sqrt{2\ln(4/\bar{\delta})}$, then with probability greater than $1 - \delta$, the constraints

$$\left(\boldsymbol{\xi} - \bar{\boldsymbol{\xi}}\right)^T \boldsymbol{\Sigma}^{-1} \left(\boldsymbol{\xi} - \bar{\boldsymbol{\xi}}\right) \leq R^2, \ (\hat{\bar{\boldsymbol{\xi}}} - \bar{\boldsymbol{\xi}})^T \boldsymbol{\Sigma}^{-1} (\hat{\bar{\boldsymbol{\xi}}} - \bar{\boldsymbol{\xi}}) \leq \rho_1, \ \boldsymbol{\Sigma} \preceq \rho_2 \hat{\boldsymbol{\Sigma}}$$

are satisfied by setting

$$\rho_1 = \frac{\bar{R}^2}{N} (2 + \sqrt{2\ln(2/\bar{\delta})})^2, \ \rho_2 = \frac{1}{1 - t\left(\bar{\delta}/4\right) - \rho_1} \tag{6.91}$$

where $\bar{R} = \hat{R}(1 - (\hat{R}^2 + 2)T(\bar{\delta})/\sqrt{N})^{-\frac{1}{2}}$, $\hat{R}$ is a sample-based approximation of R, $t(\bar{\delta}/4) = \frac{\bar{R}^2}{\sqrt{N}}(\sqrt{1 - n/\bar{R}^4} + \sqrt{\ln(4/\bar{\delta})})$.

Theorem 6.2 suggests a probabilistic manner to determine the parameters R_0, τ_1, τ_2, R_{f_i}, $\tau_{3,i}$, $\tau_{4,i}$ regarding sample numbers N_0, N_{f_i} and confidence levels $1 - \delta_0$, $1 - \delta_{f_i}$.

It is remarkable that, with respect to Lemma 6.5 and Theorem 6.2, we can, on the one hand, determine the confidence level of empirical estimates for a given sample number and, on the other hand, compute the minimum sample number for a fixed confidence level. In general, parameters ϵ_1, ϵ_2 in (6.11) and τ_1, τ_2 in (6.14) are computed by finding a minimum N_0 for a given acceptable $1 - \delta_0$ aiming at saving computational expense while without FD performance degradation. Differently, parameters ϵ_3, ϵ_4 in (6.12) and R_{f_i}, $\tau_{3,i}$, $\tau_{4,i}$ in (6.15) and $1 - \delta_{f_i}$ are computed for a given N_{f_i}. This handling is required for the fact that a large enough sample set of the residual signal in normal operation is accessible while comparatively smaller sample sets in faulty cases are availiable in practice.

6.4.2 Confidence levels of FAR and MDR

Provided the quantitative evaluation of the estimation errors under certain confidence levels, we can, together with the results in Section 6.3, intuitively evaluate the confidence levels of the achieved FAR and MDR under moments uncertainties in the probabilistic context, as stated in the following theorem.

Theorem 6.3. *Given* δ_0, $\delta_{f_i} \in (0,1)$, $i = 1, 2, \ldots M$, *empirical means* $\hat{\bar{\mathbf{z}}}_0$, $\hat{\bar{\mathbf{z}}}_{f_i}$ *and covariance matrices* $\hat{\mathbf{\Sigma}}_{z_0}$, $\hat{\mathbf{\Sigma}}_{z_{f_i}}$ *obtained over the i.i.d sample sets* $\mathcal{S}_0 = \{\mathbf{z}_0(i)\}_{i=1}^{N_0}$ *and* $\mathcal{S}_{f_i} = \{\mathbf{z}_f(i)\}_{i=1}^{N_{f_i}}$, *respectively, the FD systems designed by solving*

(i) the problems (6.21)–(6.22) and (6.34)–(6.35), wherein the parameters ϵ_1, ϵ_2, ϵ_3, ϵ_4 *are given in (6.87), (6.88) with sample numbers* N_0, N_f *satisfying (6.86),*

(ii) the multivector-valued FD problem (6.51)–(6.52), wherein $N_{f_i}, i = 1, 2, ..., M$ *are given satisfying (6.86) and the parameters* $\epsilon_{3,i}$, $\epsilon_{4,i}$ *are determined with (6.88) and*

(iii) the matrix-valued FD problems (6.51)–(6.52), (6.62)–(6.63) and (6.75)–(6.76), wherein the sample numbers N_0, N_{f_i} *are given satisfying (6.90) and parameters* R_0, τ_1, τ_2, R_{f_i}, $\tau_{3,i}$, $\tau_{4,i}$ *with* $i = 1, 2, \ldots M$ *determined according to Theorem 6.3*

can achieve the FAR not larger than α_0^{rob} *and the MDR not greater than* β^{rob} *with confidence levels not less than* $1 - \delta_0$ *and* $1 - \delta_{f_i}$, *respectively.*

6.5 Summary and notes

In this chapter, performance assessment of the DIO methods aided data-driven FD systems developed in Chapters 3–5 has been carried out under the estimation uncertainties in means and covariance matrices. Ambiguity sets with norm-bounded and box-type uncertainties have been first established to this end, with respect to which design issues of FD systems have been formulated as distribution independent RO problems in terms of the empirical means and covariance matrices of residuals. It has been theoretically proven that the derived upper bounds of FAR and MDR get poor due to the moments uncertainties. Moreover, quantitative confidence levels of the achieved FAR and MDR depending on the sample numbers have been exploited in the probabilistic context.

7 Benchmark study and real-time implementation

In this chapter, applications of the proposed FD methods in Chapters 3–6 to a laboratory setup of three-tank system will be demonstrated. For this purpose, the process model is first described. Then data-driven implementations of FD systems designed using DIO approaches in Chapters 3–5 are illustrated, followed by quantitative performance evaluation of the achieved FAR and MDR under moments uncertainties. The simulation and experimental results are given to show the effectiveness of the methods.

7.1 Process description

A three-tank system consists of tanks, pipelines and pumps that are typically used in chemical industry and thus serves as a popular benchmark example for process monitoring. A laboratory setup of three-tank system considered here is TTS20, see Fig. 7.1(a). As sketched in Fig. 7.1(b), the system consists of three water tanks that are connected through pipes and two pumps. Pumps 1 and 2 pump water to tank 1 and tank 2 with incoming mass flow rates Q_1 and Q_2, respectively. The water levels of the tanks, i.e., h_1, h_2, h_3, are measured through sensors. With regard to the parameters in Table 7.1, the dynamics of three-tank system is modeled as follows

$$A\dot{h}_1 = Q_1 - Q_{13}, \quad A\dot{h}_2 = Q_2 + Q_{32} - Q_{20}, \quad A\dot{h}_3 = Q_{13} - Q_{32}$$

where Q_{ij} is the mass flow from the ith tank to the jth tank with

$$\begin{aligned} Q_{13} &= a_1 s_{13} \mathrm{sgn}(h_1 - h_3)\sqrt{2g|h_1 - h_3|} \\ Q_{32} &= a_3 s_{23} \mathrm{sgn}(h_3 - h_2)\sqrt{2g|h_3 - h_2|} \\ Q_{20} &= a_2 s_0 \sqrt{2gh_2} \end{aligned}$$

and $s_{13} = s_{23} = s_0 = s_n$. By choosing the incoming mass flow rates as system inputs, the water levels the states and the sensor measurements the outputs, i.e.,

$$\mathbf{x} = \begin{bmatrix} h_1 \\ h_2 \\ h_3 \end{bmatrix}, \quad \mathbf{u} = \begin{bmatrix} Q_1 \\ Q_2 \end{bmatrix} = \begin{bmatrix} u_1 \\ u_2 \end{bmatrix}, \quad \mathbf{y} = \begin{bmatrix} h_1 \\ h_2 \\ h_3 \end{bmatrix}$$

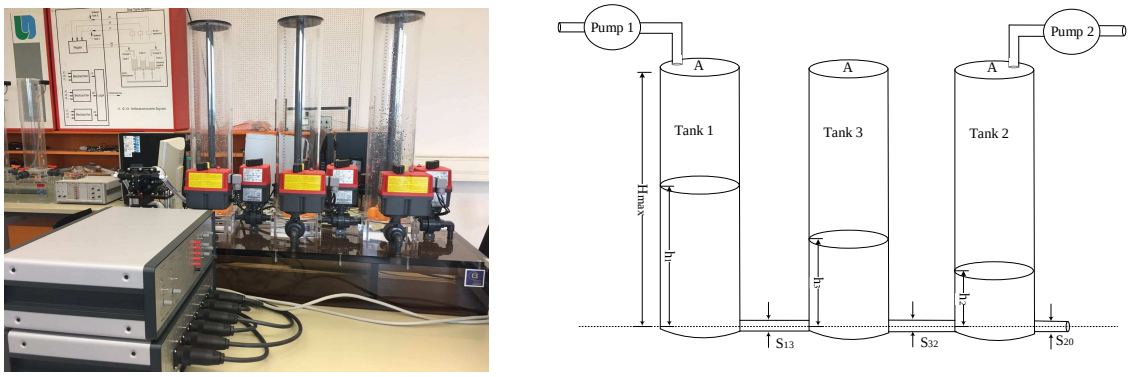

(a) (b)

Figure 7.1: Laboratory setup (a) and schematic diagram (b) of three-tank system TTS20.

Table 7.1: Parameters of three-tank system TTS20

Parameters	Symbol	Value	Unit
Cross section area of tanks	A	149	cm^2
Cross section area of pipes	s_n	0.5	cm^2
Maximal height of tanks	H_{max}	62	cm
Maximal flow rate of pump 1	$Q_{1_{max}}$	100	cm^3/s
Maximal flow rate of pump 2	$Q_{2_{max}}$	100	cm^3/s
Coefficient of flow for pipe 1	a_1	0.45	/
Coefficient of flow for pipe 2	a_2	0.60	/
Coefficient of flow for pipe 3	a_3	0.45	/

the system model subject to process noise $\boldsymbol{\omega}(t)$ and measurement noise $\boldsymbol{\upsilon}(t)$ is then described as follows

$$\begin{cases} \dot{\mathbf{x}}(t) = \phi\left(\mathbf{x}(t)\right) + \mathbf{B}\mathbf{u}(t) + \boldsymbol{\omega}(t) \\ \mathbf{y}(t) = \mathbf{x}(t) + \boldsymbol{\upsilon}(t) \end{cases} \tag{7.1}$$

where

$$\mathbf{B} = \begin{bmatrix} \frac{1}{A} & 0 \\ 0 & \frac{1}{A} \\ 0 & 0 \end{bmatrix}, \ \phi\left(\mathbf{x}(t)\right) = \begin{bmatrix} \frac{-a_1 s_{13} \mathrm{sgn}(h_1 - h_3)\sqrt{2g|h_1 - h_3|}}{A} \\ \frac{a_3 s_{23} \mathrm{sgn}(h_3 - h_2)\sqrt{2g|h_3 - h_2|} - a_2 s_0 \sqrt{2gh_2}}{A} \\ \frac{a_1 s_{13} \mathrm{sgn}(h_1 - h_3)\sqrt{2g|h_1 - h_3|} - a_3 s_{23} \mathrm{sgn}(h_3 - h_2)\sqrt{2g|h_3 - h_2|}}{A} \end{bmatrix}$$

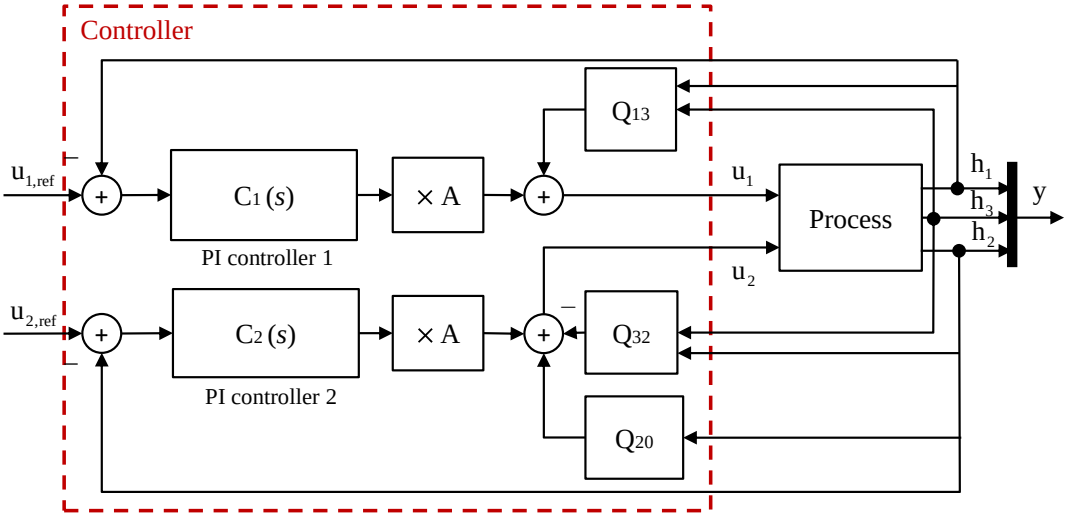

Figure 7.2: Schematic block of the controller of three-tank system.

To guarantee the system operates steadily, PI controllers are applied in TTS20, as presented in Fig. 7.2. The transfer functions of controllers 1 and 2 are as follows

$$C_1(s) = K_{p_1} + \frac{K_{i_1}}{s}, \quad C_2(s) = K_{p_2} + \frac{K_{i_2}}{s}$$

where $K_{p_1} = K_{p_2} = 0.087$, $K_{i_1} = K_{i_2} = 0.001$.

Typically, four kinds of faults are considered in three-tank systems, i.e.,

- Leakage faults $f_{l_i},\ i = 1,\ 2,\ 3$: additional mass flows out of tanks, i.e.,

  $$f_{l_i} = \theta_{l_i}\sqrt{2gh_i},\ i = 1,\ 2,\ 3.$$

  where $\theta_{l_i},\ i = 1,\ 2,\ 3$ are unknown parameters related to the size of leakage.

- Plugging faults $f_{p_i},\ i = 1,\ 2,\ 3$: the changes in Q_{13}, Q_{32}, Q_{20} with

  $$f_{p_1} = \theta_{p_1}Q_{13},\ f_{p_2} = \theta_{p_2}Q_{32},\ f_{p_3} = \theta_{p_3}Q_{20}$$

  where $\theta_{p_i} \in [-1, 0),\ i = 1,\ 2,\ 3$ are parameters related to the plugging size.

- Actuator faults $f_{a_i},\ i = 1,\ 2$: the additive faults in input $\mathbf{u}$.

- Sensor faults $f_{s_i},\ i = 1,\ 2,\ 3$: the additive faults in output $\mathbf{y}$.

It is remarkable that the leakage faults and plugging faults are component faults being multiplicative from the viewpoint of modeling. In the fashion of data-driven FD, their influence on the process can be regarded as additive without changing the system stability.

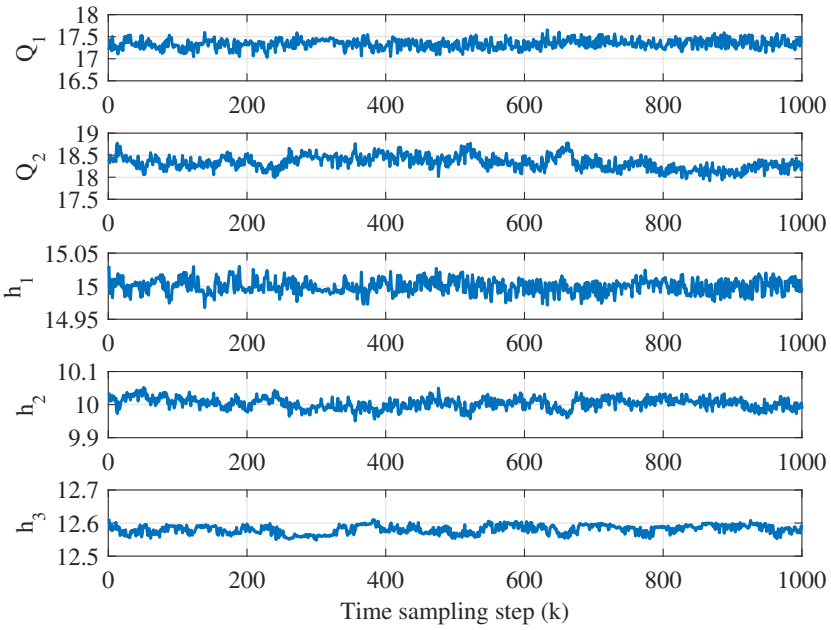

Figure 7.3: Experimental input and output of three-tank system working around steady point of $h_1 = 15cm$, $h_2 = 10cm$, $h_3 = 12.5cm$.

By linearizing the nonlinear process (7.1) at a steady operating point, a linear discrete-time model of three-tank system with stochastic noises and faults can be established as follows

$$\begin{cases} \mathbf{x}(k+1) = \mathbf{A}\mathbf{x}(k) + \mathbf{B}\mathbf{u}(t) + \mathbf{B}_f\mathbf{f}(k) + \boldsymbol{\omega}(k) \\ \mathbf{y}(k) = \mathbf{x}(k) + \mathbf{D}_f\mathbf{f}(k) + \boldsymbol{\upsilon}(k). \end{cases}$$

In the research line of data-driven FD, the system matrices and the distributional information of noises and faults are considered to be unknown.

In the following discussion, we consider the system operates steadily around the point of $h_1 = 15cm$, $h_2 = 10cm$, $h_3 = 12.5cm$ unless otherwise stated. The experimental inputs and outputs in nominal situation are shown in Fig. 7.3 with sampling time $T_s = 1s$.

7.2 FD results using vector-valued DIO methods

In this part, the applicability of the proposed FD methods in Chapters 3–4 are demonstrated through numeric simulation and experimental studies.

For verification purpose, three faulty cases listed in Table 7.2 are considered. It is assumed that only one type of fault occurs at each time sampling step k, i.e., $\mathbf{f} = [f_{l_1} \;\; f_{l_2} \;\; f_{p_2}]^T = [f_1 \;\; f_2 \;\; f_3]^T$ and in i-th faulty case $f_i \neq 0$, $f_j = 0$, $i \neq j$, $\forall i, j = 1, 2, 3$.

Table 7.2: Concerned fault modes of three-tank system

Fault mode		Parameters
Faulty case 1	$f_1 = f_{l_1}$: 5% leakage of tank 1	$\theta_{l_1} = 0.05$
Faulty case 2	$f_2 = f_{l_2}$: 7% leakage of tank 2	$\theta_{l_2} = 0.07$
Faulty case 3	$f_3 = f_{p_2}$: 6% plugging of pipe S_{32}	$\theta_{p_2} = -0.06$

Around the above operating point, the experimental process I/O data in fault-free and each faulty cases are collected.

As a common part of the DIO methods aided design of FD systems, a parity relation based primary residual generator (3.3) should be constructed using process I/O data in fault-free case. To this end, by setting $s = 10$, $N = 1000$, the matrix $\mathbf{\Psi}_s^\perp$ is then identified with Algorithm 2.2.3. On this basis, the sample sets $\mathcal{S}_0 = \{\mathbf{z}_0(j)\}_{j=1}^{N_0}$ for fault-free case and $\mathcal{S}_{f_i} = \{\mathbf{z}_{f_i}(j)\}_{j=1}^{N_{f_i}}$ for i-th faulty case with $i = 1, 2, 3$ are established, over which the empirical means $\hat{\bar{\mathbf{z}}}_0$, $\hat{\bar{\mathbf{z}}}_{f_i}$ and covariance matrices $\hat{\mathbf{\Sigma}}_{z_0}$, $\hat{\mathbf{\Sigma}}_{z_{f_i}}$ with $i = 1$, 2, 3 are then achieved with (6.5)–(6.6). Below, we first verify the effectiveness of the vector-valued DIO methods for FD as presented in Chapters 3 and 4.

7.2.1 Real-time implementations

We temporally ignore the estimation errors in means and covariance matrices and assume $\hat{\bar{\mathbf{z}}}_0 = \bar{\mathbf{z}}_0$, $\hat{\mathbf{\Sigma}}_{z_0} = \mathbf{\Sigma}_{z_0}$, $\hat{\bar{\mathbf{z}}}_{f_i} = \bar{\mathbf{z}}_{f_i}$, $\hat{\mathbf{\Sigma}}_{z_{f_i}} = \mathbf{\Sigma}_{z_{f_i}}$, $i = 1$, 2, 3. The upper bound of FAR is set as $\alpha_0 = 0.05$. For the DIO method presented in Chapter 3, the FD problem (3.10)–(3.11) is solved with Algorithm 3.2.5 for the optimal solutions of $\mathbf{w}$, b, β. The results of b, β for the concerned faulty cases are summarized in Table 7.3. To gain a deeper insight, the

Table 7.3: Experimental FD results using vector-valued DIO methods

Methods	Faults	β	β^{rob}	b	b^{rob}	α_0^l	$\alpha_0^{l,rob}$	α_0	α_0^{rob}
DIO	f_1	0.1506	0.3976	3.5660	3.8483	0.0136	0.0284	0.05	0.0883
	f_2	0.1024	0.2338	3.5990	4.1713	0.0138	0.0245	0.05	0.0883
	f_3	0.1050	0.3163	2.8992	3.4021	0.0111	0.0367	0.05	0.0883
Improved DIO	f_1	0.0875	0.1516	$b = 1$	$b^{rob} = 1$	0.0136	0.0283	0.05	0.1206
	f_2	0.0616	0.1872	$b = 1$	$b^{rob} = 1$	0.0138	0.0245	0.05	0.1206
	f_3	0.0684	0.2989	$b = 1$	$b^{rob} = 1$	0.0112	0.0374	0.05	0.1206

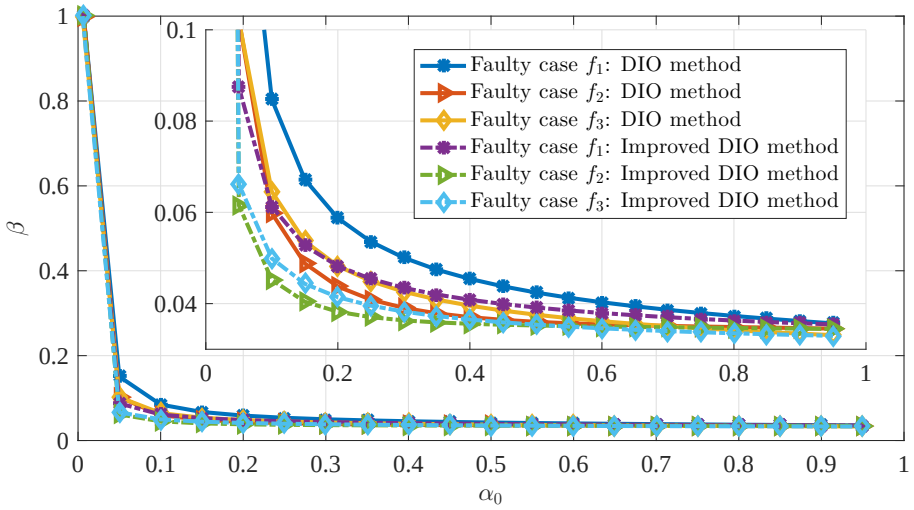

Figure 7.4: Evolutions of β over $\alpha_0 \in [0.05, 0.95]$ by using the DIO method and the improved DIO method.

evolutions of β over $\alpha_0 \in [0.05, 0.95]$ for each faulty case are studied, as demonstrated in Fig. 7.4. It is seen that the MDR gets smaller with the increase of FAR and the selection of $\alpha_0 = 0.05$ can achieve an acceptable tradeoff between FAR and MDR.

For online FD, we inject each fault into the laboratory setup of three-tank system at $k = 500$, the experimental FD results are demonstrated in Fig. 7.5 (a). As shown in Table 7.3 and Fig. 7.5 (a), good fault detectability is achieved by means of the DIO method without known precise distribution knowledge of noises and faults.

For the improved DIO method given in Chapter 4, Algorithm 4.2.7 is applied to achieve $\mathbf{w}$, β for each faulty case. Firstly, the existence condition of the optimal solutions is first checked, i.e., $\alpha_0 \in (\alpha_0^l, 1)$ with α_0^l obtained using (4.35). By solving the FD problem (4.17)–(4.18) by means of an SVD, the optimal solutions of $\mathbf{w}$, β are then obtained. The results of α_0^l and β are given in Table 7.3 and the evolutions of β over $\alpha_0 \in [0.05, 0.95]$ for each faulty case are demonstrated in Fig. 7.4. In comparison with the results using DIO method, a smaller upper bound of MDR can be achieved for an identical FAR, as stated in Remark 4.1. For online FD purpose, we introduce each fault at $k = 500$. The FD results are illustrated in Fig. 7.5 (b). We then see from Table 7.3 and Fig. 7.5 (b) that, with the utilization of the improved DIO method, the concerned faults can be well detected with a satisfactory MDR for a given FAR not larger than 0.05.

7.2.2 Performance evaluation

Under consideration of the estimation uncertainties in means and covariance matrices caused by the limited sample numbers, robustness and confidence levels of the above

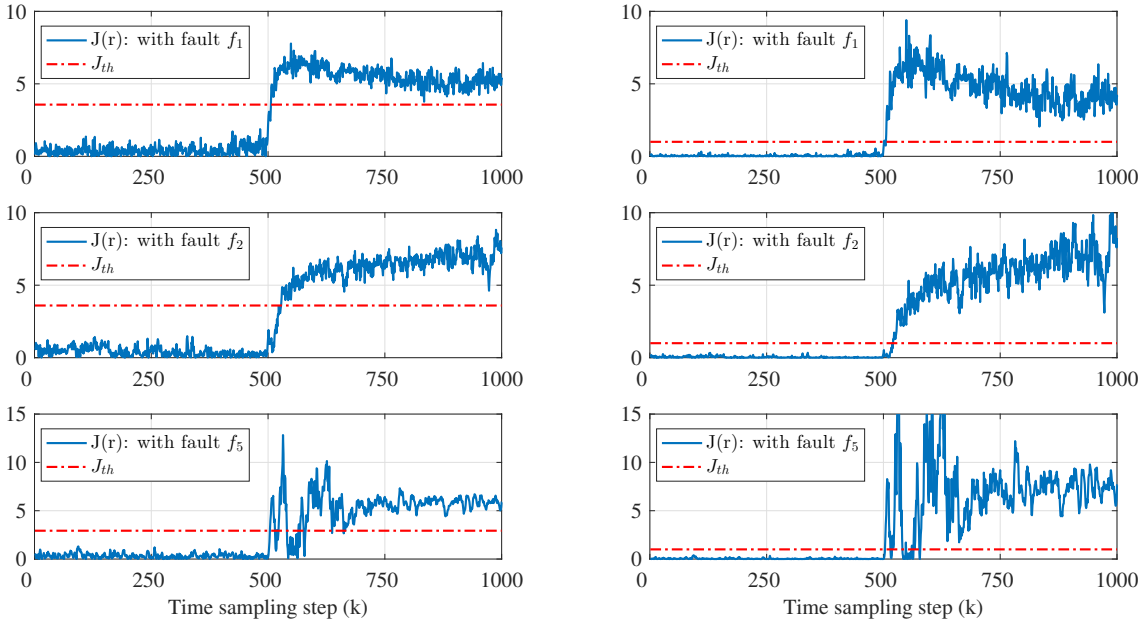

Figure 7.5: FD results using (a) the DIO method and (b) the improved DIO method.

achieved FAR and MDR can be evaluated in the probabilistic context according to the results in Chapter 6. For this purpose, we build a simulation platform of TTS20 in Matlab/Simulink towards generating process I/O data in fault-free and faulty cases. The process and measurement noises are simulated with random sequences keeping the accordance of $\hat{\bar{\mathbf{z}}}_0$, $\hat{\mathbf{\Sigma}}_{z_0}$, $\hat{\bar{\mathbf{z}}}_{f_i}$, $\hat{\mathbf{\Sigma}}_{z_{f_i}}$ with the ones in experiment study. On this basis, the parameters ϵ_1, ϵ_2, $\epsilon_{3,i}$, $\epsilon_{4,i}$ of ambiguity sets $\mathcal{P}_{0,\Delta_0}$ in (6.11) and $\mathcal{P}_{f_i,\Delta_{f_i}}$, $i = 1, 2, 3$ in (6.13) are first determined according to Lemma 6.5.

Due to the commonly sufficient large I/O samples in fault-free case, we give the confidence level of FAR being not less than $1 - \delta_0 = 0.99$ and determine a N_0 satisfying (6.86). The parameters ϵ_1, ϵ_2 are then computed with (6.87). For the faulty cases, we consider to achieve an acceptable confidence level $1 - \delta_{f_i}$ of MDR for each faulty case with fixed N_{f_i} satisfying (6.86). The parameters $\epsilon_{3,i}$, $\epsilon_{4,i}$ are obtained with (6.88). The results of ϵ_1, ϵ_2 and δ_{f_i}, $\epsilon_{3,i}$, $\epsilon_{4,i}$ for the i-th faulty case are summarized in Table 7.4. With known ϵ_1, ϵ_2, $\epsilon_{3,i}$, $\epsilon_{4,i}$, the performance of FAR and MDR under moments uncertainties, i.e., α_0^{rob}, β^{rob}, are thus achieved with (6.32), (6.29) for the DIO method and (6.48), (6.47) for the improved DIO method, respectively, as demonstrated in Table 7.3. In comparison with the results without moments certainties, we obviously have $\alpha_0^{rob} > \alpha_0$ and $\beta^{rob} > \beta$ that implies the FD performance degradation due to the corruption of uncertainties.

Table 7.4: Parameters in norm-based ambiguity sets $\mathcal{P}_{0,\Delta_0}$ and $\mathcal{P}_{f,\Delta_f}$

Faults	$N_0/N_f(\times 10^4)$	$\epsilon_1/\epsilon_3(\times 10^{-4})$	$\epsilon_2/\epsilon_4(\times 10^{-4})$	δ_0/δ_f
Fault-free	100	1.5922	0.0074	0.01
f_1	20	12.5801	2.3862	0.05
f_2	20	9.4351	1.8982	0.05
f_3	10	3.9782	2.3862	0.05

7.3 FD results using matrix-valued DIO methods

In this section, we show the effectiveness of matrix-valued DIO solutions presented in Chapter 5 to real-time FD and evaluate the FAR and MDR criteria in the probabilistic context by using the results in Chapter 6. For verification purpose, three fault modes listed in Table 7.2 are concerned subsequently. The above designed residual generator and the obtained empirical means and covariance matrices $\hat{\bar{\mathbf{z}}}_0$, $\hat{\mathbf{\Sigma}}_{z_0}$, $\hat{\bar{\mathbf{z}}}_{f_i}$, $\hat{\mathbf{\Sigma}}_{z_{f_i}}$, $i = 1, 2, 3$ are considered to be available here.

7.3.1 Real-time implementations

Multivector-valued solution

Given $\hat{\bar{\mathbf{z}}}_0$, $\hat{\mathbf{\Sigma}}_{z_0}$, $\hat{\bar{\mathbf{z}}}_{f_i}$, $\hat{\mathbf{\Sigma}}_{z_{f_i}}$, $i = 1, 2, 3$, we temporarily omit the estimation errors and consider to design an FD system with the multivector-valued DIO method. As stated in Algorithm 5.2.9, the upper bound of FAR α_0 should be set satisfying (5.22). Due to the values of α_0^l for each faulty case has been given in Table 7.3, we can directly have $\alpha_{0,max}^l = 0.0112$. Then, by setting $\alpha_0 = 0.05$, the parameter vector $\mathbf{w}_i$ and MDR criterion β_i are obtained by solving the problem (5.14)–(5.15) with $i = 1, 2, 3$. The results of β_i, $i = 1, 2, 3$ have been given in Table 7.3. According to (5.25)–(5.26), the FAR and MDR of the FD system in worst-case setting are obtained as $P_{MDR} \leq P_{FAR}^u = M\alpha_0 = 0.15$ and $P_{MDR} \leq \beta = \min\limits_{i=1,2,3} \beta_i = 0.0616$, as summarized in Table 7.5.

For online realization purpose, we inject each fault at $k = 500$ and compute the residual evaluation functions $J(r_i)$, $i = 1, 2, 3$ with (5.10). Using the decision logic (5.11) with $J_{th} = 1$, the FD results for the concerned fault modes are demonstrated in Figs. 7.6–7.8, respectively. It is seen from Table 7.5 and Figs. 7.6–7.8 that, the muletivector-valued DIO method to FD can achieve a quite lower MDR while a larger FAR.

Table 7.5: Experimental FD results using matrix-valued DIO methods

Methods	β	β^{rob}	α_0^l	$\alpha_0^{l,rob}$	P_{FAR}^u	$P_{FAR}^{u,rob}$
Multivector-valued DIO	0.0616	0.0872	0.0112	0.0374	0.15	0.3618
WC-CVaR aided DIO	0.0829	0.2860	/	/	0.05	0.05
Optimal matrix-valued DIO	0.0631	0.3235	/	/	0.05	0.05

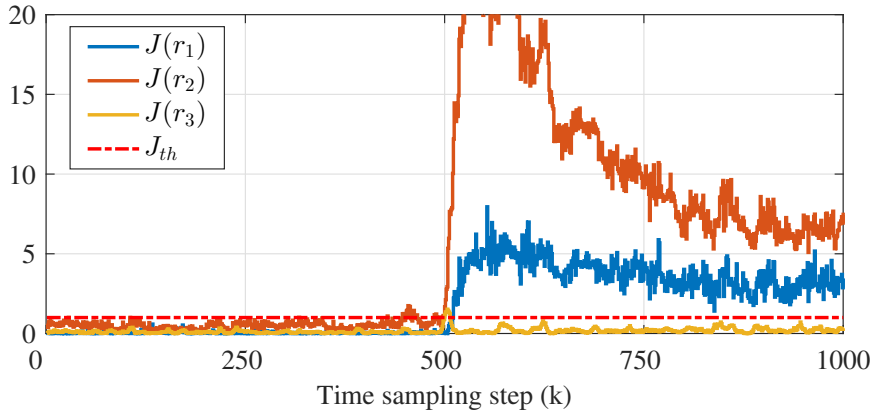

Figure 7.6: FD results using the multivector-valued DIO method for faulty case f_1.

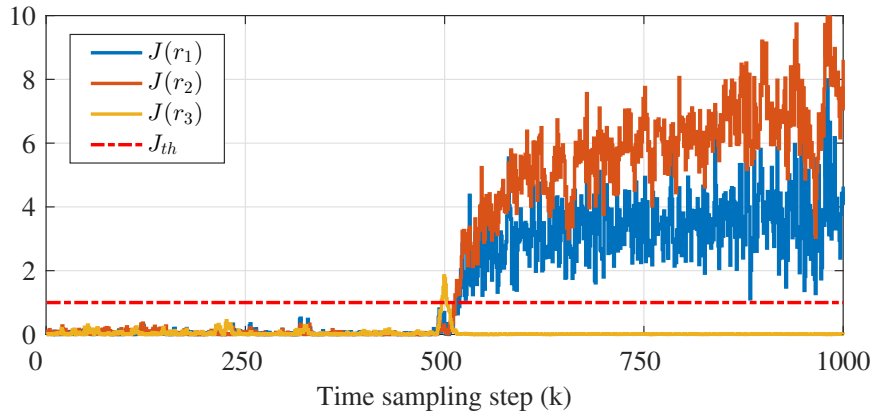

Figure 7.7: FD results using the multivector-valued DIO method for faulty case f_2.

WC-CVaR aided solution

To verify the applicability of the WC-CVaR aided DIO method for FD, Algorithm 5.3.10 is applied to FD system configuration and the key lies in solving the problem (5.51)–(5.52). Using the SDPT3 solver in CVX, the solutions of β, $\mathbf{Q}_i$, $i = 1, 2, 3$ are thus achieved and the results of β are given in Table 7.5 with the given upper bound of FAR $\alpha_0 = 0.05$. In

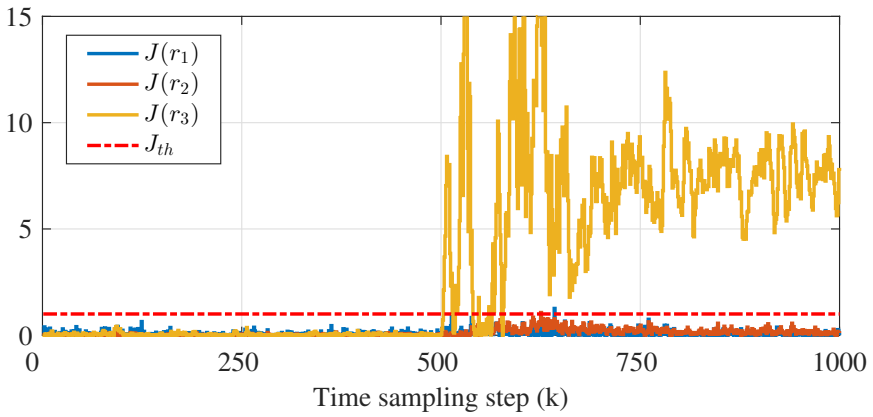

Figure 7.8: FD results using the multivector-valued DIO method for faulty case f_3.

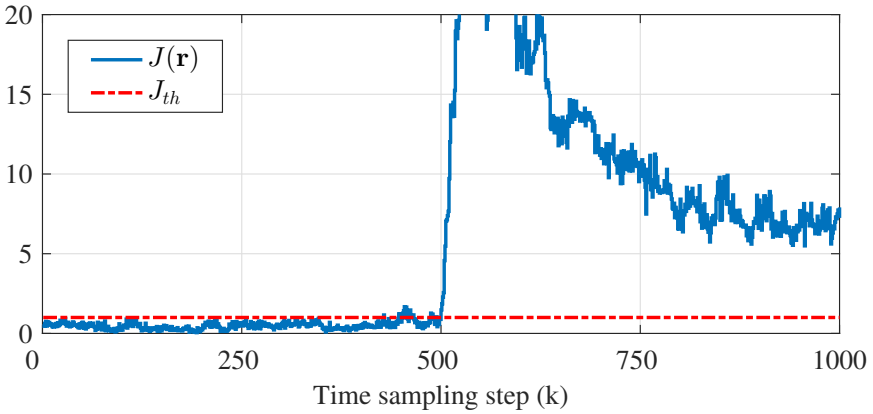

Figure 7.9: FD results using the WC-CVaR aided DIO method for faulty case f_1.

the phase of online realization, the residual evaluation function (5.29) and decision logic (5.2) are applied. With the injection of each fault at $k = 500$, the FD results are given in Figs. 7.9–7.11, respectively, from which we can see that satisfactory FD performance can be achieved in terms of a lower MDR and an acceptable FAR.

Matrix-valued optimal solution

We are now in the position of verifying the effectiveness of the optimal matrix-valued DIO method to FD. Let $\alpha_0 = 0.05$. The optimal solutions of $\mathbf{W}$, β are obtained with respect to solving the problem (5.61)–(5.62) with Algorithm 5.4.11. By using the residual evaluation function (5.53) and decision logic (5.2), the real-time FD results for each faulty case are demonstrated in Figs. 7.12–7.14, respectively. It is seen that the optimal matrix-valued DIO method can deliver good FD performance without distribution knowledge of noises and faults.

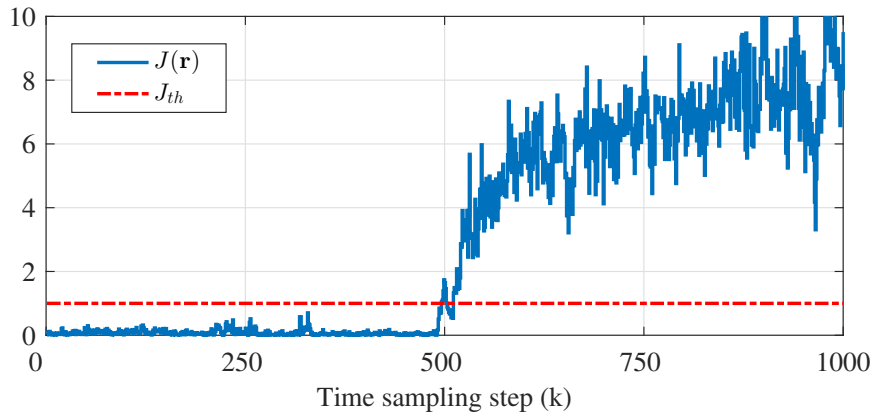

Figure 7.10: FD results using the WC-CVaR aided DIO method for faulty case f_2.

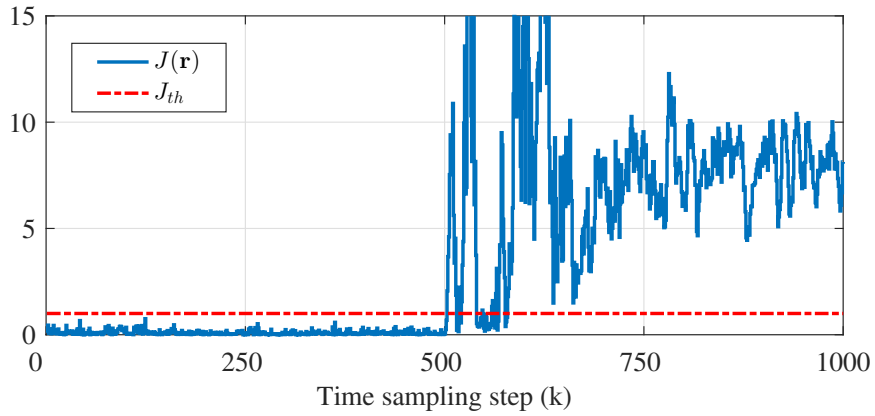

Figure 7.11: FD results using the WC-CVaR aided DIO method for faulty case f_3.

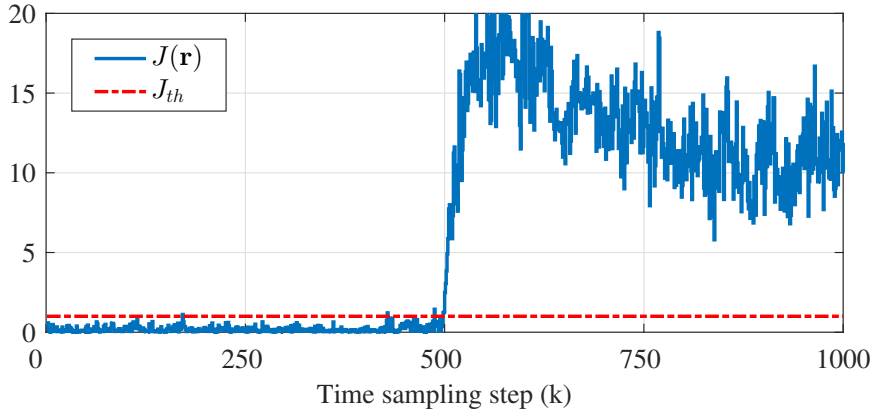

Figure 7.12: FD results using optimal matrix-valued DIO method for faulty case f_1.

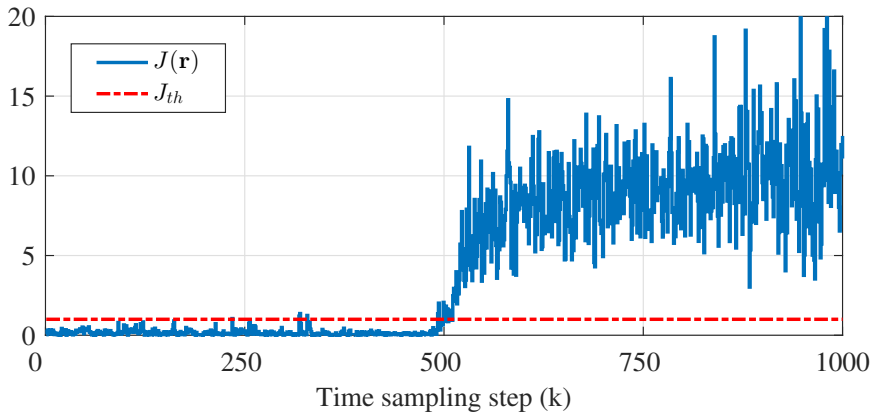

Figure 7.13: FD results using optimal matrix-valued DIO method for faulty case f_2.

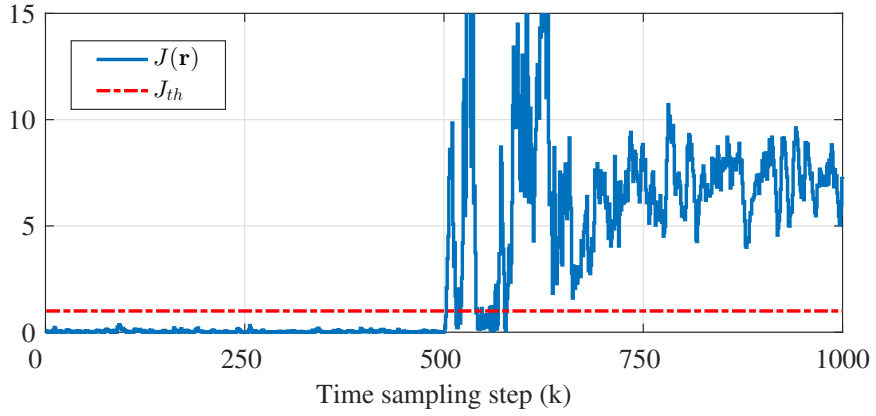

Figure 7.14: FD results using optimal matrix-valued DIO method for faulty case f_3.

Solutions without fault information

Regarding the residual evaluation function (5.53) and threshold $J_{th} = 1$, we consider to establish the FD systems without information of fault and the matrix $\bar{\mathbf{H}}_{f,s}\bar{\mathbf{H}}_{f,s}^T = \mathbf{I}$. In the stage of offline design, given $\hat{\bar{\mathbf{z}}}_0$, $\hat{\mathbf{\Sigma}}_{z_0}$ and $\alpha_0 = 0.05$, the solutions of the parameter matrix $\mathbf{W}$ are successively solved by addressing the SDP problem (5.68), the generalized eigenvalue-eigenvector problem (5.71) and the trace ratio problem (5.75), respectively, and the solutions are called *solution 1, 2* and *3*, respectively.

In the phase of online FD, the faults in Table 7.2 are individually injected at $k = 500$ and the FD results are illustrated in Figs. 7.15–7.17, respectively. It is seen from Figs. 7.15–7.17 that *solution 3* outperforms the other two solutions for the faults f_1, f_2 in terms of larger magnitudes of residual evaluation functions for the given identical threshold, and *solution 2* achieves a lower MDR for fault f_3 in comparison with the *solutions 1* and *3*. By

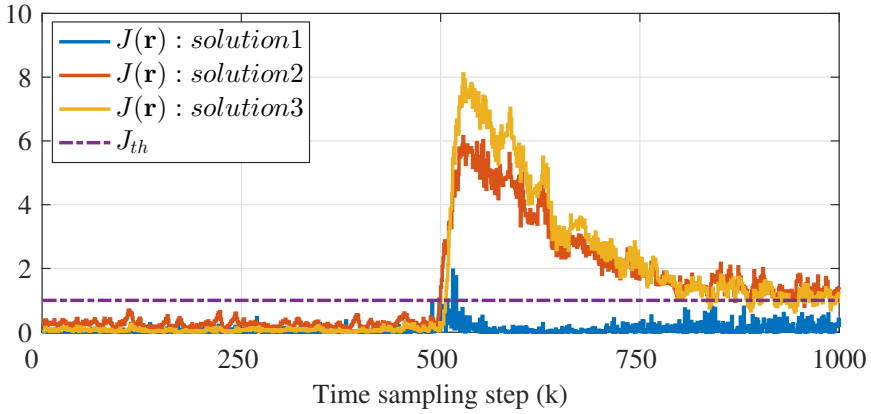

Figure 7.15: FD results using matrix-valued DIO method without fault knowledge in the presence of f_1.

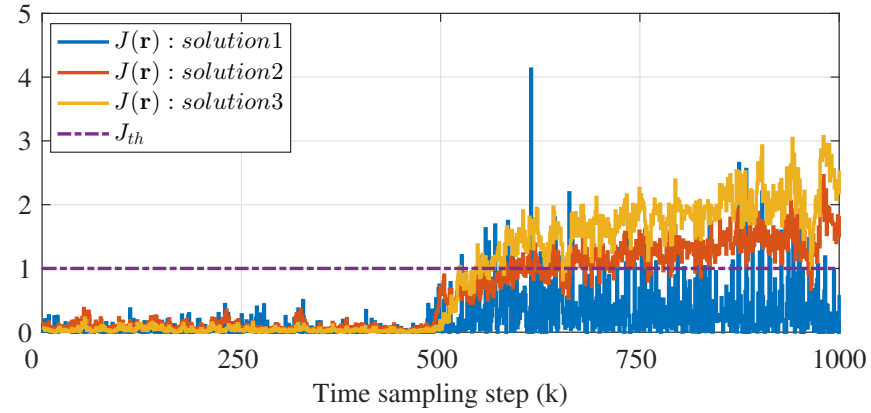

Figure 7.16: FD results using matrix-valued DIO method without fault knowledge in the presence of f_2.

comparing Figs. 7.6–7.14 and Figs. 7.15–7.17, we can see that the matrix-valued solutions obtained with fault information outperform the ones without using fault knowledge.

7.3.2 Performance evaluation

In this subsection, we evaluate the FD performance under consideration of the estimation uncertainties in means and covariance matrices.

At first, parameters in ambiguity sets $\mathcal{P}_{0,\Delta_0}(R_0, \tau_1, \tau_2)$ in (6.14) and $\mathcal{P}_{f_i,\Delta_{f_i}}(R_{f_i}, \tau_{3,i}, \tau_{4,i})$ in (6.15) with $i = 1, 2, 3$ should be determined according to Theorem 6.2. As mentioned before, we determine the parameters R_0, τ_1, τ_2 by finding an appropriate N_0 satisfying (6.90) for a given confidence level $1 - \delta_0 = 0.99$ whilst the δ_{f_i}, R_{f_i}, $\tau_{3,i}$, $\tau_{4,i}$ are computed with a fixed N_{f_i} for the i-th faulty case. By generating I/O samples in fault-free and each

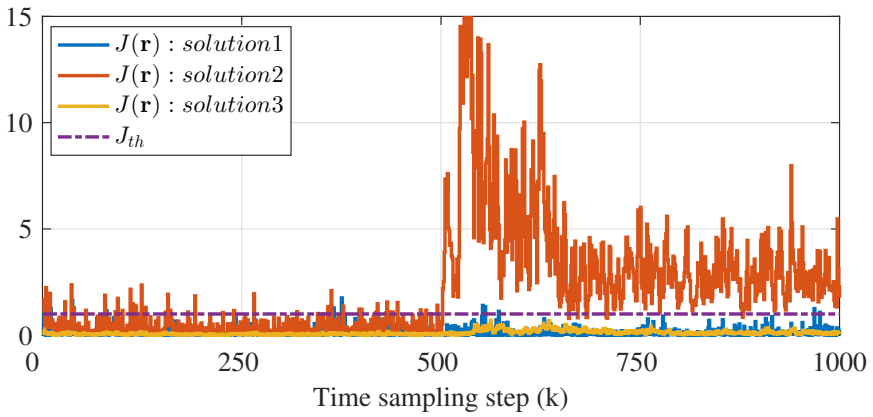

Figure 7.17: FD results using matrix-valued DIO method without fault knowledge in the presence of f_3.

Table 7.6: Parameters in box-type ambiguity sets $\mathcal{P}_{0,\Delta_0}$, $\mathcal{P}_{f_i,\Delta_{f_i}}$

Faults	$N_0/N_f(\times 10^4)$	$\tau_1/\tau_{3,i}$	$\tau_2/\tau_{4,i}$	R_0/R_{f_i}	δ_0/δ_{f_i}
Fault-free	100	0.0009	1.1198	5.0171	0.01
f_1	80	0.0010	1.1391	5.2633	0.05
f_2	50	0.0018	1.2005	5.3025	0.05
f_3	50	0.0025	1.3046	6.0201	0.05

faulty cases in the simulation platform, the parameters are then determined, as given in Table 7.6. This allows us to study the robustness of the proposed matrix-valued solutions in Chapter 6. By solving the SDP problems (6.72)–(6.73) and (6.79)–(6.80), the values of β^{rob} for each faulty case are given in Table 7.5. It is clear that the MDR performance gets poor when the means and covariance matrices involve estimation errors.

7.4 Summary and notes

In this chapter, the applicability of the DIO approaches for FD systems design and performance analysis has been illustrated through the simulation and experimental studies on a laboratory setup of three-tank system. The results show that both vector- and matrix-valued DIO approaches can well handle FD issues with a satisfactory MDR for a given acceptable FAR without precise distribution knowledge of noises and faults, even though no prior knowledge of fault is available. In addition, the worst-case FAR and MDR criteria under moments uncertainties have been derived quantitatively and the confidence levels of them have been suggested in the probabilistic context.

8 Conclusions and future work

In this thesis, data-driven design and analysis issues of optimal FD systems for stochastic dynamic processes are addressed dispensing with precise distribution knowledge of stochastic noises and faults. In Chapter 1, the motivations and objectives of this work have been presented. In response to the increasing requirements on the safety and reliability of modern industrial processes, great interest has been stimulated in data-driven FD for stochastic dynamic processes subject to distributional ambiguity due to the practically inaccessible probability distributions for noises and faults. Serving as the basis of this work, preliminaries of subspace technique aided data-driven FD and basic concepts of stochastic optimization have been reviewed in Chapter 2.

Chapter 3 focuses on a DIO approach to the design of FD systems in the context of minimizing the MDR for a prescribed FAR. On the basis of a data-driven construction of residual generator, the mean-covariance based ambiguity sets have been introduced to characterize the distribution knowledge of residuals in fault-free and faulty cases. Then, the design of FD systems has been formulated as an SP problem with DCCs, which was further reformulated as a DIO problem and solved with iterative parametric algorithms. Moreover, the worst-case FAR and MDR and a geometric interpretation of the achieved optimal solution have been discussed to gain a deeper insight into the proposed method.

Noting the conservatism of the achieved FAR criterion and the computational burden of the DIO method in Chapter 3, an improved DIO approach to data-driven FD has been demonstrated in Chapter 4. Regarding the mean-covariance based ambiguity sets, a two-sided test statistic of residual was applied as residual evaluation function and the design of FD systems has been formulated as a DIO problem in terms of the means and covariance matrices of residuals in fault-free and faulty cases. It has been theoretically proven that the targeting problem can be addressed by solving a generalized eigenvalue-eigenvector problem. Then an analytical solution has been achieved by using an SVD-based algorithm. The existence condition of the optimal solution has also been studied quantitatively.

The DIO methods given in Chapters 3 and 4 are vector-valued that concerns certain fault mode with known mean and covariance matrix. To improve the freedom of the design of FD systems towards a lower MDR, Chapter 5 is devoted to the matrix-valued DIO approaches to data-driven FD with respect to the mean-covariance based ambiguity sets, wherein both the situations of accessible and inaccessible prior knowledge of fault

have been concerned. By characterizing the fault modes with mean and covariance matrix of residual, three configurations of FD systems have been developed successively in the context of minimizing the MDR for a prescribed FAR, namely the multivector-valued scheme, the WC-CVaR aided scheme and the optimal matrix-valued method. Moreover, the matrix-valued DIO solutions to FD without fault information have also been studied.

Remarkably, the results in Chapters 3–5 have been obtained based on the true means and covariance matrices of residuals both in fault-free and faulty cases. In fact, only the empirical estimates of them can be achieved based on process I/O data. Concerning the estimation uncertainties in means and covariance matrices caused by the limited number of I/O samples, Chapter 6 has provided a quantitative analysis of the FD performance in the probabilistic context. The robustness of the FD systems designed in Chapters 3–5 against the moments uncertainties have been studied and confidence levels of the achieved FAR and MDR criteria have been suggested in the probabilistic context by constituting analytical relationships between sample numbers and estimation uncertainties.

Finally, a benchmark study on a laboratory setup of three-tank system has been demonstrated in Chapter 7 to illustrate the applicability and effectiveness of the developed DIO methods in Chapters 3–6.

As future works, the following directions are well worth considering:

- Extension of the proposed DIO methods in dealing with multiplicative faults will be performed.
- Fault isolation issues will be addressed in the framework of distribution independent optimization. On this basis, the integrated design of fault diagnosis and fault-tolerant control systems will be exploited with respect to a two-stage optimization of fault diagnosis performance and control performance.
- Different types of distribution features except for the mean and covariance matrix, e.g., Wassterin metric and KL-divergence, will be applied to model the ambiguity sets such that more precise FD performance criteria can be achieved to a better synthesis of fault diagnosis systems.

A Appendix

A.1 Proof of Theorem 3.3

Given $\boldsymbol{\xi} \in \mathbb{R}^n$, $b > 0$, if the following inequalities hold

$$\sup_{\boldsymbol{\xi} \sim (\bar{\boldsymbol{\xi}}, \boldsymbol{\Sigma})} \Pr\{\mathbf{w}^T \boldsymbol{\xi} > b\} \leq \frac{\rho}{2}, \quad \sup_{\boldsymbol{\xi} \sim (\bar{\boldsymbol{\xi}}, \boldsymbol{\Sigma})} \Pr\{-\mathbf{w}^T \mathbf{z} > b\} \leq \frac{\rho}{2} \tag{A.1}$$

according to Bonferroni inequality, we have $\sup_{\boldsymbol{\xi} \sim (\bar{\boldsymbol{\xi}}, \boldsymbol{\Sigma})} \Pr\{|\mathbf{w}^T \boldsymbol{\xi}| \geq b\} \leq \rho$. Moreover, according to Lemma 3.1, (A.1) with $\mathbf{w}^T \bar{\boldsymbol{\xi}} \leq b$ yields

$$\begin{aligned} \sup_{\boldsymbol{\xi} \sim (\bar{\boldsymbol{\xi}}, \boldsymbol{\Sigma})} \Pr\{\mathbf{w}^T \boldsymbol{\xi} > b\} \leq \frac{\rho}{2} \quad &\Leftrightarrow \quad \inf_{\boldsymbol{\xi} \sim (\bar{\boldsymbol{\xi}}, \boldsymbol{\Sigma})} \Pr\{\mathbf{w}^T \boldsymbol{\xi} \leq b\} \geq 1 - \frac{\rho}{2} \\ &\Leftrightarrow \quad b - \mathbf{w}^T \bar{\boldsymbol{\xi}} \geq \kappa(1 - \frac{\rho}{2}) \sqrt{\mathbf{w}^T \boldsymbol{\Sigma} \mathbf{w}} \\ &\Leftrightarrow \quad b - \mathbf{w}^T \bar{\boldsymbol{\xi}} \geq \bar{\kappa}(\rho) \sqrt{\mathbf{w}^T \boldsymbol{\Sigma} \mathbf{w}} \end{aligned} \tag{A.2}$$

where $\kappa(1 - \frac{\rho}{2}) = \bar{\kappa}(\rho) = \sqrt{\frac{2-\rho}{\rho}}$. When $\mathbf{w}^T \bar{\boldsymbol{\xi}} > b$, it holds $\inf_{\boldsymbol{\xi} \sim (\bar{\boldsymbol{\xi}}, \boldsymbol{\Sigma})} \Pr\{\mathbf{w}^T \boldsymbol{\xi} \leq b\} = 0$. By replacing $\mathbf{w}$, b in (A.2) with $-\mathbf{w}$, $-b$, respectively, it holds

$$\sup_{\boldsymbol{\xi} \sim (\bar{\boldsymbol{\xi}}, \boldsymbol{\Sigma})} \Pr\{-\mathbf{w}^T \mathbf{z} > b\} \leq \frac{\rho}{2} \Leftrightarrow -b + \mathbf{w}^T \bar{\boldsymbol{\xi}} \geq \bar{\kappa}(\rho) \sqrt{\mathbf{w}^T \boldsymbol{\Sigma} \mathbf{w}}. \tag{A.3}$$

When $-\mathbf{w}^T \bar{\boldsymbol{\xi}} > b$, it holds $\inf_{\boldsymbol{\xi} \sim (\bar{\boldsymbol{\xi}}, \boldsymbol{\Sigma})} \Pr\{-\mathbf{w}^T \boldsymbol{\xi} \leq b\} = 0$. Together with (A.1)–(A.3), we thus have

$$b - |\mathbf{w}^T \bar{\boldsymbol{\xi}}| \geq \bar{\kappa}(\rho) \sqrt{\mathbf{w}^T \boldsymbol{\Sigma} \mathbf{w}} \Rightarrow \sup_{\boldsymbol{\xi} \sim (\bar{\boldsymbol{\xi}}, \boldsymbol{\Sigma})} \Pr\{|\mathbf{w}^T \boldsymbol{\xi}| > b\} \leq \rho. \tag{A.4}$$

When $\left|\mathbf{w}^T \bar{\boldsymbol{\xi}}\right| > b$, it holds $\sup_{\boldsymbol{\xi} \sim (\bar{\boldsymbol{\xi}}, \boldsymbol{\Sigma})} \Pr\{|\mathbf{w}^T \boldsymbol{\xi}| > b\} = 1$. The proof is completed.

A.2 Proof of Theorem 3.4

Given $\boldsymbol{\xi} \in \mathbb{R}^n$, $\bar{\boldsymbol{\xi}} = \mathbb{E}[\boldsymbol{\xi}]$, $\mathbb{V}[\boldsymbol{\xi}] = \boldsymbol{\Sigma} \in \mathbb{S}_+^n$. Define a convex set $S = \{\boldsymbol{\xi} | (\mathbf{w}^T \boldsymbol{\xi})^2 \leq b^2\}$ with $\mathbf{w} \neq 0$, $b \neq 0$ given such that $|\mathbf{w}^T \bar{\boldsymbol{\xi}}| \geq |b|$. Let $\mathbf{a} = \boldsymbol{\Sigma}^{-\frac{1}{2}} (\boldsymbol{\xi} - \bar{\boldsymbol{\xi}})$, $\mathbf{T}^T = \mathbf{w}^T \boldsymbol{\Sigma}^{\frac{1}{2}}$. Recalling Theorem 3.1, we have

$$\sup_{\boldsymbol{\xi} \sim (\bar{\boldsymbol{\xi}}, \boldsymbol{\Sigma})} \Pr\left\{(\mathbf{w}^T \boldsymbol{\xi})^2 \leq b^2\right\} = \frac{1}{1 + d^2}, \; d^2 = \inf_{(\mathbf{w}^T \boldsymbol{\xi})^2 \leq b^2} \mathbf{a}^T \mathbf{a}.$$

Let $c = \mathbf{w}^T\boldsymbol{\xi}$, $\bar{c} = \mathbf{w}^T\bar{\boldsymbol{\xi}}$. Then $c = \mathbf{T}^T\mathbf{a} + \bar{c}$. Formulate a Lagrangian function as follows

$$L(\mathbf{a}, \lambda) = \mathbf{a}^T\mathbf{a} + \lambda\left(c^T c - b^2\right) = \mathbf{a}^T\mathbf{a} + \lambda\left[\theta(\mathbf{a}) - \tau\right]$$

with $\tau = b^2 - \bar{c}^T\bar{c}$, $\theta(\mathbf{a}) = \mathbf{a}^T\mathbf{T}\mathbf{T}^T\mathbf{a} + \mathbf{a}^T\mathbf{T}\bar{c} + \bar{c}^T\mathbf{T}^T\mathbf{a}$. Note that the Lagrangian function $L(\mathbf{a}, \lambda)$ is maximized w.r.t. $\lambda \geq 0$ and minimized w.r.t. $\mathbf{a}$, i.e., $d^2 = \min\limits_{\mathbf{a}} \max\limits_{\lambda \geq 0} L(\mathbf{a}, \lambda)$. At the optimum of d^2, we have

$$\frac{\partial L(\mathbf{a}, \lambda)}{\partial \mathbf{a}} = 2\left[\left(\mathbf{I} + \lambda\mathbf{T}\mathbf{T}^T\right)\mathbf{a} + \lambda\mathbf{T}\bar{c}\right] = 0, \quad \frac{\partial L(\mathbf{a}, \lambda)}{\partial \lambda} = \theta(\mathbf{a}) - \tau = 0.$$

It implies $\left(\mathbf{I} + \lambda\mathbf{T}\mathbf{T}^T\right)\mathbf{a} = -\lambda\mathbf{T}\bar{c}$, $\tau = \theta(\mathbf{a})$. Then

$$\mathbf{a} = -\lambda\left(\mathbf{I} + \lambda\mathbf{T}\mathbf{T}^T\right)^{-1}\mathbf{T}\bar{c} = \mathbf{m}\mathbf{T}\bar{c} \tag{A.5}$$

where $\mathbf{m} = -\lambda\left(\mathbf{I} + \lambda\mathbf{T}\mathbf{T}^T\right)^{-1}$, $\mathbf{m}^T = \mathbf{m}$.

Let $k = \mathbf{T}^T\mathbf{T} = \mathbf{w}^T\boldsymbol{\Sigma}\mathbf{w}$, $t = \mathbf{T}^T\mathbf{m}\mathbf{T}$. Then it holds $t = -\frac{\lambda k}{\lambda k + 1}$. By substituting a in (A.5) and τ to $\theta(a)$, we have

$$\theta(\mathbf{a}) = \left(t^2 + 2t\right)\bar{c}^T\bar{c} = b^2 - \bar{c}^T\bar{c} \leq 0.$$

It follows $t = \sqrt{\frac{b^2}{\bar{c}^T\bar{c}}} - 1$. At the optimal, we have

$$d^2 = \mathbf{a}^T\mathbf{a} = \frac{t^2}{k}\bar{c}^T\bar{c} = \left(\frac{\sqrt{\mathbf{w}^T\bar{\boldsymbol{\xi}}\bar{\boldsymbol{\xi}}^T\mathbf{w}} - \sqrt{b^2}}{\sqrt{\mathbf{w}^T\boldsymbol{\Sigma}\mathbf{w}}}\right)^2. \tag{A.6}$$

Because of $|\mathbf{w}^T\bar{\boldsymbol{\xi}}| \geq |b|$, it thus holds

$$\begin{aligned}\sup_{\boldsymbol{\xi}\sim(\bar{\boldsymbol{\xi}},\boldsymbol{\Sigma})} \Pr\left\{|\mathbf{w}^T\boldsymbol{\xi}| \leq |b|\right\} &= \sup_{\boldsymbol{\xi}\sim(\bar{\boldsymbol{\xi}},\boldsymbol{\Sigma})} \Pr\left\{(\mathbf{w}^T\boldsymbol{\xi})^2 \leq b^2\right\} = \frac{1}{1+d^2} \leq \beta \\ &\Leftrightarrow \quad d^2 \geq \frac{1-\beta}{\beta} \Leftrightarrow |\mathbf{w}^T\bar{\boldsymbol{\xi}}| - b \geq \kappa(\beta)\sqrt{\mathbf{w}^T\boldsymbol{\Sigma}\mathbf{w}}\end{aligned}$$

with $\kappa(\beta) = \sqrt{(1-\beta)/\beta}$, $b > 0$. When $|\mathbf{w}^T\bar{\boldsymbol{\xi}}| < b$, $d^2 = 0$, then $\sup\limits_{\boldsymbol{\xi}\sim(\bar{\boldsymbol{\xi}},\boldsymbol{\Sigma})} \Pr\left\{|\mathbf{w}^T\boldsymbol{\xi}| \leq |b|\right\} = 1$. The proof is completed.

Bibliography

[1] "$https://www-user.tu-chemnitz.de/\ helmberg/sdp_software.html$."

[2] R. V. Beard, "Failure accomodation in linear systems through self-reorganization." Ph.D. dissertation, Massachusetts Institute of Technology, 1971.

[3] D. Bertsimas, M. Sim, and M. Zhang, "Adaptive distributionally robust optimization," *Management Science*, vol. 65, no. 2, pp. 604–618, 2019.

[4] C. M. Bishop, *Pattern recognition and machine learning*. Springer, 2006.

[5] J. Blesa, V. Puig, J. Saludes, and R. M. Fernández-Cantí, "Set-membership parity space approach for fault detection in linear uncertain dynamic systems," *International Journal of Adaptive Control and Signal Processing*, vol. 30, no. 2, pp. 186–205, 2016.

[6] R. Boscolo, H. Pan, and V. P. Roychowdhury, "Independent component analysis based on nonparametric density estimation," *IEEE Transactions on Neural Networks*, vol. 15, no. 1, pp. 55–65, 2004.

[7] B. Cai, L. Huang, and M. Xie, "Bayesian networks in fault diagnosis," *IEEE Transactions on Industrial Informatics*, vol. 13, no. 5, pp. 2227–2240, 2017.

[8] L. Cai, X. Tian, and S. Chen, "Monitoring nonlinear and non-gaussian processes using gaussian mixture model-based weighted kernel independent component analysis," *IEEE Transactions on Neural Networks and Learning Systems*, vol. 28, no. 1, pp. 122–135, 2017.

[9] G. Calafiore, U. Topcu, and L. El Ghaoui, "Parameter estimation with expected and residual-at-risk criteria," *Systems & Control Letters*, vol. 58, no. 1, pp. 39–46, 2009.

[10] G. C. Calafiore and L. El Ghaoui, "On distributionally robust chance-constrained linear programs," *Journal of Optimization Theory and Applications*, vol. 130, no. 1, pp. 1–22, 2006.

[11] A. Charnes and W. W. Cooper, "Chance-constrained programming," *Management Science*, vol. 6, no. 1, pp. 73–79, 1959.

[12] J. Chen and R. J. Patton, *Robust model-based fault diagnosis for dynamic systems*. Springer Science & Business Media, 2012.

[13] R. Chen, "Outlier detection using distributionally robust optimization under the wasserstein metric," *https://hdl.handle.net/2144/29592*, 2017.

[14] R. Chen and I. C. Paschalidis, "A robust learning approach for regression models based on distributionally robust optimization," *Journal of Machine Learning Research*, vol. 19, no. 1, pp. 517–564, 2018.

[15] W. Chen, M. Sim, J. Sun, and C.-P. Teo, "From cvar to uncertainty set: Implications in joint chance-constrained optimization," *Operations Research*, vol. 58, no. 2, pp. 470–485, 2010.

[16] Z. Chen, M. Sim, and P. Xiong, "Tractable distributionally robust optimization with data," *http://www. optimization-online. org/DB_FILE/2017/06/6055.pdf*, 2017.

[17] Z. Chen, M. Sim, and H. Xu, "Distributionally robust optimization with infinitely constrained ambiguity sets," *Operations Research*, vol. 67, no. 5, pp. 1328–1344, 2019.

[18] A. K. Cline and I. S. Dhillon, "Computation of the singular value decomposition," *in Handbook of Linear Algebra. Edited by L. Hogben. CRC Press, Boca Raton, FL, 45.1-45.13*, 2006.

[19] E. Delage and Y. Ye, "Distributionally robust optimization under moment uncertainty with application to data-driven problems," *Operations Research*, vol. 58, no. 3, pp. 595–612, 2010.

[20] S. X. Ding, *Data-driven Design of Fault Diagnosis and Fault-tolerant Control Systems*. Springer, 2014.

[21] S. X. Ding, P. Zhang, E. L. Ding, and B. Huang, "Subspace method aided data-driven design of fault detection and isolation systems," *Journal of Process Control*, vol. 19, no. 9, pp. 1496–1510, 2009.

[22] S. X. Ding, *Model-based fault diagnosis techniques: design schemes, algorithms, and tools*. Springer, 2013.

[23] ——, *Data-driven design of fault diagnosis and fault-tolerant control systems*. Springer, 2014.

[24] S. X. Ding, L. Li, and M. Krüger, "Application of randomized algorithms to assessment and design of observer-based fault detection systems," *Automatica*, vol. 107, pp. 175–182, 2019.

[25] M. Farina and R. Scattolini, "Model predictive control of linear systems with multiplicative unbounded uncertainty and chance constraints," *Automatica*, vol. 70, pp. 258–265, 2016.

[26] R. Fazai, K. Abodayeh, M. Mansouri, M. Trabelsi, H. Nounou, M. Nounou, and G. Georghiou, "Machine learning-based statistical testing hypothesis for fault detection in photovoltaic systems," *Solar Energy*, vol. 190, pp. 405–413, 2019.

[27] J. Feng, J. Wang, H. Zhang, and Z. Han, "Fault diagnosis method of joint fisher discriminant analysis based on the local and global manifold learning and its kernel version," *IEEE Transactions on Automation Science and Engineering*, vol. 13, no. 1, pp. 122–133, 2015.

[28] P. M. Frank and S. X. Ding, "Survey of robust residual generation and evaluation methods in observer-based fault detection systems," *Journal of Process Control*, vol. 7, no. 6, pp. 403–424, 1997.

[29] V. Gabrel, C. Murat, and A. Thiele, "Recent advances in robust optimization: An overview," *European Journal of Operational Research*, vol. 235, no. 3, pp. 471–483, June 2014.

[30] L. E. Ghaoui, M. Oks, and F. Oustry, "Worst-case value-at-risk and robust portfolio optimization: A conic programming approach," *Operations Research*, vol. 51, no. 4, pp. 543–556, 2003.

[31] A. Giantomassi, F. Ferracuti, S. Iarlori, G. Ippoliti, and S. Longhi, "Electric motor fault detection and diagnosis by kernel density estimation and kullback–leibler divergence based on stator current measurements," *IEEE Transactions on Industrial Electronics*, vol. 62, no. 3, pp. 1770–1780, 2015.

[32] G. H. Golub and H. A. Van der Vorst, "Eigenvalue computation in the 20th century," *Journal of Computational and Applied Mathematics*, vol. 123, no. 1-2, pp. 35–65, 2000.

[33] G. H. Golub and Q. Ye, "Inexact inverse iteration for generalized eigenvalue problems," *BIT Numerical Mathematics*, vol. 40, no. 4, pp. 671–684, 2000.

[34] A. Gramacki, *Nonparametric kernel density estimation and its computational aspects*. Springer, 2018.

[35] Y.-F. Guo, S.-J. Li, J.-Y. Yang, T.-T. Shu, and L.-D. Wu, "A generalized foley–sammon transform based on generalized fisher discriminant criterion and its application to face recognition," *Pattern Recognition Letters*, vol. 24, no. 1-3, pp. 147–158, 2003.

[36] G. A. Hanasusanto, V. Roitch, D. Kuhn, and W. Wiesemann, "A distributionally robust perspective on uncertainty quantification and chance constrained programming," *Mathematical Programming*, vol. 151, no. 1, pp. 35–62, 2015.

[37] B. Hassibi and T. Kaliath, "H^∞ bounds for least-squares estimators," *IEEE Transactions on Automatic Control*, vol. 46, no. 2, pp. 309–314, 2001.

[38] Y. Hong, M. Kim, H. Lee, J. J. Park, and D. Lee, "Early fault diagnosis and classification of ball bearing using enhanced kurtogram and gaussian mixture model," *IEEE Transactions on Instrumentation and Measurement*, vol. 68, no. 12, pp. 4746–4755, 2019.

[39] A. R. Hota, A. Cherukuri, and J. Lygeros, "Data-driven chance constrained optimization under wasserstein ambiguity sets," in *2019 American Control Conference (ACC)*. Philadelphia, PA, USA, 2019, pp. 1501–1506.

[40] B. Huang and R. Kadali, *Dynamic modeling, predictive control and performance monitoring: a data-driven subspace approach*. Springer, 2008.

[41] K. Huang, H. Yang, I. King, M. Lyu, and L. Chan, "The minimum error minimax probability machine," *Journal of Machine Learning Research*, vol. 5, pp. 1253–1286, 2004.

[42] K. Huang, H. Yang, I. King, and M. R. Lyu, "Maximin margin machine: learning large margin classifiers locally and globally," *IEEE Transactions on Neural Networks*, vol. 19, no. 2, pp. 260–272, 2008.

[43] R. Isermann, *Fault-diagnosis systems: an introduction from fault detection to fault tolerance*. Springer Science & Business Media, 2006.

[44] Y. Jia, F. Nie, and C. Zhang, "Trace ratio problem revisited," *IEEE Transactions on Neural Networks*, vol. 20, no. 4, pp. 729–735, 2009.

[45] B. Jiang, Z. Guo, Q. Zhu, and G. Huang, "Dynamic minimax probability machine-based approach for fault diagnosis using pairwise discriminate analysis," *IEEE Transactions on Control Systems Technology*, vol. 27, no. 2, pp. 806–813, 2019.

[46] B. Jiang, Y. Luo, and Q. Lu, "Maximized mutual information analysis based on stochastic representation for process monitoring," *IEEE Transactions on Industrial Informatics*, vol. 15, no. 3, pp. 1579–1587, 2019.

[47] B. Jiang, X. Zhu, D. Huang, J. A. Paulson, and R. D. Braatz, "A combined canonical variate analysis and fisher discriminant analysis (cva–fda) approach for fault diagnosis," *Computers & Chemical Engineering*, vol. 77, pp. 1–9, 2015.

[48] B. Jiang, H. Chen, H. Yi, and N. Lu, "Data-driven fault diagnosis for dynamic traction systems in high-speed trains," *Scientia Sinica Informationis*, vol. 50, no. 4, pp. 496–510, 2020.

[49] R. Jiang and Y. Guan, "Data-driven chance constrained stochastic program," *Mathematical Programming*, vol. 158, no. 1-2, pp. 291–327, 2016.

[50] T. Jiang, K. Khorasani, and S. Tafazoli, "Parameter estimation-based fault detection, isolation and recovery for nonlinear satellite models," *IEEE Transactions on Control Systems Technology*, vol. 16, no. 4, pp. 799–808, 2008.

[51] B. Krawczyk, L. L. Minku, J. Gama, J. Stefanowski, and M. Woźniak, "Ensemble learning for data stream analysis: A survey," *Information Fusion*, vol. 37, pp. 132–156, 2017.

[52] M. Krüger, *Randomized Algorithms Aided Analysis and Design of Model-Based Fault Detection Systems*. Ph.D. dissertation of University of Duisburg-Essen, 2018.

[53] G. R. G. Lanckriet, L. E. Ghaoui, C. Bhattacharyya, and M. I. Jordan, "A robust minimax approach to classification," *Journal of Machine Learning Research*, vol. 3, pp. 555–582, Dec. 2002.

[54] G. R. Lanckriet, N. Cristianini, P. Bartlett, L. E. Ghaoui, and M. I. Jordan, "Learning the kernel matrix with semidefinite programming," *Journal of Machine learning research*, vol. 5, no. Jan, pp. 27–72, 2004.

[55] L. Li, H. Luo, S. X. Ding, Y. Yang, and K. Peng, "Performance-based fault detection and fault-tolerant control for automatic control systems," *Automatica*, vol. 99, pp. 308–316, 2019.

[56] H. Liang, Z. Zhang, and C. K. Ahn, "Event-triggered fault detection and isolation of discrete-time systems based on geometric technique," *IEEE Transactions on Circuits and Systems II: Express Briefs*, vol. 67, no. 2, pp. 335–339, 2019.

[57] H. Luo, K. Li, O. Kaynak, S. Yin, M. Huo, and H. Zhao, "A robust data-driven fault detection approach for rolling mills with unknown roll eccentricity," *IEEE Transactions on Control Systems Technology*, 2019.

[58] M. Mahsereci and P. Hennig, "Probabilistic line searches for stochastic optimization," *The Journal of Machine Learning Research*, vol. 18, no. 1, pp. 4262–4320, 2017.

[59] D. Martínez-Rego, O. Fontenla-Romero, A. Alonso-Betanzos, and J. C. Principe, "Fault detection via recurrence time statistics and one-class classification," *Pattern Recognition Letters*, vol. 84, pp. 8–14, 2016.

[60] B. L. Miller and H. M. Wagner, "Chance constrained programming with joint constraints," *Operations Research*, vol. 13, no. 6, pp. 930–945, 1965.

[61] K. Natarajan, M. Sim, and J. Uichanco, "Tractable robust expected utility and risk models for portfolio optimization," *Mathematical Finance: An International Journal of Mathematics, Statistics and Financial Economics*, vol. 20, no. 4, pp. 695–731, 2010.

[62] J. Neyman and E. S. Pearson, "On the problem of the most efficient tests of statistical hypotheses," *Philosophical Transactions of the Royal Society of London*, vol. 231, no. 694-706, pp. 289–337, 1933.

[63] T. T. Ngo, M. Bellalij, and Y. Saad, "The trace ratio optimization problem," *SIAM Review*, vol. 54, no. 3, pp. 545–569, 2012.

[64] N.-T. Nguyen, J.-M. Kwon, and H.-H. Lee, "Fault diagnosis of induction motor using decision tree with an optimal feature selection," in *the 7th International Conference on Power Electronics*. Daegu, South Korea, 2007, pp. 729–732.

[65] A. Prekopa, "On probabilistic constrained programming," in *Proceedings of the Princeton symposium on mathematical programming*, vol. 113. Princeton, NJ, 1970, p. 138.

[66] R. T. Rockafellar and S. Uryasev, "Optimization of conditional value-at-risk," *Journal of Risk*, vol. 2, pp. 21–42, 2000.

[67] A. H. Sameh and J. A. Wisniewski, "A trace minimization algorithm for the generalized eigenvalue problem," *SIAM Journal on Numerical Analysis*, vol. 19, no. 6, pp. 1243–1259, 1982.

[68] S. Schaible, "Fractional programming," in *Handbook of global optimization*. Springer, 1995, pp. 495–608.

[69] O. Shamir, "Fundamental limits of online and distributed algorithms for statistical learning and estimation," *Advances in Neural Information Processing Systems*, pp. 163–171, 2014.

[70] C. Shang and F. You, "Distributionally robust optimization for planning and scheduling under uncertainty," *Computers & Chemical Engineering*, vol. 110, pp. 53–68, 2018.

[71] ——, "A data-driven robust optimization approach to scenario-based stochastic model predictive control," *Journal of Process Control*, vol. 75, pp. 24–39, 2019.

[72] M. Z. Sheriff, M. Mansouri, M. N. Karim, H. Nounou, and M. Nounou, "Fault detection using multiscale pca-based moving window glrt," *Journal of Process Control*, vol. 54, pp. 47–64, 2017.

[73] B. W. Silverman, *Density estimation for statistics and data analysis*. Routledge, 2018.

[74] S. Song, Y. Gong, Y. Zhang, G. Huang, and G.-B. Huang, "Dimension reduction by minimum error minimax probability machine," *IEEE Transactions on Systems, Man, and Cybernetics: Systems*, vol. 47, no. 1, pp. 58–69, 2017.

[75] A. Stief, J. Ottewill, J. Baranowski, and M. Orkisz, "A pca-two stage bayesian sensor fusion approach for diagnosing electrical and mechanical faults in induction motors," *IEEE Transactions on Industrial Electronics*, vol. 66, no. 12, pp. 9510–9520, 2019.

[76] B. P. Van Parys, D. Kuhn, P. J. Goulart, and M. Morari, "Distributionally robust control of constrained stochastic systems," *IEEE Transactions on Automatic Control*, vol. 61, no. 2, pp. 430–442, 2015.

[77] H. Wang, S. Yan, D. Xu, X. Tang, and T. Huang, "Trace ratio vs. ratio trace for dimensionality reduction," in *2007 IEEE Conference on Computer Vision and Pattern Recognition*. Minneapolis, MN, USA, 2007, pp. 1–8.

[78] Z. Wang, Q. Bian, H. Xin, and D. Gan, "A distributionally robust co-ordinated reserve scheduling model considering cvar-based wind power reserve requirements," *IEEE Transactions on Sustainable Energy*, vol. 7, no. 2, pp. 625–636, 2015.

[79] W. Wiesemann, D. Kuhn, and M. Sim, "Distributionally robust convex optimization," *Operations Research*, vol. 62, no. 6, pp. 1358–1376, 2014.

[80] G. Xu and S. Burer, "A data-driven distributionally robust bound on the expected optimal value of uncertain mixed 0-1 linear programming," *Computational Management Science*, vol. 15, no. 1, pp. 111–134, 2018.

[81] L. Yang, S. Song, S. Li, Y. Chen, and C. L. P. Chen, "Discriminative dimension reduction via maximin separation probability analysis," *IEEE Transactions on Cybernetics*, 2019.

[82] W. Yang and H. Xu, "Distributionally robust chance constraints for non-linear uncertainties," *Mathematical Programming*, vol. 155, no. 1-2, pp. 231–265, 2016.

[83] S. Yin, S. X. Ding, A. Haghani, H. Hao, and P. Zhang, "A comparison study of basic data-driven fault diagnosis and process monitoring methods on the benchmark tennessee eastman process," *Journal of Process Control*, vol. 22, no. 9, pp. 1567–1581, 2012.

[84] S. Yin, S. X. Ding, X. Xie, and H. Luo, "A review on basic data-driven approaches for industrial process monitoring," *IEEE Transactions on Industrial Electronics*, vol. 61, no. 11, pp. 6418–6428, 2014.

[85] L. Zhang, J. Lin, and R. Karim, "Adaptive kernel density-based anomaly detection for nonlinear systems," *Knowledge-Based Systems*, vol. 139, pp. 50–63, 2018.

[86] Q. Zhang, "Adaptive kalman filter for actuator fault diagnosis," *Automatica*, vol. 93, pp. 333–342, 2018.

[87] M. Zhong, S. X. Ding, J. Lam, and H. Wang, "An lmi approach to design robust fault detection filter for uncertain lti systems," *Automatica*, vol. 39, no. 3, pp. 543–550, 2003.

[88] M. Zhong, Y. Song, and S. X. Ding, "Parity space-based fault detection for linear discrete time-varying systems with unknown input," *Automatica*, vol. 59, pp. 120–126, 2015.

[89] M. Zhong, Y. Song, T. Xue, and W. Li, "Parity space-based fault detection by minimum error minimax probability machine," *IFAC-online paper*, vol. 1, no. 1, p. 1, 2018.

[90] M. Zhong, T. Xue, Y. Song, S. X. Ding, and E. L. Ding, "Parity space vector machine approach to robust fault detection for linear discrete-time systems," *IEEE Transactions on Systems, Man, and Cybernetics: Systems*, 2019.

[91] K. Zhou and J. C. Doyle, *Essentials of robust control*. Prentice hall Upper Saddle River, NJ, 1998, vol. 104.

[92] J. Zhu, Z. Ge, and Z. Song, "Non-gaussian industrial process monitoring with probabilistic independent component analysis," *IEEE Transactions on Automation Science and Engineering*, vol. 14, no. 2, pp. 1309–1319, 2016.

[93] S. Zymler, D. Kuhn, and B. Rustem, "Distributionally robust joint chance constraints with second-order moment information," *Mathematical Programming*, vol. 137, no. 1-2, pp. 167–198, 2013.

[94] ——, "Worst-case value at risk of nonlinear portfolios," *Management Science*, vol. 59, no. 1, pp. 172–188, 2013.

List of publications

Journal Papers

1. **T. Xue**, M. Zhong, L. Li, and S. X. Ding. An optimal data-driven approach to distribution independent fault detection, *IEEE Trans. Ind. Inf., 2020, doi: 10.1109/TII.2020.2976043.*

2. **T. Xue**, M. Zhong, S. X. Ding, and H. Ye. Stationary wavelet transform aided design of parity space vectors for fault detection in LDTV systems, *IET Control Theory & Applications, 2018, vol. 12, no. 7, pp: 857–864.*

3. M. Zhong, **T. Xue**, Y. Song, S. X. Ding and E. L. Ding. Parity space vector machine approach to robust fault detection for linear discrete-time systems, *IEEE Trans. Syst., Man, Cybern., Syst., 2019, doi: 10.1109/TSMC.2019.2930805.*

4. M. Zhong, **T. Xue**, and S. X. Ding. A survey on model-based fault diagnosis for linear discrete time-varying systems, *Neurocomputing, 2018, vol. 306, pp: 51–60.*

Conference Papers

1. **T. Xue**, M. Zhong, L. Luo, L. Li, and S. X. Ding. Distributionally robust fault detection by using kernel density estimation, *in proceedings of the 21th IFAC World Congress of the International Federation of Automatic Control, Berlin, Germany, July 2020.*

2. M. Zhong, **T. Xue**, S. X. Ding, and H. Ye. A wavelet-based parity space approach to fault detection of linear discrete time-varying systems, *in proceedings of the 20th IFAC World Congress of the International Federation of Automatic Control, Toulouse, France, July 2017.*